THE UNIVERSITY OF HULL

An Investigation of Glycidyl Methacrylate Terpolymers for Mixed Mode LC Separations

Being a thesis submitted for the Degree of Doctor of Philosophy

The University of Hull

By

AHMED A. ALKARIMI

April 2018

Table of Contents

Table of Figures

Table of Tables

Abstract

Enhancing efficient separation techniques for use in proteomics or metabolomics is a growing area in recent years. Monolithic columns, as innovative separation materials have gained more attention and acceptance for proteomic and metabolic separation as alternatives to conventional packed columns. Moreover, monolithic columns have advantages over conventional columns such as fast and easy modifications, no requirement for retaining frits, ability to improve analyte mass transfer, lower back pressure due to high porosity, and broad selectivity.

Five monomers were used to prepare the monolithic columns alongside glycidyl methacrylate, styrene, 2-(diethylamino)ethyl methacrylate, butyl methacrylate, lauryl methacrylate, and stearyl methacrylate. Ethylene glycol dimethacrylate (EDMA) was used as cross-linker, while 2,2-dimethoxy-2-phenylacetophenone was used as initiator. The v/v ratio between the two monomers has been investigated, while the ratio between the monomer to cross-linker was not changed. Three ratios (90:10, 50:50, and 10:90)% between the two monomers were used to prepare monoliths with appropriate surface area and pore size that can be used to separate small and macro molecules.

The results indicated that the glycidyl methacrylate-co-stearyl methacrylate-co-ethylene glycol dimethacrylate monolith was formed at all the ratios tested, yet (30:70, 20:80, and 10:90) ratios that gave higher average surface area compared to other ratios. The average surface area was between 19.5938-21.0283 m^2 g^{-1}, and the average pores size was 5.12, 4.80, and 4.2 nm for (30:70, 20:80, and 10:90)% of GMA:SMA respectively. Correct formation of the monolith was proven using different techniques such as FTIR, and ^{1}HNMR.

Mixed mode properties were investigated by ring opening the epoxy group of glycidyl methacrylate to form free hydroxyl functions to give HILIC/revers phase functionality and by converting the epoxy groups to sulphonate groups to give cation exchange/revers phase properties.

The effect of several porogenic solvents and the irradiation time on the monolith formation were investigated to obtain even higher surface areas. The best results were obtained using a 50:50 v/v ratio of 1-propanol to methanol with an irradiation time of 23 minutes. The monolithic column produced gave average surface areas of 73 $m^2 g^{-1}$ and was tested for the separation of proteins, however, base line separation could only be achieved with the strong cation exchange/revers phase monolith.

Base line separation was obtained with all proteins samples tested, depending on the pI value of each protein, also, with peptides, hydrophobic compounds, and a mixture of hydrophilic and hydrophobic compounds, which was a better result compared to the HILIC/RP monolithic columns.

The strong cationic exchange/ reversed phase monolithic columns were also prepared inside a glass microchip device and used for LC separation. The result showed base line separation was obtained for pharmaceutical and hydrophobic compounds.

Acknowledgements

I would like to express my heartful thanks to the Iraqi Ministry of Higher Education and Scientific Research (HESR), the Iraqi cultural attaché in London and Ireland, and the University of Babylon for their financial support and encouragement to conduct my study.

I take this opportunity to express my profound gratitude and deep regards to my supervisor (Dr. Kevin Welham) for his exemplary guidance, monitoring and constant encouragement throughout the course of this work.

Furthermore, I would also like to thank with much appreciation the University of Hull, Chemistry Department, teaching lab staff for their help with HPLC system, and Mr. Tony Sinclair for his help with SEM analysis. As well as, special thanks to all my friends for their support.

I would also like to express my big thanks to my parents, my brothers and my sisters for their unceasing encouragement and prayers, and great special thanks to my wife and my children for all their patience, love, help, care and generous support in every aspect of my life.

Ahmed

Abbreviations

ID	Internal diameter
OD	Outer diameter
min	Minute
h	Hours.
ºC	Celsius
PSI	Pressure per square inch
SEM	Scanning Electron Microscopy
BET	Brunauer-Emmett-Teller
HPLC	High Performance Liquid Chromatography
UV	Ultraviolet light
PS-DV	Poly styrene-Divinyl benzene
AIBN	2,2'- Azobisisobutyronitrile
TSP	3-(Trimethoxysilyl) propyl methacrylate
DVB	Divinyl benzene
DAP	2, 2-Dimethoxy-2-phenylacetophenone
GMA	Glycidyl methacrylate
EDMA	Ethylene glycol dimethacrylate
STY	Styrene
LMA	Lauryl methacrylate
SMA	Stearyl methacrylate
HILIC	Hydrophilic interaction chromatography
NP	Normal phase
RP	Reversed phase

TFA	Trifluroacitic acid
AFM	Atomic Force Microscopy
MIP	Mercury Intrusion Porosimetry
CEC	Capillary Electro Chromatography
2D-HPLC	Two Dimension High Performance Liquid Chromatography
EOF	Electro Osmotic Flow
TEOS	Tetraethoxysilane
TMOS	Tetramethoxysilane
PEO	Polyethylene oxide
TSP	3-(Trimethoxysilyl) propyl methacrylate
BP	Benzoyl peroxide
EDMA	Ethylene glycol dimethacrylate
ISEC	Inverse Size Exclusion Chromatography
TLC	Thin layer chromatography
GC	gas chromatography
HETP	high equivalent to a theoretical plate
N	theoretical plates
CX	Cationic exchange
SCX	Strong cationic exchange
3SPMA	3-sulfopropyl methacrylate
HI	Hydrophilic interaction
ODA	Octadecyl acrylate
TPGDA	Tripropylene glycol diacrylate
TMPTMA	Trimethylolpropane trimethacrylate

PETA	Pentaerythritol triacrylate
VPBA	Vinylphenylboronic acid
WAX	Weak anion exchange
WCX	Weak cation exchange

1 Introduction

1.1 General introduction

Monoliths is a Greek word consisting of two idioms (mono), and (lithos), which means (one) and (stone) respectively. While, geologically, it is well-defined as a single massive rock that have different shapes and sizes of holes, a good example of this sort of the rocks was the rocks that have been collected and utilized by Chinese empress in architect work and palaces design. The monolithic rock is shown in Figure (1.1). [1]

Figure 1.1 Photograph of the porous monolith erected at the entrance of the Summer Palace Park, Beijing, China.[1]

The first efforts to prepare porous monolithic stationary phase was in the period of 1960 to 1970 by Kubin *et al*, to prepare a swollen polymer gel, and by Ross and Jefferson to prepare porous polyurethane, all these efforts were unsuccessful due to the limited permeability of the monolith.[2,3] In the 1980 an innovative approach was developed to form porous monoliths as separating media by using the manufacturing technology developed for polymeric ultrafiltration membranes.[4] Later, a novel monolithic stationary phase was developed in disk format by Belenkii, Svec, and Tennikova as a cooperative group in 1989, for high performance chromatography of proteins, biopolymers, and nucleic acids.[5,6]

In the early 1990 monolithic columns based on inorganic matrices were obtained, and the sol–gel approach was presented by the Tanaka group after fabrication of a silica monolith.[7,8] Since then, two kinds of monolithic materials have been developed for chromatographic separations, the first is a monolith based on organic precursors and the second one is based on inorganic polymers, theses monolithic materials have been used as popular media in widely research areas, for instance, electrophoresis, high performance liquid chromatograph, and on-chip chromatography.[9]

Belenkii *et al.* in the middle of 1990 investigated the chromatography of proteins on monolithic porous disks with several chemical structures and configurations. They advised to usage the process of gradient elution for these purposes, because they investigated that the proteins can be separated by gradient chromatography using monolithic disks of small thickness.[10] Svec prepared novel monolithic stationary phases utilizing macro porous polymeric materials were

investigated in situ polymerization processes in capillaries or tubes forming the chromatographic column.[11]

Tanaka improved monolith stationary phases based on silica, which are prepared in situ in capillaries or columns by using the poly condensation method with tetraethoxysilane.[12,13] Later, Karger *et al*. demonstrated the effective separation of tryptic protein hydrolysates by using a 20-µm ID capillary monolithic column fabricated in fused silica.[14] Over the last few decades, monolithic materials have been investigated and developed by enormous number of researchers and companies using these materials in a range of different sectors due to their dynamic transport and time saving process.[15]

1.2 Monolithic materials

Monolithic materials have been employed in the last decades as an inventive and valuable generation of polymers that can be utilized in diverse sectors, these polymeric materials can prepared in simple way using homogenous or a heterogenous mixture inside mould(s), the materials have large interconnected pores or channels, therefore, they can be used with high flow rates with moderate back pressures.[16]

Heterogenous polymers-based monoliths are prepared from a suspension polymerization reaction in particle form, while homogenous polymers are prepared using polymerization mixture consists of a single phase, the possible combination of monomers used in the preparation of continuous polymers is higher than that in the case of suspension polymerization reactions. For this reason, a greater diversity of surface chemical structures could be obtained. Nevertheless, the reaction conditions optimized for a specific system cannot be

transferred directly to another system. The reaction conditions for each special system must be optimized.[16]

The polymerization mixture should always include a vinylic monomer as cross-linker (it must have at least two double bonds) and an inert solvent(s) (called porogen, porogenic mixture or pore forming agent).[17] The presence of the inert solvent is crucial for the preparation of macroporous polymers, hence, different classes of solvents are used, those that solvate the polymeric chains during formation (good solvents), and those that do not solvate the polymeric chains in formation (poor solvents) [18], such as supercritical carbon dioxide[19,20], linear polymers[21], and a mix of good/poor solvents[22].

The macroporous polymers have a porous structure formed during preparation and maintained in any solvent or in dry state, the inner structure consists of aggregates of microglobules of interconnected polymers forming pores and their rigidity results from their high degree of single monomer and cross-linkings.[2]

Homogenous polymers (single phase polymers), these macroporous monolithic have been used as a new and useful generation of macroporous polymers prepared in a more simple way respect to suspension.[16]

The structure of monolith column can be viewed as a network of interconnected large flow-through pores, that shows high axial permeability with a large internal pore surface area which providing less back pressure than that of a conventional packed column, in addition these channels allow better contact between the analyte and the active sites of the stationary phase.[23] The structures of packed columns and the monolithic columns is shown in Figure (1-2).[24]

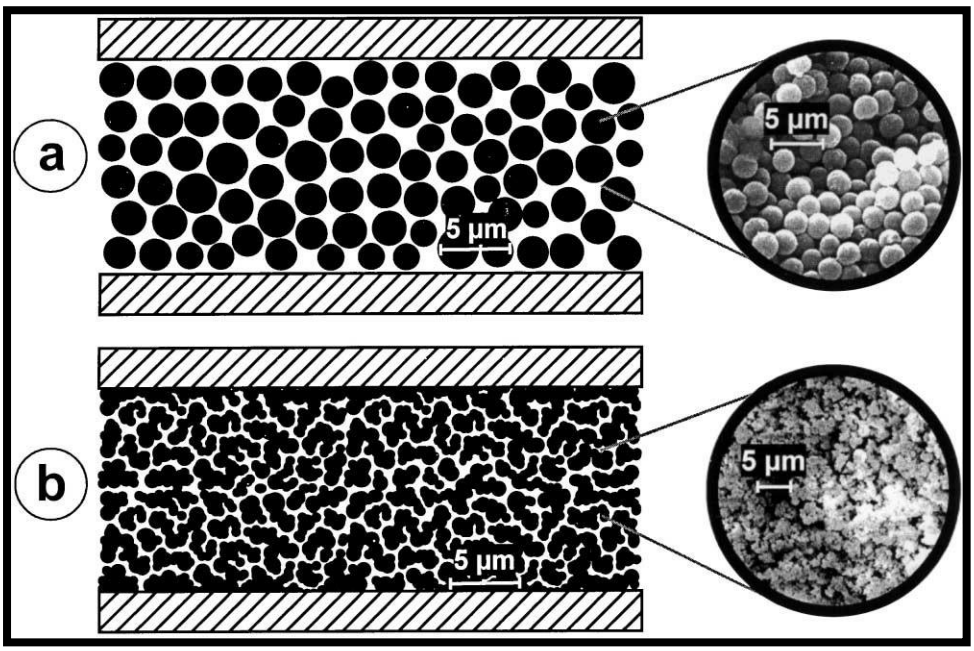

Figure 1.2 The structural difference of (a) the packed column, (b) the monolithic column.[24]

Monolithic columns have three kinds of the pores structure, firstly, macropores or through-pores (> 50 nm), secondly, mesopores (2-50 nm), and finally, micropores (< 2 nm), the advantages of this pore structure are the macropores (through-pores) are used to control the column permeability by reducing the backpressure of the column when high flow rate applied, because they allow to the solvent to pass throw the monolithic column faster than the packed column as shown in Figure (1-3).[25,26] The mesopores are responsible for increasing the surface area of the monolith and increasing the load ability of the monolith, this pore structure affects the rapid extraction with high flow rate and moderate backpressure. While, the micropores are played a crucial role for sorption capacity for small solutes in the total surface area.[20]

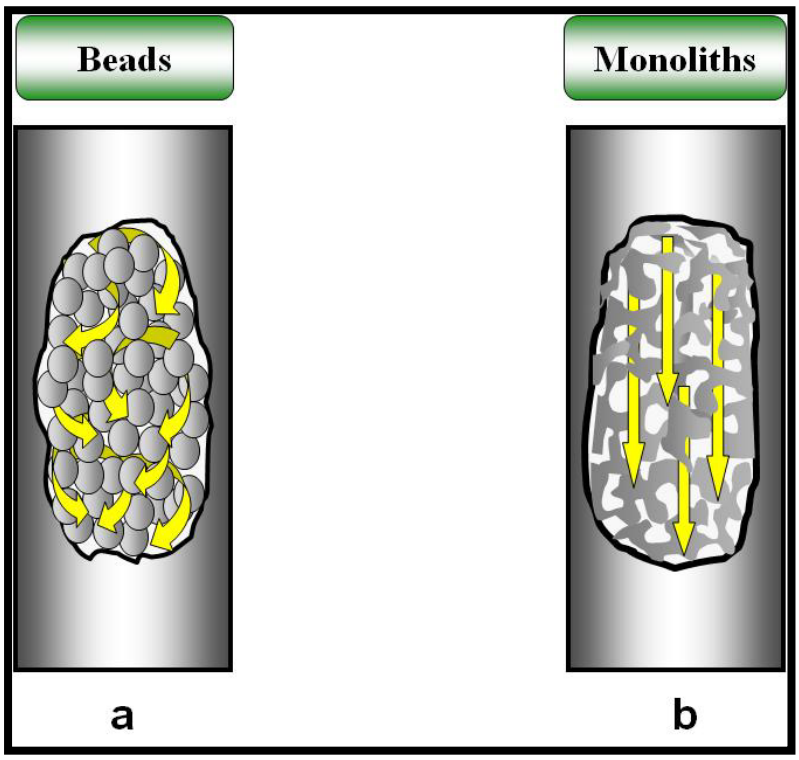

Figure 1.3 The difference in mobile phase movement in (a) packed column and (b) monolithic column. [26]

The physical properties of monolithic materials can be studied by using different techniques, such as scanning electron microscopy (SEM), transmission electron microscopy (TEM), and atomic force microscopy (AFM). [27] The three techniques provide significant data covering the morphology of the monolithic materials, and can be used to measure the monolithic porous properties such as the size of the pores and to determine the hydrodynamic features and mechanical strength of the column.[28] Mercury intrusion porosimetry (MIP) is used to study the porosity and pore size distribution of monolithic columns, the (MIP) ability is to measure the large pores between 10 nm to 150 nm.[29] Inverse size exclusion chromatography (ISEC) is utilized to measure the small pores which are less than 50 nm, Brunauer-Emmett-Teller (BET) procedure was used to study the pore size

distribution by measuring the volume of N_2 gas that is adsorbed on to the surface of the monolithic materials.[29,30]

Monolithic columns can be prepared using two different methods depending on the monomer(s) used in polymerization process, therefore, when the monomer is organic materials the monolith called organic based monolith, while when alkoxysilane (silica-based monolith) used the monolith called inorganic monolith or silica-based monolith.[31] Both types have many useful properties such as higher permeability, lower flow resistance, significantly shorter separation times, and moderate operation pressures compared to conventional packed columns. These features allow them to find many applications including pharmaceutical, environmental, industrial, forensic, clinical, and food analysis, by using chromatographic technique for example high performance liquid chromatography (HPLC), gas chromatography (GC), and capillary electrochromatography (CEC).[32]

1.3 Organic based monoliths

Organic polymeric materials serve as valuable alternatives stationary phases for liquid chromatography (LC). These materials offer low back pressures depending on their structures, as well as stability across varied pH ranges. They are prepared by a one-step method and can be fixed in a plastic tube or a column following chemical modification.[12, 33] Polymer-based monolithic columns were chromatographically investigated with compressed aqueous polyamide beds (gel chromatography) in the late 1980s by Hjertn *et al.*[34,35] Then, from the early 1990s, these columns have been investigated for high-performance LC (HPLC) and CEC applications.[36] The concept of the polymer-based monolith was claimed by patent

by Frechet and Svec in 1988 as a chromatographic column with a specific bimodal pore (double pore) size distribution.[37] Meanwhile, the other type of monolithic column composed of nonporous particles of PS-DVB were investigated and used in protein separation.[38] Moreover, in the early 1990s, a new monolithic column technology was developed and applied to rapidly separate biomolecules, the important feature of these materials is the presence of large through-pores (macropores), which allow the use of high flow rates with low back pressures.[39]

There are three kinds of organic-based monoliths are exist nowadays.[40] The first type is the thin disk (up to 3 mm), which are prepared in flat cylindrical molds. The second type is the cylindrical monolithic rod-like column (Figure (1.4) formed by in situ polymerization methods in stainless-steel or glass tubing. The length of this column is 30–50 mm, and the i.d. is 1–8 mm. These columns are used for the expeditious separation of proteins.[41,42] The third and final type is the monolithic capillary, which is widely used for capillary electrochromatography and capillary HPLC.[43]

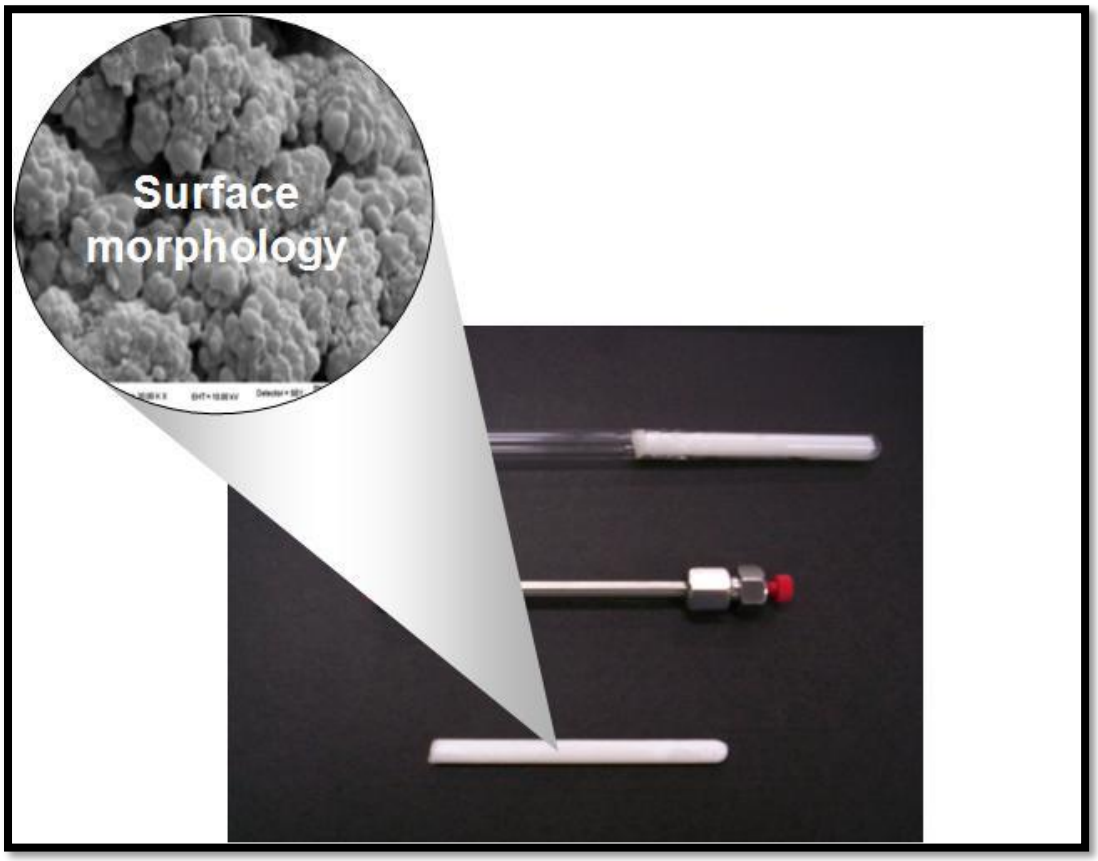

Figure 1.4 Types of cylindrical monolithic columns.[16]

Organic-based monoliths are prepared from a homogeneous polymerization mixture, which includes functional and cross-linking monomers, along with porogenic solvents and a radical initiator.[44] The monomer mixture is purged in a tube, and the two ends of the tube are closed. The polymerization process is started by UV radiation or heating for up to 24 h, after which monomers are polymerized to form a polymeric skeleton.[45] The polymerization reaction occurs within a mold that controls the shape of the support. The active functional groups on the polymer surface are dependent on the monomer type employed. Methacrylates, acrylamides, and styrene are commonly utilized as monomers to produce porous polymer monolith.[34]

Organic-based monoliths hold the following significant advantages over the packed columns: [46,47]

1- Fast and easy modifications.
2- No requirement for retaining frits.
3- Ability to improve the analyte mass transfer.
4- Lower back pressure due to high porosity.
5- Broad selectivity.

Organic-based monoliths are the ideal media for separating large molecules, such as, nucleic acids,[48] peptides,[24] synthetic polymers,[49] and proteins,[50] due to the significant convective mass transfer and appropriate surface area.

The drawback of organic polymer monoliths is the poor separation of small molecules under normal chromatographic conditions. This disadvantage is due to the low mesopore volume and high porosity of the material.[51,52] Given its porosity, the monolith gel swells in the mobile phase and performs poorly in separating low-molecular-weight compounds.[52] Scholars have attained substantial progress in improving the separation efficiency for small molecules to 70,000–80,000 plates·m^{-1} to achieve this goal, various factors and steps have been adjusted to investigate the porosity and mass transfer in organic-based monoliths. These factors include:[44, 53-57]

(1) Changing the initiation conditions and temperature of the polymerization process.

(2) Controlling the time of the polymerization reaction.

(3) Carefully optimizing the chemistry and proportions of the polymerization mixture (functional monomers, crosslinkers and porogenic solvents).

(4) post-polymerization and modifications of the monolith.

(5) Combining extra structural elements into the monolithic skeleton.

These factors are played significant role in producing organic based monoliths to separate low molecular weight compounds by chromatographic methods.

1.4 Silica-based monoliths

Despite their internal structure with dominant flow-through pores, silica-based and organic polymer monoliths considerably differ in pore morphology. The discrepancy is apparent in the micrographs in Fig. (1.5). Silica-based monoliths exhibit a bimodal pore structure with obvious 7–12 nm mesopores (~13%) and relatively high specific surface area of several hundreds of square meters per gram. This specific surface area is similar to the 150–400 $m^2.g^{-1}$ range that is typical for the particles packed in conventional columns.[8, 58]

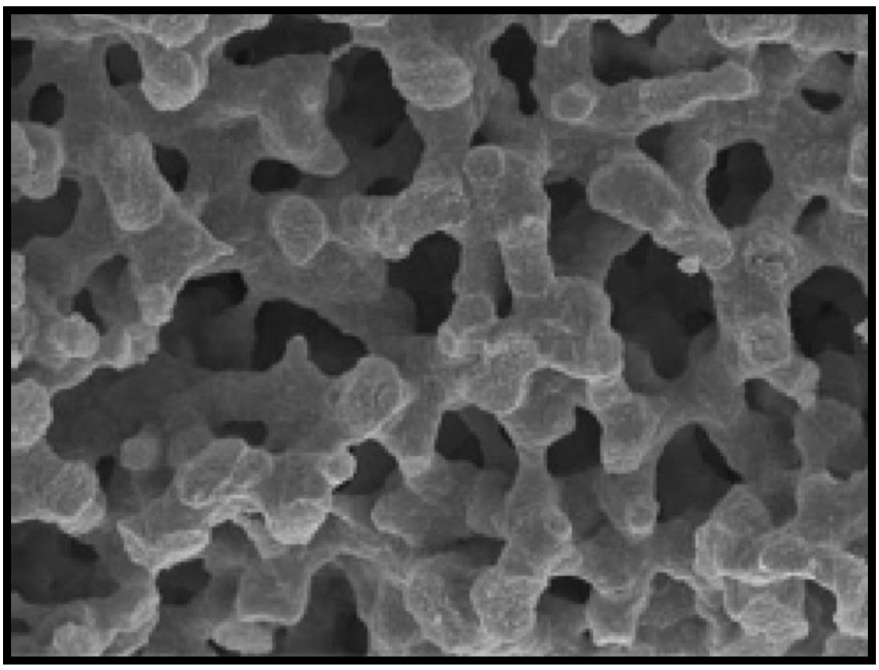

Figure 1.5 The bimodal pore structure of silica-based monoliths.[9]

Hence, silica monoliths are ideal for separating small molecules, their mesopores sizes allow the easy penetration of the molecules to the adsorption sites, as well as fast diffusion, which result in a high separation efficiency.[58] Like silica gel particles, monolithic silica rods can be chemically modified by binding with various nonpolar or weakly or strongly polar functionalities for various LC applications. Chemically bonded silica-based monoliths enable the rapid separation of low-molecular-weight samples, with column efficiencies of up to 100,000 theoretical plates.m^{-1}.[59] Commercial silica-based monolithic columns with chemically bonded alkyls have been widely used to separate various low molecular weight compounds, including in food analysis.[60]

Examples of these columns include Chromolith C18 or Chromolith C8 from Merck (Darmstadt, Germany). They provide lower column pressures and considerably shorter separation times than those of the columns packed with fully porous and even fused-core particles, although occasionally, at the cost of lower

chromatographic efficiency. Moreover, the method transfer between the particulate and monolithic columns often requires the adjustment of separation conditions.[58, 61]

Unfortunately, silica monoliths generally have poor performance when separating macromolecular compounds, such as proteins and other biopolymers, than when doing so for low molecular weight compounds.[9]

Monolithic silica materials have been proven to be useful materials for chromatography, in the last years these materials have been employed instead of particle packed columns due to high porosity of these materials, which resulting from the network structure of the mesopores and the macropores.[62] The mesopores and macropores are offered low mobile phase stream hydraulic resistance and a large surface area for analyte retention.[13]

The monolithic silica materials have no interstitial void volume, therefore, mobile phase streams through the support pore channels, and leads to improve the analyte's molecule mass transfer rate through the beds.[30]

Currently, monolithic silica columns are available commercially in varied sizes. Examples of these columns include traditional analytical columns of 4.6 mm i.d. and 1–10 cm length, capillary columns of 50–200 μm i.d. and 15–30 cm length, and preparative scale columns of 25 mm i.d. and 10 cm length.[63]

The sol–gel reaction that consisting tetraethoxysilane (TEOS) or tetramethoxysilane (TMOS), is the main method to prepare silica monolith, it was described and improved by Nakanishi and coworkers.[12, 64]

In the early of 1980 the silica sol-gel technology was invented; however, it was not used until the beginning of the 1990 when Nakanishi and Soga reported the sol-gel process. Tanaka and co-workers in 1996 prepared a well-ordered

bicontinuous silica monolith structure with a sharp bimodal pore size distribution with a variety of mesopores and macropores using a sol–gel process and first indicated the application of the monolith in HPLC.[7, 8, 65]

There are three reactions that form the sol-gel phase, firstly, the hydrolysis of an alkoxysilane, secondly, the condensation of hydrated silica to form siloxane bonding (≡Si-O-Si≡), and finally, the polycondensation of the linkage of an additional silanol group to form cyclic oligomers, these reactions are shown in Figure (1.6).

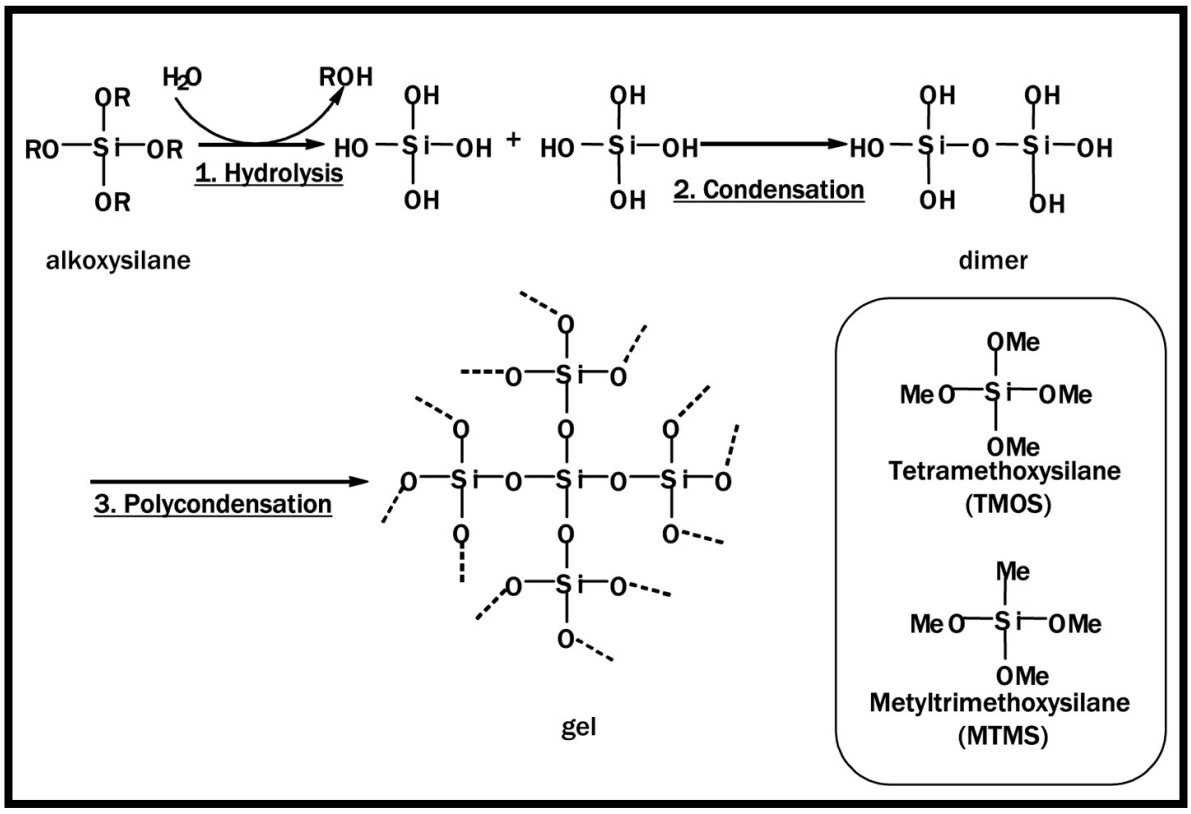

Figure 1.6 The sol-gel reactions involved in forming silica polymers.[66]

There are several factors that affect the properties of the sol-gel matrix, for example, temperature, reagent concentrations, pH, reaction time, the nature of the catalyst, and the rate of hydrolysis and condensation. Tetraethoxysilane

(TEOS) or tetra-methoxysilane (TMOS) are popular starting reagents since they can be hydrolyzed directly and condensed under mild conditions.[67]

The monolithic silica gel can be synthesized by adding applicable quantities of polyethylene oxide (PEO) as a polymer and tetramethoxysilane (TMOS) as a source of silica in an aqueous acidic solution. The methods of sol-gel transition and phase separation can occur at the same time and control the monolith's structure [59]. PEO is the main factor that can be used to control the macropores and the skeleton diameter in the reactant mixture, simultaneously lower macropores volume and skeleton diameter or higher macropores volume and thinner skeletons can be controlled by TMOS.[65]

The disadvantages of Monolithic Silica Columns are: [63, 68]

1- High porosity leads to a high permeability of a monolithic silica column, but the column is inevitably accompanied by a low phase ratio (through-pore size / skeleton).
2- Small surface area since the quantity of silica present in a column is less than in a particle-packed column, this leads to short retention time.
3- The *k* values (column permeability) are smaller than the particle-packed columns by 2 – 5 times, and depend on the total porosity. The *k* values are 90 – 95% for a capillary type column and 80 – 85% for a conventional size column.
4- The sample loading capacity is not as small as estimated from the phase ratio. The loading capacity depends on the separation conditions, and the mobile phase also plays a key role in this matter. A good example is a second dimensional column in 2D-HPLC, low retention is a clear

drawback, as the volume of large injection require extremely retentive columns for conserving the column efficiency.

5- Small internal porosity, resulting in a small range for size exclusion mode elution, the labour-intensive preparation of individual columns with possible reproducibility problems, and limited availability.

6- Low pH range (2-8).

1.5 Hybrid Organic – Inorganic Monolith

This kind of monolith contains two or more components combined at the molecular or nanometer level, it has significant advantages such as high selectivity, high surface area, thermal stability, excellent mechanical strength, long life, flexibility, and excellent biocompatibility.[69-73] Excellent performance is obtained when the organic functional groups are distributed equally within the inorganic matrix structure.[74-76]

Hybrid organic–inorganic monoliths are classified into two types according to the chemical composition, the first one is hybrid polymer-based monolith, Different monomers can be used to polymerize inside sealed column, therefore, the produced monoliths have integrated structures, such as, greater flexibility and higher external porosity compared with particulate-based column.[36, 77] Bai *et al.* have been investigated novel procedure to prepare an innovative hybrid polymer-based monolith for HPLC, the atom transfer radical polymerization (ATRP) has been depending on vinyl ester resin as a monomer and $NaHSO_3$ as initiator to adjust the free radical activity and controlling the molecular mass in polymerization process.[73] Hybrid polymer-based monoliths have been used in different applications such as separation materials, catalysis and sensors [78(89)].

The disadvantages of this kind of monolith are swelling when using organic solvents leading to mechanical instability.[79]

The second type is a monolith made from a silica precursor which has organic moieties, it was synthesized by the sol–gel process involving organic and inorganic polymers to form network combination copolymer.[80-82] Hybrid monoliths have a range of applications in optics,[83] electronics,[84] and biology.[85, 86]

Noble *et al*. investigated polyfunctional siloxane network monolith depending on siloxane–silica nanocomposites, the monolith was prepared by utilising the 1,3,5,7-tetramethyl-tetrakis (ethyltriethoxysilane)-cyclotetrasiloxane and TEOS using sol-gel procedure, with cetyltrimethylammonium bromide as cationic surfactant, the produced monolith has well-defined of porosity.[87]

Moreover, poly(methyl methacrylate) (PMMA)/SiO2 hybrid monolith was prepared using sol-gel technique based on TEOS to use as a matrix for organic dyes and rare earth ions, in addition to optical devices.[88] There are many papers have been published to investigate this sort of the monolith in different sectors, although, silica-based monolithic materials have some advantages, for example a good mechanical stability and organic solvent resistance, however, it has some disadvantages such as a narrow pH range (2–8). In addition, the preparation process is difficult to control.[15]

1.6 The polymerization process

The polymerization process involves preparation of the polymer mixture for organic monolith that consists methacrylate derivative monomer(s), cross-linker, porogenic solvent, and initiator. After that, the polymerization mixture was exposed to thermal or UV light source, to initiate the free radical polymerization process, the steps of free radical polymerization are shown below:[89, 90]

1- Initiator cleavage step, this step consists decomposing of the initiator 2, 2-dimethoxy-2-phenylacetophenone using UV light at 365 nm to form benzoyl fragment that initiate the polymerization reaction and into acetal fragment as inhibitors to inhibit the polymerization process.[90]

2- Initiation step, this step involves attacking of free radical (benzoyl fragment) into the double bond in the monomer to form new free radical on the monomer that could be attacked the double bond of the cross-linker or other monomer.

3- Propagation step, this step involves free radical reactions between the monomers and cross-linker to growing the polymer chain.

4- Termination step, in this step the polymerization process was terminated due to all free radicals are reacted with each other.

The polymerization steps are shown in Figures (1.7-1.10)

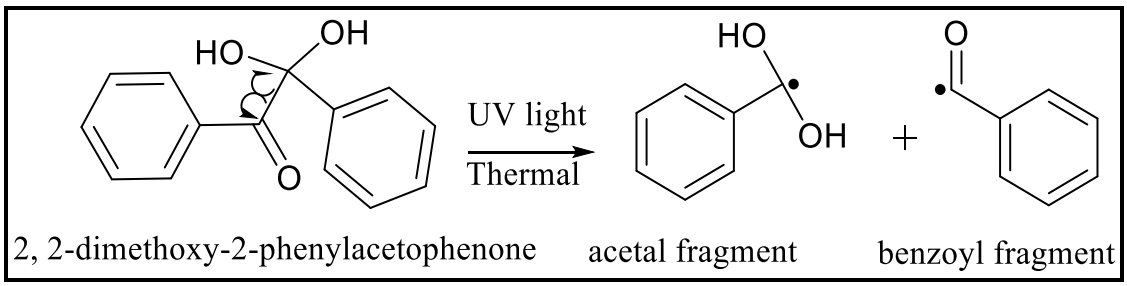

Figure 1.7 Initiator cleavage step.

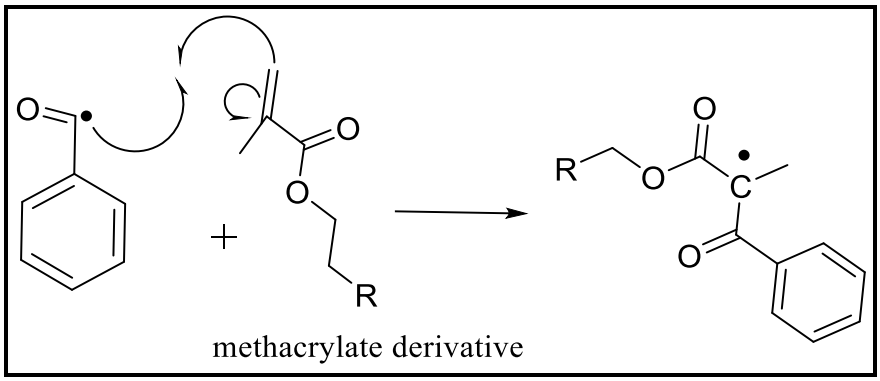

Figure 1.8 Initiation step.

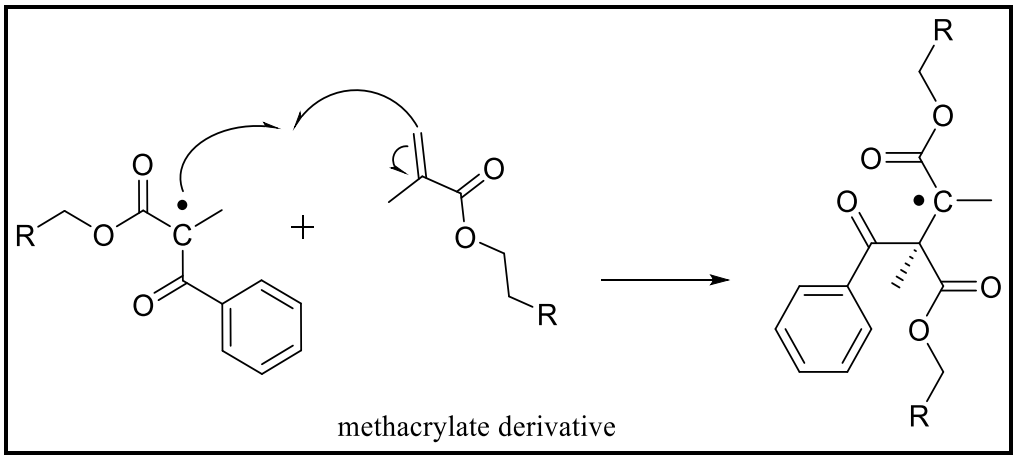

Figure 1.9 Propagation step

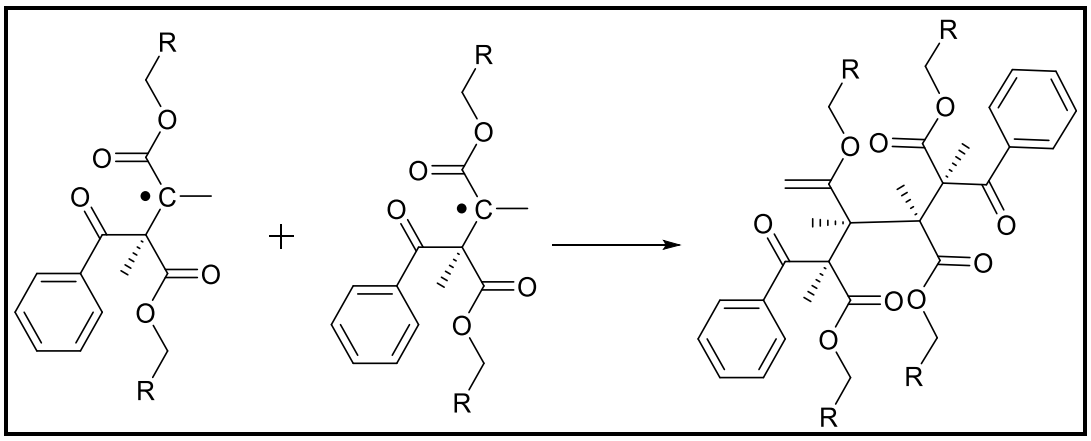

Figure 1.10 Termination step

1.7 Chromatography

Chromatography is defined as a technique that is used for separation and/or identification the analytes in a mixture; the basic principle for this technique is the components in a mixture have different tendencies to adsorb onto a surface or dissolve in a solvent.[91]

The first scientist that recognized chromatography as an efficient method of separation was the Russian botanist Tswett he used a simple form of liquid-solid chromatography to separate number of plant pigments.[92] The coloured bands that produced on the adsorbent bed induced the term chromatography for this type of separation (colour writing), the modern chromatography has little to do with the colours, yet the name has still used for all separation techniques.[92]

There are several types of chromatography currently in use such as paper chromatography; thin layer chromatography (TLC); gas chromatography (GC); liquid chromatography (LC); high performance liquid chromatography (HPLC); ion exchange chromatography; and gel permeation or gel filtration chromatography, all chromatographic methods require one static part (the

stationary phase) and one moving part (the mobile phase), these techniques are depending on one of the following phenomena: adsorption; partition; ion exchange; or molecular exclusion.[93]

1.8 Theories of chromatography[94, 95]

The phenomenon of band broadening in sample separation has brought attention of many chromatographers to tackle this problem. It occurs when sample mixture has been moved down through the column due to the interactions of different components which will be retained by diverse degrees with the stationary phase, these interactions with the sinuous path of the sample through the packed column will lead to increase the band width. The band broadening value should be kept to a minimum to obtained good separation degree of the components in the sample.

There are two chromatographic theories have been utilized to describe the band broadening and column efficiency, firstly the plate theory which was produced by Martin and Synge and secondly, is the rate theory which has been developed by van Deemter *et al*, these two theories are used in modern chromatograph.

1.8.1 The plate theory [93, 96]

The principle of the plate theory assumes that there is an instant equilibrium set up for the solute between the mobile phase and stationary phase, and It is considered the chromatographic column contains a number of thin sections (plate) each one is allowing the solute to equilibrate between the mobile phase and the stationary phase. Therefore, when the column has a greater number of

theoretical plates (N), it will be more efficient. Yet, it does not take in consideration the effects of band broadening on separation, in addition it does not take in consideration the effect of chromatographic variables, for example, stationary phase loading, flow rate on column, performance particle size, and eluent viscosity.

The number of theoretical plates (N) value can be calculated from the equation below.

$$N = L/H \tag{1.1}$$

Where, H is the high equivalent to a theoretical plate (HETP), L is the length of the column (millimetres), and N is the number of theoretical plate, however, from equation (1.1) it can be seen that the low value of the (HETP) can lead to high efficiency of the column by increasing the (N) value, this could be achieved when using low flow rate of the mobile phase, high oven temperature, small particle size of stationary phase, less viscous mobile phases, and small size of the solute molecule.

The (N) value can be calculated using different methods depending on the width of the peak as shown in equations (1.2) for the peak half-height method and equation (1.3) for the Tangent method.

$$N = 5.54\,(t_R / w_{50})^2 \tag{1.2}$$

$$N = 16\,(t_R / w_T)^2 \tag{1.3}$$

Where (t_R) is the retention time of the solute, (w_{50}) is the half peak width, and (w_T) is the total peak width. The Tangent method considered more popular method

that used for the calculation of (N) value due to the simplicity. The t_R, $W_{0.5}$, and W_T are shown in Figure (1.11)

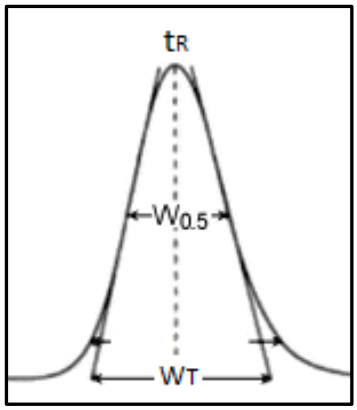

Figure 1.11 The peak half-height and the Tangent methods that used to calculate the number of theoretical plate (N)

1.8.2 The rate theory [93, 95, 97, 98]

This theory was established by van Deemter *et al* in 1956 to illustrate the band broadening and column efficiency, it considers the diffusional factors that lead to the band broadening in the column and avoids the hypothesis of an instantaneous equilibrium inherent in the plate theory, the van Deemter equation is shown in equation (1.4).

$$H = A + B/\mu + C\,\mu \qquad (1.4)$$

Where (H) is the efficiency of the column, (μ) is the average linear velocity of the mobile phase, (A) is the eddy diffusion, (B) is longitudinal diffusion, and (C) is the resistance to mass transfer, the hypothetical van Deemter plot is shown in Figure (1.11).

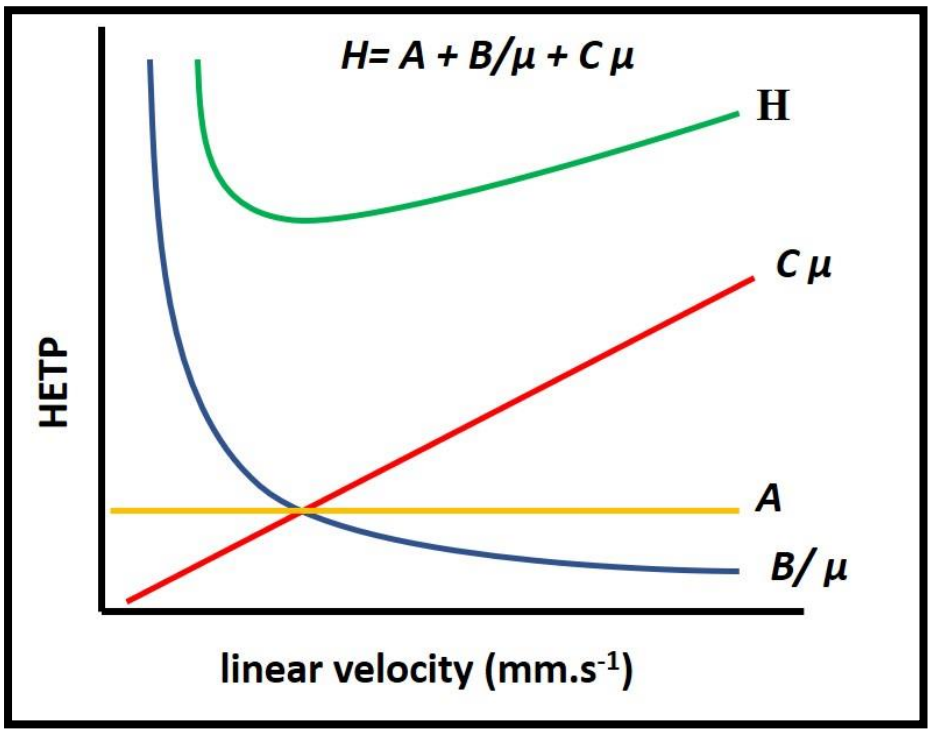

Figure 1.12 The hypothetical van Deemter plot adopted from reference 112.

According to van Deemter plot, the efficiency is dependent on diffusion effect (B) at flow rates below the optimum, while, it is decreased at higher flow rates due to the mass transfer factor (C) become significant.

The solute will transport through the column by two mechanisms, convective transport, and diffusive transport. The diffusion of the solute (mass transfer) is restricted to transport through stagnant pools of the liquid in the stationary phase, and by convective transport between the particles in the column. Therefore, van Deemter equation was developed by (Huber) to include fourth term that should be considered to describe column efficiency as shown in equation (1.5)

$$H = A + B/\mu + C_s\,\mu + C_m\,\mu \qquad (1.4)$$

Where (C_s) and (C_m) are the contributions to zone broadening from resistance to mass transfer in the stationary phase and the mobile phase, respectively.

According to van Deemter equation, the efficiency of the column (H) is represented the band broadening, therefore, it should be kept minimum by determination the conditions of the experiments to minimize the zone dispersion, this goal can be achieved by:

1- Reducing eddy diffusion by choosing well packed column, small particle stationary phase, and narrow size distribution of the particle.
2- Decrease the longitudinal diffusion by using high flow rate of mobile phase, the system tubing should be narrow and short, and using correct fitting, ferrules, and nuts.
3- Minimizing the effect of mass transfer, by using stationary phase with small particles, reducing the mobile phase flow rate, and heating the column because at elevated temperature the diffusion process is increased.

1.9 High pressure liquid chromatography (HPLC) technique

Liquid chromatography is a common name that can describe any chromatographic technique which has a liquid mobile phase, samples separation can be happen when optimum set of conditions are applied.[93] However, the analytes in the sample will interact with the two phases in diverse ways; High-performance liquid chromatography (HPLC) is the title that can illustrate the liquid chromatographic technique that uses liquid mobile phase which has been pumped through stationary phase column using mechanical pump.[93] The typical HPLC system contains solvent(s) reservoir, pump(s), injector, stationary phase column, and detector, which can be shown in Figure (1.12).

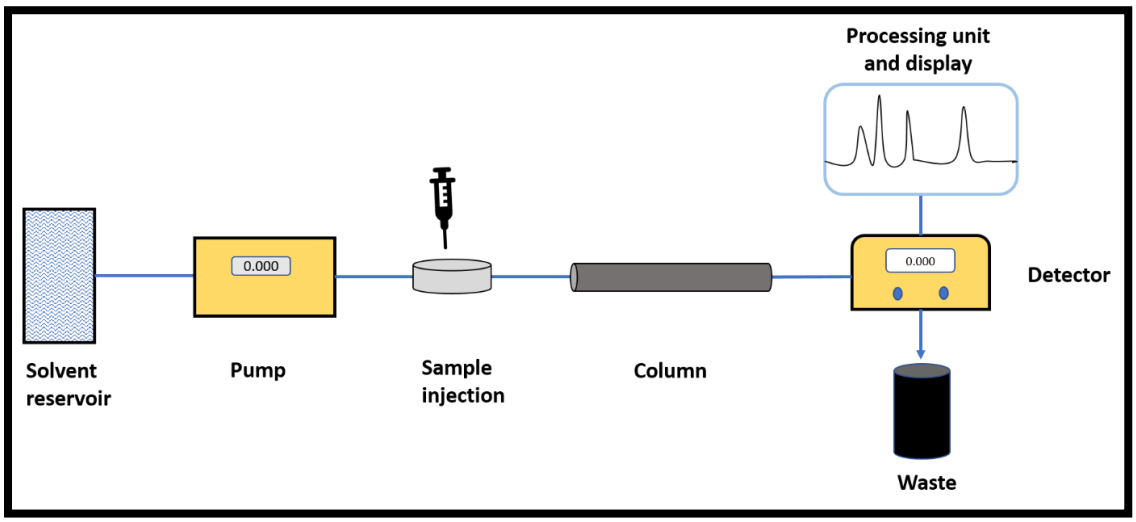

Figure 1.13 The HPLC system diagram.

The stationary phase column for HPLC usually contains packed material such as alkyl silica bonded, when the sample injects inside the injector by the syringe it will travel through the column by pumped mobile phase(s) to reach the detector that can display the retention times of each analyte in the sample, however, the retention time of each analyte is varied depending on the specific chemical and physical interactions between the analyte with the stationary phase, and the analyte with the mobile phase solvent(s).[99] The composition of mobile phase and stationary phase plays a key role in determining the amount of the analyte(s) that is retained inside the column, therefore, the retention time will be varied for specific analyte that elutes from the column toward the detector.[100]

Water and organic solvent are considered the common mobile phase solvents used in HPLC reservoir, however, the most common organic solvents are methanol and acetonitrile.[99, 101] There are some separations has been achieved using the gradient analysis by varying the mobile phase composition during the analysis, gradient analysis technique can separate the target analyte in the sample as affinity function of the analyte toward the mobile phase.[101]

High-pressure liquid chromatography (HPLC) is considered one of the most popular techniques used in biochemistry and analytical chemistry for purification, chemical separations, identification, clinical and pharmaceutical applications, environmental, forensics, food and flavour analysis.[101, 102]

1.10 High-pressure liquid chromatography modes

There are diverse types of chromatographic modes such as normal phase, reversed phase, ion exchange, and size exclusion that can be used in chromatographic analysis, these modes depend on the properties of stationary phase.[112]

1.10.1 Normal phase liquid chromatography (NPLC)

Normal phase liquid chromatography consist of polar stationary phases with cyano group, amino group, or a diol group, and organosilane's alkyl group ($(-CH_2)_3CN$) inside packed columns, while the mobile phase is nonpolar or moderately polar, for instance, hexane for eluting the analytes.[103] All compounds that retained inside the NPLC columns depend on their polarity; therefore, less polar compounds move faster and detected first, while the polar compounds are detected next according to the difference in their polarity.[100]

This mode can perform separation using two different mechanisms, adsorption or partitioning mechanism, the more likely mechanism is adsorption, there are two models which have been used to illustrate the adsorption mechanism.[100] Firstly, the competition model which assume that the stationary phase are covered with mobile phase molecules, therefore, the adsorption will happen due

to the competition between the solute and mobile phase molecules on the adsorption sites.[104] secondly, the solvent interaction model, this model proposed that a bilayer is formed by solvent molecules around the particles of stationary phase, this bilayer depends on the solvent concentration, therefore, the retention will be as a result of the interaction of solute molecules with the second layer of the adsorbed molecules of mobile phase.[105] These models for normal phase mechanisms are shown in Figure (1.13).[92]

The adsorption strengths are increased with increasing the analyte polarity, therefore the interactions between polar analyte and polar stationary phase will increase the elution time, and the analyte moves slowly.[100] However, polarity can sometimes play a secondary role relative to a solute's ability to show a specific interaction with active sites on the stationary phase surface.[106]

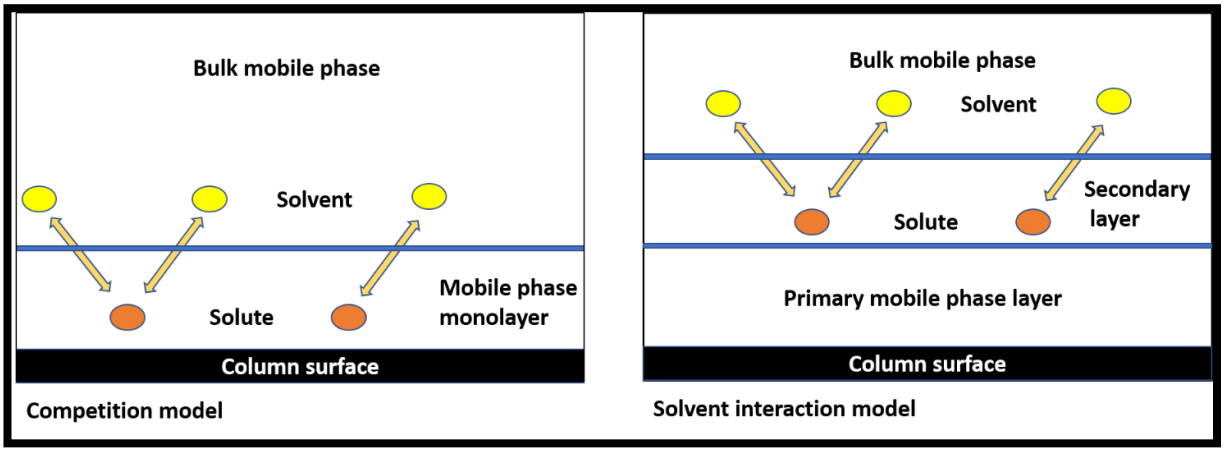

Figure 1.14 The mechanism of normal phase chromatography (competition and solvent interaction model) adopted from reference (111).

1.10.2 Reversed phase liquid chromatography (RPLC)

Reversed phase is considered a popular mode in HPLC techniques, nowadays it is used in more than 65% (may be 90%) of all HPLC separations, due to the versatility, simplicity, and scope to handle compounds of a varied molecular mass and polarity.[107, 108]

Normally, the mobile phases for RPLC are polar solvents such as, acetonitrile, water and methanol, while the stationary phases are nonpolar compounds, such as (C8) n-Octyl or (C18) n-Octadecyl hydrocarbon chains.[101] Reversed-phase chromatography can call also chemically bonded stationary phases, because the functional group in the analyte is bonded to the stationary phase group such as silica, therefore, bonded-phase chromatography is the other name for reversed-phase chromatography in the literature.[109]

The separation mechanism in RPLC depends on two main concepts, the solvophobic and the partitioning concept; the solvophobic concept proposes that the stationary phase behaves more like a solid than a liquid, therefore, the retention of analyte molecules is dependent on hydrophobic interactions between the mobile phase and the analyte molecules.[110, 111] When the analyte molecules are bonded to the stationary phase surface, they will reduce the surface area of analyte exposed to the mobile phase, consequently, when the surface tension of the mobile phase is increased the adsorption will increase, therefore, the analyte molecules are retained due to the solvophobic interactions with the mobile phase rather than with the stationary phase.[112]

The partitioning concept is proposed that the analyte molecules are embedded completely in the stationary phase chains, and do not adsorbed on the surface of

the stationary phase, therefore these molecules are partitioned between the stationary phase and the mobile phase.[113, 114]

The certain type of the retention mechanism is still a matter of debate, the chain length of stationary phase is played a significant role in the retention process, so when bonded material chain length is increased, the mechanism will be approaching from partitioning mechanism, while it will be similar to adsorption mechanism with shorter chain lengths.[115, 116] The solvophobic and partitioning retention mechanisms are shown in Figure (1.14)

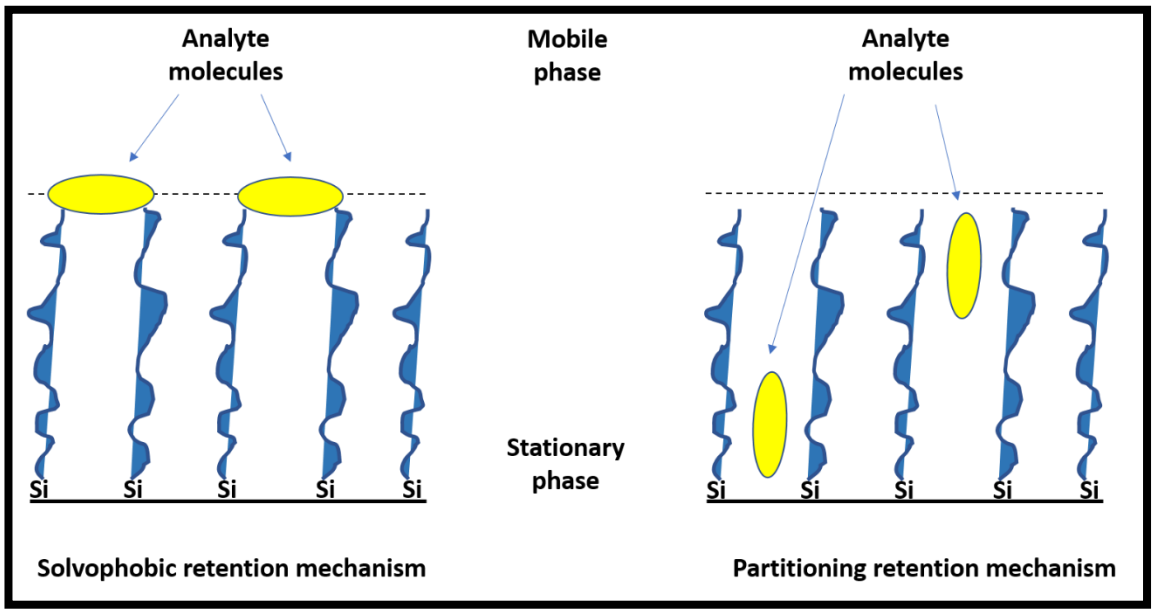

Figure 1.15 The solvophobic and partitioning retention mechanisms was adopted from reference 115.

Reversed phase chromatographic methods are used in many applications in purification and biochemical separation, however, molecules that have some degree of hydrophobic character can be separated by reversed phase chromatography with excellent recovery and resolution.[117]

1.10.3 Ion-Exchange chromatography (IEC)

Ion-exchange chromatography is a significant type of chromatographic technique that can be used to separate and determine different ionic compounds.[118] The separation process is depending on the ionic interactions between the ionic functional groups, which are fixed to the stationary phase with ions present in the solute as shown in Figure (1.15), stationary phase is classified as a cationic exchanger when it carries negative charge, while when it has positive charge it will be anion-exchanger.[119] However, this type of chromatography was used precisely for separation of different charged molecules.[119, 120] Moreover, It was used for proteins purification, peptides, enzymes, amino acids, nucleic acids, antibodies, organic compounds, and simpler carbohydrates.[121-127]

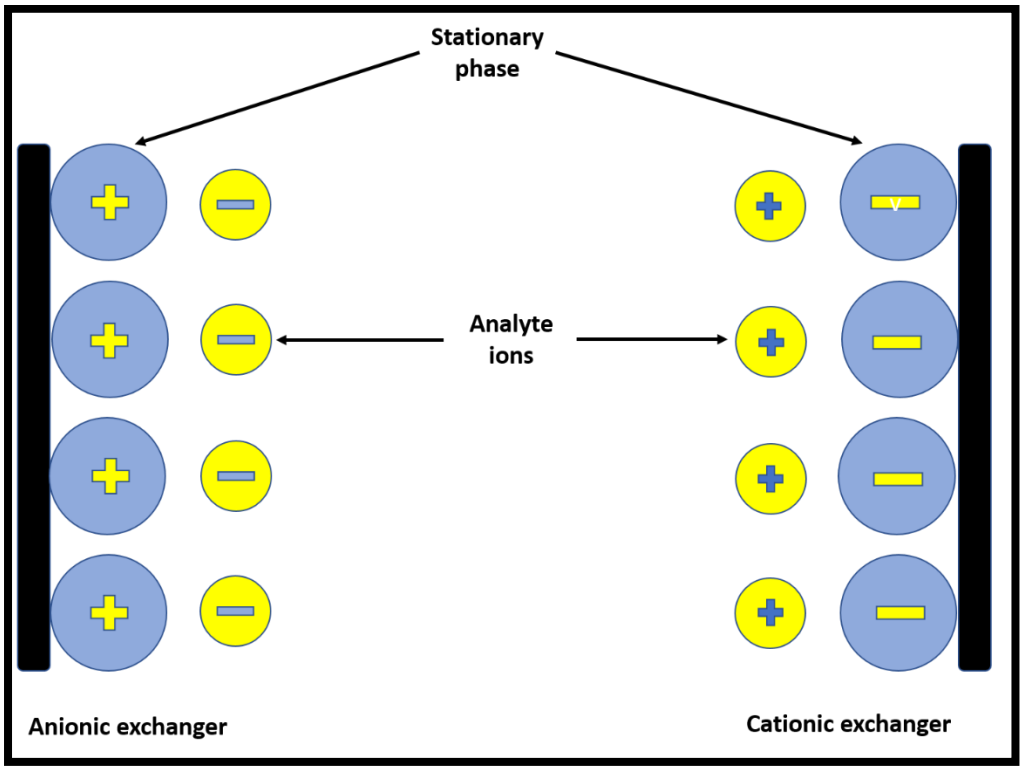

Figure 1.16 Anionic and cationic exchangers.

Stationary phase of ion-exchange chromatography is functionalized silica, synthetic polymeric resins such as methacrylic acid-divinylbenzene or styrene-

divinylbenzene copolymers that treated with some reagents, and some inorganic materials.[128] Functionalized silica is a good stationary phase for ion-exchange chromatography, yet it has a limitation toward pH value above pH (8) and below pH (2) which can lead to instability of the silica when it used as stationary phase, this drawback lead to use synthetic polymers which can be utilized over a much wider pH range (pH 12 or above), yet it is suffering from some degree of swelling.[129]

The mobile phase in ion-exchange chromatography is an aqueous solution of a salt or mixture of salts (could be buffer), with a slight ratio of organic solvent.[115]

As mentioned above the stationary phase has ionizable functional groups which have opposite charge to the analyte charge, while the mobile phase is an aqueous buffer system, therefore, the ion-exchange mechanism is that the analyte ions are distributed in a state of equilibrium between the stationary and mobile phase, this equilibrium can show two possible formats, cation and anion exchange mechanisms depending on counter ions, the separation process happens as a significance differences in the charge density, size, and structure of the diverse ionic solutes.[130]

1.10.4 Size-Exclusion chromatography (SEC)

Size-exclusion chromatography was described firstly by Synge and Tiselius, they mentioned that the principle of this technique is based on the size of the molecules [131]. Separation process depending completely on the molecular weight of the analysed samples, therefore, to separate the big molecules (macromolecules), the difference in the molecular weight between them should be double, while, for the small molecules it is required more than tenfold difference in the molecular weight to get significant resolution.[132]

Size-exclusion chromatography can be divided into two types, gel-permeation chromatography (GPC) and gel-filtration chromatography (GFC), these two kinds are classified based on the packing materials and the mobile phase; to start with GPC, the stationary phase is hydrophobic materials used for polymer characterization such as cross-linked gels or polystyrene divinylbenzene gels, the mobile phase for GPC is an organic solvents.[92]

GFC stationary phases are hydrophilic compounds such as silica gel, polydextrans, and poly vinyl alcohol, while the mobile phase is an aqueous mobile phase or aqueous buffer, in both kinds of SEC modes the mobile phases are chosen for their ability to dissolve the sample not for their selectivity, moreover, the mobile phases viscosity should be low and compatible with the packing material and the detector.[115]

The SEC mechanism based on the ability of the sample molecules to penetrate in to the stationary phase pores, therefore, depending on the pore size of the stationary phase, the small sample molecules penetrate inside these pores, while the big molecules are unable to penetrate deeply inside the pores and travel to the end of the column, and the bigger molecules are moved straight away toward

the end of the column without any retention.[133] The principle of size-exclusion mechanism is shown in Figure (1.16)

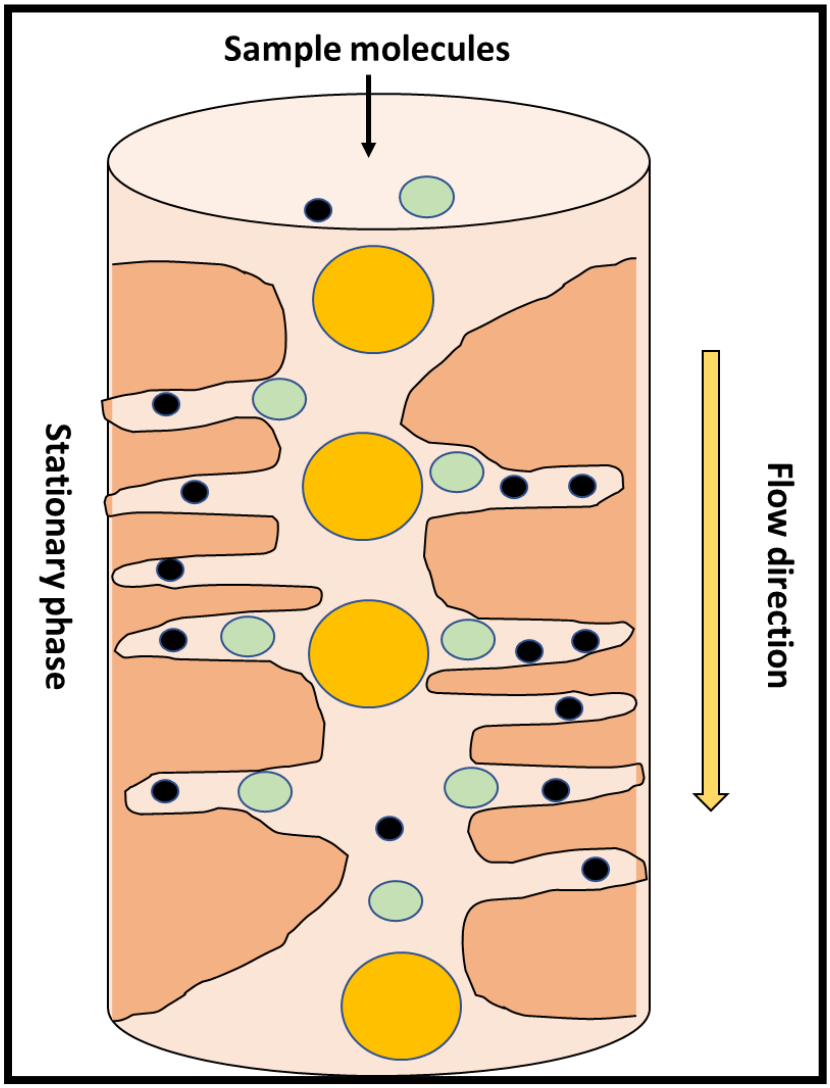

Figure 1.17 The principle of size-exclusion mechanism

1.11 Mixed-mode chromatography

Mixed-mode chromatography is the chromatographic method that involves a combination of different retention mechanisms which can be used to separate samples that have different chromatographic behaviors.[134] The term mixed-mode liquid chromatography first appeared in 1986 by combining ion exchange and reversed phase mixed mode column to separate proteins.[135] Since then, mixed mode chromatography has been used in a variety of analyses by utilizing more than one kind of interaction between analytes and stationary phase to achieve significant and efficient separation.[136] The advantages of mixed mode over the single mode separation media caught attention of the biotechnology and pharmaceutical industries, therefore, it became a popular tool in quality control and downstream processing.[137] Nowadays, many mixed mode columns combining reversed phase, hydrophilic interaction, hydrophobic interaction, and different ion exchange mechanisms are available from commercial sources.[137]

The stationary phases of this chromatographic mode can be designed depending on different procedures such as:

1- A mixture of diverse particles or groups are bonded to various categories of ligands.[138]

2- Supporters with different immobilized ligands.[139, 140]

3- Single ligand was functionalized with diverse chemical functions.[173, 141]

Mixed-mode chromatography has significant advantages compared with single-mode chromatography, these advantages can be summarised as,[136] (i) high selectivity because different samples can be separated such as neutral, negative, and positive substances in single run using reversed-phase/anion–cation

exchange column.[142] (ii) high loading capacity,[143, 144] that can be provided a new perspective to improve of semi-preparative and preparative chromatography.[145, 146] (iii) Avoiding the over consuming and the waste of materials when using mixed-mode column compared with two single-mode columns.[136, 147]

Monolithic materials have been investigated as stationary phases for LC separation as monolithic columns, these columns were used for numerous separation modes such as revers phase,[148-150] hydrophilic interaction,[151] ion exchange.[152] Recently the attention is toward the monolithic columns with mixed mode, for example reversed phase / ion exchange (RP/IE), hydrophilic interaction / ion exchange (HI/IE). Mixed mode of RP/IE monolithic columns have been used in CEC, as well as many research groups have investigated different mixed mode monoliths, such as reversed phase/strong cation exchange, reversed phase /weak anion exchange, reversed phase /strong anion exchange, and reversed phase /zwitterion exchange.[153-163] The ratio of organic to aqueous solvents in the mobile phase has usually played an important role in determining the retention mechanism of the column, therefore, one retention mechanism will be dominate under the conditions used.[138, 164]

Numerous methodologies have been developed to introduce ion exchange functionalities into the polymeric monolith backbone to form mixed-mode monolithic columns for LC separation, such as adsorption,[165-168] post modification, [152, 169] and one step copolymerization.[153] The most direct and easiest way to fabricate these monoliths is the one step copolymerization, although the ion exchange capacity on the surface of macro porous monoliths is lower than that of monoliths prepared using the other two approaches (adsorption and post modification).[149] Nonetheless, due to the incompatible solubility of

nonpolar long alkyl chain functional monomers with relatively polar ion exchange functional monomers, the hydrophobicity of most reported one step copolymerized monoliths was based on short alkyl chain monomers or just cross linker.[170]

Several investigations have been made in mixed mode chromatography as an effective separation technique, for example, Lammerhofer *et al*. prepared normal phase/weak and strong anion exchange mixed mode monolithic columns for CEC to separate basic polar, neutral, and weakly acidic compounds such as, aromatic amines, xanthines, and phenols.[171]

Nogueira *et al*. investigated a reversed phase (RP)/weak anion exchange (WAX) stationary phase for capillary chromatography to separate peptides and detached all major impurities in a single chromatographic step, sample-loading capacity, selectivity, and productivity have improved by approximately 15 times higher than using RP in chromatographic analysis.[144]

Many research groups have used hydrophobic interaction (HI) mode as a complement to a normal phase (NP) mode, they used hydrophobic interaction/ion exchange (IE) stationary phase mixed mode to separate numerous polar compounds for example, phenols, nucleic acid bases, nucleosides, protein.[172-175]

Mant *et al*. stated that hydrophilic interaction chromatography (HILIC)/ cationic exchange (CEX) mixed-mode system has exhibited many advantages over RPLC in peptides separation, such as, stronger separation efficiency, unique selectivity, and a wider range of applications, also they found that highly charged peptides were clearly determined using low acetonitrile (ACN) levels, and the

peptides were eluted using an ionic mechanism.[122, 176, 177]

1.11.1 Glycidyl methacrylate copolymers as mixed-mode monolith column for chromatographic separation

Glycidyl methacrylate or (2,3-Epoxypropyl methacrylate) that is shown in Figure (1.18) is an ester of methacrylic acid and glycidol, it is a common monomer used in the creation of epoxy resins, it has attracted attention due to the ability of pendent epoxide groups to participate in many chemical reactions.[178]

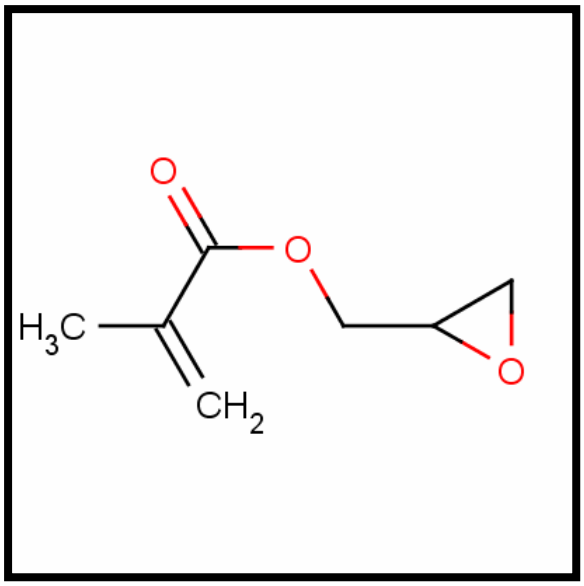

Figure 1.18 Glycidyl methacrylate

The strain in the three-membered ring is considered the main factor in the high reactivity of the epoxide group, therefore, this group provides a good opportunity for chemical modification for numerous applications, for example, glycidyl methacrylate has been utilized for binding enzymes and other biologically active species.[179] It has also been used as a negative electron-beam resist in electronic applications.[180]

The polymerization process of glycidyl methacrylate to form different polymers takes place in solution utilizing a solvent that can dissolve the GMA monomer

and poor solvent for the polymer, the GMA copolymers are prepared using different methods, however, all these methods are based on free radical initiation usually organic peroxides or azo-catalysts as initiators of the polymerization reaction.[181] Researchers have proven that glycidyl methacrylate undergoes radical polymerization entirely on its methacrylic double bond, whereas, the oxirane function does not participate.[182]

After formation of the copolymer the epoxy ring can allow a wide range of chemical conversions and modify the functional sites on the polymer surface by entering many reactions as shown in Figure (1.19).[183]

Significant surface modifications can be achieved by introducing precise ligands essential for bio affinity chromatography, these reactions are shown in Figure (1.20).[183]

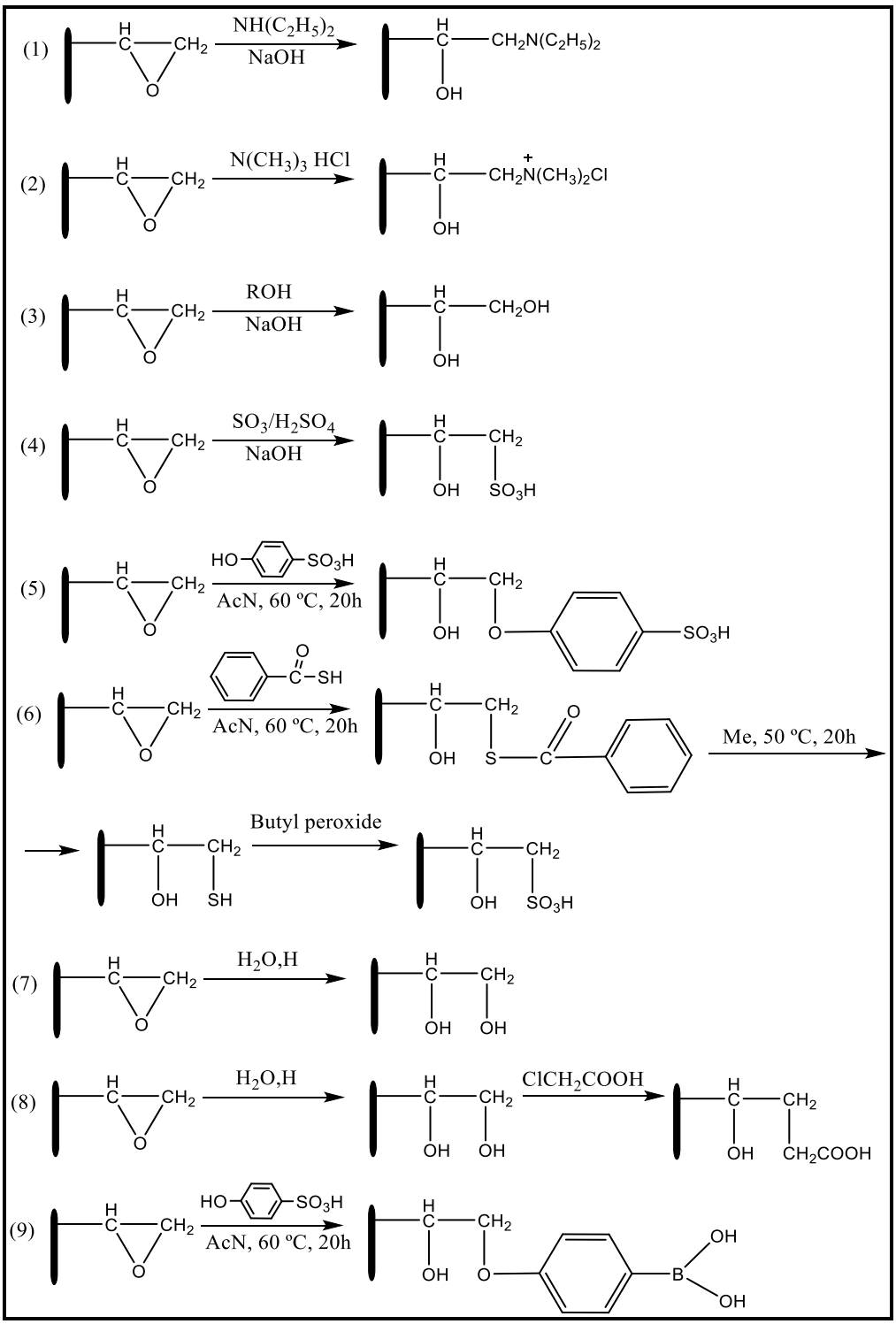

Figure 1.19 Chemical conversion of epoxy groups (1, 2) amination; (3, 4) alkylation; (5, 6). sulfonation; (7) hydrolysis; (8) carboxymethylation; (9) modification with p-hydroxy phenylboronic acid. [183]

.

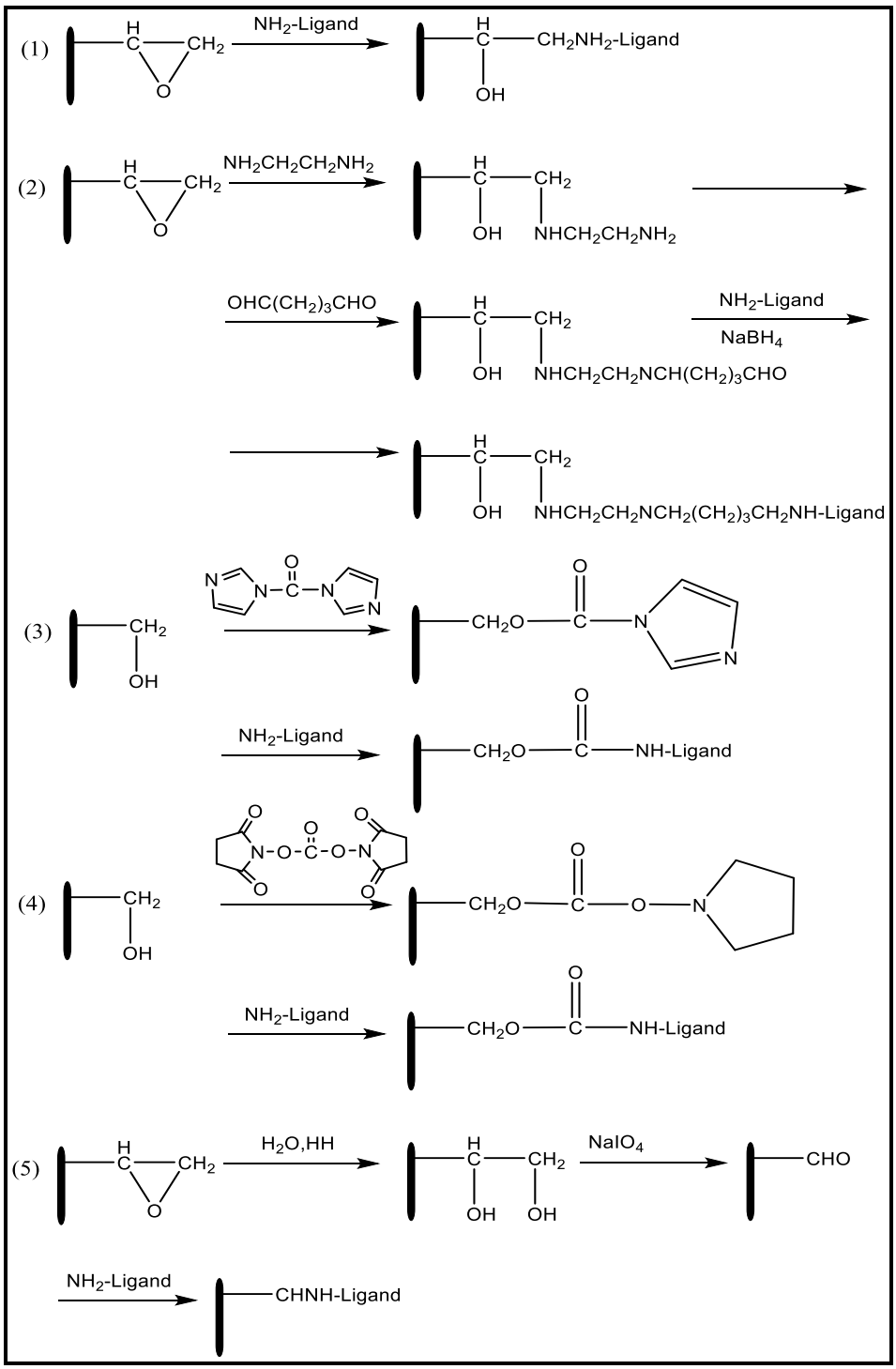

Figure 1.20 Several methods for affinity functionalization (1) Direct immobilization via epoxy groups, Immobilization via intermediate modifications: (2) with diamine and glutaraldehyde; (3) with carbonyl diimidazole; and (4) with disuccinimidyl carbonate. (5) Oxidation of hydroxyl-groups followed by a ligand attachment.[183]

Glycidyl methacrylate is a moderately polar compound because it has an ester bond and a carbonyl group, therefore, it is frequently utilized in revers phase chromatography.[184] The dual properties of GMA as a nonpolar and polar compound, in addition to the easy preparation and post functionalization of GMA copolymers, therefore, it has been used in several methods of chromatographic separation, for example, revers phase,[185] hydrophilic interaction liquid chromatography (HILIC),[186] and ion exchange chromatography[187] to separate peptides and proteins,[188] polymer separation,[189, 190] small polar molecules and alkyl benzenes.[191-193]

The copolymerization of monomers having different functional groups is considered an efficacious method that could be applied to prepare multi-functional polymers, therefore, as described earlier GMA is a functional monomer that can be used in many post polymerisation reactions to prepare polymers with desired functionalityt.[194, 195] Moreover, it was used in industrial applications such as, drug delivery for pharmaceutical compounds, nonlinear optical material, dental mixtures, leather adhesives, and resins for ion exchange chromatography, surface modifiers, and surface coatings.[196-200]

All these properties, reactions and applications of GMA have caught the attention of many researchers to investigate this monomer in copolymerisation reactions to try and form novel stationary phases for LC separation.[201]

Svec and Frechet in 1995, prepared porous poly(glycidyl methacrylate-co-ethylene dimethacrylate) rods using free radical polymerization within the confines of a 300 × 8 mm I.D. chromatographic column. The GMA was modified using diethylamine to produce an ion-exchange chromatographic mode. This

column showed significant dynamic capacity exceeding 300 mg at a flow velocity of 200 $cm.min^{-1}$. A mixture of proteins was separated such as chicken egg albumin, bovine serum albumin, lysozyme, soybean trypsin inhibitor, and conalbumin in single run. The mobile phase used was a gradient analysis (0.01 M Tris-HCl buffer pH 7.6 to 1 M NaCI in the buffer in 10 min) the flow rate was 0.5 $mL.min^{-1}$. The total injected protein was 7.5 mg, and the detection was UV detection at 280 nm.[202]

Camilla et al. prepared porous poly(glycidyl methacrylate-co-ethylene dimethacrylate) monoliths with different porous properties. The free radical polymerization was initiated utilizing cerium(IV), the prepared monolith was then grafted with poly(2-acrylamido-2-methyl-1-propanesulfonic acid) chains. This monolith column was used for proteins separation (myoglobin, chymotrypsinogen, and lysozyme) by ion-exchange chromatography in less than 1.5 min, this column had good efficiency and was not affected by high flow rates due to the presence of large through pores.[203]

Poly(glycidyl methacrylate-co-ethylene dimethacrylate) monolithic columns were also investigated by Jorge Cesar Masini using thermal free radical polymerization at 60 °C for 24h inside a 2.1 mm i.d. activated fused silica-lined stainless steel tubing, the monolithic column has been modified with iminodiacetic acid (in 2M Na_2CO_3, pH10.5) using azobisisobutyronitrile as initiator, this column was used to separate cytochrome C, ribonuclease A, lysozyme, and myoglobin. All proteins were separated using (20 mM KH_2PO_4/K_2HPO_4) pH 7.0 and salt gradient (NaCl), however, myoglobin was not retained.[204]

A strong anion exchange monolithic column of poly(glycidyl methacrylate-co-divinyl benzene) inside the capillary column by *in-situ* polymerization using 1-decanol and tetrahydrofuran as porogens. Epoxy groups were changed to obtain quaternary ammonium functionalities. This column has been shown high pressure stability of material even at high flow rates. The monolithic column was used for separation of nucleotide mono, di, and triphosphates, using a phosphate buffer at pH 8.0. Nine different nucleotide CMP, AMP, ADP, GMP, CDP, UTP, CTP, ATP and GTP can be separated within 6 min. The mobile phase was, (A) 20 mM KH_2PO_4, 20% acetonitrile, pH 8.0, (B) 1 M NaCl in A.[152]

Strong cation-exchange glycidyl methacrylate (GMA) and ethylene dimethacrylate monolithic capillary columns (250 µm i.d) were prepared using free radical polymerization for ion chromatography, the epoxy groups have been sulfonated using (1M) Na_2SO_3. The performance of the monolithic columns were investigated through the separation of a model mixture cations for example, Na^+, NH_4^+, K^+, Mg^{2+}, and Ca^{2+}, employing 10 mmol L^{-1} $CuSO_4$ as eluent and indirect UV detection.[205]

Hydrophilic interaction/cation-exchange and RP/cation-exchange stationary phase for CEC capillary monolithic column was prepared using thermal polymerization of 3-sulfopropyl methacrylate potassium salt (SPMA), glycidyl methacrylate (GMA), and ethylene dimethacrylate (EDMA), 1,4-butanediol and dimethylformamide (DMF) was used as a binary porogenic solvent. The epoxy groups were hydrolysed using hydrochloric acid to form diol groups which can be enhanced the polarity of the stationary phase. It was found that, by varying the

acetonitrile ratio in the mobile phase, the two mixed-mode mechanisms can be achieved in different mobile phase condition. At high acetonitrile content, the hydrophilic interaction/cation-exchange interaction mechanism can be observed, on the other hand, with low acetonitrile content, the reversed-phase/cation-exchange interaction mechanism can be observed. It was noticed that this monolithic column has good efficiency and high selectivity to separate basic compounds and neutral polar analytes, such as narcotic pharmaceuticals, nucleic acid bases, alkaloids, anilines, and phenols.[206]

Atefeh Darvishi *et al*. prepared two types of monolithic column, first one the glycidyl methacrylate- co- stearyl methacrylate and the second one is glycidyl methacrylate- co- ethylene dimethacrylate-co-stearyl methacrylate using thermal free radical copolymerization at 70 °C. The porogenic solvent was toluene, and the initiator was 2,2-azobisisobutyronitrile. The copolymer compositions were determined by ^{1}H NMR spectroscopy. Moreover, the swelling behaviour and the thermal properties of the monolithic columns were investigated using diverse types of nonpolar and polar solvents. It was noticed that the melting temperature (Tm) values are decreased, while the glass transition temperature (Tg) values are increased in cross-linked copolymers compared with none cross-linked polymers. In addition, the cross-linked polymers exhibited swelling behaviour in nonpolar solvents, yet the swelling values were in the acceptable range, therefore, the polymers can be utilised with nonpolar solvents. Furthermore, when the monolithic columns contain high percentage of the GMA, they have been shown lower swelling ratio in nonpolar solvents, while, it was higher in polar solvent.[194]

GMA-co-SPMA-co-EDMA double mixed mode of HI/cation-exchange and RP/ cation-exchange monolithic column was prepared for CEC separation of five alkaloids such as, morphine, narkotine, thebaine, papaverine, and codeine, using binary porogenic solvent consisting of 1, 4-butanediol and dimethylformamide. After that, epoxy groups were changed to diol groups by hydrolyzed reaction using HCl. The ACN content played a major role in column behavior mechanism, main when the ACN ratio in the mobile phase is more than (80% v/v) the HI/cation exchange mode was observed, and it was (HILIC) useful mode to separate pharmaceutical compounds.[207]

The monolithic column octadecyl methacrylate-co-3-sulfopropyl methacrylate-co-ethylene dimethacrylate was prepared for capillary CEC analysis, using 1,4-butanediol and cyclohexanol porogenic solvent. The sulfonate groups are used to provide electroosmotic flow (EOF) that essential to transport the mobile phase through the monolithic capillary, and to show hydrophilic interaction, while the octadecyl hydrocarbon chains are provided nonpolar sites to separate neutral molecules. It was found that, the percentage of SPMA and the composition of porogenic solvent are key factors that could affect the optimum EOF velocity, therefore, at 0.6% SPMA highest efficiency and significant chromatographic retention are obtained, this column was used to separate adenosine, uridine, guanine, guanosine, and adenine in single chromatographic run.[208]

A butyl methacrylate-co-2-acrylamide-2-methyl-1-propansulphonic acid-co-ethylene glycol dimethacrylate monolithic column was prepared using photo polymerisation, the polymerisation solution involved azobisisobutyronitrile as initiator and the porogenic solvent was a mixture of 1-propanol, 1,4-butanediol and water, the monolith was formed after 16 h inside a UV transparent capillary tube with a length of 35 cm for CEC separation. This column provided a plate number over 210000 plates.m^{-1} with desired pore properties. However, this column was used to separate thiourea and eight aromatic compounds (benzene, benzyl alcohol, toluene benzaldehyde, ethylbenzene, propyl benzene, amyl benzene, and butylbenzene), in addition it was also used to separate four different peptides in a single run.[209]

Lazara *et al.* prepared glycidyl methacrylate-co-methyl methacrylate-co-ethylene glycol dimethacrylate monolithic separation medium using a photo polymerisation reaction initiated by 2,2-dimethoxy-2-phenyl-acetophenone, and the porogenic solvent was a mixture of 1-propanol/formamide. The monolith was fabricated inside the microchip device and used for CEC separation coupled with mass spectrometric detection to separate peptides and digested proteins. After formation of the monolithic polymer, the epoxy groups of GMA were reacted with N-ethylbutylamine to offer the positive charge on the monolith surface to minimize electrostatic interactions between the positively charged peptides and the surface of the monolith. The microchip was tested by separating a tryptic digest bovine haemoglobin. It was found that by utilising mass spectrometric detection, sequence coverage of 70–80% was achieved.[210]

Lauryl methacrylate-co-ethylene dimethacrylate monolithic column was prepared inside capillary tubing of 75 µm i.d using cyclohexanol and ethylene glycol as porogenic solvents and the initiator was azobisisobutyronitrile, the polymerisation reaction was carried out under UV light for 2 hr. The C12 monolithic capillary column was investigated for the separation of commercial digested cytochrome c containing 12 hydrophobic peptidic fragments using nano LC–MS. The results showed that this column was able to separate/or desalt these peptides, the column performance was similar to the standard commercial columns used for proteomic analysis. The separation efficiency was up to 145×10^3 ($plates.m^{-1}$). [211] The comparison of this study with other works are shown in Tables (1.1) and (1.2)

Table 1.1 Summary of data obtained from this research

Type of the column	**Dimensions of the column**	**Technique**	**Samples**
HILIC/RP GMA-co-SMA-co-EDMA	Borosilicate tube 50 mm x 1.5 mm i.d	HPLC	Hydrophobic compounds, Pharmaceutical compounds, Hydrophilic and hydrophobic
SCX/RP GMA-co-SMA-co-EDMA	Borosilicate tube 50 mm x 1.5 mm i.d	HPLC	Hydrophobic compounds, Pharmaceutical compounds, Hydrophilic and hydrophobic mixture, peptides, proteins
SCX/RP GMA-co-SMA-co-EDMA	Glass microchip device, 30 mm x 0.5 mm channel	HPLC	Hydrophobic compounds pharmaceutical compounds

Table 1.2 Summary of the data from previously reported research.

Type of the column	Dimensions of the column	Technique	Samples
Ion-exchange GMA-co-EDMA, the GMA was modified using diethylamine.[202]	Stainless-steel tube of a 300 x 8 mm I.D.	HPLC	Proteins
Ion-exchange GMA-co-EDMA, GMA was grafted with poly(2-acrylamido-2-methyl-1-propanesulfonic acid.[203]	50 mm × 8 mm i.d. fused silica-capillary	HPLC	Proteins
GMA-co-EDMA, GMA was modified with iminodiacetic acid.[204]	2.1 mm i.d. fused silica-lined stainless steel tubing,	Sequential injection chromatography	Proteins,
HI /SCX and RP/SCX GMA-co-3SPMA-co-EDMA.[206]	100 mm id fused-silica capillary.	CEC	Narcotic pharmaceuticals, nucleic acid bases, alkaloids, anilines, and phenols.

Mixed mode of HI/cation-exchange and RP/ cation-exchange GMA-co-SPMA-co-EDMA.[207]	30 cm x 100 µm id	CEC	Alkaloids compounds
GMA-co-ODA and GMA-co-ODA-co-EDMA.[194]	Test tube		Characterization of the monolith only
GMA-co-MMA-co-EDMA, GMA was modiied with N-ethylbutylamine.[210]	Microchip device	CEC	Separating a tryptic digest bovine haemoglobin
GMA-co-TPGDA-co-EDMA.[212]	30 mm x 4.6 mm i.d stainless-steel.	HPLC	Benzene derivatives
silica-particles-supported SCX GMA-co-PETA, GMA was sulfonated with Na_2SO_3.[213]	6.5 cm capillary tube within 150µm id.	(µ-LC)	Monovalent inorganic cations, and nucleotides.
GMA-co-TMPTMA.[214]	quartz tubes		Characterization only

RP, HI, and CX GMA-co-4VPBA-co- EDMA.[215]	25 cm 100 µm i.d. fused-silica capillary	Nano LC separation	Alkaloids, and proteins
GMA-co-SPMA-co-EDMA.[216]	30 cm 100 µm i.d. capillary	Pressurized CEC	Narcotine, papaverine, thebaine, codeine, and morphine.
WAX GMA-co-EDMA, GMA was modified with diethyl amine.[217]	100-mm silicosteel tubing 1.02 mm i.d. and 1/16 o.d.	HPLC	Ligodeoxythymidilic and DNA
Mixed-mode GMA-co-EDMA, GMA was functionalized with thiols and coated with gold nanoparticles.[218]	12 cm · 100 µm capillary column	HPLC	Proteins
WAX GMA-co-EDMA, GMA was functionalized using trimethylamine.[219]	Teflon-coated fused-silica capillaries, 7.5 cm 100 mm id	CE	Five inorganic anions
SCX GMA-co-EDMA, GMA was modified using Na_2SO_3 solution.[205]	15-cm 250- µm -i.d. fused-silica capillary	Capillary LC	Separation of a model mixture of Na^+, NH_4^+, K^+, Mg^{2+}, and Ca^{2+}

WAX GMA-co- EDMA, GMA was modified with polyethyleneimine.[220]	100 mm × 4.6 mm I.D. stainless steel tube	HPLC	Proteins
WCX GMA-co-EDMA, GMA was modified with ethylene diamine followed by chloroacetic acid.[221]	Stainless-steel tube of 50 x 7.9 mm ID.	HPLC	Proteins
SAX GMA-co-DVB, GMA was modified with diethylamine followed by alkylation with diethyl sulfate.[152]	Capillary tube 65 x 0.2 mm id	µLC	Nucleotides and oligonucleotides
GMA-co-EDMA modified with diethyl amino hydroxypropyl.[11]	30 mm X 8mm i.d.	HPLC	Model protein mixture (ovalbumin, cytochrome C, and lysozyme)

It can be seen from the Tables (1.1) and (1.2) that, a single mixed mode monolithic column HILIC/RP or SCX/RP GMA-co-SMA-co-EDMA can be used to separate different samples such as hydrophobic, hydrophilic, pharmaceutical compounds, in addition to peptides and proteins using HPLC. Other studies showed generally single mode use of monolithic columns or mixed mode use but for a narrower range of samples than used in this study.

1.12 Microchip device

Microchip devices or lab on a chip can be defined as a network of micro channels that have been milled or etched into solid materials using different techniques such as wet etching and photolithography which are considered the most common methods that used to prepare the microfluidic device.[222] The microchip materials have been chosen depending on compatibility of the analyte, in addition to the cost and the availability, however, it could be plastic, glass, ceramic, polymeric materials, or silicon.[223] Silicon and glass are common materials that used for lab on a chip device because they are more popular and easy to fabricate using the traditional methods.[224] In addition, these materials have advantages such as high thermal conductivity for the silicon that can be used in fast temperature ramping, while the glass materials can be used for detection due to the optical transparency.[225, 226]

There are many advantages of microchip devices such as reducing the volumes of expensive analytes or the solvents volume that could be not available in substantial amounts. Moreover, reducing the reaction time due to the small size of the reactors, and enhancing the performance of the analytical device by increasing the reproducibility, and the selectivity.[227] Furthermore, the interactions

between the analytes and the reactants are higher than the interactions in the conventional analytical methods. The reason behind that is the increasing of the ratio between the inner surface area of the channel to the volume occupied by the solution. So far, the reaction will be more efficient compared with other analytical techniques.[228]

As mentioned above the microchip devices have channels, the size of these channels could be millimeters or micrometers, therefore, a small volume of the sample can be used such as microliters, nanoliters, picoliters, and femtoliters[229]. Samples and solvents could be pumped through these channels using hydrodynamic pump that can be used with any types of the solvents and samples, the other pump is electro kinetic pumps or electroosmotic flow (EOF) which can be used with ionic or polar chemicals only without using external pump.[222, 230] The difference between the hydrodynamic pump and electroosmotic flow is the flow profile in electroosmotic flow is flat while in hydrodynamic pump is parabolic, the flat flow profile has advantage over the parabolic flow profile due to reducing the dispersion and improving the resolution by making the signal sharp and high.[223]

Monolithic materials have been investigated by *in-situ* polymerization inside the micro fluidic devices for CEC, LC, solid phase extraction, enzyme reactors, proteomic.[231]

1.13 Additional separation technique

These include electrophoretic separations which, although not part of the current research, they have been included for completeness.

1.13.1 Capillary electrophoresis (CE)

Capillary electrophoresis (CE) is a technique that used electrical field to separate different samples in a mixture when the sample molecules have positive or negative electrical charges, when these ions are moved in a freedom movement they will try to find regions that have opposite charge, for example electrodes. Therefore, cations move toward the cathode and anions will move toward the anode. [232, 233]

The movement of these ions are affected by two factors, the first factor is the ion electrophoretic mobility which is summation of the mobility of the electroosmotic flow and the electrophoretic mobility of the analyte, the electrophoretic mobility depends on the dielectric constant and the viscosity of the electrolyte, in addition to the charge density of the solute, moreover, it is based strongly on the temperature, therefore when the temperature is increased by 1 Kelvin the mobility will increase by 2%.[234]

The second factor is the direction and the speed of the electroosmotic flow (EOF), EOF is the movement of the liquid that in interaction with a solid surface when a tangential electric field is applied, EOF occurs in any electrophoretic system and is significant factor in CE due to very high ratio between the surface area and the volume inside a capillary.[235]

The EOF may be persuaded to move in the same direction as the analyte ions to increase the speed of the analyte to reach the detector, or in the opposite

direction from the analyte ions, to improve resolution, the EOF is affected by different parameters such as, (i) the pH of the solution, it is increased when the pH is increasing, (ii) applied voltage, it is increased when high voltage is used, (iii) the ionic strength, it decreases with increasing of ionic strength.[236, 237]

As described before CE can be used to separate charged molecules such as proteins, peptides, DNA, and inorganic ions using a low volume of these samples with short analysis time, yet this technique has limitations, the main limitation of CE is that neutral molecules will not be affected by the electrical field, however, these molecules are unseparated from other natural species and eluted when the EOF is applied; to tackle this problem, the surfactant micelles should be added to the buffer solution to interact with the sample molecules chromatographically and allowing the neutral molecules to be determined[238], Figure (1.20) shows the CE diagram.[239]

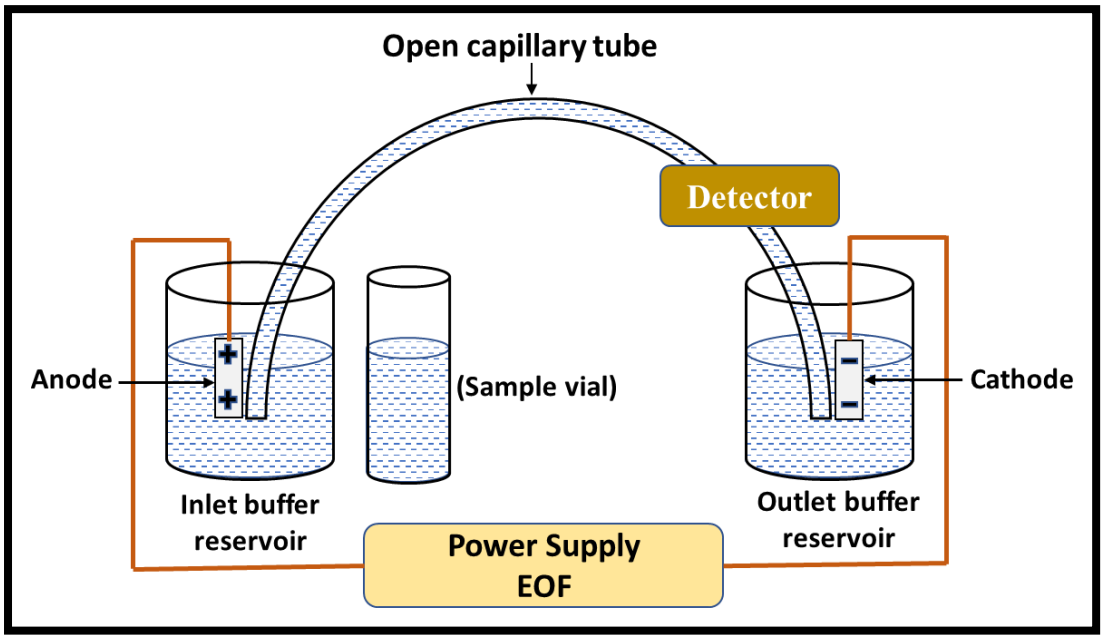

Figure 1.21 Capillary electrophoresis (CE) diagram (adopted from reference 148).

1.13.2 Capillary electrochromatography (CEC)

Capillary electrochromatography (CEC) is a miniaturized and hybrid separation technique that can be used to separate and identify a wide spectrum of compounds. This technique combines two principles, the chromatographic principle in which the sample is distributed between two phases like (HPLC), and electro migration principle that is using electroosmotic and electrophoretic aspect (CE), the analytes may be separated according to differences in partitioning ratio between the stationary and the mobile phase, and/or to differences in electrophoretic mobility, the separation process in CEC can be achieved by applying an electric field through the packed capillary column.[238, 240]

CEC differs from HPLC in the flow of mobile phase, because in HPLC this is typically provided by a high-pressure mechanical pump, while in CEC, the mobile phase is driven by an electric field to give flow (EOF) which passes through the stationary phase.[241] The stationary phase of capillary electrochromatography is unmodified silica gel or coated silica gel, this stationary phase of CEC can be packed into a capillary which is called a packed column, or attached to the capillary wall as open tube, or can be added to the mobile phase as pseudo stationary phase.[241, 242]

The advantages of CEC are: [160,243]

1- It can be used to separate neutral and ionic samples without adding surfactant micelles.
2- Economic technique because it uses a low volume of the solvent and sample consumption (nanoliters).
3- Short analysis times.

4- It also offers much greater separation efficiencies than HPLC because it uses plug-like flow principle, while HPLC technique uses a parabolic flow which can lead to band broadening when the plate number is low.

5- The water-insoluble compounds can be separated easily compared with CE.

The limitations of CEC are: [244, 245]

1- Bubble formation inside the column, which can lead to breakdown of the current and the electroosmotic flow.

2- The drying of the packed capillary due to resistive heating.

3- Low column capacity which could reduce the separation efficiency.

The CEC diagram is shown in Figure (1.21).[239]

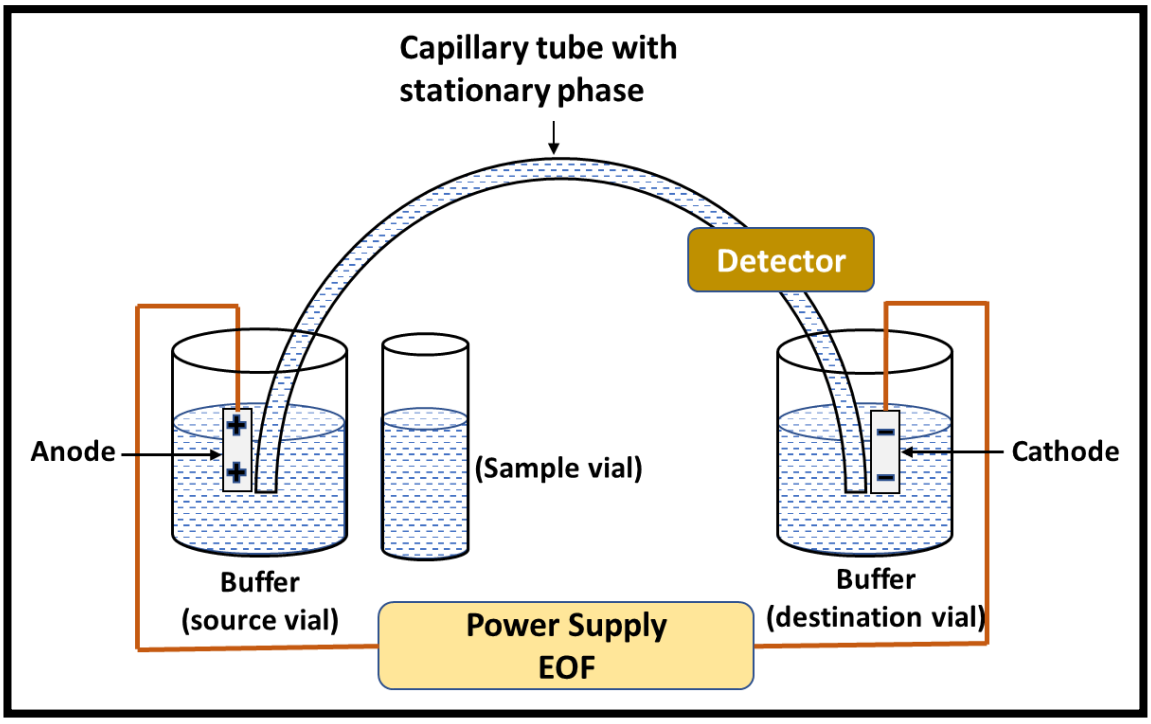

Figure 1.22 Capillary electrochromatography (CEC) diagram (adopted from reference 148).

1.14 Aim of this study

This study aims to prepare and investigate new monolithic columns depending on glycidyl methacrylate as the major component combined with other monomers that have different properties to be used for liquid chromatography. The monoliths produced should allow mixed mode separation and possibly extend the range of molecules separated in a single analysis.

Glycidyl methacrylate monomer has been chosen to prepare the copolymers due to the significant ability of pendent epoxide groups to participate in many chemical reactions and modifications for numerous applications. Therefore, these properties have been used to prepare and investigate mixed-mode monolithic columns that may be used to extend and identify the range of compounds with different properties.

Objectives:

1- Investigation of the parameters that effect of the morphology (the pore size and the surface area) of the prepared monolith, including the irradiation time, monomer ratios, and porogenic solvents.

2- Characterization of the monoliths using different techniques, such as FT-IR, ^{1}HNMR, SEM, BET, CHN, EDX.

3- Investigation of the produced monoliths as a mixed mode separation media including RP, IE, and HILIC to separate samples that have different properties using HPLC technique.

4- Preparation of the monolith inside the microchip device by *in-situ* polymerisation and use it for LC separation

2 Experimental

All chemicals were purchased from (Sigma-Aldrich, Poole, UK) unless listed without further purification, besides deionized water (milli-q water) was used in all experiments.

2.1 Fabrication of the monolithic materials

The monolith was fabricated inside a (60 mm borosilicate tube with an inner diameter of (1.5 mm), and an outer diameter of (3.0 mm) (Smith Scientific, Kent, UK). A reducing stainless steel union 1/8" to 1/16" adapter (Kinesis, Cambs, UK) was used to connect the borosilicate tube with the polyetheretherketone (PEEK) tubing (Thames Restek Ltd., Saunderton, UK), microtight adapter (Kinesis, Cambs, UK) was used to connect the PEEK tubing to the glass syringe (SGE, Kinesis, Cambs, UK). All solutions were injected using a syringe pump (Bioanalytical System Inc., West Lafayette, USA) inside the borosilicate tube for polymerization process. Figure 2.1 shows a photograph of the experimental setup for fabrication of the polymer-based monolith.

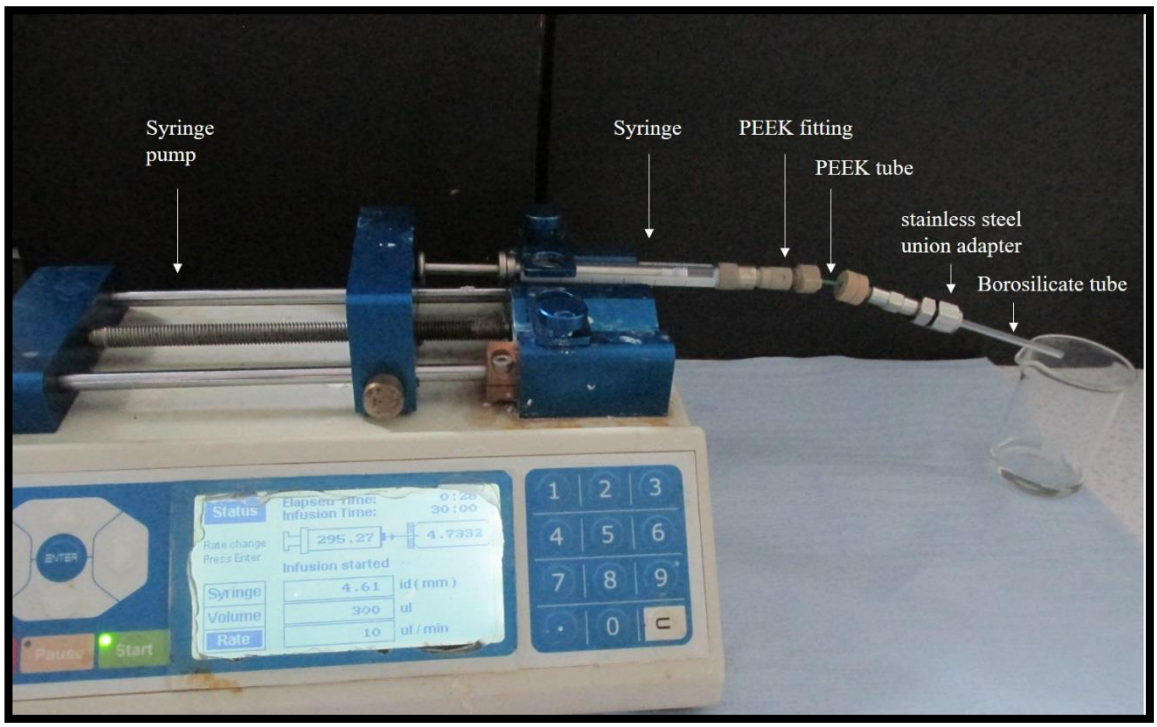

Figure 2.1 Photograph of the experimental setup for fabrication of the polymer-based monolith.

2.1.1 Silanization Step[246]

The borosilicate tube was first silanized to anchor the monolith to the inner wall of the tube. This step can be achieved by washing the tube with acetone (Fisher Scientific, Lough, UK) followed by water, then activation of the inner surface of the borosilicate tube by pumping the sodium hydroxide (Fisher Scientific, Lough, UK) solution 0.2 M at 5.0 µL.min^{-1} using syringe pump for 1 hour. After that it was washed with water, followed by hydrochloric acid solution (Fisher Scientific, Lough, UK) 0.2 M at 5.0 µL.min^{-1} for 1 hour, the next step is to flush with water, then ethanol (Fisher Scientific, Loughbrouh, UK) and it was finally silanized with a solution of 3-(trimethoxysilyl) propylmethacrylate (γ-MAPS) 20 % in ethanol (pH = 5.0 adjusted with acetic acid (Fisher Scientific, Loughbrouh, UK) at 5.0 µL.min^{-1} for 1 hour. The borosilicate tube was finally dried using nitrogen gas and

left overnight. After that the borosilicate tube was ready for polymerization reaction to form the monolith.

2.1.2 In-situ polymerization of the monolith[205]

The free radical photo initiation polymerization was used to prepare the monolith inside the borosilicate tube at room temperature. Basically, the Ueki *et al*. method was applied with some modifications to prepare the polymerization mixture, however, 2, 2-dimethoxy-2-phenyl acetophenone 99 % (DMPA) was used as the initiator instead of 2, 2-azoisobutyronitrile (AIBN). Monovinyl monomers (0.9 mL) which are glycidyl methacrylate (GMA) with other monomers and ethylene glycol dimethacrylate 98 % (EDMA) (0.3 mL) cross-linker.

The monomers and cross-linker were dissolved into a binary porogenic solvent, propan-1-ol (1.05 mL) (Fisher Scientific, Loughbrouh, UK), butane- 1.4-diol (0.6 mL) (Alfa Aesar, UK), the initiator (1 wt %) corresponding to the amount of total monomers weight was added to the monomer solution, the mixture was sonicated using ultrawave sonicator (Cardiff, UK) for 10 min to dissolve the initiator, then purging with nitrogen for 5 min to remove the oxygen.

The borosilicate tube (1.5 mm i.d) and (3 mm o.d.) was filled with the polymerization mixture to a length of (6 cm) by syringe and closed from both sides by blocked rubber, after that it was placed under the UV light lamp (Cambridge UK) (the distance between the lamp and the borosilicate tube was 5 cm) and exposing to the UV light using UV lamp at 365 nm for anticipated irradiation time. Then flushed with ethanol and water to remove any remaining starting materials. After that the two edges of the borosilicate tube were covered by blocked rubber were cut using glass cutter to produce monolithic column inside the borosilicate

tube with 5 cm length. The monolithic columns were connected to the HPLC Varian Prostar system (Perkin Elmer U.S Instrument Division Norwalk, CT 06859 California USA), that consisted of UV detector Varian Prostar module 340, oven Varian Prostar module 520, and solvent delivery Varian Prostar module 210 for LC separation.

2.2 Mixed mode monolithic columns

The mixed mode monolithic columns were prepared according to the methods illustrated in sections 2.1.1 and 2.1.2. A range of diverse types and ratio of the monomers have been investigated, while the (v/v) ratio between the monomers to cross-linker was constant (3:1). The types of monomers that were used to prepare mixed mode monolithic columns are shown in Table (2.1)

Table 2.1 Monomers that used to form mixed mode monolithic columns

No.	**Monomers ratio (v/v)**	**Monomer (1) mL**	**Monomer (2) mL**	**Cross-linker mL**
1	90:10	GMA (0.81)	Sty (0.09)	EDMA (0.30)
2	50:50	GMA (0.45)	Sty (0.45)	EDMA (0.30)
3	10:90	GMA (0.09)	Sty (0.81)	EDMA (0.30)
4	90:10	GMA (0.81)	LMA (0.09)	EDMA (0.30)
5	50:50	GMA (0.45)	LMA (0.45)	EDMA (0.30)
6	10:90	GMA (0.09)	LMA (0.81)	EDMA (0.30)
7	90:10	GMA (0.81)	SMA (0.09)	EDMA (0.30)
8	50:50	GMA (0.45)	SMA (0.45)	EDMA (0.30)
9	10:90	GMA (0.09)	SMA (0.81)	EDMA (0.30)
10	90:10	GMA (0.81)	BMA (0.09)	EDMA (0.30)
11	50:50	GMA (0.45)	BMA (0.45)	EDMA (0.30)
12	10:90	GMA (0.09)	BMA (0.81)	EDMA (0.30)
13	90:10	GMA (0.81)	2DEAMA (0.09)	EDMA (0.30)
14	50:50	GMA (0.45)	2DEAMA (0.45)	EDMA (0.30)
15	10:90	GMA (0.09)	2DEAMA (0.81)	EDMA (0.30)

2.3 Investigation of irradiation time

The irradiation time was investigated for all the mixed mode monolithic column that given in Table (2.1) to obtain the effective irradiation time that can be formed the monolith properly inside the borosilicate tube. It varied between columns depending on the type of the co-monomer, therefore the irradiation time was in the range 1-7 hours. The morphological properties for all the columns were tested using scanning electron microscope (SEM) images (Zeiss EVO 60 USA) and Brunauer-Emmett-Teller (BET) model (Surface Area and Porosity Analyser, Micromeritics Ltd., DunsTable, UK)

2.4 Glycidyl methacrylate-co-lauryl methacrylate-co-ethylene glycol dimethacrylate- monolithic column (GMA-co-LMA-co-EDMA)

Glycidyl methacrylate-co-lauryl methacrylate-co-ethylene glycol dimethacrylate monolithic columns were prepared using the methods described in 2.1.1 and 2.1.2 using the effective irradiation time. The monolithic columns have been tested by SEM and BET to determine the morphological properties of the monolith, also the permeability of the monolith has been determined. After that the monolith were connected to the LC system to try separate different samples.

2.4.1 Application of glycidyl methacrylate-co-lauryl methacrylate-co-ethylene glycol dimethacrylate-monolithic column (GMA-co-LMA-co-EDMA)

GMA-co-LMA-co-EDMA monolithic columns were tested with a diverse types of compounds with different range of the molecular weight, such as hydrophilic, hydrophobic, peptides, and proteins. All these samples were prepared by preparing a stock solution of each compound, then prepared the desire concentration from the stock solution. After that, these compounds were tested individually to determine the retention time for each one, then they have been tested as a mixture.

2.5 Glycidyl methacrylate-co-stearyl methacrylate-co-ethylene glycol dimethacrylate- monolithic column (GMA-co-SMA-co-EDMA)

Glycidyl methacrylate-co-lauryl methacrylate monolithic column has been investigated for LC separation using the methods that illustrate in 2.1.1 and 2.1.2 and effective irradiation time. The permeability and the morphological properties of the monolith columns have tested by SEM and BET. Next, the monolith has been connected to the LC system to try separate different samples.

2.5.1 Investigation of the ratio between GMA:SMA

The ratio between GMA:SMA as a co monomers was investigated to prepare significant monolithic column that could be used in LC separation to separate different samples with high separation efficiency by using the methods that described in 2.1.1 and 2.1.2 and Table (2.1), the ratio is shown in Table (2.2)

Table 2.2 The ratio between GMA:SMA

	GMA %	SMA%
1	90	10
2	50	50
3	40	60
4	30	70
5	20	80
6	10	90

2.5.2 Investigation of the irradiation time

The irradiation time was investigated for each ratio between the GMA:SMA that illustrate in Table (2.2) to prepare monolithic column that has high surface area and reasonable pore size. After preparing the desire monolith column, different techniques were used to characterize the monolith properties and used for LC separation.

2.5.3 Investigation of porogenic solvents

The porogenic solvent can play important role in the monolith formation, therefore, the composition of the porogenic solvent by using 1-propanol besides other solvent that listed in Table (2.3) was investigated to form the monolith using the procedure that described in 2.1.1 and 2.1.2 using different solvents alongside with 1-propanol, the surface area and pore size were investigated for all the columns. The types of the solvents are shown in Table (2.3)

Table 2.3 The types of porogenic solvents

	Porogenic solvents	
1	1-propanol	1,4-butan-diol
2	1-propanol	Water
3	1-propanol	Methanol
4	1-propanol	Ethanol
5	1-propanol	Hexanol
6	1-propanol	1-dodecanol
7	1-propanol	Acetonitrile
8	1-propanol	Chloroform

2.5.4 Investigation of 1-propanol to methanol ratio as a porogenic solvent

The monolith was formed using previous methods that described in 2.1.1 and 2.1.2, the ratio between 1-propanol to methanol was 63% to 37% from the total porogenic solvent. However, it was investigated to get desire surface area and pore size for the monolith, the ratio was illustrated in Table (2.4)

Table 2.4 The ratio between 1-propanol/methanol

	1-propanol %	**Methanol %**
1	70	30
2	65	35
3	60	40
4	55	45
5	50	50
6	45	55
7	40	60
8	35	65
9	30	70

2.6 Ring opening reaction of glycidyl methacrylate-co-stearyl methacrylate-co-ethylene dimethacrylate monolithic column

The epoxy ring in glycidyl methacrylate monomer was opened using two reactions, firstly, hydrolysis the epoxy ring and forming diol group that can be used in hydrophilic/hydrophobic interactions. Secondly, sulfonation of the epoxy ring to form cationic/hydrophobic interactions using sodium sulfate.

2.6.1 Hydrolysis of epoxy ring[206]

After formation of glycidyl methacrylate-co-ethylene dimethacrylate-co-stearyl methacrylate monolithic column as described in 2.1.1 and 2.1.2, the epoxy ring was hydrolyzed to form diol group by pumping 1 M hydrochloric acid at 5 µL min^{-1} for 3 hours. Then, the monolithic column was closed from each side by rubber and kept in column block heater at 60 ºC for 6 hours (Perkin Elmer U.S Instrument Division Norwalk, CT 06859 California USA), to allow the epoxy groups to change to diol groups. After that, the column was washed with water until the pH of the outlet solution was 7.

2.6.2 Sulfonation of epoxy ring[247]

The epoxy group was sulfonated by pumping a sulfonation solution using syringe pump that contained tetra-n-butylammonium bisulfate (1.356 g; 0.4 mol L^{-1}.) (TBABS) as cationic surfactant and 2.52 g (1 mol L^{-1}.) of sodium sulphite anhydrous was dissolved in 10 mL of distilled water for 6 hours at 5 µL min^{-1} in

column block heater at 80 ºC. Then the monolith was washed with 10 mM nitric acid at 5 µL min^{-1} for 1 hour, finally washed with water for 6 hours.

2.7 Applications of glycidyl methacrylate-co-stearyl methacrylate-co-ethylene dimethacrylate- monolithic column

After opening the glycidyl methacrylate epoxy ring as described in 2.6 the monolithic column performance was investigated to separate diverse range of samples such as, hydrophobic, hydrophilic, peptides, and proteins. Samples were prepared by preparing a stock solution of each compound, then prepared the desire concentration from the stock solution. All the samples have been tested individually to determine the exact retention time for each analyte, then a mixture of analytes have been tested.

2.8 Design and fabrication of microchip device for LC separation

A glass microchip was made from B-270 crown glass (SKAN), it consisted of two layers each one has 3 mm thickness, while the dimensions of the chip were 50 mm length and 15 mm width.

The top layer consists two holes (1.5 mm diameter) which was created using traditional glass drilling techniques for inlet and outlet of the mobile phase. The second layer consisted of the milled channel that was created using Datron M7 CNC-machine (Datron Dynamics, Inc. Milton Keynes UK), the dimensions of the channel were 30 mm length, 1 mm width, and 500 µm depth, the two layers were thermally bonded at 585 °C for 3 hours in a custom-made oven, the chip design is illustrated in Figure (2.2).

When the chip was ready to use, the monolith was fabricated inside the chip using the same methods that illustrated in 2.1.1 and 2.1.2, then the chip was connected to HPLC system to investigate separation different samples.

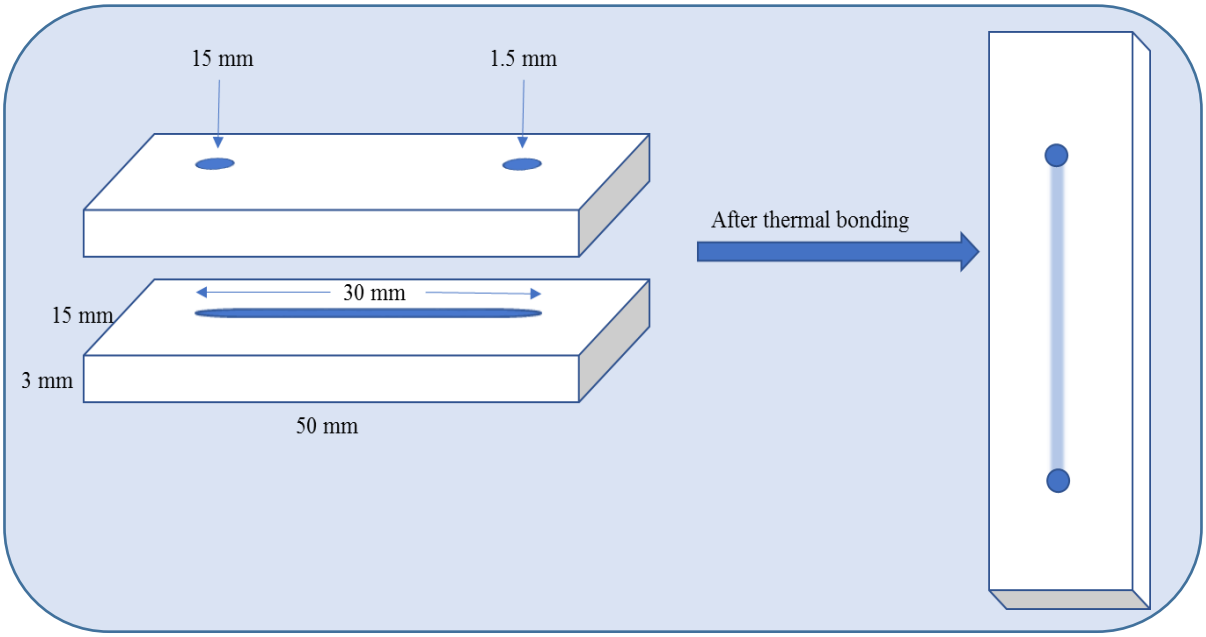

Figure 2.2 Microchip device design for LC separation.

2.9 Characterization of monolithic material

2.9.1 Scanning electron microscope (SEM)

A scanning electron microscope (Zeiss EVO 60) was used to characterize the morphology of the monolithic columns that have been prepared. Samples were coated with a thin layer of gold-platinum (thickness around 2 nm) by a Sputter Coating machine (Polaron SC7640 USA). After that images were obtained by utilizing an accelerating voltage of 20 kV and a probe current of 100 pA in high vacuum mode.

2.9.2 Brunauer-Emmett-Teller (BET) analysis

The surface area, and average pore size of the monolith were investigated using the Brunauer-Emmett-Teller (BET) model analyzer BJH (Barrett-Joyner-Halenda) model. The monolith was prepared inside (1 mL) a disposable plastic syringe `using the method that described in 2.1.2 without the silanization step to remove the monolith easily from the plastic syringe. Then, the unreacted materials were removed by washing with ethanol and water. The monolith was dried in column block heater at 60 ºC. The BET isotherms of nitrogen adsorption and desorption at 77 K were used to find the surface area, and average pore size of the monolith

2.9.3 Measuring porosity[248]

Fletcher *et al.* method was used to calculate the total porosity of the monolithic columns by weighing the monolithic column when it was dried (i.e. with all pores containing only air) and when it was filled with deionized water by pumping the deionized water using syringe pump for 3 hrs. to ensure that all the monolith was filled completely with deionized water. The porosity was measured using equation below:

$$\mathbf{Ø_t = (W_M - W_T) / dLR^2\pi} \qquad (2.2)$$

Where $\mathbf{Ø_t}$ is the porosity, $\mathbf{W_M}$ are the weights of the monolith when filled with water, $\mathbf{W_T}$ the weights of the monolith when dried, **d** is the density of water (at 23 ºC = 0.9975 g cm^{-3}), **L** is the length of the monolithic column, and **R** is the cylindrical radius of the column. L, and d were measured using Draper 0-150

mm/0-6" Digital Vernier Caliper (Toolbox Ltd., Lincoln, U). The measurement was repeated three times to get the average and minimize the human error.

2.9.4 Permeability of the monolith

The monolith permeability was studied by evaluating the backpressure that generated using HPLC system pump (solvent delivery Varian Prostar module 210) when the Milli-q water was pumped through the monolithic column at different flow rates.[200], when the pressure was stable the value of the pressure was recorded.

2.9.5 FT-IR spectroscopy

The FT-IR spectra were obtained using Thermo Scientific Nicolet 380 FT-IR (Thermo Scientific, Hemel Hempstead, UK), equipped with attenuated total reflectance (ATR) and all samples were in direct contact with the ATR diamond crystal. The transmittance spectra (4000–500 cm^{-1}) were collected at a resolution of 4 cm^{-1} with 4 scans.

2.9.6 ^{1}H NMR spectroscopy

Glycidyl methacrylate, stearyl methacrylate, ethylene glycol dimethacrylate, and glycigdyl methacrylate-co-ethylene glycol dimethacrylate-co- stearyl methacrylate were characterized by ^{1}HNMR on a Jeol JNM ECP 400 MHz Spectrophotometer, the reference was (DMSO δ_H = 2.50 ppm). Chemical shifts (δ) were given in ppm and coupling constants (*J*) was given in Hertz (Hz). Peak splitting patterns were denoted by the following notations: broad (br), singlet (s),

doublet (d), triplet (t) and multiplet (m), the ^{1}H NMR results for GMA, SMA, EDMA, and GMA-co-SMA-co-EDMA polymer are shown below respectively:

^{1}HNMR (400MHz, DMSO-D6) δ 5.68 (dd, J = 6.5 Hz, 2H), 5.16 (m, 2H), 4.09 (m, 3H), 3.50 – 3.27 (m, 4H), 2.70 – 2.56 (m, 2H), 1.88 (s, 0H).

^{1}H NMR (400 MHz, DMSO-D6) δ 3.66 (s, 0H), 5.88 (dd, J = 4.9, 4.6 Hz, 2H), 4.32 (d, J = 5.2 Hz, 1H), 4.09 (t, J = 6.6 Hz, 2H), 3.60 – 3.58 (m, 4H), 2.69 – 2.66 (m, 3H), 1.60 (d, J = 6.8 Hz, 1H).

^{1}H NMR (400 MHz, DMSO-D6) δ 6.33 (dd, J = 17.3, 1.7 Hz, 1H), 5.94 (dd, J = 10.3, 1.7 Hz, 1H), 4.17 (t, J = 6.7 Hz, 2H), 3.39 – 3.34 (m, 2H), 1.93 – 1.81 (m, 3H).

^{1}H NMR (400 MHz, DMSO-D6) δ 4.02 – 4.00 (m, 2H), 4.09 (d, J = 6.5 Hz, 1H), 3.50 – 3.27 (m, 10H), 2.70 – 2.56 (m, 24H), 1.88 (s, 0H). 3.64 (m, 4H), 1.76 – 1.50 (m, 24H), 2.09-0.81 (dt, J = 11.5, 5.3 Hz, 3H).

2.9.7 Energy dispersive X-ray (EDX) analysis

The INCA 350 energy dispersive X-ray EDX (Oxford Instruments, Abingdon, UK) system analysis was used to investigate and determine the chemical composition of the monolithic materials before and after opening the epoxy ring of the glycidyl methacrylate-co-stearyl methacrylate-co-ethylene dimethacrylate monolithic column.

3 Results and discussion: fabrication of monolithic columns

The fabrication of the monolithic columns was investigated inside a (60 mm) borosilicate tube with an inner diameter of (1.5 mm), and an outer diameter of (3.0 mm) that is shown in Figure (3.1) using two steps, silanization step, and *in-situ* polymerization step.

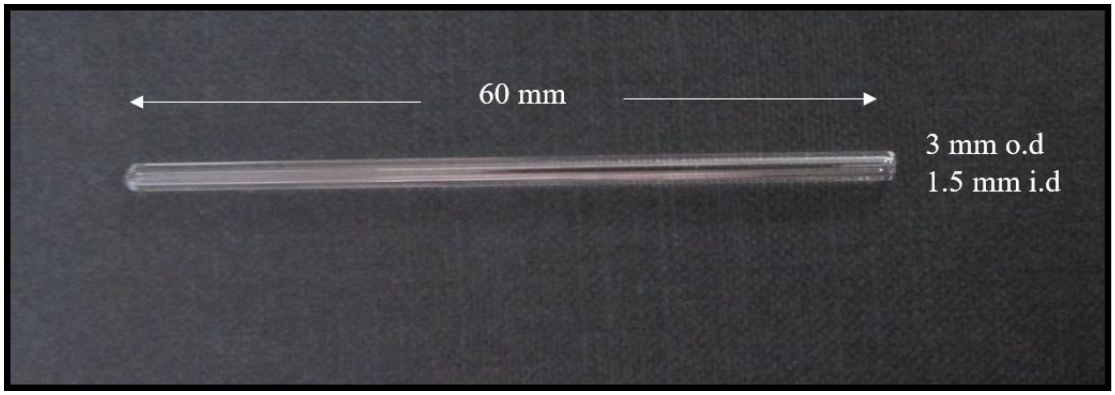

Figure 3.1 A photograph for the borosilicate tube before silanization step.

3.1 Silanization step

This silanization process considers the main step in the formation of the monolith inside the borosilicate tube. It involved reacting (3-trimethoxysilyl) propyl methacrylate with the silanol groups (Si-OH) on the inner wall of the borosilicate tube. The main advantage of this process is to anchor the monolith to the inner wall of the tube and prevent the formed monolith from pushing out the borosilicate tube when using high flow rate. Moreover, it helps prevent the shrinking effect during the polymerization process. In addition, if the analyte sample has proteins, the silanization step will avoid the interactions between the silanol groups and proteins.[249]

The silanization process involves various stages, in all these stages the solutions were pumped inside the borosilicate tube using syringe pump at flow rate 5 µL min^{-1} for 1 hr. The first stage was washing the inner wall of the tube by rinsing with acetone to remove any organic materials, then flushing with deionized water to remove any remaining of the acetone. After that hydrolyzed the siloxane groups and increase the silanol groups' density using basic solution (0.2 M NaOH) followed by washing with deionized water to remove any remaining basic solution.[250]

Moreover, hydrochloric acid (0.2 M) solution was used to remove and neutralize remaining alkali metal ions, then the borosilicate tube was rinsed with deionized water to remove any hydrochloric acid remaining, after that it was flushed with ethanol to remove any deionized water.

Finally, (3-trimethoxysilyl) propyl methacrylate, which is a bifunctional reagent, was injected inside the glass tube and allowed to react for 1 hour, following this the tube was dried with nitrogen gas. Now the trimethoxysilane groups are anchored to the silanol groups on the glass surface and the attached methacrylate groups will contribute in the polymerization reaction, binding the monolith *in-situ* to the inner walls of the glass tube.[30] The silanization steps are shown in Figure (3.2).

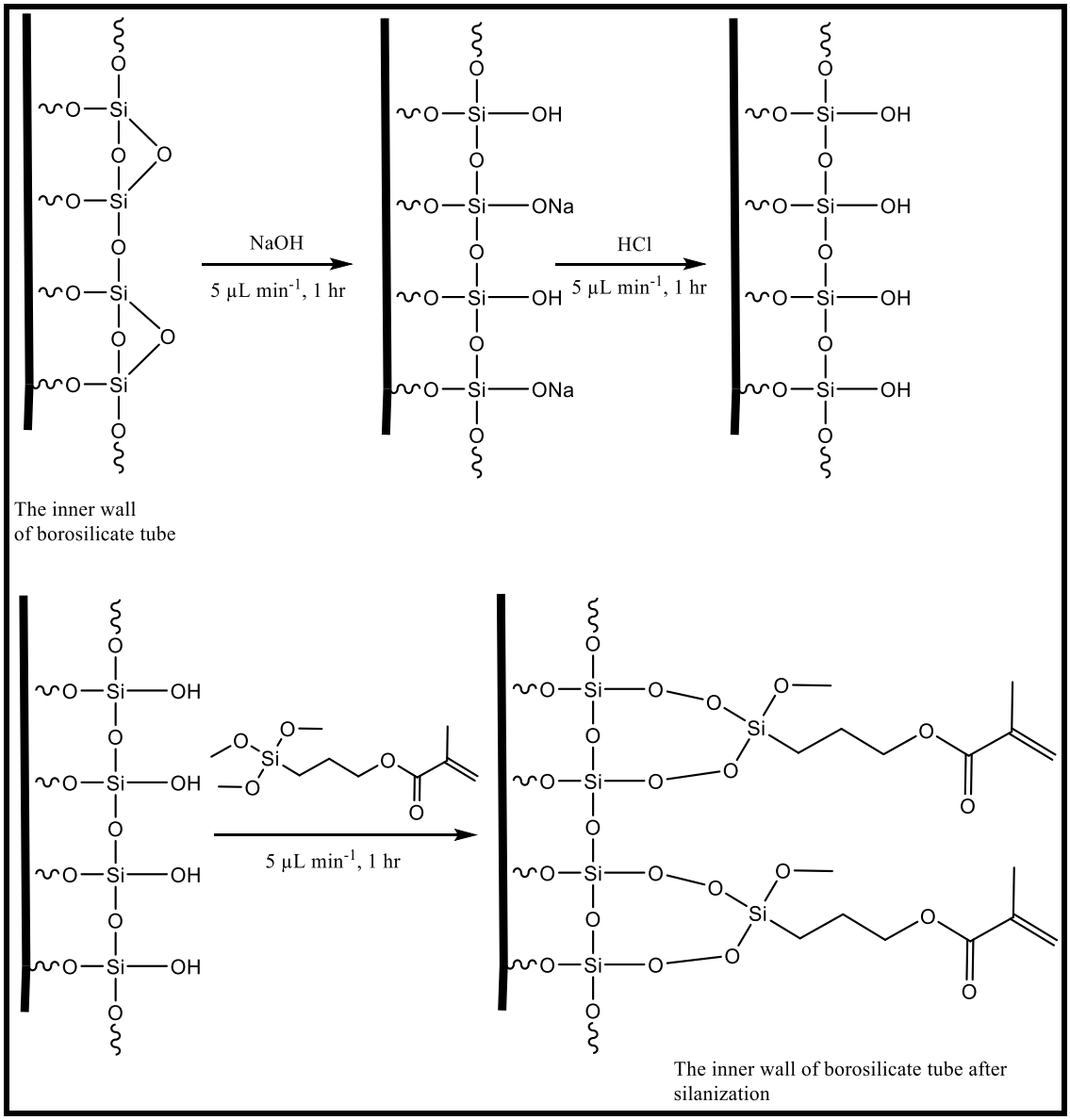

Figure 3.2 Silanization steps of borosilicate tube.

3.2 *In-situ* polymerization of the glycidyl methacrylate copolymers monolithic columns

Glycidyl methacrylate copolymer monolithic columns as illustrated in Table (3.1), have been investigated inside the borosilicate tube by *in-situ* polymerization reaction to produce mixed mode monolithic columns. The prepared columns have been tested for use in LC separation, instead of using one column for each mode (hydrophobic, hydrophilic, and ionic exchange) to save the time, effort, money and enhance the reproducibility of the analysis. The polymerization mixture included four main reagents, initiator, monomers, cross linker, and porogenic solvent, each one has a vital role in the polymerization reaction and the final morphology of the polymer. [251] 2,2-dimethoxy-2-phenylacetophenone (DMPA) was used as initiator instead of the more common initiator 2,2-azoisobutyronitrile (AIBN), this was because of some disadvantages when using (AIBN), for instance voids can be formed due to the rapid reaction and generation of N_2 gas during the polymerization process.[251]

Methacrylate derivative compounds based on glycidyl methacrylate (GMA) and other monomers have been chosen as a monomers, because GMA has two functional groups, a methacrylic double bond which participates in the photo polymerization reaction and an epoxide groups that can be used in many chemical reactions in post polymerization modification reactions to produce different functional groups which can provide for multiple possible separation mechanism.[178, 182]

The cross-linker, ethylene glycol dimethacrylate (EDMA) is a common crosslinking agent used to prepare rigid macro porous methacrylate monolithic polymers with glycidyl methacrylate and other monomers.[252] Crucially, the

diethylene glycol chains provide a significant flexibility to the crosslink and reducing many negative factors such as avoiding failure of the material caused by internal stress during the polymerization process, and osmotic shock can be avoided when using a broad range of salt concentration or organic solvent gradients or different pH solutions.[183]

The percentage of cross linker to the monomer should be constant because any change will effect on the porous properties, and the monolith chemical composition. For example, if the percentage of cross linker is increased, the average pore size is decreased due to formation of highly and rapidly cross-linked micro globules, these may be beneficial to gain a monolith that has a large surface area such as hundreds of square meters. However, monoliths that have high surface area will have limited permeability for solvents, increased backpressure, and be less suitable for HPLC separation, therefore the ratio of cross-linker to the monomer should be constant.[18]

A binary porogenic solvent consisting of 1-propanol, and 1,4-butan-diol was used in the polymerization mixture. The main role for the porogenic solvent is to solubilize the monomers, cross-linker, and initiator, while it needs poor solubility for the polymer to produce a homogeneous polymer solution that can be used for the polymerization reaction.[253]

The types of the co-monomers with the ratio of each monomer are shown in the Table (2.1), however, the amount of the cross-linker ethylene glycol dimethacrylate (EDMA) (0.3 mL), and the binary porogenic solvent, propan-1-ol (1.05 mL), butane- 1.4-diol (0.6 mL) in the polymerization mixture were constant in all the experiments. While the initiator was (1%) corresponding to the amount

of total monomers weight was added to the monomer solution. The formed monolithic column inside the borosilicate tube is shown in Figure (3.3).

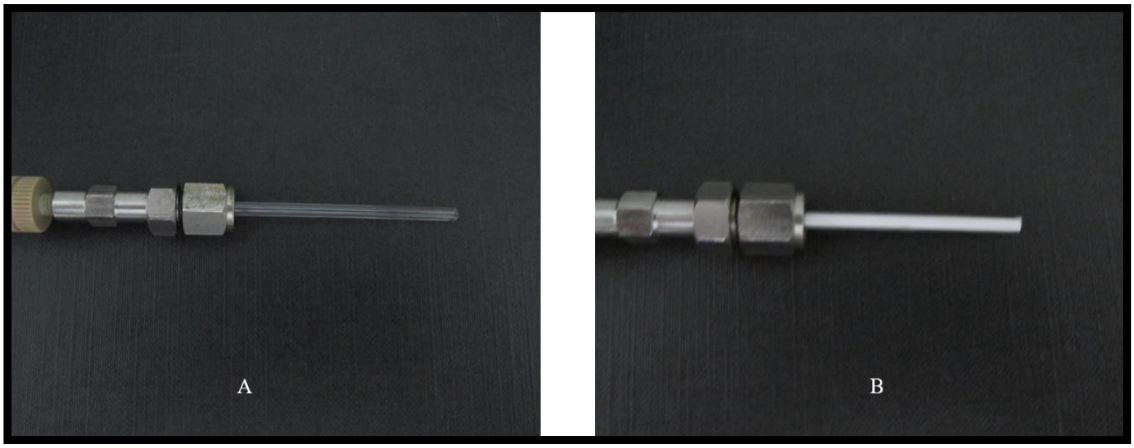

Figure 3.3 (A) The borosilicate tube after silanization step, (B) the borosilicate tube after *in-situ* polymerization.

3.3 Investigation of some mixed mode monolithic columns

Mixed mode monolithic columns were prepared to try separating different samples depending on two or more interaction mechanisms between the stationary phase and analytes. The types of interactions are based on the functional groups on the surface of the monolith which can participate to achieve significant separation.

These columns were prepared according to the methods presented in sections (2.1.1) and (2.1.2) using five types of monomers alongside glycidyl methacrylate as shown in Figure (3.4). Different ratios of the monomers were investigated to obtain a suitable monolithic column that could be used for LC separation.

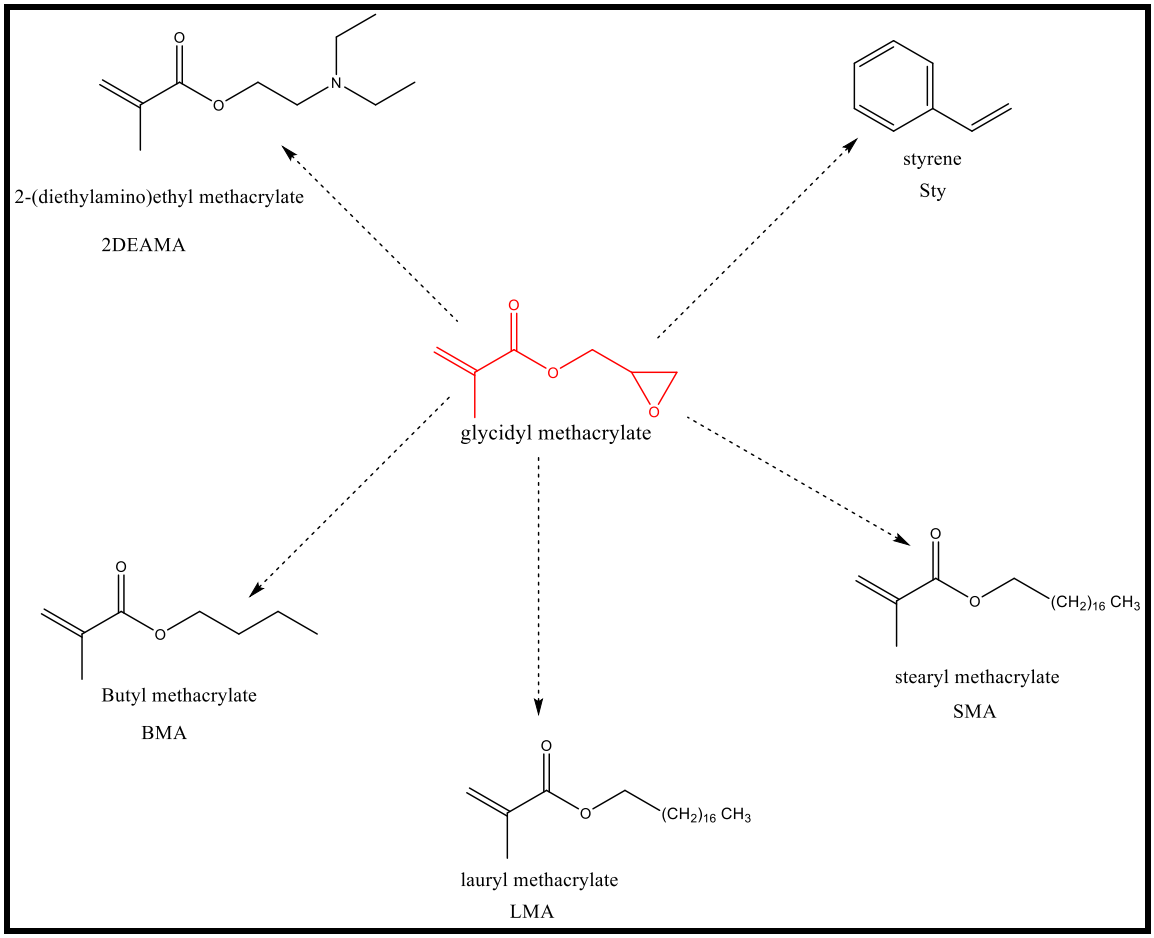

Figure 3.4 The five types of the co-monomers that used to form the mixed-mode monolithic columns alongside with glycidyl methacrylate.

As can be seen in Table (2.1) and Figure (3.4), five types of co-monomers were used to form mixed mode monolithic columns alongside the glycidyl methacrylate. However, these monomers have different properties, therefore, different monolithic columns with different chromatographic properties can be produced.

Initially, a (GMA-co-Sty-co-EDMA) monolithic column was formed using (90:10) % of GMA:Sty after 360 minutes of irradiation time. The formed monolith was tested by BET analysis to determine the surface area and the pore size. It was found that this monolithic column has low average surface area 1.2104 m^2 g^{-1}, with average pore size of 17.84 nm. The chromatographic performance of the

monolithic column was investigated by connecting the column to an HPLC system to try separate different analytes. The results were showed this column has a poor separation ability to separate different samples because the peaks were not resolved properly. It could be due to the low surface area which lead to poor interactions between the sample and the stationary phase. Consequently, less distribution of the analytes between the stationary phase and mobile phase. Other monomer ratios were investigated to form the monolithic column, however, the monolith did not form using any of these other ratios.

The (GMA-co-2DEAMA-co-EDMA) monolithic column was formed after 240 minutes with (90:10) %, and after 290 minutes with (50:50) % of GMA:2DEAMA. While, the monolith was not formed with (10:90)% of GMA:2DEAMA.

The BET analysis results showed that the average surface area and the average pore size for (90:10)% GMA:2DEAMA were 3.0530 $m^2 g^{-1}$, and 14.02 nm, while, 2.2716 $m^2 g^{-1}$, and 15.80 nm, for (50:50)% GMA:2DEAMA. The chromatographic behavior of these columns was also poor, and no separation was achieved

The GMA-co-BMA-co-EDMA monolithic columns showed a slightly higher surface area than the monolithic columns prepared using Sty, and 2DEAMA. The monolith was only formed using (10:90) % GMA:BMA. The average surface area was 4.9582 $m^2 g^{-1}$, with an average pore size of 15.03 nm when irradiated for 110 minutes. The monolithic columns showed poor performance as a LC column because all the peaks were broad and could not recognize the sample peaks in a mixture. The poor separation could be due to the low surface area that reduce the binding sites on the surface of the monolith that lead to low interactions between the sample and the monolith.

When it comes to LMA, and SMA, the surface area and the pore size values were significantly improved compared to the other monomers. GMA-co-LMA-co-EDMA monolithic column was formed using three ratios with different irradiation time, however, the (10:90) % of GMA:LMA monolithic column had the higher average surface area 11.4328 $m^2.g^{-1}$ and the average pore size was 4.26 nm after 140 minutes irradiation time. The GMA-co-SMA-co-EDMA monolithic column was formed properly with the three ratios, more details will be discussed in chapter 5.

3.4 Summary

To sum up, five types of co-monomers were used to prepare mixed-mode monolithic columns alongside glycidyl methacrylate. It was found that the lauryl methacrylate and stearyl methacrylate as co-monomers alongside with glycidyl methacrylate produced monolithic columns that had a high surface area and reasonable pore size compared to the other co-monomers. These monolithic columns could be used to separate different samples in liquid chromatographic separation.

4 Results and discussion: fabrication and applications of glycidyl methacrylate-co-lauryl methacrylate-co-ethylene glycol dimethacrylate monolithic column

4.1 Preparation of glycidyl methacrylate-co-lauryl methacrylate-co-ethylene glycol dimethacrylate monolithic column

Glycidyl methacrylate-co-lauryl methacrylate-co-ethylene glycol dimethacrylate monolithic column was prepared using the methods presented in 2.1.1 and 2.1.2. However, different (v/v) ratios of the monomers (90:10), (50:50), and (10:90) of GMA:LMA was used to obtain significant columns in term of surface area and pore size that could be used for LC separation.

4.1.1 Effect of irradiation time

The irradiation time is one of the main factors besides the polymerization mixture materials that participate in polymerization reaction. The UV light can cleavage the initiator (2,2-dimethoxy-2-phenylacetophenone) to form free radicals that can start the polymerization process as shown in Figure (4.1) in cleavage step. In addition, it is play a key role in formation of the final morphological shape of the polymer.

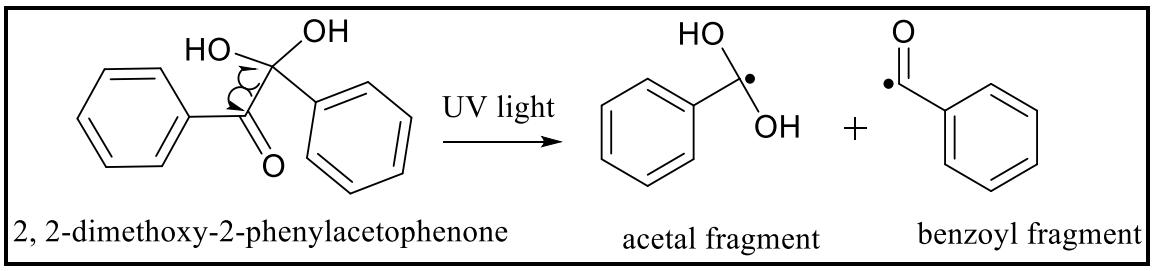

Figure 4.1 The cleavage of 2, 2-dimethoxy-2-phenylacetophenone to form radicals that can initiate the polymerization reaction

Photo polymerization at (365 nm) was used to form the monolith inside the borosilicate tube instead of thermal polymerization, because it has many advantages such as, control of the pore size, short preparation time, avoidance of elevated temperatures that lead to cracking the polymer, control over the placement and length of the porous matrix, and high mechanical strength.[254] Further, photo polymerization was used in subsequent experiments because it allows control over the distance (the length) of the irradiated area by masking the rest of the borosilicate or microchip area compared with thermal polymerization that could not be so easily controlled.[255] The most suitable irradiation time was investigated to form a monolith with a suitable pore matrix containing macropores and mesopores, and able to provide significant separation.

As described above the irradiation time is the main factor that changes the monomers mixture to the solid polymer, therefore when the photoreactions continue, the polymer chains are growing. Consequently, the polymer branches are increased rapidly, and form a dense monolith due to formation of a micro porous structure as show in Figure (4.2) (C). In contrast, when the irradiation time decreases it could lead to formation of less polymerized material inside the borosilicate tube or the microchip and the monolith will not form properly and affect the fabricated monolith performance as shown in Figure (4.2) (A), while the

appropriate irradiation time that gives reasonable back pressure and surface area is shown in Figure (4.2) (B)[256]

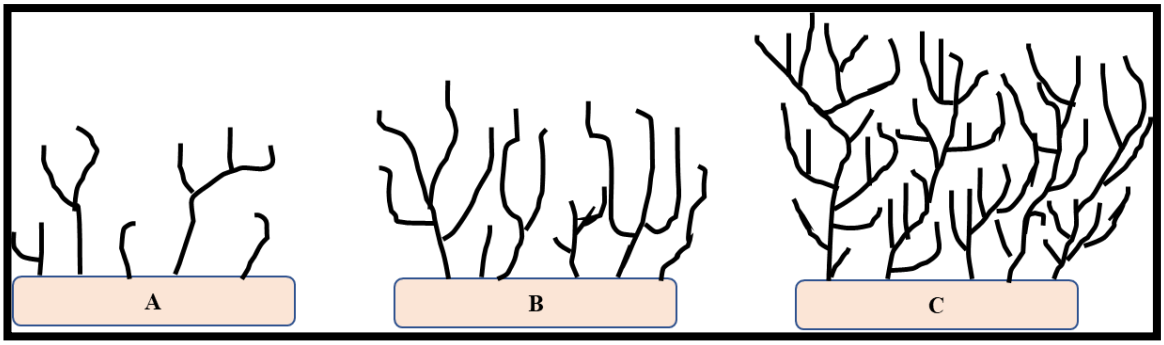

Figure 4.2 Effect of increasing irradiation time on the branches of polymers chains.

The effect of irradiation time was investigated with all three different percentages of monomers (90:10), (50:50), and (10:90) to form suitable morphological properties of the monolithic column, the effect of the irradiation time is shown in Table (4.1).

Table 4.1 Effect of irradiation time on the monolith formation

Irradiation time (min)	(**90% GMA, 10% LMA) (v/v)**	**(50% GMA, 50% LMA) (v/v)**	**(10% GMA, 90% LMA) (v/v)**
30	The monolith did not form	The monolith did not form	The monolith did not form
40	The monolith started forming	The monolith did not form	The monolith did not form
50	The monolith formed with back pressure 290 psi	The monolith did not form	The monolith did not form
60	The monolith formed with back pressure 350 psi	The monolith was start forming	The monolith did not form
70	The monolith formed with back pressure 480 psi	The monolith formed with back pressure 368 psi	The monolith did not form
80	The monolith formed with back pressure 481 psi	The monolith formed with back pressure 501 psi	The monolith did not form
90	The monolith formed with back pressure 482 psi	The monolith formed with back pressure 502 psi	The monolith was start forming

100	The monolith formed but it was blocked	The monolith formed with back pressure 507 psi	The monolith formed with back pressure 460 psi
110	-----	The monolith was formed but blocked	The monolith formed with back pressure 573 psi
120	-----	-----	The monolith formed with back pressure 651 psi
130	-----	-----	The monolith formed with back pressure 653 psi
140	-----	-----	The monolith formed with back pressure 654 psi
150	-----	-----	The monolith formed but it was blocked

Table (4.1) showed that the monolith was formed properly using 90% GMA:10% LMA (v/v) between (50-90) minute. The higher back pressure was achieved between 70-90 minutes due to increasing the branches of the monomers and increasing the surface area, while at 100 minutes the monolithic column was blocked and could not wash. It could be the monolith was too dense with lack of

macropores. When it comes to the 50% GMA:50% LMA (v/v) it can be noticed that the monolith was started forming at higher irradiation time that used to form the monolith using (90:10) GMA:LMA. It was formed in the range (70-100) minute. The 10% GMA:90% LMA (v/v) showed that the monolith was formed properly in (100-140) minute using (10:90) GMA:LMA, which is higher irradiation time compared with (50:50), and (90:10) GMA:LMA. That is indicated the polymer formation time is increased with increasing the percentage of the LMA, it could be due to increasing the percentage of the aliphatic chains in LMA that need more time to react with GMA and EDMA may be due to steric factors effect.

Once the monolith had formed properly with good back pressure and after washing with deionized water then dried well, the surface area, and pore size were investigated using BET analysis for the dried monoliths formed after 70, 80, and 120 minute for (90:10), (50:50)% and (10:90) GMA: LMA respectively. Since, the difference in the back pressure in that range of each monolith was not very significant, and avoiding the possible thermal polymerization effect from long irradiation time, the BET results for these monoliths are shown in Figure (4.3)

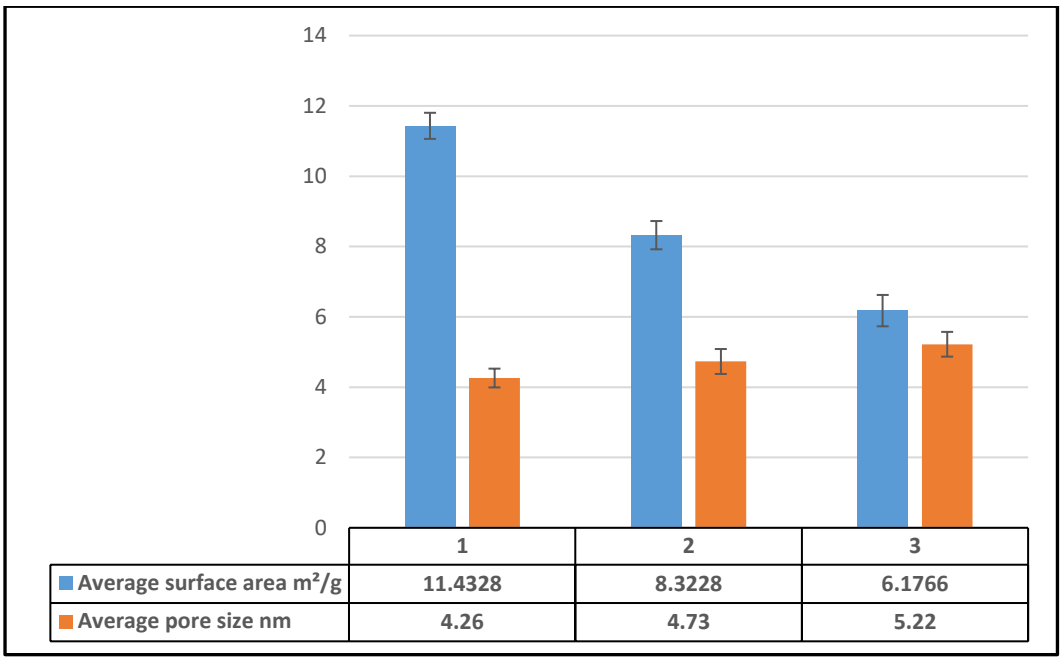

Figure 4.3 The morphological properties for glycidyl methacrylate-co-lauryl methacrylate-co-ethylene glycol dimethacrylate monolithic column, 1(10:90), 2(50:50), and 3(90:10) of GMA:LMA, SD (n=3)

It can be seen from Figure (4.3), the 10:90 GMA:LMA ratio gave significant average surface area compared with other ratios, because the monolith has a higher surface area than the others according to BET analysis. Consequently, the number of mesopores and micropores will be increased with increase the surface area. Therefore, the interactions between the surface of the monolith with the sample will be increased, however, the separation process will be enhanced. Therefore this column has been chosen for LC separation.

4.1.2 SEM analysis of glycidyl methacrylate-co- lauryl methacrylate-co-ethylene dimethacrylate monolithic column (10% GMA, 90% LMA)

The morphology of the monolith was visualized using scanning electron microscopy (SEM). The SEM image for the glycidyl methacrylate-co-lauryl methacrylate-co-ethylene dimethacrylate monolithic column is shown in Figure (4.4). It can be seen from Figure (4.4) that the structure of monolithic media can be viewed as a network of interconnected large flow-through pores.[23] These pores allow the mobile phase to rapidly pass through the monolithic column, consequently, it will enhance the permeability by reducing the back pressure.[23] In addition, the cluster of the monolith has many mesopores, and micropores, the advantages of this pore structure are responsible for increasing the surface area of the monolith and increasing the load ability of the monolith. Moreover, they influence on the rapid extraction with high flow rate and moderate backpressure.[20]

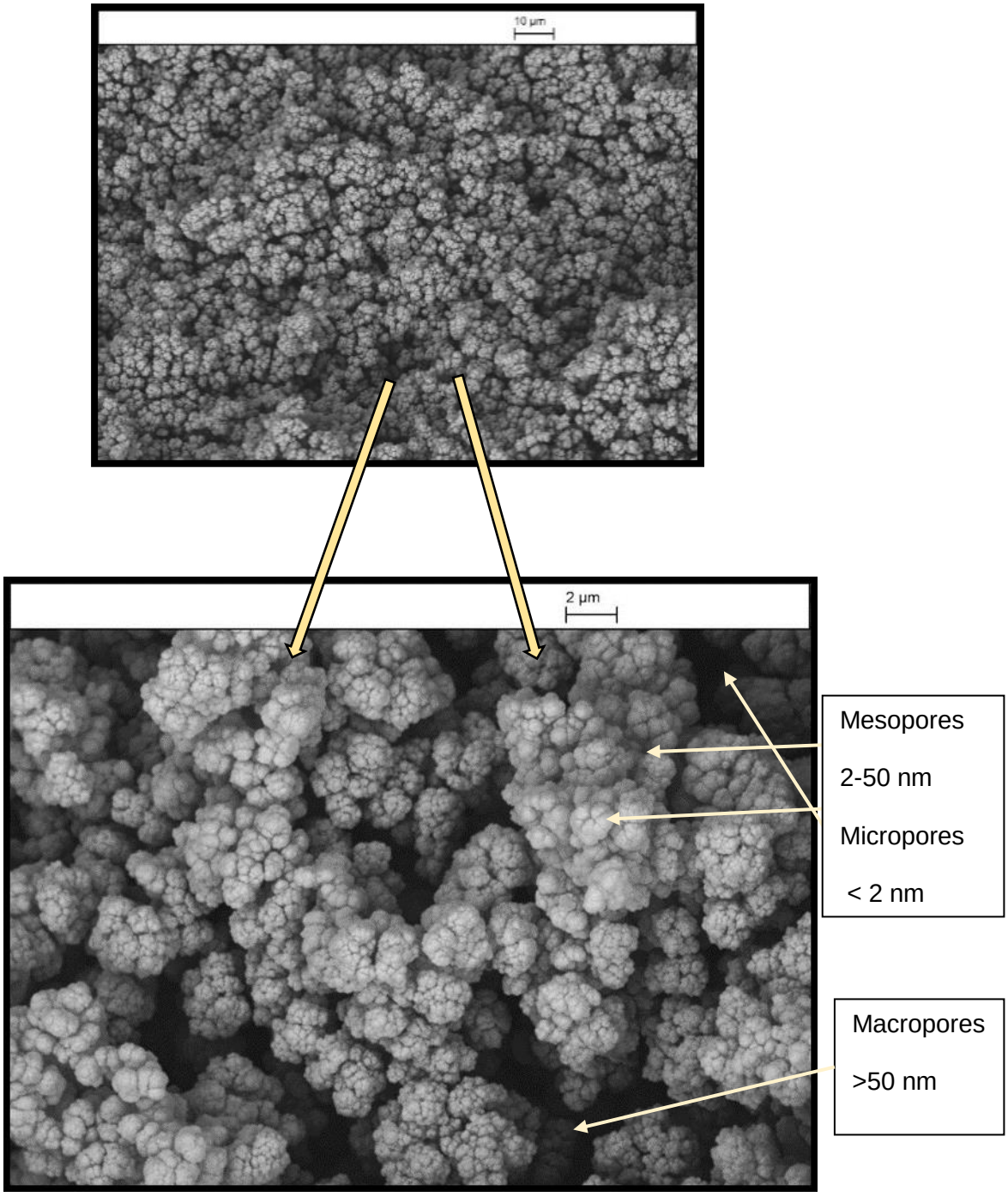

Figure 4.4 SEM image for the glycidyl methacrylate-co-lauryl methacrylate -co-ethylene dimethacrylate monolithic column

4.1.3 Permeability and the porosity of the monolith

The permeability of (10:90) % GMA:LMA monolithic column monolithic was examined by evaluating the backpressure generated from HPLC system pump using milli-q water at different flow rates through the monolith.[200] The result is shown in Figure (4.5)

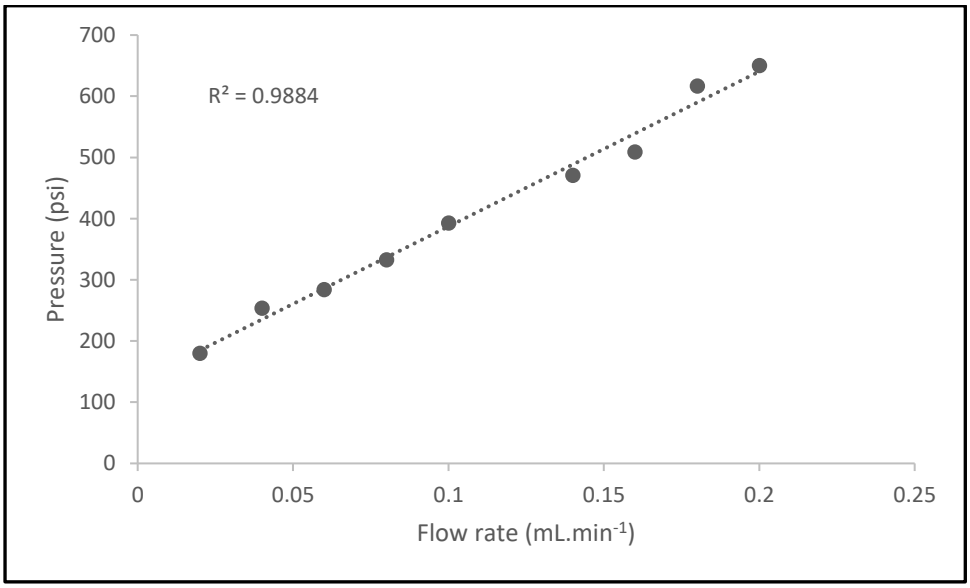

Figure 4.5 The relationship between the back pressure and the flow rate for the glycidyl methacrylate-co- lauryl methacrylate-co-ethylene dimethacrylate monolithic column.

It can be seen from Figure (4.5) that the back pressure was increased with increasing the flow rate up to 0.2 mL.min^{-1}, the pressure was stable at the value of 650 psi. After that the system leaked, it could be due to the porosity of the monolith, or the stainless-steel fitting did not grip the borosilicate tube sufficiently causing leakage above 0.2 mL.min^{-1} flow rate. However, the 0.2 mL.min^{-1} was used in the further experiments. The porosity of the glycidyl methacrylate-co-lauryl methacrylate-co-ethylene dimethacrylate monolithic was calculated using

the method that described in 2.9.3. the result showed the porosity of the column was 0.0463.

4.2 Applications of glycidyl methacrylate-co- lauryl methacrylate-co-ethylene dimethacrylate monolithic column

This column was tested with different samples to investigate it is separation ability and chromatographic properties, all the samples were tested individually three times each (n=3), then mixed together and tested three times (n=3) for reproducibility and to determine the exact retention time for each compound. Different solvents have been used such as acetonitrile, methanol, ethanol, and 2-propanol with deionized water to obtain the final separation. Results showed that acetonitrile and water was the best solvent mixture compared with other solvents, therefore these solvents were used in all the following experiments.

4.2.1 Separation of hydrophobic compounds

A mixture of naphthalene and benzophenone was used to evaluate the separation ability of the column. These compounds have been used because they differ in the molecular weight and the hydrophobicity. Therefore, they could interact with the stationary phase in different ways, and that could be used to separate these compounds. Gradient analysis method was used for each compound and the mixture because the isocratic method did not produce a good separation for the tested compounds. In addition it was mentioned elsewhere that the isocratic system could not provide fine separation if the monolithic column

does not have enough mesopores[191]. The gradient analysis no. (1) is shown in Table (4.2) was used for this experiment. The result is shown in Figure (4.6).

Table 4.2 Solvent compositions for gradient analysis no. (1)

Time/ min.	Water %	Acetonitrile %	Flow rate mL/min
0:00	95	5	0.2
2:00	95	5	0.2
25:00	50	50	0.2
33:00	50	50	0.2
33:30	95	5	0.2
35:00	95	5	0.2

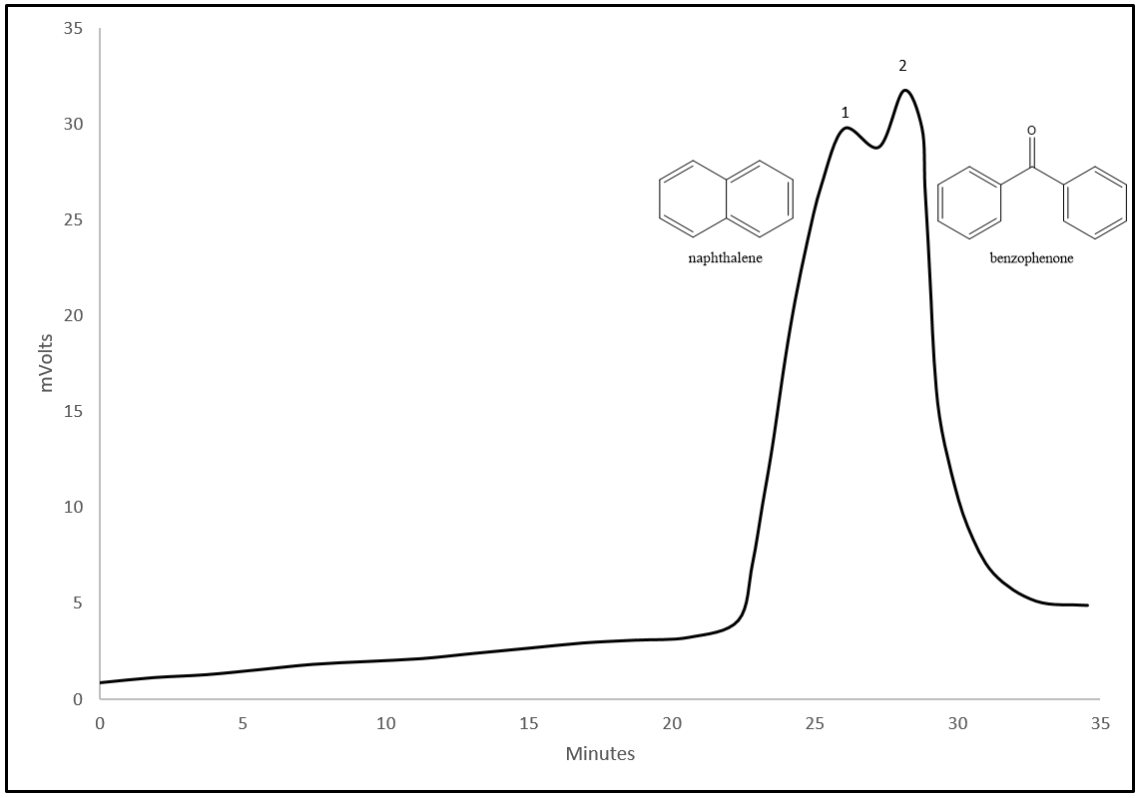

Figure 4.6 Chromatogram of a mixture of (1) naphthalene, and (2) benzophenone, 10^{-4} M with gradient analysis no (1), the injection volume (2.5 µL), and the detection wavelength 254 nm.

The experimental result of small molecules showed that this column has limited ability to separate these two compounds with hydrophobic properties. The two peaks were close to each other and did not separate completely.

It can be noticed that the two compounds are hydrophobic, and the stationary phase is 90% lauryl methacrylate in addition to the hydrophobic part from the glycidyl methacrylate, therefore, the analytes will be partitioning between the mobile phase and the hydrophobic stationary phase of the monolithic column. Consequently, the solutes will diffuse into the pores of the stationary phase and interact with the alkyl chains by hydrophobic interactions. Therefore, to decrease the C-term in van Deemter equation, the mass transfer from the stationary phase to the mobile phase should be increased, however, the amount of less polar solvent should be increased to enhance the mass transfer by reducing the retention factor of the analytes.[257] The gradient program was used to increase the organic solvent percentage to see if this allows faster desorption of the molecules from the monolith surface and reduces band broadening. The new gradient no. (2) is shown in Table (4.3), and the result is shown in Figure (4.7)

Table 4.3 Solvent compositions for gradient analysis no. (2)

Time/ min.	Water %	Acetonitrile %	Flow rate mL/min
0:00	95	5	0.2
2:00	95	5	0.2
12:00	10	90	0.2
30:00	10	90	0.2
33:30	95	5	0.2
35:00	95	5	0.2

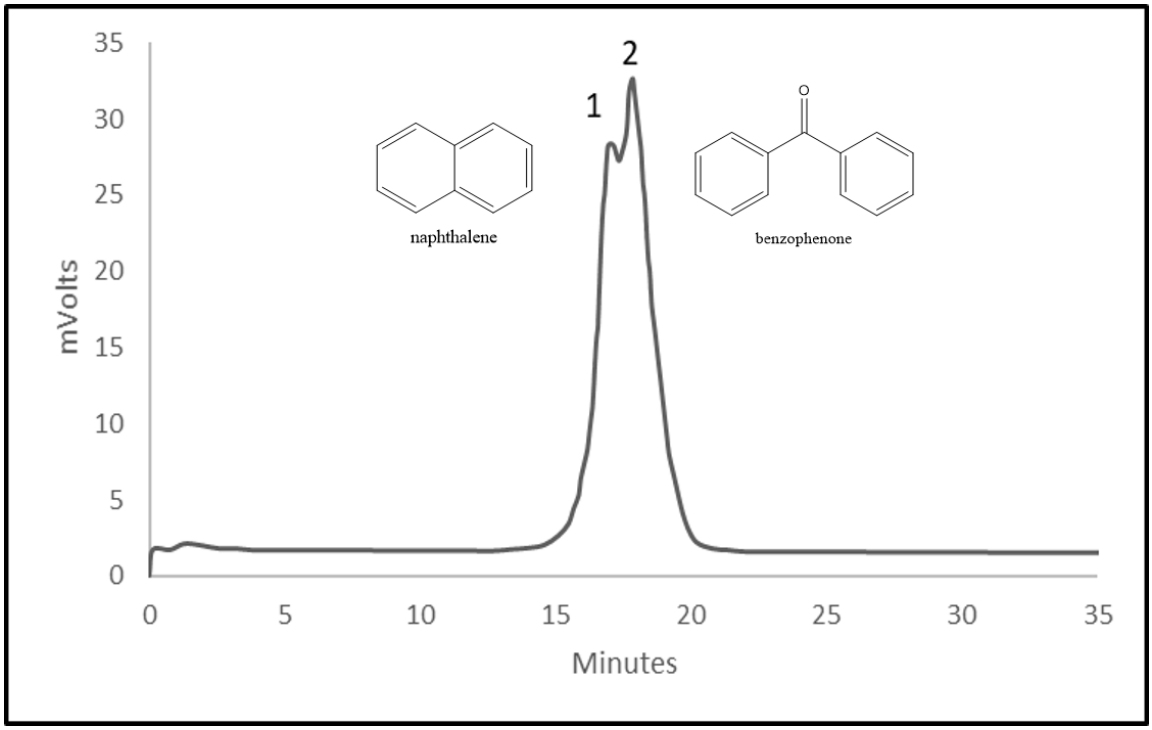

Figure 4.7 Chromatogram of a mixture of (1) naphthalene, and (2) benzophenone, 10^{-4} M with gradient no. (2), the injection volume (2.5 µL), and the detection wavelength 254 nm.

From Figure (4.7) it can be seen that the two peaks are sharper compared with the peaks in Figure (4.6), due to changing the gradient analysis and increase the organic solvent ratio, which lead to maintain the peak shape and reduce the analysis time by decreasing the retention time for each compound. The increasing of acetonitrile percentage from (50 to 90) % increased the mass transfer rate from the stationary phase to the mobile phase, which led to increasing the desorption rate over the adsorption rate, and allowing the solute molecules to leave the surface pores of the stationary phase and be released to the mobile phase.

While the shape and the retention time of the peaks were enhanced, the base line separation was not achieved, it could be due to the mesopores and the surface area were not enough to increase the mass transfer and reduce the convection, that lead to enhance the chromatographic separation efficiency[258].

According to the plate theory, the other factor that can affect the base-line separation is the number of theoretical plates (N), therefore, the (N) and (Rs) values were calculated. The results are shown in Table (4.4).

Table 4.4 The average number of theoretical plates (N) and the resolution value (Rs) for naphthalene, and benzophenone (n=3)

N	481
Rs	0.33

From Table (4.4) it can be seen that the (N) value was poor, which is could be due to the low surface area of the monolith. Therefore, the resolution value (Rs) was low which causing non-line separation.

4.2.2 Separation of a hydrophobic and hydrophilic mixture

A mixture of hydrophilic and hydrophobic compounds was used to test the separation ability of glycidyl methacrylate-co-lauryl methacrylate-co-ethylene dimethacrylate monolithic column to separate samples with different chromatographic properties (hydrophobic and hydrophilic), the results are shown in Figures (4.8) and (4.9) using the same gradient in Table (4.3)

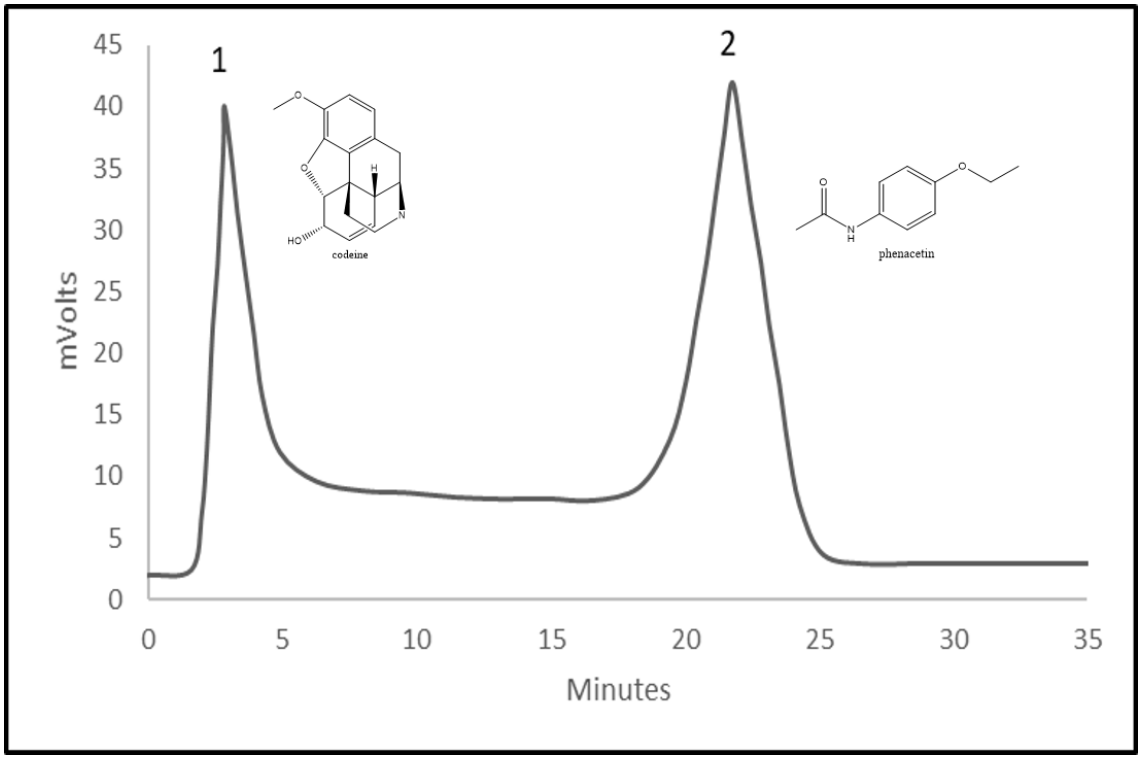

Figure 4.8 Chromatogram of a mixture of (1) codeine, and (2) phenacetin 10^{-4} M with gradient no. (2) the injection volume (2.5 µL), and the detection wave length 254 nm.

Codeine and phenacetin as pharmaceutical hydrophilic and hydrophobic compounds depending on the partition coefficient (log P) to determine the hydrophobicity of each compound the (P) value was (1,19) for codeine, and the solubility in the water (9 $g.L^{-1}$). While, phenacetin was (1.58) and the solubility

(0.76 $g.L^{-1}$), benzophenone (3.18) and the solubility in the water was (0.137 $g.L^{-1}$).[259] According to the (log P) value it can be considered that codeine is a moderately hydrophilic compound and phenacetin is hydrophobic compound.

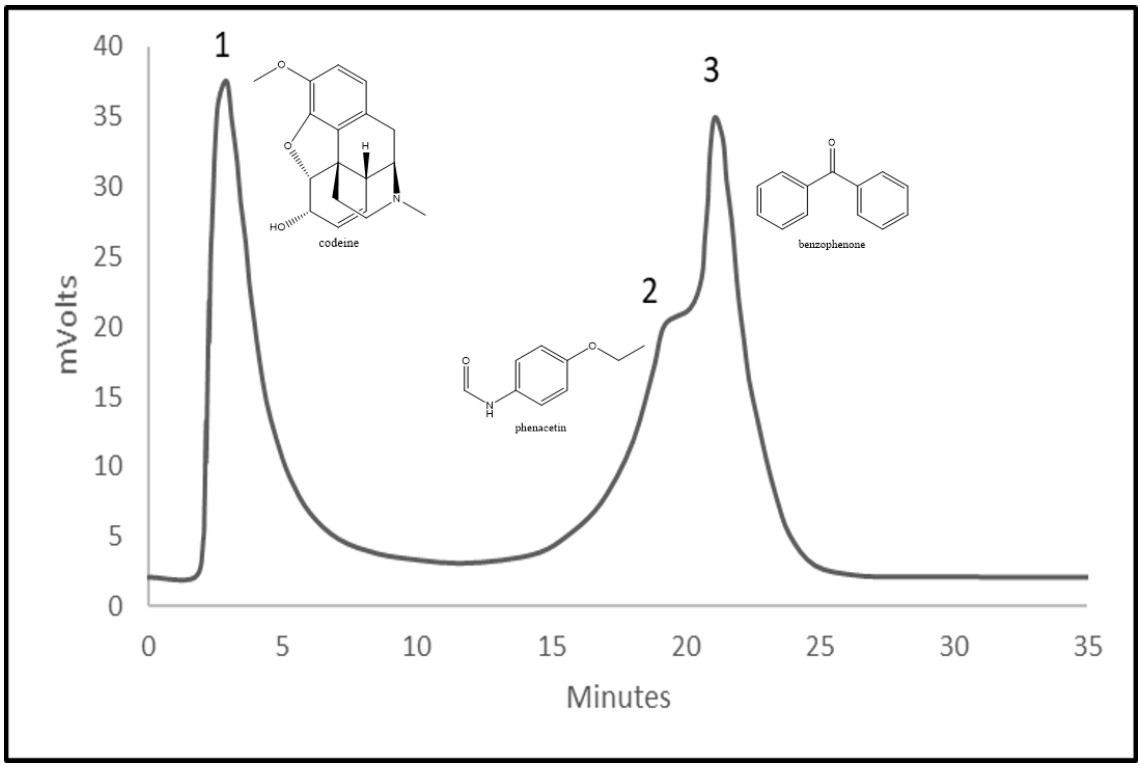

Figure 4.9 Chromatogram of a mixture of (1) codeine, (2) phenacetin, and (3) benzophenone, 10^{-4} M with gradient no. (2), the injection volume (2.5 µL), and the detection wavelength 254 nm.

From these two Figures (4.8) and (4.9), it can be seen that this column could be used to separate hydrophilic from hydrophobic compounds using high ratio of organic solvent, while the separation of hydrophobic compounds was not significant. It can be concluded that the mechanism of separation could be mixed mechanism (HILIC) due to the hydrophilic part GMA monomer and (RP) due to the LMA monomer. So far, the elution order of the compounds has followed the

hydrophobicity order, therefore, more investigations about mixed mode mechanism were carried using another test of different compounds.

4.2.3 Separation of peptides and proteins

GMA-co-LMA-co-EDMA monolithic columns were used to try separating peptides and proteins, the results were not acceptable because they were not reproducible. The retention time varied with each run giving broad peaks at various times, making it impossible to assign a retention time to each peak reliably as can be seen in Figures (4.10-4.12) using gradient no (3). In addition, this column could not separate a mixture of proteins in a single run, even when different solvents and different gradient analyses were investigated.

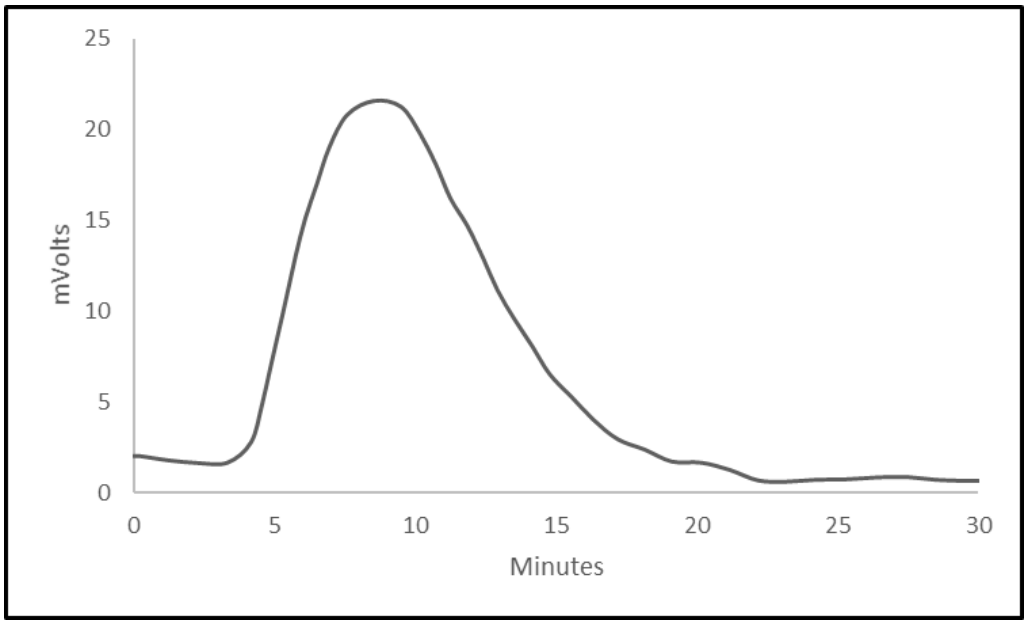

Figure 4.10 Chromatogram of cytochrome c, 10^{-4} M with gradient, the injection volume (2.5 µL), and the detection wavelength 254 nm.

It can be seen from Figure (4.10) that cytochrome c was eluted with very broad peak and could not recognize the exact retention time.

Table 4.5 Solvent composition for gradient analysis no. (3)

Time/ min.	Water %	Acetonitrile %	Flow rate mL/min
0:00	50	50	0.2
2:00	50	50	0.2
12:00	10	90	0.2
25:00	10	90	0.2
26:30	50	50	0.2
30:00	50	50	0.2

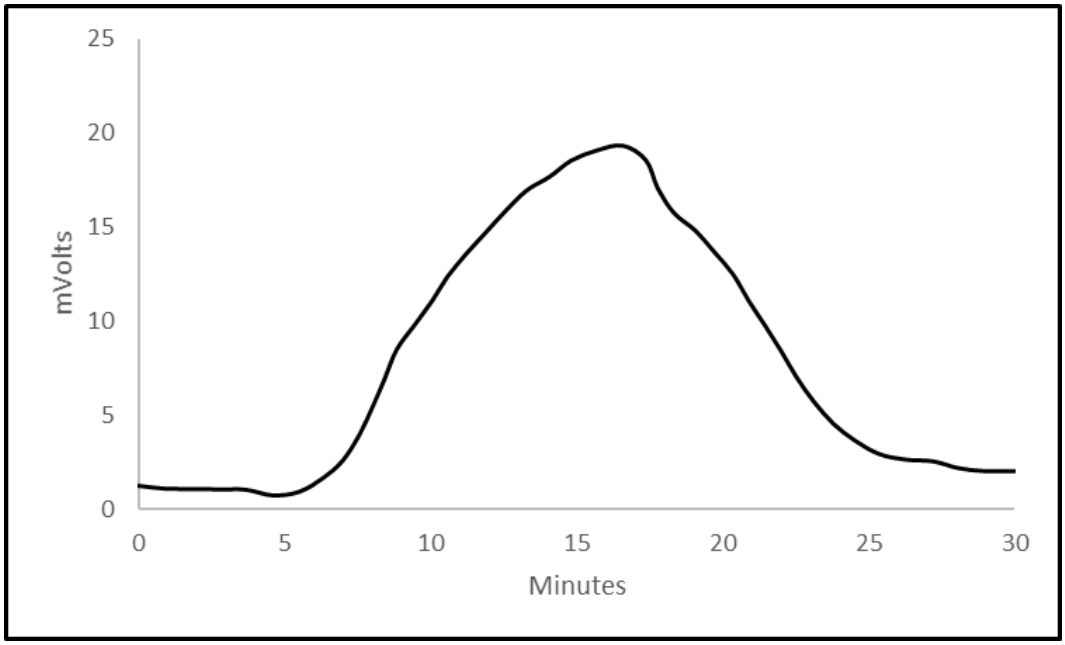

Figure 4.11 Chromatogram of myoglobin, 10^{-4} M with gradient, the injection volume (2.5 µL), and the detection wavelength 254 nm.

From Figure (4.11), it is clearly seen the lack in column behavior with large molecules, due to the broad peak and could not specify the exact retention time.

A commercial peptide (Glu-Gln-Arg-Leu-Gly-Asn-Gln-His-Leu-Met) was tested using (GMA-co-LMA-co-EDMA) monolithic column, the results were showed that this column has poor separation and could not use for LC separation of macromolecules as showed in Figure (4.12).

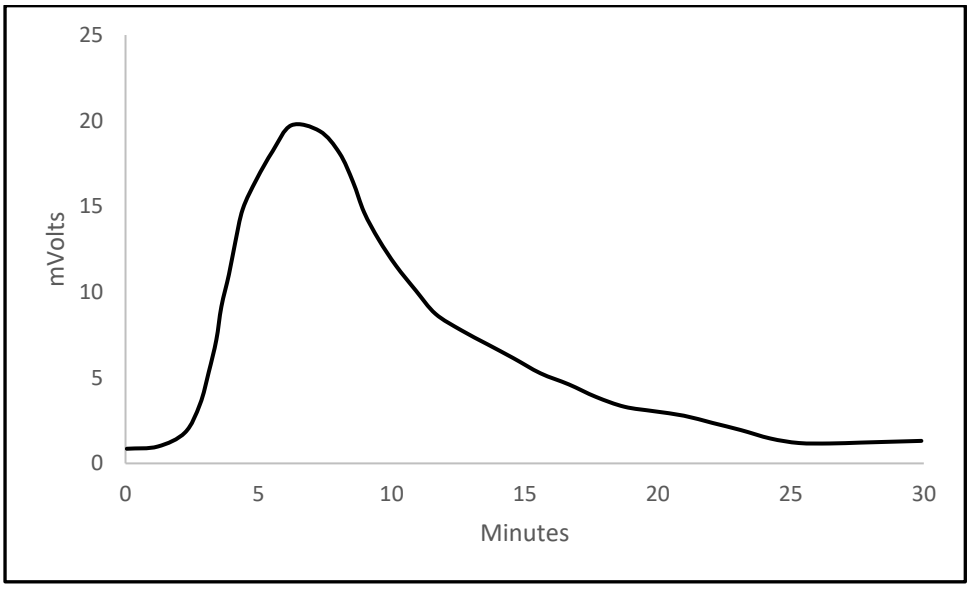

Figure 4.12 Chromatogram of commercial peptide (Glu-Gln-Arg-Leu-Gly-Asn-Gln-His-Leu-Met) chromatograph, 10^{-4} M with gradient, the injection volume (2.5 µL), and the detection wavelength 254 nm.

The commercial peptide gave a broad peak when it was tested by GMA-co-LMA-co-EDMA monolithic column as showed in Figure (4.12).

The macromolecules results showed that the monolithic column has limited ability to separate these molecules. It could be due to the low surface area of the monolith which lead to decrease the interactions with the macromolecules giving poor separation.

4.3 Mixed mode evidence

Mixed mode mechanism was tested by using LMA-co-EDMA, and GMA-co-LMA-co-EDMA monolith columns to test a mixture of four compounds with gradient analysis no. (4), the results are shown in Figures (4.13) and (4.14)

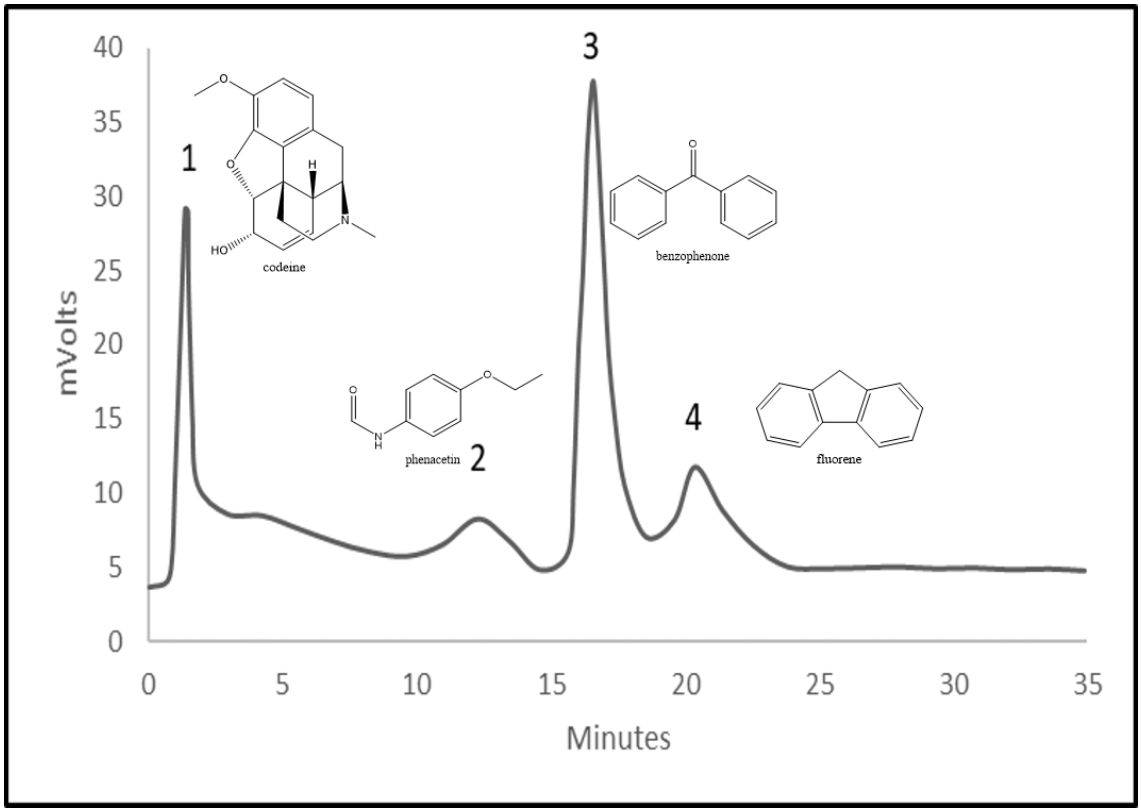

Figure 4.13 Chromatogram of a mixture of (1) codeine, (2) phenacetin, (3) benzophenone, (4) fluorene, 10^{-4} M with gradient no. (4), using LMA-co-EDMA monolithic column, the injection volume (2.5 µL), and the detection wavelength 254 nm.

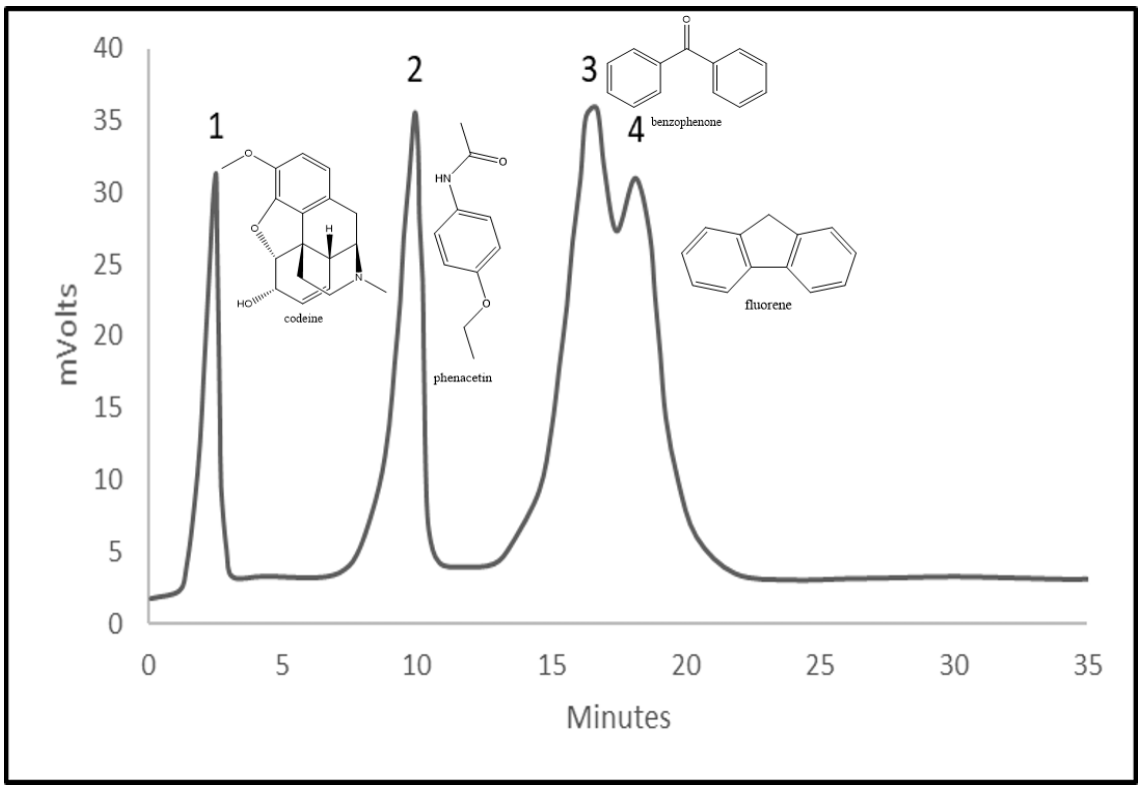

Figure 4.14 Chromatogram of a mixture of (1) codeine, (2) phenacetin, (3) benzophenone, and (4) fluorene 10^{-4} M with gradient no. (3), using GMA-co-LMA-co-EDMA monolithic column, the injection volume (2.5 µL), and the detection wavelength 254 nm.

Table 4.6 Solvent composition for gradient analysis no. (4)

Time/ min.	Water %	Acetonitrile %	Flow rate mL/min
0:00	95	5	0.2
2:00	95	5	0.2
12:00	5	95	0.2
30:00	5	95	0.2
30:30	95	5	0.2
35:00	95	5	0.2

It was found from Figure (4.13) that the LMA-co-EDMA monolithic column behaves as a revers phase C12 column, and the elution order follows the hydrophobic interactions, with base-line separation for all four compounds. While the peak shapes were broad except for codeine and benzophenone.

Figure (4.14) showed a slight change in the retention time of each sample with the same elution order as the LMA monolithic column when using GMA-co-LMA-co-EDMA monolithic column, while the peak shape for phenacetin was enhanced to be sharper than in Figure (4.13). Moreover, the based-line separation between benzophenone and fluorene was decreased significantly. The N and Rs values were calculated to compare the separation efficiency of the two columns, the results are shown in Table (4.7).

Table 4.7 The N and Rs values for the GMA-co-LMA-co-EDMA and LMA-co-EDMA monolithic columns

Compounds	**GMA-co-LMA-co-EDMA column**	**LMA-co-EDMA column**
N value	497	348
Rs codeine and phenacetin	11.3	4.8
Rs phenacetin and benzophenone	2.8	1.5
Rs benzophenone and fluorene	0.63	1.23

It can be seen from Table (4.7) that the N value for GMA-co-LMA-co-EDMA monolithic column is higher compared with LMA-co-EDMA monolithic column. In

addition, the Rs was increased for codeine and phenacetin, and for phenacetin and benzophenone, however, for benzophenone and fluorene was decreased. These result lead to the conclusion that the presence of GMA in the stationary phase of the GMA-co-LMA-co-EDMA monolithic column lead to a decrease in the hydrophobic properties and changed the chromatographic behavior of the monolithic column, which could now work as a mixed-mode column HLIC-RP.

4.4 Summary

The GMA-co-LMA-co-EDMA monolithic columns can be prepared using different monomers ratios, these ratio can effect on the surface area and the pore size of the monolith. The results are shown in Table (4.8).

Table 4.8 the effect of the monomers ratio on the surface area and the pore size of the GMA-co-LMA-co-EDMA monolithic columns

Monomers ratio (v/v) GMA:LMA mL	**Surface area m^2g^{-1}**	**Pore size nm**
90:10 %	6.1766	5.22
50:50 %	8.3228	4.73
10:90 %	11.4328	4.26

As can be seen from Table (4.8) the monolith was formed with all the ratios that used. However, the (10:90) % of GMA:LMA had a higher surface area compared with other ratios, therefore this ratio was used to prepare the monolithic column to investigate separation different samples.

The monolithic column was demonstrated to separate different samples such as hydrophilic, and hydrophobic molecules the results are shown in Table (4.9).

Table 4.9 The applications of GMA-LMA-co-EDMA monolithic columns

Monomers ratio (v/v) GMA:LMA	**Monolithic column applications**
90:10 %	Poor separation
50:50 %	Poor separation
10:90 %	Good separation media for small molecules. Poor separation for peptides and proteins.

It can be seen from Table (4.9) that (10:90)% GMA:LMA showed good separation with small molecules. However, large molecules (peptides and proteins) were not separated. While other percentage of GMA, LMA (50:50) % and (90:10) % were prepared and investigated to separate the same samples as used with (10:90) % GMA, LMA monolithic column.

In addition, the results showed that the hydrophilic compounds are eluted first followed by hydrophobic compounds, this could be, because the surface of the monolith has a 90% of LMA, therefore, the hydrophilic properties of the GMA that can give hydrophilic properties to the monolith, was poor compared with the hydrophobic properties.

The literature indicates that monolithic columns with surface areas of tens of $m^2.g^{-1}$ may have lack micropores and mesopores which can lead to a decrease in the mass transfer resistance[52]. Therefore, this may be the reason for a lack of base-line separation of some compounds tested here.

For all the reasons above the monolithic column could not separate macromolecules due to the low surface area that cannot provide more theoretical plate to retain these molecules.

Due to the broad peaks with small molecules and the lack of separation for peptides and proteins with GMA-co-LMA-EDMA monolithic column, other monomers were used to try to enhance the peak shape, N, and Rs values.

5 Results and discussion: fabrication and applications of glycidyl methacrylate-co-stearyl methacrylate-co-ethylene dimethacrylate monolithic column

Glycidyl methacrylate-co-stearyl methacrylate-co-ethylene glycol dimethacrylate monolithic columns were prepared using the method previously described in section 2.1.1 and 2.1.2. The SMA monomer was used for many reasons, as can be seen with the LMA monomer the surface area was increased with increasing percentage of aliphatic chains. Therefore, high surface area and reasonable pore size could be obtained using SMA with longer aliphatic chains. This also could be enhanced the chromatographic separation of different samples. In addition, SMA can be used with various types of nonpolar solvents due to its higher affinity to ward these solvents.[194] So far, when it copolymerized with different monomers the lipophilic nature of the aliphatic alkyl chains for SMA produced polymers with different properties, for example, amphoteric polymers,[260]copolymers with self-assembling amphiphilic characters,[261] and particle stabilizers.[262]

To form the GMA-co-SMA-co-EDMA monolith columns different percentages of the monomers (90:10)%, (50:50)%, and (10:90)% of GMA:SMA were studied to produce monolithic columns with higher surface area and suitable pore sizes for range of separations. The literature shows that, the ratio of the monomers is a very significant parameter from both an industrial and academic perspectives, because it has a high impact on the ability to tailor of the copolymers, so that the chemical and physical properties can be used for different applications.[194, 263]

5.1 Effect of irradiation time

The effect of irradiation time on monolith formation was investigated for all three monomers percentages (90:10)%, (50:50)%, and (10:90)% of GMA:SMA to produce monolith with suitable morphological properties. In the photo polymerization reaction, the free radicals formed when ultraviolet light was absorbed by the initiator molecules as showed previously in Figure (4.1), and propagate the growing chains and cross-links. This process increases with increased the irradiation time. Therefore, the polymerization rate also is increased by higher monomer diffusion rates. Eventually, the polymerization reaction reaches a higher double bond conversion and the photo polymerization reaction is decreased rapidly due to restricted monomer mobility.[264]

The most suitable irradiation time was investigated using 365 nm UV-light to form a monolith with a suitable pore matrix containing macropores and mesopores, and able to provide significant separation. The effect of the irradiation time is shown in Table (5.1).

Table 5.1 Effect of irradiation time on the monolith formation.

Irradiation time (min)	(**90:10)% (v/v) GMA:SMA**	(**50:50)% (v/v) GMA:SMA**	(**10:90)% (v/v) GMA:SMA**
60	The monolith did not form	The monolith did not form	The monolith did not form
70	The monolith did not form	The monolith did not form	The monolith did not form
80	The monolith was formed with back pressure 479 psi	The monolith did not form	The monolith did not form
90	The monolith was formed with back pressure 493 psi	The monolith was start forming	The monolith did not form
100	The monolith was formed with back pressure 527 psi	The monolith was formed with back pressure 485 psi	The monolith did not form
110	The monolith was formed but blocked	The monolith was formed with back pressure 518 psi	The monolith did not form
120	------	The monolith was formed with back pressure 535 psi	The monolith was start forming

130	------	The monolith was formed but blocked	The monolith was formed with back pressure 590 psi
140	------	------	The monolith was formed with back pressure 667 psi
150	------	------	The monolith was formed with back pressure 690 psi
160	------	------	The monolith was formed with back pressure 695 psi
170	------	------	The monolith was formed but blocked

From table (5.1), it can be seen that the monolith was forming after 80 minutes using (90:10)% (v/v) GMA:SMA with back pressure 479 psi and the maximum back pressure was 527 psi after 100 minutes irradiation time. When compared to the GMA-co-LMA-co-EDMA monolithic column with the same ratio, it was found that the GMA:SMA monolithic column was formed at higher irradiation time with higher back pressure because the GMA:LMA has maximum back pressure 482 psi after 90 minutes irradiation time. This would indicate some morphological changes in the monolith related to the increased the alkyl chain length

The irradiation time effect on the (50:50)% (v/v) GMA:SMA was investigated, and the results indicated that the monolith was formed with higher irradiation time 100 minutes irradiation time with back pressure 485 psi, and the highest back pressure was 535 psi after 120 minutes irradiation time. These results can be compared to (90:10)% (v/v) GMA:SMA, as well as the (50:50)% of (v/v) GMA:LMA which gave the maximum pack pressures of 527 psi, and 507 psi after 100 minutes irradiation time respectively.

The effect of irradiation time on the monolithic column that formed using (10:90)% (v/v) of GMA:SMA confirmed the previous experiment results, which indicated that increasing the SMA percentage lead to an increased irradiation time, consequently increasing the back pressure. The maximum back pressure was 695 psi after 160 minutes, however, when the results are compared to the same ratio with GMA:LMA (654 psi after 140 minutes irradiation time), it was found that the GMA:SMA monolith column was formed after longer irradiation time with higher back pressure.

It can be seen from Table (5.1) that the monolith was formed properly between (80-100) minute for the (90:10)% GMA:SMA, (100-120) minute for (50:50)% GMA:SMA, and (130-160) minute for (10:90)% GMA:SMA. The results indicated that the polymer formation time is increased with increasing percentage of the SMA, this may be due to increasing in the steric effects due to the longer aliphatic chains in SMA. The literature has mentioned that the long aliphatic chains of the monomer will reduce the monomer mobility, which in turn effects the termination rate[265]. However, according to chain length dependent termination (CLDT) the termination process is diffusion-controlled, therefore, the length of the growing chains has a high impact on the termination kinetic constant. So far, when the

polymerization process is developed the length of free radical long chains are increased too, leading to a decrease in the mobility of these chains, subsequently the termination kinetic constant will be suppressed and the polymerization process will require a longer time.[266]

More investigations have been carried out to investigate the percentage of SMA and its effect on surface area, and pore size, because the (10:90)% GMA:SMA could exhibit hydrophobic properties over hydrophilic properties. Moreover, the monolithic column could not show clearly mixed-mode mechanism. Therefore, different percentage such as (60, 70, and 80)% of SMA with GMA have been investigated. The irradiation time for each percentage was investigated to determine the optimum irradiation time that could give reasonable back pressure and BET results, the irradiation time for each percentage has been shown in Table (5.2)

Table 5.2 Effect of irradiation time on the monolith formation

Irradiation time (min)	(**40:60)% (v/v) GMA:SMA**	(**30:70)% (v/v) GMA:SMA**	(**20:80)% (v/v) GMA:SMA**
80	The monolith did not form	The monolith was not formed	The monolith was not formed
90	The monolith was start forming	The monolith was not formed	The monolith was not formed
100	The monolith was formed with back pressure 552 psi	The monolith starts forming	The monolith starts forming
110	The monolith was formed with back pressure 560 psi	The monolith was formed with back pressure 660 psi	The monolith starts forming
120	The monolith was formed with back pressure 568 psi	The monolith was formed with back pressure 677 psi	The monolith was formed with back pressure 663 psi
130	The monolith was formed but blocked	The monolith was formed with back pressure 680 psi	The monolith was formed with back pressure 679 psi
140	------	The monolith was formed but blocked	The monolith was formed with back pressure 685 psi
150	------	------	The monolith was formed but blocked

It is clearly seen from Table (5.2) that the monolith was formed between 100-120 minutes with maximum back pressure 568 psi at 120 minutes of irradiation time, which is higher than the monolith that was formed using (50:50)% (v/v) GMA:SMA.

The same concept can be seen when using (30:70)% (v/v) GMA:SMA, the irradiation time was increased with increasing the percentage of SMA. The monolith was formed between 110-130 minutes and the highest back pressure was 680 psi. When it comes to the (20:80)% (v/v) GMA:SMA, the results were as expected, the monolith was formed at higher irradiation time with increasing the SMA percentage, the effective irradiation time that formed the monolith with 685 psi back pressure was 140 minutes.

The results of irradiation time effect showed that after using (50:50)% of GMA:SMA, the irradiation time to form the monolith was increased by 1 minute for each one percent increase in SMA except for the monolith formed using (10:90)% GMA:SMA which does not fit this pattern.

After the monoliths were formed properly with suitable back pressure which means high surface area to increase the binding sites, with reasonable pore sizes to separate small and large molecules. The monoliths washed with ethanol and deionized water, then dried well. The nitrogen adsorption analysis was investigated using a BET analyzer for the monolith formed at 100 minute for (90:10)%, 120 minute for (50:50)%, 120 minutes for (40:60)%, 130 minutes for (30:70)%, 140 minutes for (20:80)% and 160 minute for (10:90)% of GMA:SMA respectively. All these results were tested to determine the optimum surface area, and pore size of the monolithic columns that can be used for LC separation. The BET analyzer results for the monoliths are shown in Figure (5.1)

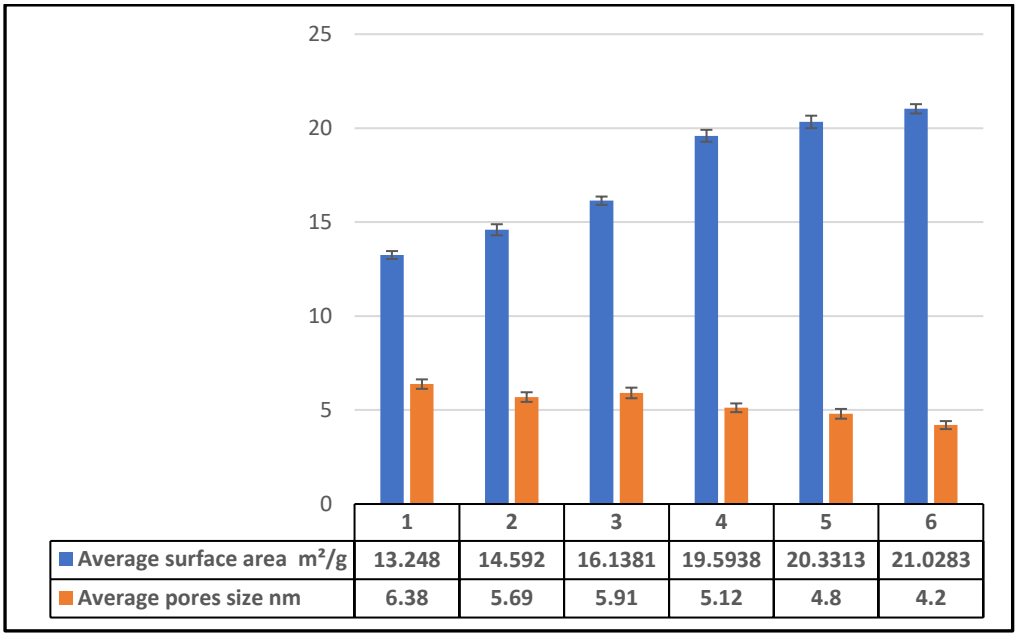

	1	2	3	4	5	6
Average surface area m²/g	13.248	14.592	16.1381	19.5938	20.3313	21.0283
Average pores size nm	6.38	5.69	5.91	5.12	4.8	4.2

Figure 5.1 The morphological properties for glycidyl methacrylate-co-stearyl methacrylate-co-ethylene dimethacrylate monolithic columns, 1(90:10)%, 2(50:50)%, 3(40:60)%, 4(30:70)%, 5(20:80)% and 6(10:90)% of GMA:SMA, SD (n=3).

It can be seen from Figure (5.1) that the average surface area was increased with increasing of SMA ratio, this could be due to the long alkyl chain that can provides more surface area when compared to the LMA monomers that have C12 chain in GMA-co-LMA-co-EDMA monolith. Thus, the number of mesopores and micropores will be increased with increase the surface area, which lead to increase the interactions between the surface of the monolith with the sample and enhancing the separation process.

It can be seen that the higher average surface area of the monolithic columns between 19.5938-21.0283 m^2 g^{-1}, was achieved with a reduction in the average pores size was 5.12, 4.80, and 4.2 nm for (30:70, 20:80, and 10:90)% of GMA:SMA respectively. However, the monolithic column prepared using

(30:70)% of GMA:SMA has been chosen for LC separation, due to the higher average pores size compared to the (20:80, and 10:90)% of GMA:SMA, which can give the monolith higher permeability and less pack pressure. In addition, the (30:70)% is less hydrophobic and more hydrophilic properties. In addition it has higher average surface area than the monoliths prepared using (90:10)%, (50:50)%, and (40:60)%, that can provide high interactions with the analyte molecules due to more binding sites. Furthermore, it could be more probability to prepare mixed mode monolithic columns that can be used to separate different samples.

5.2 Permeability and porosity of the monolith

The permeability of (30:70)% (v/v) GMA:SMA monolithic column was examined by evaluating the backpressure generated from HPLC system pump using milli-q water at different flow rates through the monolith.[200] The results were shown in Figure (5.2)

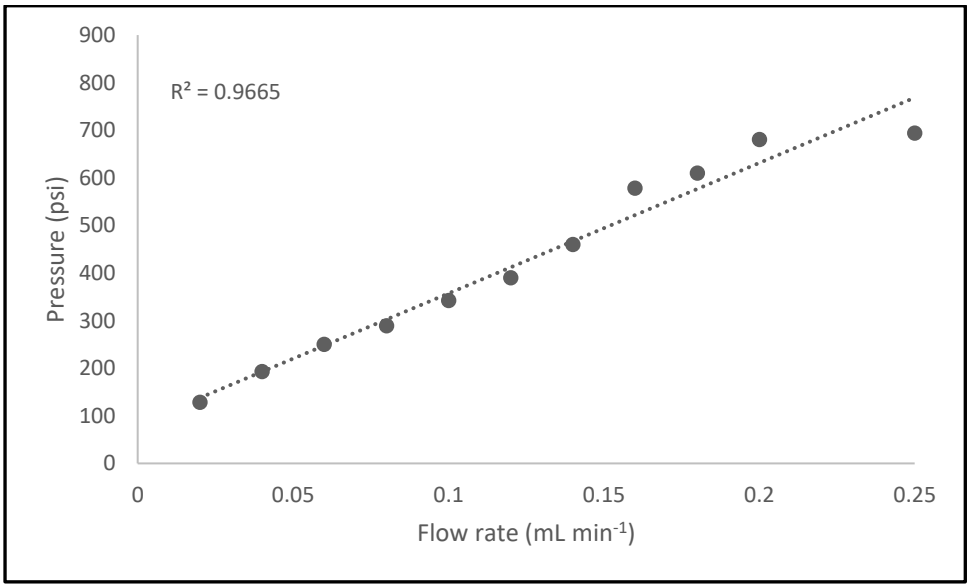

Figure 5.2 The relationship between the back pressure and the flow rate for the glycidyl methacrylate-co- stearyl methacrylate-co-ethylene dimethacrylate monolithic column.

It can be seen from Figure (5.2) that the back pressure increased with increasing flow rate up to 0.25 mL min^{-1}, the pressure was stable at the value of 680 psi with flow rate 0.2 mL min^{-1}. After that the pressure was increased slightly from 680 psi to 694 psi when the flow rate was 0.25 mL min^{-1} and system leaked, it could be the porosity of the monolith, or the stainless-steel fitting did not grip the borosilicate tube sufficiently causing leakage above 0.2 mL min^{-1} flow rate. However, the 0.2 mL min^{-1} was used in the further experiments.

The monolithic column porosity was calculated as described earlier in section 2.9.3. It was found that the porosity of the glycidyl methacrylate-co-stearyl methacrylate-co-ethylene dimethacrylate monolithic column was 0.0716.

5.3 SEM analysis of glycidyl methacrylate-co- stearyl methacrylate-co-ethylene dimethacrylate monolithic column (30% GMA, 70% SMA)

The SEM image for GMA-co-SMA-co-EDMA monolithic column is shown in Figure (5.3). It can be clearly seen that the structure of the monolith is a network of interconnected large flow-through pores, it can be seen that these pores are bigger than that noticed in GMA-co-LMA-co-EDMA monolithic columns. Therefore, the porosity and permeability of the GMA-co-SMA-co-EDMA were enhanced due to these macro pores which are controlling the permeability of the column by reducing the backpressure. Moreover, there are other types of pores which have different functions these pores are mesopores, and micro pores, mesopores are responsible for increasing the surface area of the monolith and increasing the load ability of the monolith, while the micro pores play a crucial role in the separation process. Other investigations using FTIR and ^{1}HNMR have been used to further characterize the polymer structure.

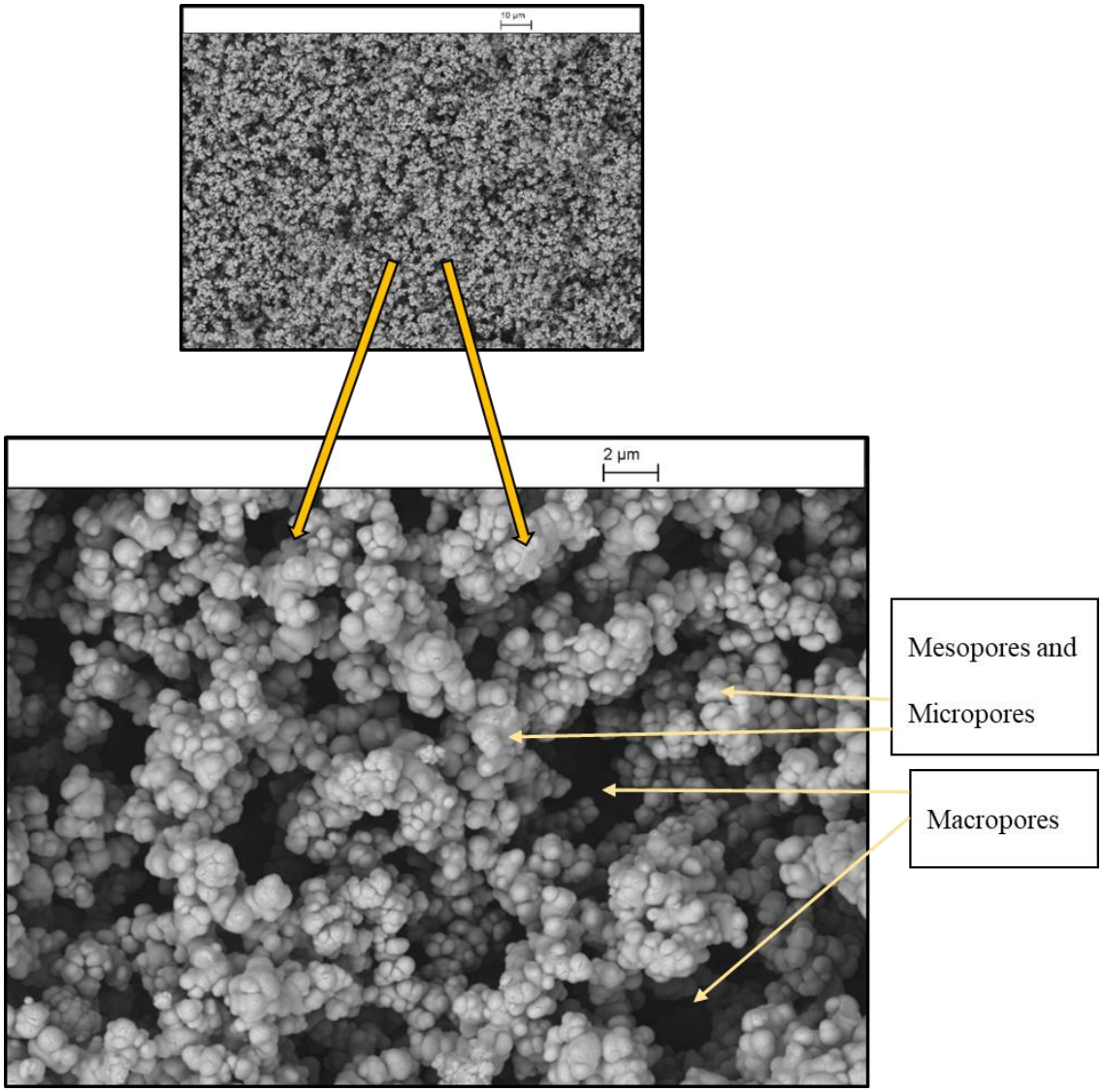

Figure 5.3 SEM image for glycidyl methacrylate-co- stearyl methacrylate-co-ethylene glycol dimethacrylate monolithic column.

5.4 FTIR analysis

FTIR analysis was used to characterize the main peaks in the monomers and the co-polymer to indicate the polymer formation.

Glycidyl methacrylate FTIR spectrum showed the three main prominent transmittance peaks that could be used to indicate to participate of GMA in polymerization reaction. The three peaks are 1717.53 cm^{-1} of (C=O),1637.94 cm^{-1} for (C=C), and 907.79 cm^{-1} for (epoxy group) which result from the vibrational stretching of these functional groups.[178] The FTIR spectrum is shown in Figure (5.4).

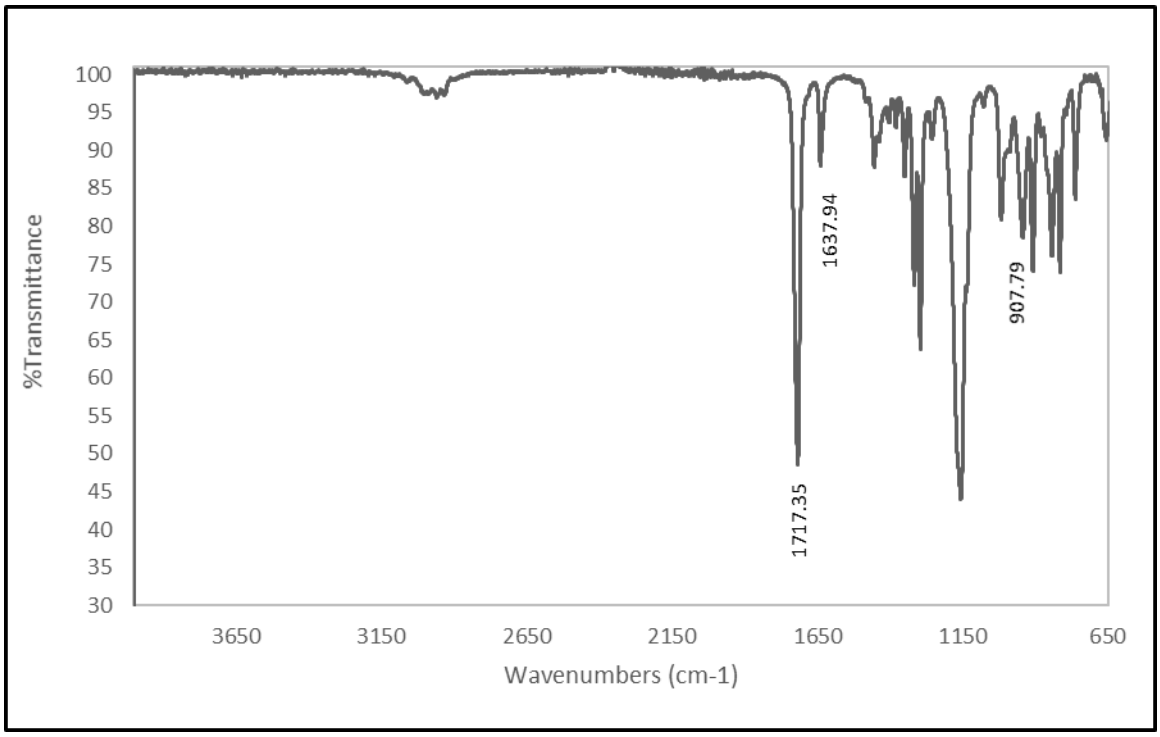

Figure 5.4 FTIR spectrum of GMA from 4000 cm^{-1} to 650 cm^{-1}.

For stearyl methacrylate the two most prominent transmittance peaks are 1720.59 cm^{-1} (C=O) and at 1639.13 for (C=C), the FTIR spectrum is shown in Figure (5.5).

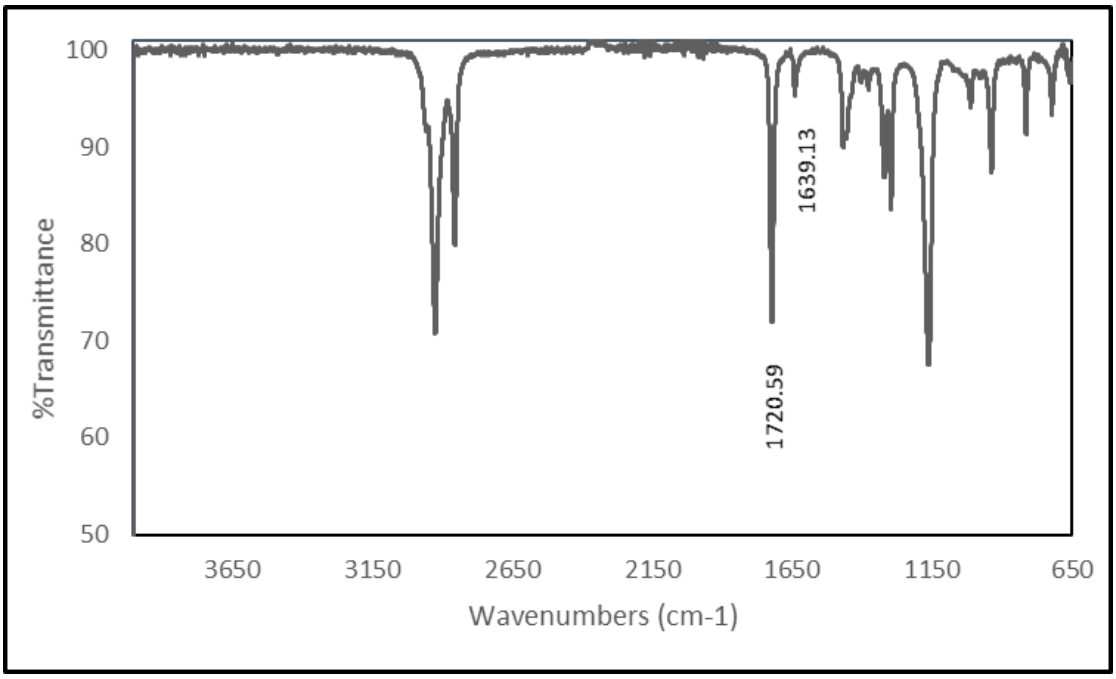

Figure 5.5 FTIR spectrum of SMA from 4000 cm^{-1} to 650 cm^{-1}.

Specific transmittance peaks for ethylene dimethacrylate at 1637.86 cm^{-1} and 1716.89 cm^{-1} indicate the presence of (C=C) and (C=O) groups, the FTIR spectrum is shown in Figure (5.6).

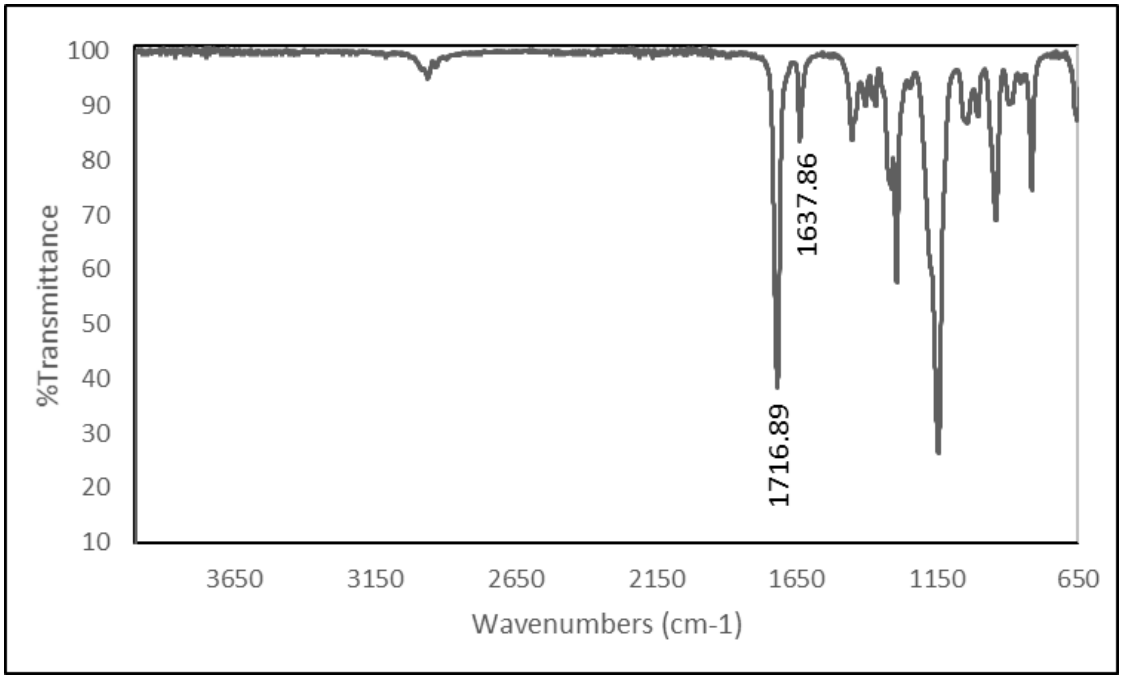

Figure 5.6 FTIR spectrum of EDMA from 4000 cm^{-1} to 650 cm^{-1}.

On the other hand, FTIR analysis results of glycidyl methacrylate-co-stearyl methacrylate-co-ethylene glycol dimethacrylate polymer showed two peaks at 1726.41 cm^{-1} for (C=O) group and slight shift in epoxy group toward 910.07 cm^{-1}. While (C=C) peak a round 1637 cm^{-1} has disappeared as can be seen in Figure (5.7), this is a good evidence for the formation of the polymer by incorporation of both monomers and cross-linker using (C=C) bonds.[178]

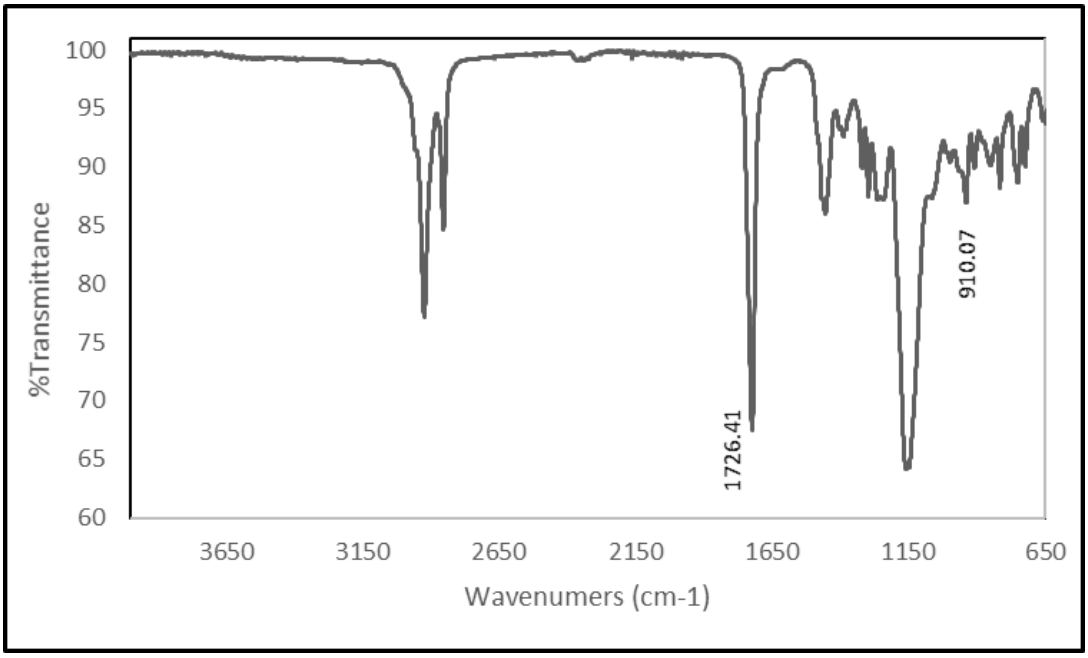

Figure 5.7 FTIR spectrum of GMA-co-SMA-co-EDMA monolithic column from 4000 cm^{-1} to 650 cm^{-1}

The ^{1}HNMR analysis have been investigated to demonstrate the formation of the monolith. The results are shown that the ($C=CH_2$) bonds around (5-6) ppm in the monomers and cross linker have disappeared in the polymer ^{1}HNMR spectrum, and appeared another band around (4.0-4.02) ppm which is corresponding to changing ($RCH=CH_2$) to (R_2CH-CH_3) that indicated the formation of the polymer via the double bonds reaction. Moreover, the chemical shift at (3.64) ppm is attributed to the epoxy group, means the epoxy group did not affect after the polymerization. These results are closed to the ^{1}HNMR spectrum for similar compounds.[194]

5.5 Applications of glycidyl methacrylate-co-stearyl methacrylate-co-ethylene glycol dimethacrylate monolithic column.

Glycidyl methacrylate-co-stearyl methacrylate-co-ethylene glycol dimethacrylate monolithic columns was prepared using the method described in section 2.1.1 and 2.1.2 and monomers ratio was (30:70)% of GMA:SMA and irradiation time 120 minute. The epoxy ring was opened to form diol groups that can increase the hydrophilic properties of the monolithic column using 1 M hydrochloric acid that was pumped at 5µL min^{-1} for 3 hours. Then, the monolithic column was kept in a column block heater at 60 ºC for 6 hours[206]. The FTIR analysis results showed that the peak at 910.07 cm^{-1} for the epoxy ring in the monolithic column had disappeared and a new peak at 3237.51 cm^{-1} was formed which indicate that the (-OH) was formed and the epoxy ring was opened as can be seen in Figure (5.8).

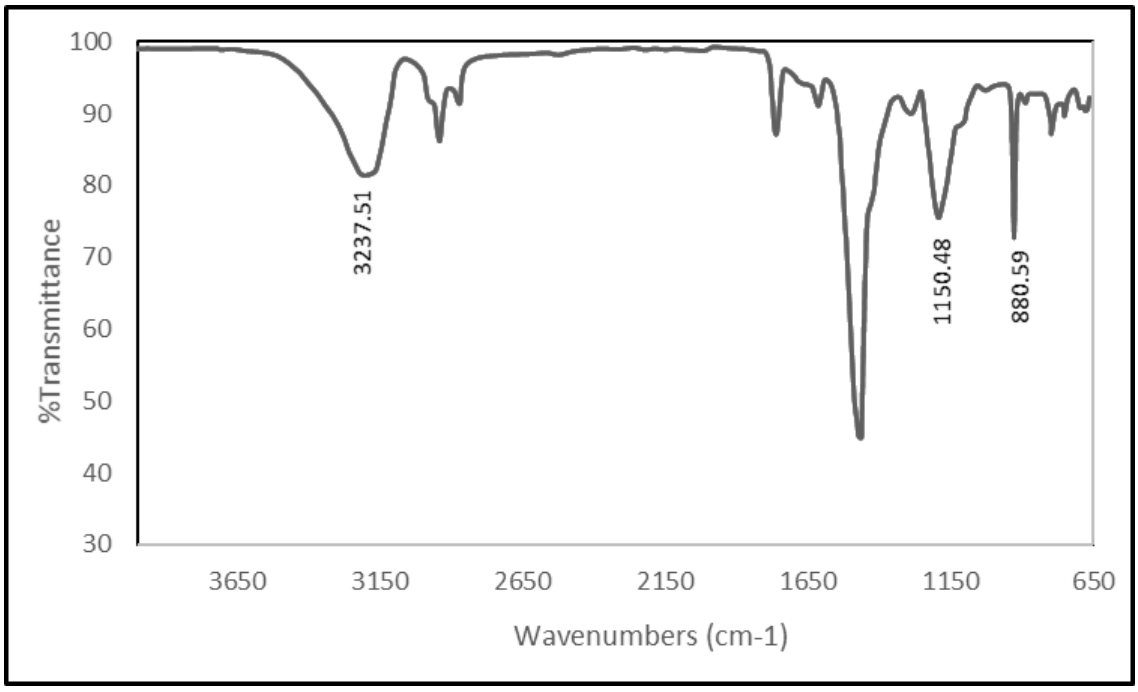

Figure 5.8 FTIR spectrum of GMA-co-SMA-co-EDMA monolithic column after opening the epoxy ring from 4000 cm^{-1} to 650 cm^{-1}

The monolith that formed inside the borosilicate tube is shown in Figure (5.9), it was connected to HPLC system and used in the further experiments.

The reproducibility of the monolithic column preparation is a significant factor that could affect the monolith separation behavior, therefore, three monolithic columns were prepared from three different polymerization mixtures. These monolithic columns were examined using SEM, nitrogen adsorption analysis using BET analyzer, and FT-IR, the results indicated that there were no significance differences between the prepared columns.

This column was tested with different samples, such as hydrophobic, hydrophilic, peptides and proteins, three times (n=3) each for more reproducibility to investigate the separation ability as a mixed mode column for LC separation

Different solvents have been used such as acetonitrile, methanol, ethanol, and 2-propanol in addition to the deionized water to get fine separation, the result showed that acetonitrile and water was the best solvent compared with the others in terms of the peak width and separation ability, therefore these solvents were used in all the flowing experiments. In addition, all tests were repeated three times for more reproducibility and accuracy.

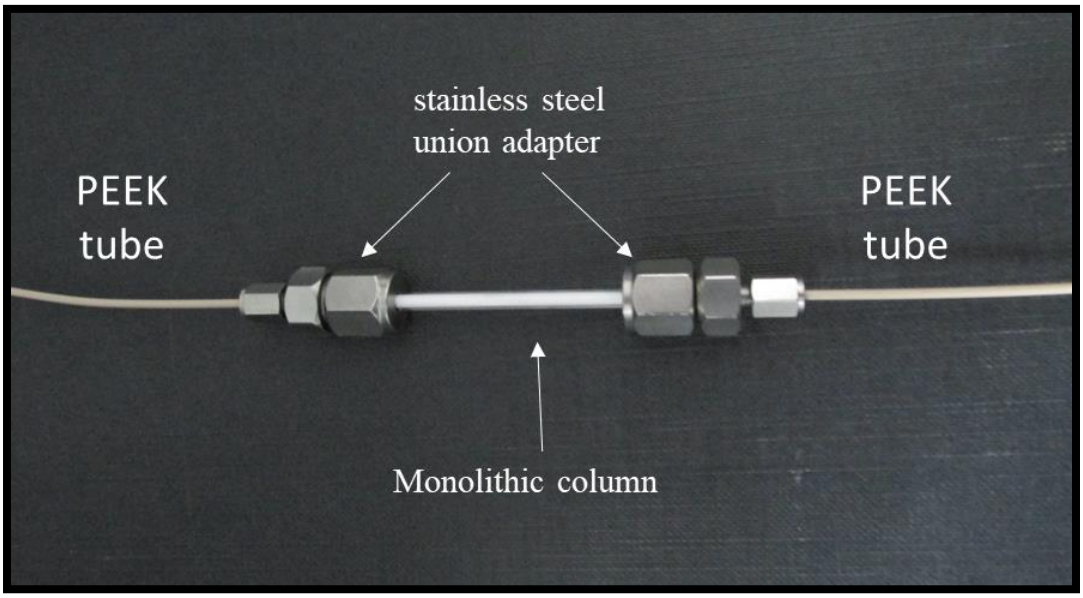

Figure 5.9 The GMA-co-SMA-co-EDMA monolithic column that was formed inside the borosilicate tube and connected to HPLC system.

5.5.1 Separation of a mixture of hydrophobic compounds

The GMA-co-SMA-co-EDMA monolithic columns were investigated to separate four different compounds (toluene, naphthalene, anthracene, and pyrene), the results are shown in Figure (5.10)

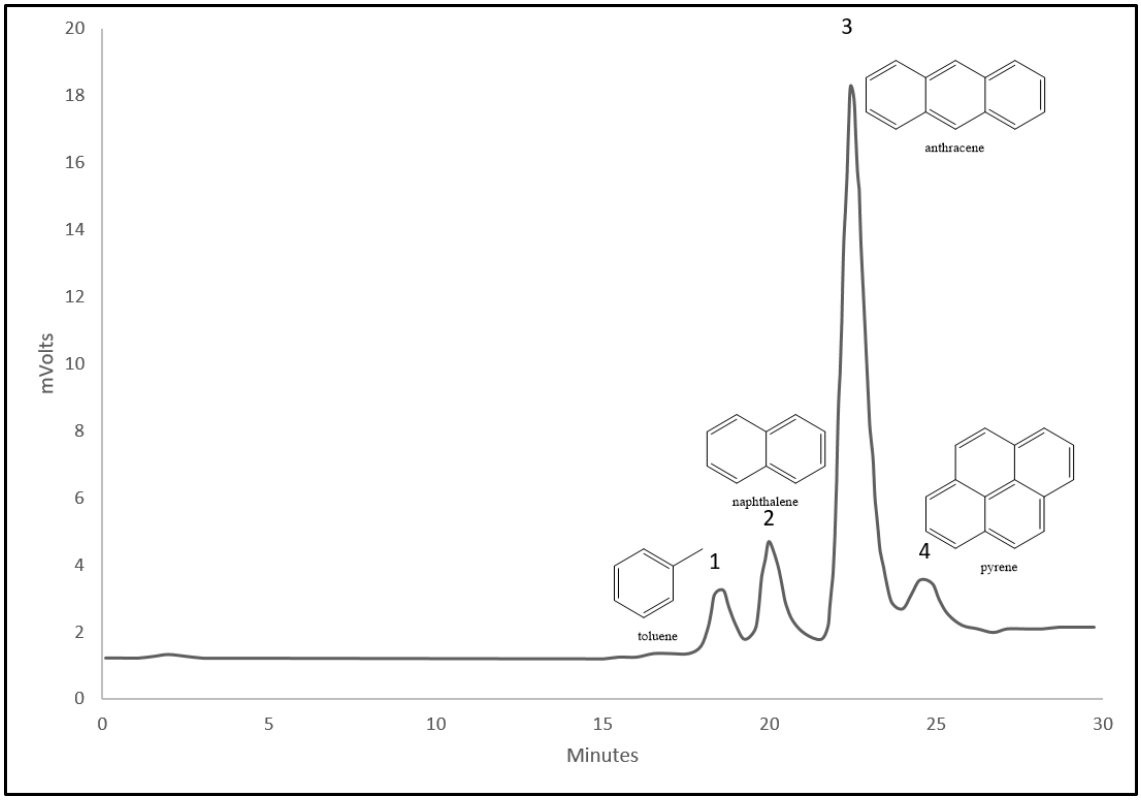

Figure 5.10 Chromatogram of a mixture of (1) toluene, (2) naphthalene, (3) anthracene, and (4) pyrene, 10^{-5} M mixture of each with gradient no. (5) the injection volume (2.5 µL), and the detection wavelength 254 nm.

The separation of four hydrophobic compounds was successfully achieved using GMA-co-SMA-co-EDMA monolithic column as shown in Figure (5.10). The separation for a mixture of four hydrophobic compounds was better than that obtained with GMA-co-LMA-co-EDMA (10:90)% GMA:LMA monolithic columns. According to the plate theory, when the N value increases the efficiency of the column is increased due to increasing the interactions between the solute and

the stationary phase. Therefore, the high surface area of the GMA-co-SMA-co-EDMA monolithic column can increase the N value due to increase the binding sites that allow more interactions between the stationary phase and the samples, the N and Rs values were calculated in Table (5.4).

In addition, according to the van Deemter concept, the H value should be kept to minimum to reduce the band broadening and get fine separation. This can be obtained by decreasing the resistance to mass transfer (C-term) between the mobile and stationary phase, although reducing the retention factor of the analytes.[257] Gradient analysis system gradient no (5) was used instead of isocratic system because it was mentioned elsewhere that the isocratic system could not provide fine separation if the monolithic column does not have enough mesopores.[191] However, the solute molecules are equilibrated between the mobile phase and stationary phase, therefore, to increase the diffusion of the solute molecules to the pores of the stationary phase the amount of less polar solvent should be increased to enhance the mass transfer by reducing the retention factor of the analytes.[257] The gradient program was obtained to increase the organic solvent percentage to see if this allows faster desorption of the molecules from the monolith surface and reduces band broadening. The flow rate for the gradient analysis was 0.2 mL min^{-1} which it was the maximum flow rate that could be used with this column to reduce longitudinal diffusion of the solute molecules (B-term) in van Deemter equation.

The results were showed that the four hydrophobic compounds can be separated according to the hydrophobicity order with different peaks height. The main reason is the detector wavelength was 254 nm and each compound have different maximum absorption wave length depending on the functional groups in

each compound, therefore this difference in the peak height is due to the difference in the wavelength of maximum absorption.

Table 5.3 Solvent composition of gradient analysis no. (5)

Time/ min.	**Water %**	**Acetonitrile %**	**Flow rate mL min^{-1}**
0:00	95	5	0.2
3:00	95	5	0.2
15:00	20	80	0.2
26:00	20	80	0.2
27:00	95	5	0.2
30:00	95	5	0.2

Table 5.4 The average number of theoretical plates (N) and the resolution value (Rs) for toluene, naphthalene, anthracene, and pyrene with HILIC/RP monolithic columns (n=3)

N	3215
Rs for Toluene and Naphthalene	1.41
Rs for Naphthalene and Anthracene	1.70
Rs for Anthracene and Pyrene	0.59

The literature mentioned that the resolution value (R) when it was 0.8 can be consider acceptable value, while for the quantification analysis it should be more than 1.0 and it would be significant at 1.5.[223] It can be noticed from Table (5.4) that Rs values were less than 0.8 for the anthracene and pyrene, it was 0.5880 due to the band broadening of the pyrene which could be reduced by increasing the percentage of the acetonitrile that could increase the desorption rate between

the stationary phase and the pyrene molecules to give fine separation. Others Rs values were near to 1.5 for toluene and over 1.5 for naphthalene and anthracene, these results could indicate that the GMA-co-SMA-co-EDMA could be used to separate four hydrophobic compounds in single run.

5.5.2 Separation of pharmaceutical compounds

Separation of three pharmaceutical compounds caffeine, paracetamol, and ibuprofen was investigated using GMA-co-SMA-co-EDMA monolithic column. The prepared monolithic column with hydroxyl groups on the surface of the monolith that formed due to opening the epoxy ring of GMA can give hydrophilic properties beside the hydrophobic properties. Therefore, the monolithic column could be used as mixed-mode monolithic column RP/HILIC.

Hydrophilic interaction liquid chromatography (HILIC) can be defined as "partitioning between the (hydrophobic) mobile phase and a layer of mobile phase enriched with water and partially immobilized on the stationary phase" [267]. However, the retention of the analytes solutes are decreased when the polarity of the mobile phase is increased, while, it will increase with increasing of the polarity of the analyte.[268]

Gradient analysis that shown in Table (5.9) was used to achieve good separation of the three compounds, the results are shown in Figure (5.11)

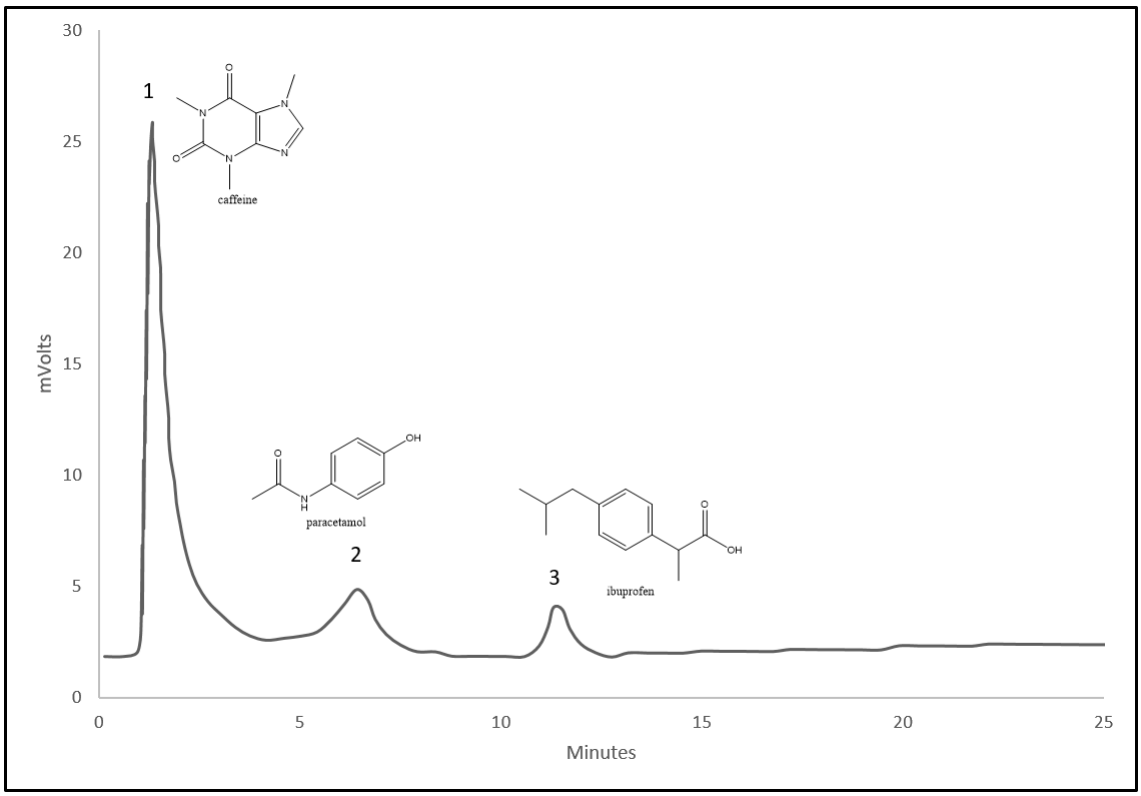

Figure 5.11 Chromatogram of a mixture of (1) caffeine, (2) paracetamol, and (3) ibuprofen, 10^{-5} M mixture of each with gradient no. (6) the injection volume (2.5 µL), and the detection wavelength 254 nm.

Table 5.5 Solvent composition of gradient analysis no.(6)

Time/ min.	Water %	Acetonitrile %	Flow rate mL/min
0:00	25	75	0.2
2:00	25	75	0.2
16:00	90	10	0.2
21:00	90	10	0.2
22:00	25	75	0.2
25:00	25	75	0.2

From Figure (5.11) it can be seen that, all the pharmaceutical compounds separated successfully by using this column and using gradient analysis, the peaks were separated with increasing the percentage of water, this could indicate a HLIC mechanism due to hydrophilic interactions between the polar surface of the monolithic column and the compounds that have hydrophilic functional groups. On the other hand, paracetamol, and ibuprofen have benzene ring in addition to aliphatic hydrocarbon groups in ibuprofen. These groups could be interacted with the hydrophobic surface of the monolith by hydrophobic interactions leading to increase the retention time of each compounds as can be seen in Figure (5.11) by RP mechanism. Therefore, it could be concluded that the mechanism could be mixed-mode mechanism. The N and Rs values are shown in Table (5.16)

Table 5.6 The average number of theoretical plates (N) and the resolution value (Rs) for phenacetin, codeine, and anthracene with HILIC/RP monolithic columns (n=3)

N	1147
Rs Caffeine and Paracetamol	2.19
Rs Paracetamol and Iuprofen	2.73

5.5.3 Separation of hydrophobic and hydrophilic compounds

A mixture of hydrophobic and hydrophilic compounds was tested using GMA-co-SMA-co-EDMA monolithic column, to further investigate the separation ability of this column, results are shown in Figures (5.12) using the gradient shown in Table (5.7)

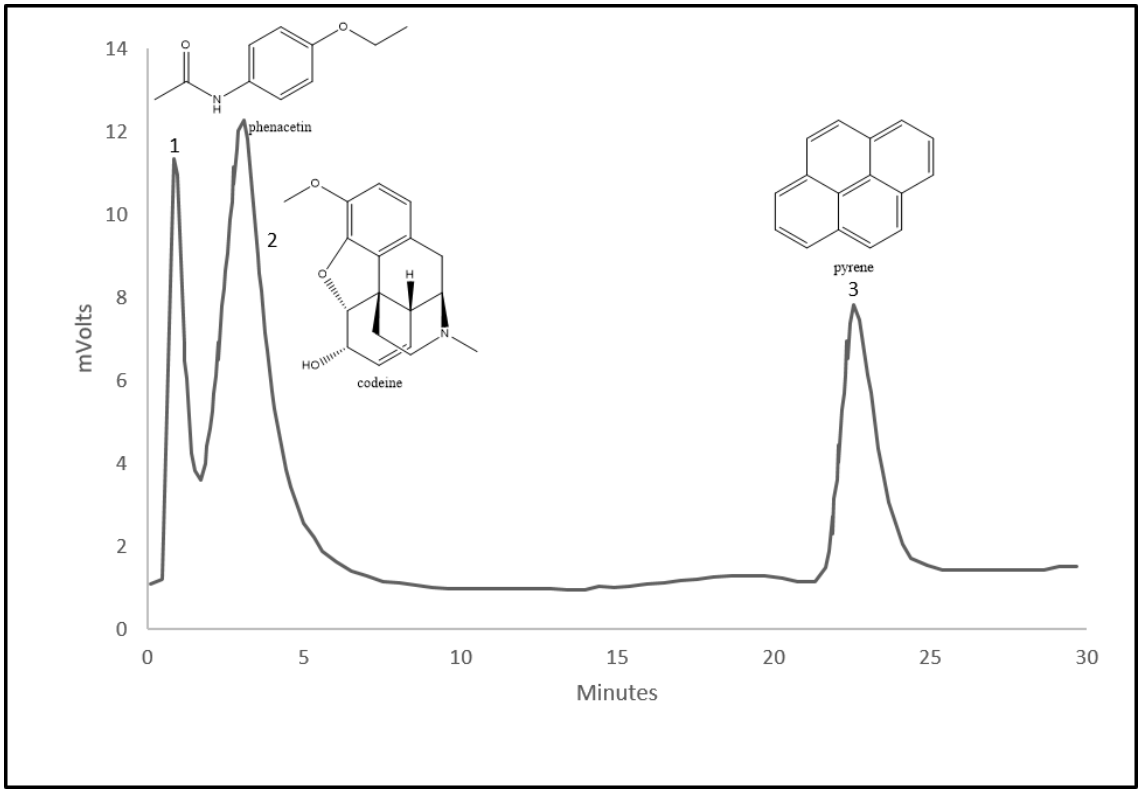

Figure 5.12 Chromatogram of a mixture of (1) phenacetin, (2) codeine, and (3) pyrene, 10^{-5} M mixture of each with gradient no. (7) the injection volume (2.5 µL), and the detection wavelength 254 nm.

Table 5.7 Solvent composition of gradient analysis no.(7)

Time/ min.	Water %	Acetonitrile %	Flowrate mL/min
0:00	90	10	0.2
3:00	90	10	0.2
15:00	10	90	0.2
25:00	10	90	0.2
27:00	90	10	0.2
30:00	90	10	0.2

This experiment showed that the GMA-co-SMA-co-EDMA monolithic column has a considerable ability to separate three different compounds that have hydrophobic and hydrophilic properties. It can be seen from Figure (5.12), the hydrophilic compounds depending on log P (phenacetin log P 1.58, and codeine log P 1.19). they were eluted early and did not follow the hydrophobicity order because phenacetin is more hydrophobicity than codeine[259] was eluted with high percentage of water. While, the hydrophobic compound was eluted later due to high interactions between the hydrophobic surface and hydrophobic compound, which needs more time to desorb the analyte molecules from the surface of the monolith. Besides, the two hydrophilic compounds are separated due to hydrophilic surface, this suggests that this column works as a mixed-mode column. The number of theoretical plate (N) and the resolution (Rs) were calculated for each peak, the results are shown in Table (5.8)

Table 5.8 The average number of theoretical plates (N) and the resolution value (Rs) for phenacetin, codeine, and anthracene with HILIC/RP monolithic columns (n=3)

N	2897
Rs for Phenacetin and Codeine	0.76
Rs for Codeine and Pyrene	6.25

A further test to separate a variety of compounds was carried out using cyclohexanol and cumene which is more hydrophobic compound than cyclohexanol using GMA-co-SMA-co-EDMA monolith column, the results are shown in Figure (5.13)

It is clearly seen that the two compounds can be separated as showed in Figure (5.13). However, the sequence of elution was followed the hydrophobicity order, that could be due to the 70% of SMA which could allow more interactions with the hydrophobic part in cyclohexanol compared to hydrophilic groups that could interact with the polar surface area on the monolithic. Moreover, the cyclohexanol peak was broader than the cumene, it could be the cyclohexanol molecules were diffused inside the pores of the monolithic surface and could interact with the hydrophobic and hydrophilic sites on the surface of the monolithic column. Therefore, the retention factor was increased and the mass transfer between the surface of the monolith and the mobile was decreased, which lead to retard the cyclohexanol molecules more on the surface and delay the elution of the molecules which causing the band broadening.

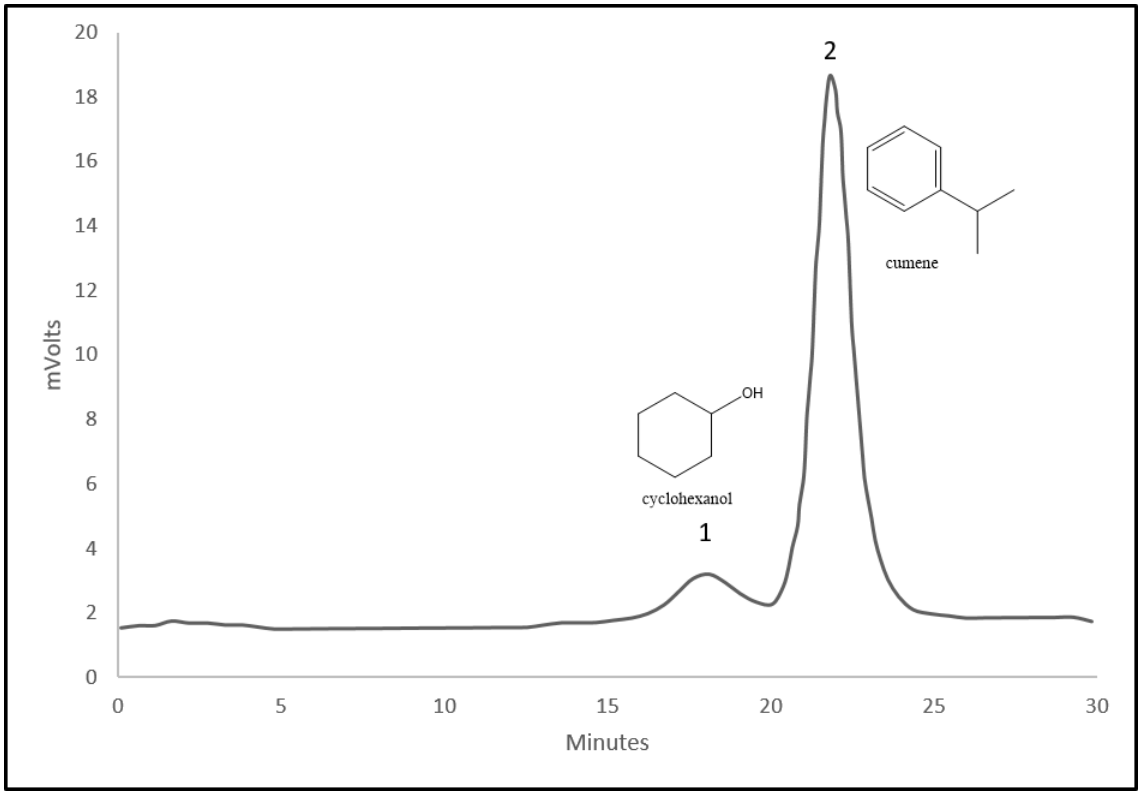

Figure 5.13 Chromatogram of a mixture of (1) cyclohexanol, and (2) cumene, 10^{-5} M mixture of each with gradient no. (7) the injection volume (2.5 µL), and the detection wavelength 254 nm

5.5.4 GMA-co-SMA-co-EDMA monolithic column with digested cytochrome C

After the success in separation of small molecules using the GMA-co-SMA-co-EDMA monolithic column, the work was carried on investigating the ability of the monolithic column to separate large molecules such as peptides and proteins. Commercial tryptic digested cytochrome C was utilized to test the separation efficiency of GMA-co-SMA-co-EDMA monolithic column, using gradient analysis specified in Table (5.9), the results are shown in Figure (5.14)

Table 5.9 Solvent composition of gradient analysis no.(8)

Time/ min.	Water %	Acetonitrile %	Flowrate mL/min
0:00	95	5	0.2
5:00	95	5	0.2
20:00	10	90	0.2
25:00	10	90	0.2
26:00	95	5	0.2
30:00	95	5	0.2

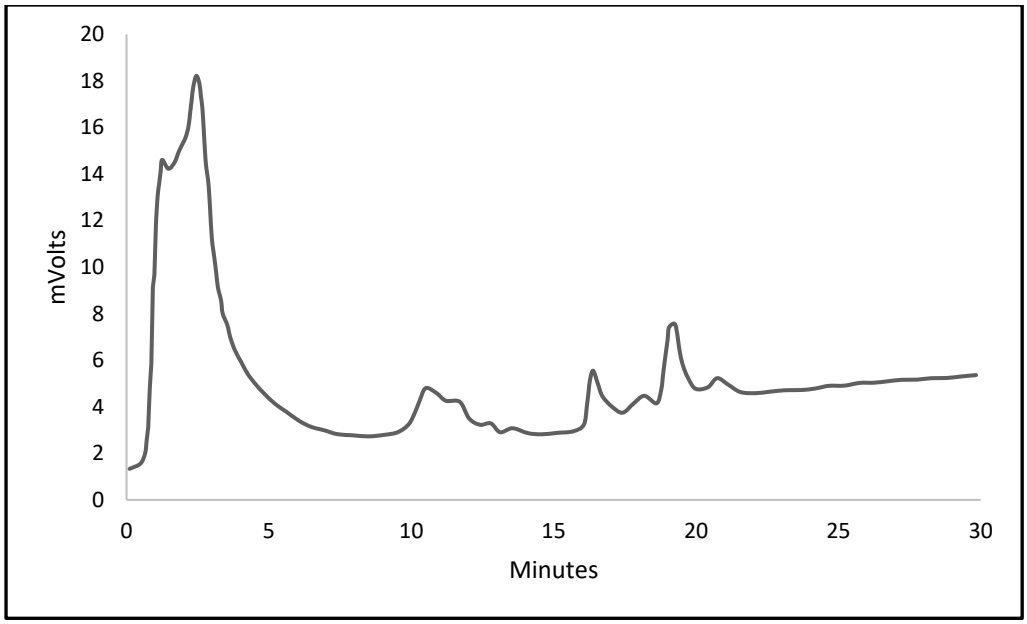

Figure 5.14 Chromatogram of commercial tryptic digested cytochrome C with gradient no. (8) the injection volume (2.5 µL), and the detection wavelength 254 nm.

It can be seen from Figure (5.14), the tryptic digested cytochrome C showed about 10 peaks it was tested using GMA-co-SMA-co-EDMA monolithic column. it could be due to different peptides are produced that could have the same amino

acids sequence when the protein is digested. A gradient analysis system was used as shown in Table (5.9) to separate these peptides because it was pointed in the literatures that the retention factors of the peptides are dependent on the mobile phase composition. However, the logarithm of the retention factor varies linearly with time in a gradient analysis according to the linear solvent strength (LSS) model was applied.[269]

The results were showed that the monolithic column has better separation efficiency compared to GMA-co-LMA-co-EDMA monolithic column, when the gradient analysis was used. This may be due to the columns ability to retain these peptides for different retention times. Yet, the base line separation was not obtained with most of the fragments. It could be the peptides were diffused inside the pores on the surface of the monolith, and the desorption rate could be lower than the diffusion rate, which lead to increases the retention factors by decreasing the mass transfer from the stationary phase to the mobile phase, causing the band broadening. In addition, the complexity of the trypsin digested cytochrome C to separate.

5.5.5 Proteins investigation by GMA-co-SMA-co-EDMA monolithic column

Proteins separation was investigated by GMA-co-SMA-co-EDMA monolithic column, using different proteins such as cytochrome c, insulin, myoglobin, and lysozyme. However, all the results showed that the monolithic column exhibits the same behavior with all proteins because all proteins have the same retention time using isocratic or gradient analysis, therefore it could not separate a mixture of these proteins properly, the results for cytochrome c, and insulin are shown in Figures (5.15) and (5.16).

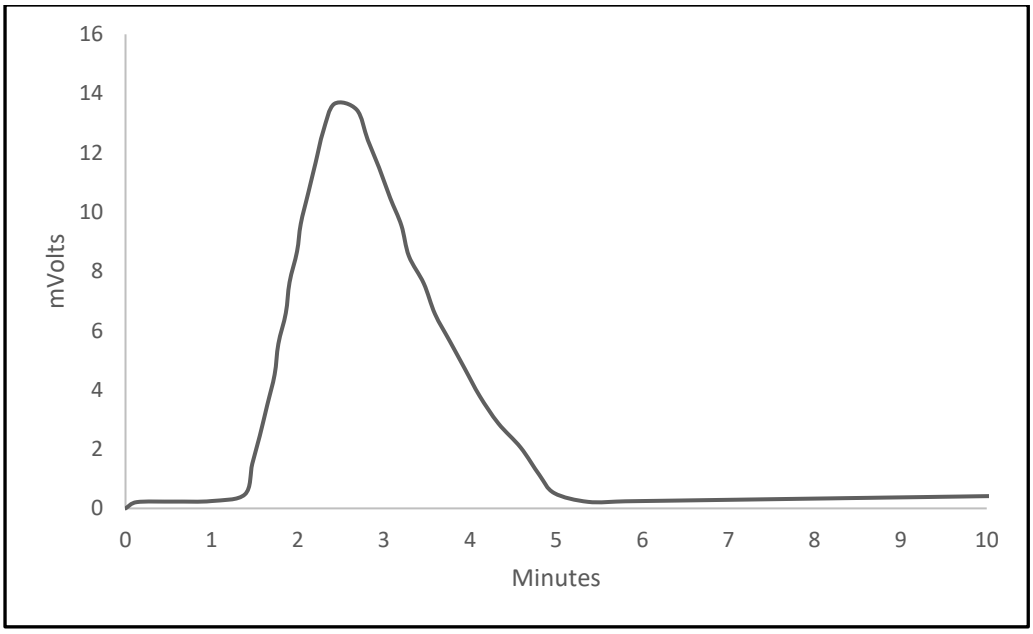

Figure 5.15 Chromatogram of insulin 10^{-5} M, with gradient no. (8) the injection volume (2.5 µL), and the detection wavelength 254 nm.

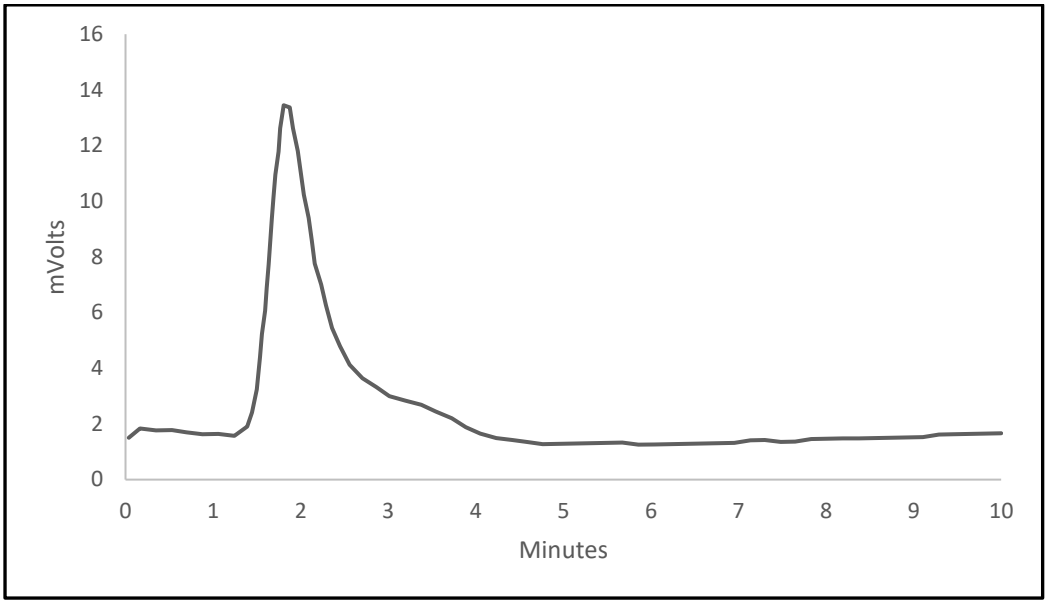

Figure 5.16 Chromatogram of cytochrome c insulin 10^{-5} M, with gradient no. (8) the injection volume (2.5 µL), and the detection wavelength 254 nm.

From Figures (5.15) and (5.16), it can be concluded that using gradient analysis method to obtain significant separation was not successfully achieved. However, proteins are eluted at the same retention time in each experiment. To explain that, there is a likely reason for that, it could be the surface area for this monolithic column is not enough to capture of proteins, because the number of meso and micro pores on the surface area are low compared with the size of proteins therefore, all the proteins are eluted quickly.

5.6 Mixed mode evidence

Mixed mode behavior for GMA-co-SMA-co-EDMA monolithic column was investigated and proven using GMA-co-SMA-co-EDMA monolithic column, and SMA-co-EDMA monolithic column. Same mixture of hydrophilic and hydrophobic compounds (phenacetin, codeine, and pyrene) that used in the previous experiment in section (5.6.3) were used with the same analysis conditions. The results were shown in Figures (5.17) and (5.18).

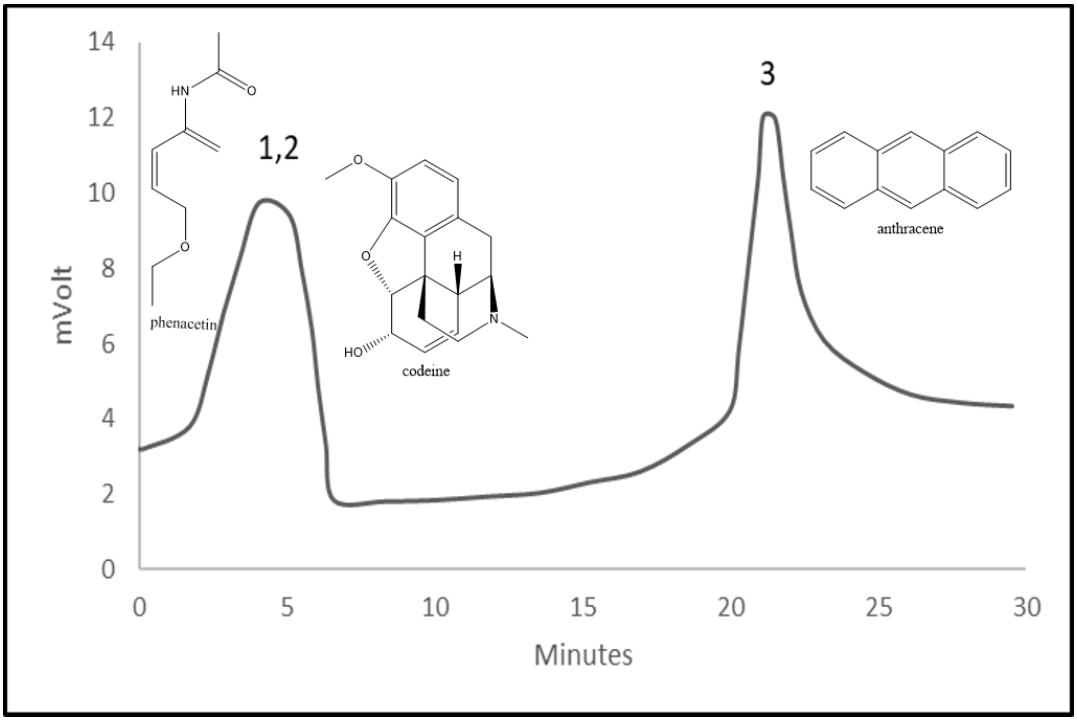

Figure 5.17 Chromatogram of a mixture of (1) phenacetin, (2) codeine, and (3) anthracene, 10^{-5} M using SMA-co-EDMA monolithic column, with gradient no. (7) the injection volume (2.5 µL), and the detection wavelength 254 nm.

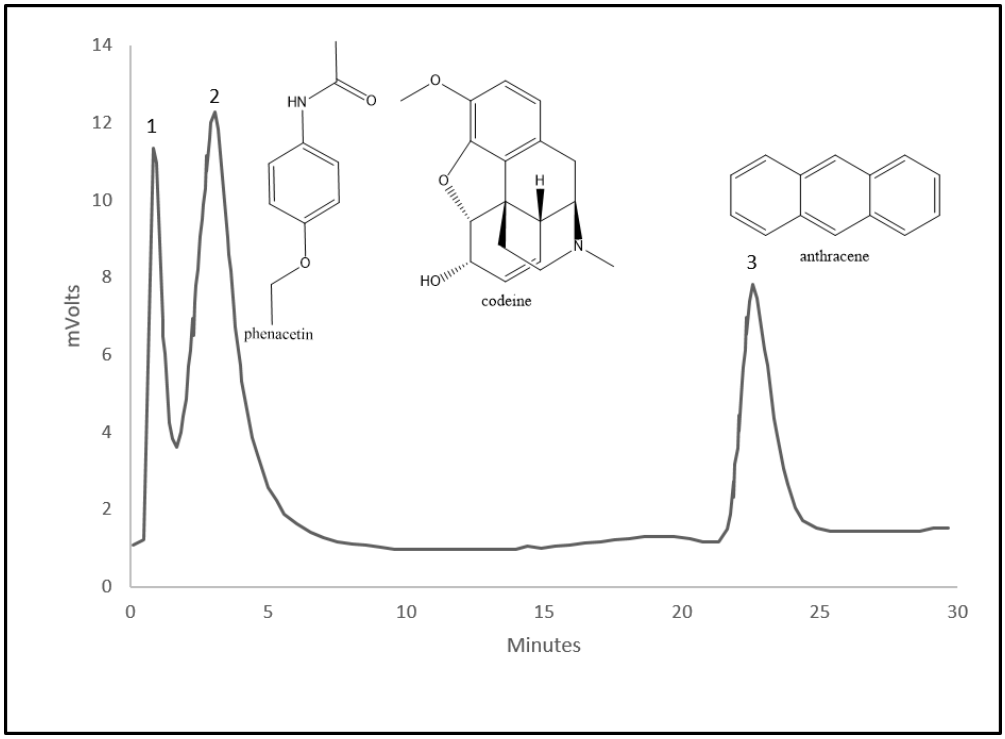

Figure 5.18 Chromatogram of a mixture of (1) phenacetin, (2) codeine, (3) anthracene 10^{-5} M using GMA-co-SMA-co-EDMA monolithic column, with gradient no. (7) the injection volume (2.5 µL), and the detection wavelength 254 nm.

It can be clearly seen from Figures (5.17) and (5.18), there is a significant difference between the two figures, firstly, in Figure (5.17) there are two peaks the first one was a broad peak for codeine and phenacetine at 4.8 min, the second peak was pyrene at 24.8 min. Whereas, in Figure (5.18) the number and the retention time of the peaks are different, because there are three peaks for all the compounds, they are 0.9 min for phenacetine, 3.2 min for codeine, and 23.1 min for anthracene. In addition, the peak shape was broad in Figure (5.17), whereas, in Figure (5.18) it was sharper. All these results showed that each column has different chromatographic properties. However, the SMA-co-EDMA monolithic column was acted as a hydrophobic column due to the elution order

was followed the hydrophobicity order codeine, phenacetin, and pyrene. In addition it has a hydrophobic mechanism and properties. While, the GMA-co-SMA-co-EDMA was acted as a mixed mode monolithic column due to the elution order was not followed the hydrophobicity order because phenacetin was eluted before codeine. That can indicate that the monolithic column has HILIC mode due to diol group generated from opening the epoxy ring for GMA and RP mode that comes from SMA. Consequently, the mechanism and the properties for the GMA-co-SMA-co-EDMA monolithic column is a mixed mode mechanism.

To summarize the previous results, it can be said that the GMA-co-SMA-co-EDMA monolithic columns were prepared using different ratios of GMA:SMA (90:10)%, (50:50)%, (40:60)%, (30:70)%, (20:80), and (10:90)%. The nitrogen adsorption analysis using BET analyzer results showed that the average surface area of the monoliths was increased with increasing the ratio of SMA.

The (30:70)% of the GMA:SMA was chosen in the all experiments because the average surface area of the monolith was higher than other monoliths that formed using GMA:SMA with lower ratio. While, above the (30:70) ratio the average surface area of the monoliths was increased steadily. So far, these columns have not been choosen because, they have higher hydrophobic properties and less hydrophilic properties due to low ratio of GMA, that could lead to decreasing the probability of obtaining mixed mode monolithic columns.

The GMA-co-SMA-co-EDMA monolithic columns prepared with (30:70)% of GMA:SMA showed good separation compared with GMA-co-LMA-co-EDMA monolithic columns when small molecules have been tested. Because base line was obtained with samples that separated using GMA-co-SMA-co-EDMA.

The GMA-co-SMA-co-EDMA monolithic columns showed acceptable separation for the commercial digested cytochrome c peptides using a gradient analysis. Proteins are eluted at the same retention time in each experiment and could not separate a mixture of proteins using GMA-co-SMA-co-EDMA monolithic column. To explain that, there is a likely reason for that, it could be the average surface area for this monolithic column is not enough to capture of proteins, because the number of meso and micro pores on the surface area are low compared with the size of proteins therefore, all the proteins are eluted quickly.

However, from all the experiment results that stated above, the work was carried on investigating monolithic columns that have higher surface area than the prepared monolithic columns with reasonable pores size. The new monolithic columns could be used as mixed mode monolithic columns to separate macro molecules such as proteins and peptides with base line separation, in addition to the small molecules.

5.7 Investigation of the types of porogenic solvents on the formation of GMA-co-SMA-co-EDMA monolithic column

The effect of porogenic solvents on the monolith formation was investigated in an attempt to obtain higher surface area compared with that of the monoliths that previously prepared using 1-propanol, and 1,4-butan di-ol. All the experiments were carried out at room temperature, therefore, the solvents with lower boiling point can be used.

It was declared that the porogenic solvents composition can control the porosity of the monolith[39, 209]. However, the investigating of porogenic solvent types was tried to improve the surface area and the pores size, so that, the monolith could

be used to separate large molecules such as proteins that could not be separated in the previous experiments. The high surface area with reasonable pores size are significant factors that can effect on the column efficiency, because when the surface area is increased the binding sites on the monolith will increase too leading to enhance the separation efficiency of the monolithic columns[270].

Different porogenic solvents such as methanol, ethanol, hexanol, 1-dodecanol, acetonitrile, and chloroform have been tried with 1-propanol to prepare the monolithic columns with (30:70)% of GMA:SMA, with an irradiation time of 120 min using the procedure described in sections 2.1.1, 2.1.2. All the monoliths were prepared inside I mL vials without a silanization step, then they have been characterized by BET measurements to determine their average surface areas, and average pores size. The porogenic solvents used and the BET results are shown in Figures (5.19), and (5.20).

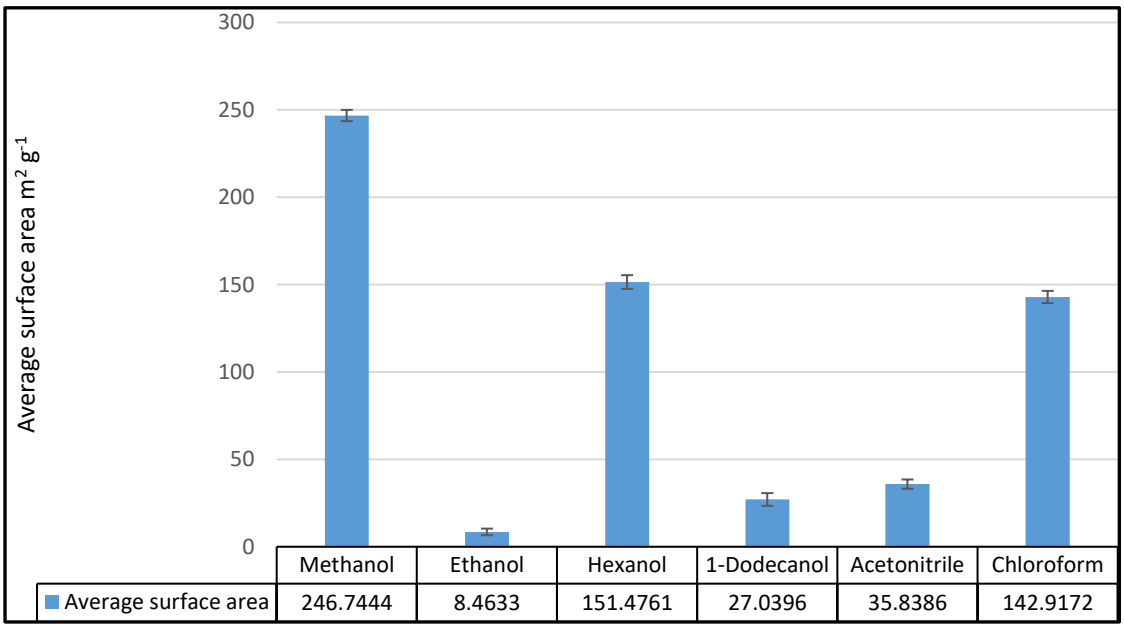

Figure 5.19 The effect of the porogenic solvents on the average surface area of glycidyl methacrylate-co-stearyl methacrylate-co-ethylene dimethacrylate monolithic columns, SD (n=3).

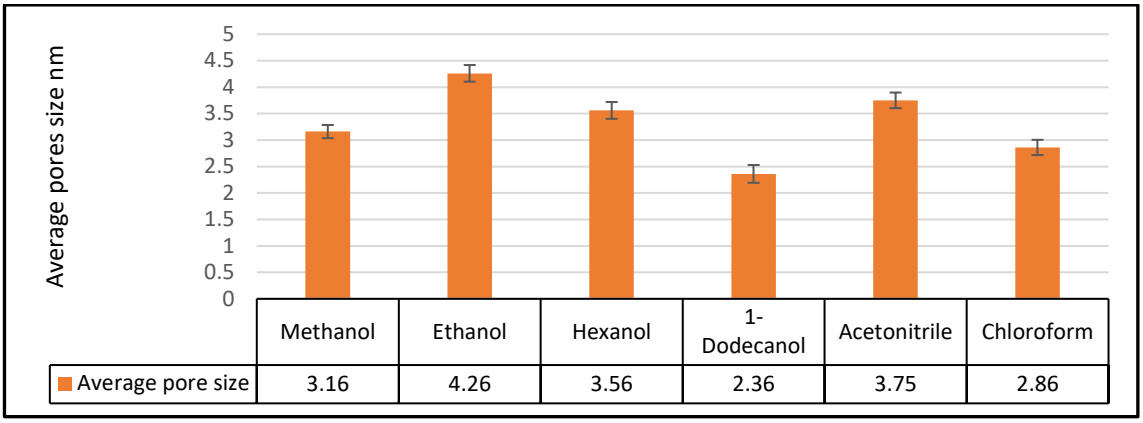

Figure 5.20 The effect of the porogenic solvents on the average pores size of glycidyl methacrylate-co-stearyl methacrylate-co-ethylene dimethacrylate monolithic columns, SD (n=3).

From Figures (5.19), and (5.20) it can be clearly seen that the monoliths were prepared with significantly higher surface area (246.7444 m^2 g^{-1}). Moreover, the average pore size was (3.16 nm) when using methanol with 1-propanol compared with other porogenic solvents. This is because, the mixture of methanol and 1-propanol may be a good solvent for the monomer and cross-linker, yet it is a poor solvent for the polymer. Therefore, the mixture of methanol and 1-propanol was used in further experiments to form the monolith inside the borosilicate tube and investigated as a mixed mode column for LC separation.

The effect of the porogenic solvent types on the surface area and the pores size was mentioned in the literatures. For example, Alzahrani investigated the effect of the porogenic solvent types of the monolithic columns prepared using BMA-co-EDMA. The porogenic solvents were (methanol, acetonitrile), (methanol, chloroform), (methanol, ethyl acetate), (methanol, ethanol), (methanol, tetrahydrofuran), (methanol, hexane), (methanol, 1-propanol), and (methanol, cyclohexanol). The results showed that the higher surface area was 56.89$m^2.g^{-1}$

for the monolithic columns that prepared using (methanol, 1-propanol) porogenic solvents, and the pores size was 8.45 nm.[29]

Yu *et al.*, investigated different solvents besides methanol to prepare GMA-co-EDMA monolithic columns. The porogenic solvents composition was (methanol, ethanol), (methanol, tetrahydrofuran), (methanol, acetonitrile), (methanol, chloroform), (methanol, ethyl acetate), and (methanol, hexane).

The results stated that the higher surface area was obtained using (methanol, acetonitrile) porogenic solvent compared with other porogenic solvents. The surface area was 110.5 m^2 g^{-1}, and the pores size was 41 nm.[252]

5.7.1 Investigation of 1-propanol to methanol ratio on the formation of GMA-co-SMA-co-EDMA monolithic columns

The ratio of the porogenic solvents (1-propanol: methanol) was investigated using the method described in sections 2.1.1 and 2.1.2 with an irradiation time of 120 min to try and obtain higher surface area, with reasonable pore size. As can be seen from the previous experiment (5.8) the monolith was formed with high surface area when the porogenic solvent mixture was methanol, and 1-propanol. while, the average pores size was 3.16 nm which means that the monolith could have low permeability.

However, the ratio between 1-propanol, and methanol was investigated to try preparing monolithic columns having good permeability. The results of BET analysis for each experiment were shown in Figures (5.21), and (5.22).

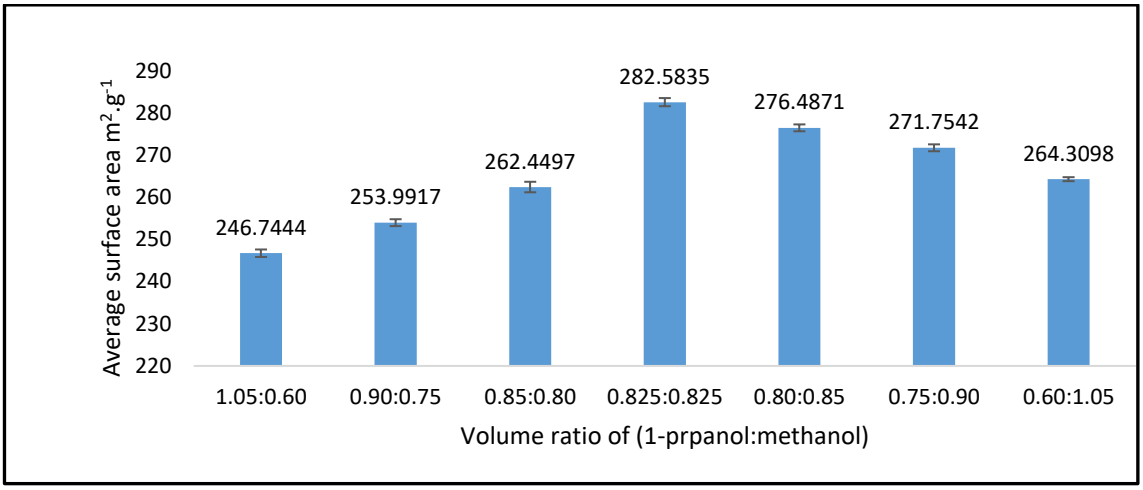

Figure 5.21 The average surface area of the monoliths that prepared with different volume ratio of 1-propanol:methanol, SD (n=3).

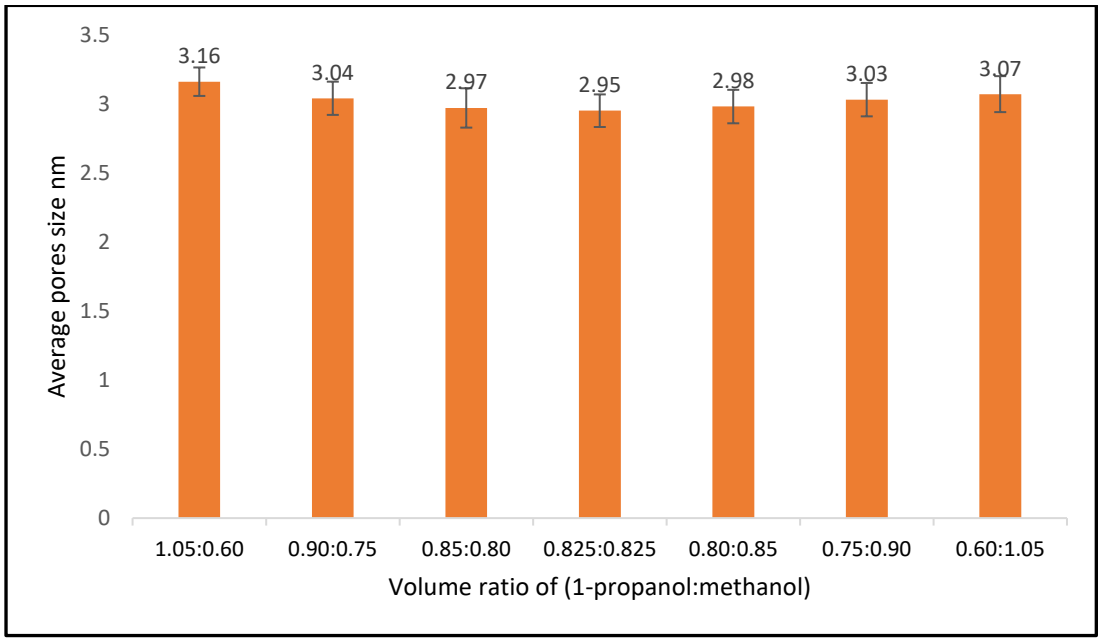

Figure 5.22 The average pores size of the monoliths that prepared with different volume ratio of 1-propanol:methanol, SD (n=3).

From Figures (5.21), and (5.22) it could be seen the role of the composition of porogenic solvent in monolithic formation, the morphological and the hydrodynamical properties. However, the average surface area of the monolith was increased with increasing the volume of the methanol up to (0.825:0.825)

after that the average surface area was decreased. It could be the solubility of the monomers and the cross-linker in (0.825 mL) of 1-propanol, and (0.825 mL) methanol was higher than the other ratios in the porogenic solvent composition, while the mixture was poor solvent for the monolith. In addition, the average pores size was decreased slightly with increasing the surface area and the lowest value was (2.95 nm) for the monolith that formed using (0.825 mL) of 1-propanol, and (0.825 mL) methanol as porogenic solvent. After that the average pores size was increased slightly with decreasing the average surface area of the formed monoliths. Moreover, the changing of the porogenic solvent composition ratio can lead to dramatic change in the porosity of the monolith because the composition could be less suitable to control the morphological properties.[253] So far, the (0.825 mL) of 1-propanol, and (0.825 mL) methanol volume ratio was used in the further experiments.

After formation the monoliths inside the borosilicate tube it was found that it was very difficult to wash with ethanol at different flow rates, because the system was leaked every time. The monolith could be blocked due to the high surface area and low pores size that can lead to increase the back pressure inside the column and prevent the solvent from passing through the interconnected channels due to the leakage in macropores. Therefore, these columns that prepared using (0.825 mL) of 1-propanol, and (0.825 mL) methanol porogenic solvent with 120 minutes irradiation time could not be used for LC separation. However, further investigations have been carried on getting suitable monolith with desired surface area, pores size, good permeability and porosity by investigating the irradiation time to reduce the number of the branches and reduce the back pressure as

described in section 4.1.1. The SEM images of the monolith are shown in Figure (5.23)

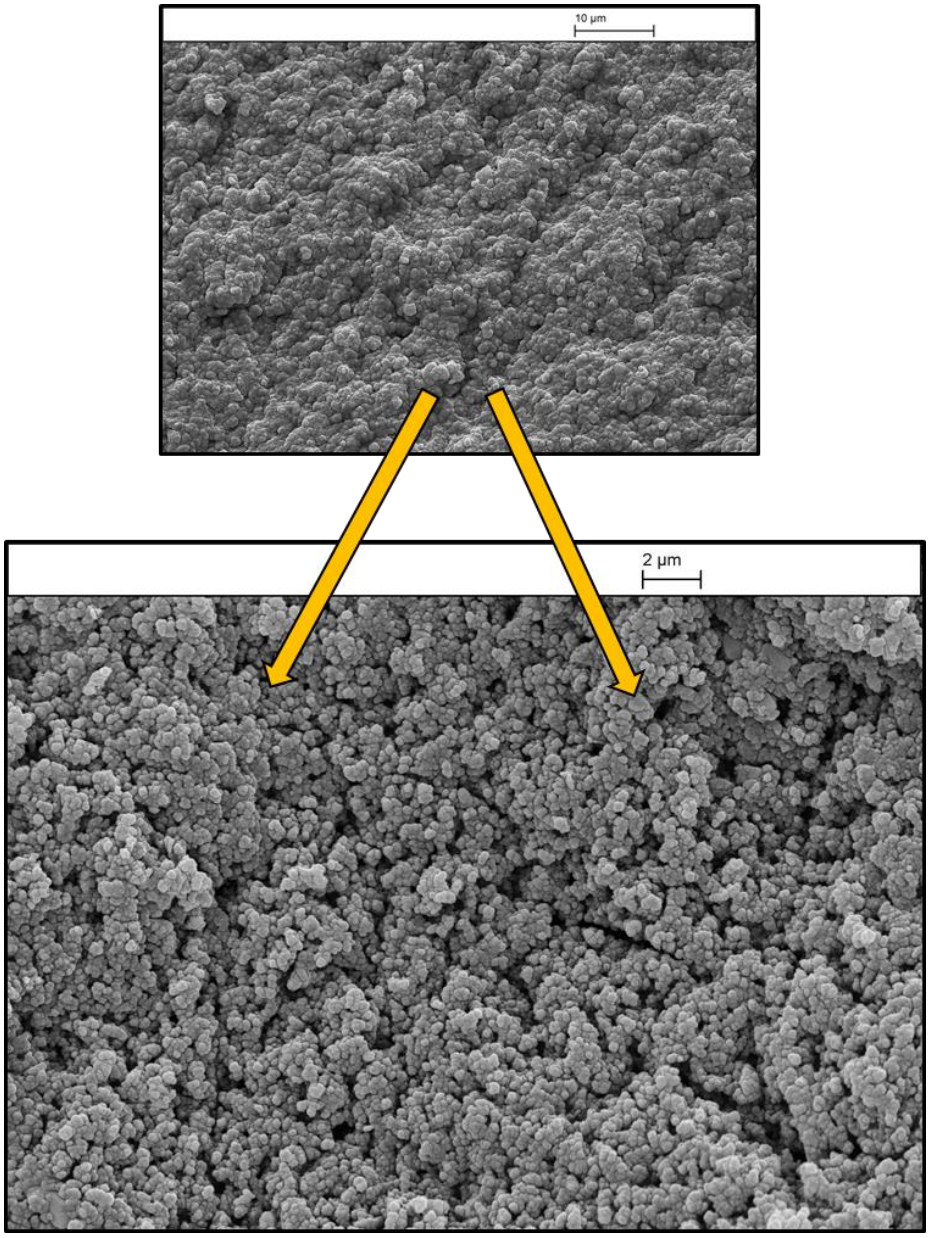

Figure 5.23 SEM images for GMA-co-SMA-co-EDMA monolith prepared using 1-propanol and methanol porogenic solvent, with irradiation time 120 minutes.

It is clearly seen from Figure (5.23) that, the monolith was formed with high surface area and low pores size. Therefore, this monolith could not be used as monolithic column for LC separation due to the high back pressure generated.

5.7.2 Investigation of irradiation time on the monolith formation using 1-propanol and methanol porogenic solvent

The effect of irradiation time on the formation of GMA-co-SMA-co-EDMA monolithic column using (0.825 mL) of 1-propanol, and (0.825 mL) methanol has been investigated. So far, to obtain the appropriate irradiation time that can be used to prepare monolith with suitable back pressure, surface area, and pore size that can have ability to separate large molecules. The effect of irradiation time is shown in Table (5.10)

Table 5.10 The effect of irradiation time on the monolith formation using 1-propanol and methanol porogenic solvent

No.	Irradiation time (min)	Result
1	120	The monolith was formed but blocked
2	60	The monolith was formed but blocked
3	26	The monolith was formed but blocked
4	25	The monolith was formed with back pressure 787 psi
5	24	The monolith was formed with back pressure 784 psi
6	23	The monolith was formed with back pressure 782 psi
7	22	The monolith was formed with back pressure 767 psi
8	20	The monolith was started formation
9	18	The monolith did not form

It can be seen from Table (5.10) that the irradiation time was dropped significantly when 1-propanol and methanol mixture was used as a porogenic solvent in the

monolith formation. However, the irradiation time that used to form the monolith was 120 minutes when 1-propanol and 1,4-butan di-ol mixture was used as a porogenic solvent, while, the monolith was formed between (22-25) minute using (0.825 mL) of 1-propanol, and (0.825 mL) methanol as a porogenic solvent. Moreover, it can notice that there is no noticeable difference in the back pressure of the monolith that formed between (23-25) minute, therefore the (23) minute was used in further experiment. The monolith was tested to determine the average surface area and the average pores size, the results were shown in Figure (5.24).

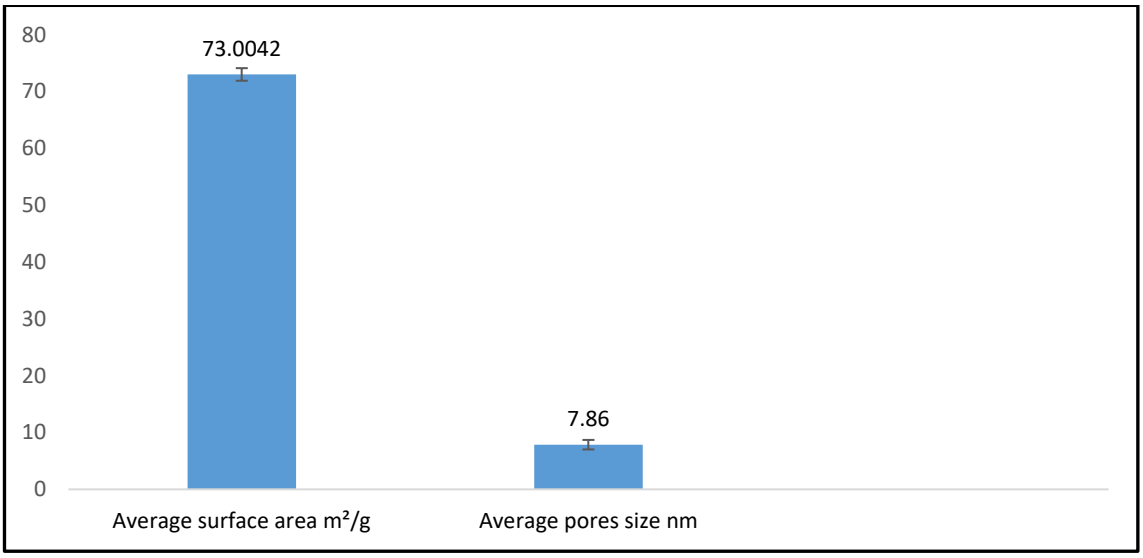

Figure 5.24 The average surface area and the average pores size of the GMA-co-SMA-co-EDMA monolithic columns that prepared using (0.825 mL) propanol, and (0.825 mL) methanol with 23-minute irradiation time, SD (n=3).

The BET results show that this monolith has a higher surface area and pore size than the same monolith that formed using (1-propanol, 1,4-butan di-ol) porogenic solvent. In addition, the irradiation time was decreased significantly using (1-propanol, methanol) porogenic solvent it was 23 minutes. While, the same

monolith was formed after 120 minutes using (1-propanol, 1,4-butan di-ol). Therefore, these conditions were used in subsequent the experiments. The SEM images of the monolith were shown in Figure (5.25)

It can notice from Figure (5.25) the effect of the porogenic solvent composition on the surface area and the pores size of the monolith. So far, the pores size was increased and the surface area was decreased significantly in the GMA-co-SMA-co-EDMA monolith that prepared using 23 minutes irradiation time compared with the same monolith that prepared using 120 minutes.

The effect of methanol ratio on the surface area and the pores size was investigated by Cong *et.al.* when poly(2-hydroxyethyl methacrylate-co-ethylene dimethacrylate) monolith was prepared using methanol and hexane as porogenic solvent. The results showed that average pores size was increased and the surface area decreased with increasing the ratio of methanol up to 60% with suitable irradiation time.[252]

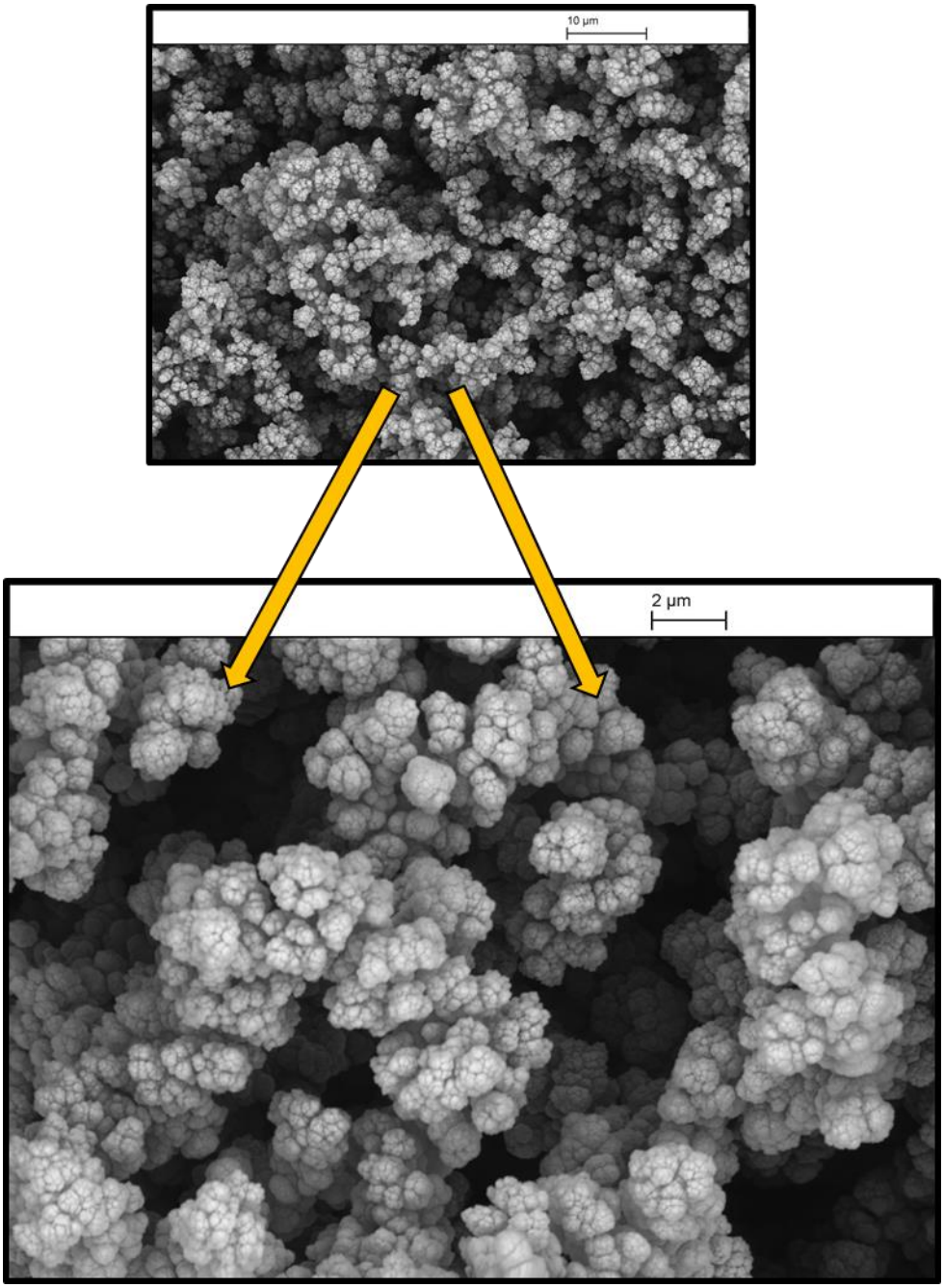

Figure 5.25 SEM images for GMA-co-SMA-co-EDMA monolith prepared using 1-propanol and methanol porogenic solvent, with irradiation time 23 minutes.

5.7.3 Measuring the porosity of the monolithic column

The total porosity of the monolith was calculated using the method of Fletcher *et al*. by using equation (5.1).[248]

It was found that the porosity of the glycidyl methacrylate-co-stearyl methacrylate-co-ethylene dimethacrylate monolithic column was (0.0983).

5.7.4 Permeability of the monolith

The permeability of (30:70) % GMA:SMA monolithic column monolithic was examined by testing the backpressure generated from HPLC system pump using milli-q water at different flow rates through the monolith.[200] The results were shown in Figure (5.26)

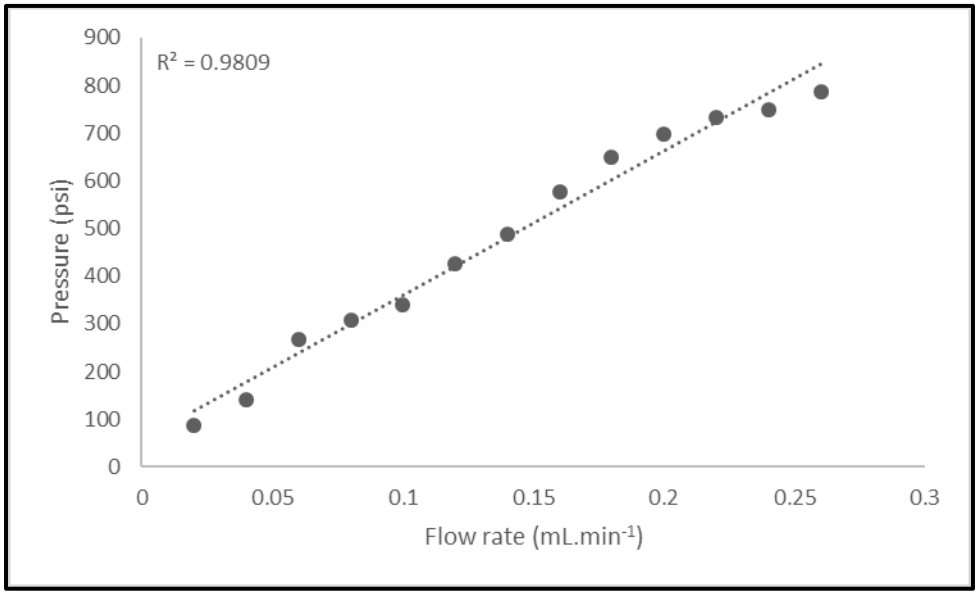

Figure 5.26 The relationship between the back pressure and the flow rate for the glycidyl methacrylate-co- stearyl methacrylate-co-ethylene dimethacrylate monolithic column.

It can be seen from Figure (5.26) that the back pressure was increased with increasing the flow rate up to 0.26 mL min^{-1}, the pressure was stable at the value of 687 psi with flow rate 0.26 mL min^{-1}. After that the pressure was dropped due to the system leaked. As can be seen that the flow rate was increased compared with the flow rates that used with other monolithic columns that prepared using (1-propanol and 1,4-butan di-ol) porogenic solvent due to the high porosity and the permeability of the monolithic columns due to high pores size.

5.7.5 Proteins separation using GMA-co-SMA-co-EDMA monolithic column.

The monolithic column that prepared inside the borosilicate tube using 30% GMA (0.27 mL), 70% GMA (0.630 mL), EDMA (0.30 mL), methanol (0.825 mL), 1-propanol (0.825 mL), and irradiation time (23 min) was connected to LC system to attempt separating mixture of proteins. Three different proteins that have different molecular weight have been used apo-transferrin (80.0 kDa), bovine serum albumin (69.324 kDa), and cytochrome c (12.384 kDa), each protein was tested individually for three times to determine the exact retention time. Separation of three proteins using gradient analysis no (9) are shown in Figure (5.27)

Table 5.11 Solvent composition of gradient analysis no.()

Time/ min.	Water %	Acetonitrile %	Flowrate mL/min
0:00	90	10	0.2
2:00	90	10	0.2
12:00	10	90	0.2
17:00	10	90	0.2
18:00	90	10	0.2
20:00	90	10	0.2

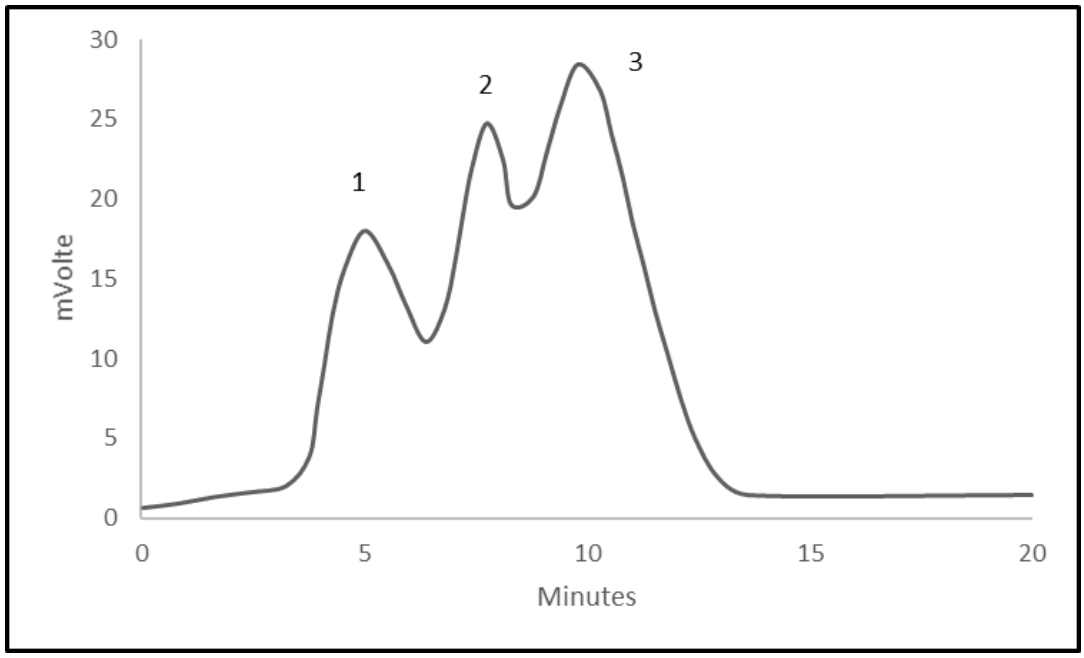

Figure 5.27 Chromatogram of proteins mixture (1) apo-transferrin, (2) bovine serum albumin, and (3) cytochrome C, 10^{-5} M mixture of each with gradient no. (9) the injection volume (2.5 µL), and the detection wavelength 254 nm.

From Figure (5.27) it can see the separation ability of the monolithic columns that prepared using methanol and 1-propanol as a porogenic solvent was enhanced compared with the other columns that prepared using 1-propanol and 1,4-butandi-ol.

The increasing in the surface area of the monolith will provide more binding sites on the surface of the monolith, however, more interactions between the amino acids residues of the proteins and the surface of the monolith could be obtained and enhanced the separation ability of the monolithic column. In addition, the large pores size allows to the macromolecules to diffuse into the pores of the stationary phase and interact and retained by hydrophobic and hydrophilic interactions. Moreover, high flow rate could be used with reasonable back pressure to reduce the eddy diffusion effect.

All samples that have been tested individually showed clear retention times, yet the peaks were broad, therefore when the protein mixture was tested it showed acceptable ability to separate these proteins. However, the peaks were broad and there is overlap between these peaks and complete resolution and base line separation was not possible as shown in Figure (5.27). It could be due to the mass transfer between the stationary phase and the mobile phase was lower than that from the mobile phase to the stationary phase. So far, the C-term in van Deemter will increase causing the band broadening.

It was mentioned that the separation mechanism of the prepared monolithic column is RP/HILIC mechanism due to mixed mode monolithic column, however this mechanism does not enhance the peak width and make it sharper. Therefore, another option has been investigated. This involved changing the monolithic column to strong cationic exchange/ hydrophobic mixed mode monolithic column

by opening the epoxy ring of glycidyl methacrylate using Na_2SO_3 to form a cationic exchanger.

5.8 Strong cationic exchange/hydrophobic mixed mode monolithic column

Glycidyl methacrylate-co-stearyl methacrylate-co-ethylene glycol dimethacrylate monolithic columns were prepared using 1-propanol and methanol porogenic solvents with an irradiation time of 23 minutes. These monoliths were then modified to give properties of strong cationic exchange and try enhancing the peaks shape of the protein samples by using electrostatic interactions along with hydrophobic interactions. In addition, the electrostatic interactions of charged molecules in ion exchange chromatography are stronger and operate longer over distances then other interactions[271].

5.8.1 Opening the epoxy ring of glycidyl methacrylate to form cationic exchanger

The epoxy groups in glycidyl methacrylate-co-stearyl methacrylate-co-ethylene glycol dimethacrylate monolithic columns can be opened using a sulfonation reaction by pumping a sulfonation solution as described in section (2.5.2) from a syringe pump.

The direct sulfonation of epoxy groups with Na_2SO_3 solution was not achieved due to the higher affinity of the sulfite groups to water than to the hydrophobic polymer chains suspended in water. Moreover, the phase separation stops the sulfite groups approaching to in close contact with the epoxy groups in the polymers which is necessary for the reaction. Therefore, phase transfer catalyst

was used as an ionic surfactant carrier to carry the an ionic reagent from the aqueous phase to the organic phase, making the sulfonation reaction possible[247]. Epoxy ring opening reaction is shown in Figure (5.28)

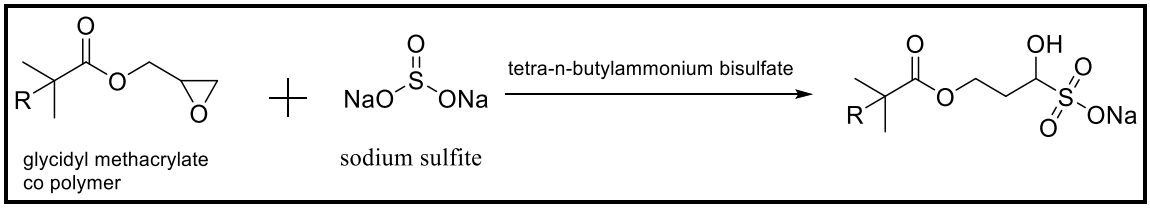

Figure 5.28 Opening the epoxy groups of the GMA in GMA-co-SMA-co-EDMA monolithic columns by sulfonation reaction to form SCE/RP monolithic columns

The ring opening reaction and formation of a cationic exchanger was proven using different techniques such as FTIR, EDX, and CHN as described below.

5.8.2 FTIR analysis

The FT-IR technique was used to characterize the main peaks from the co-polymer after ring opening reaction. The results showed clearly changing the epoxy ring to (-OH) and (R-SO_3Na) groups as shown in Figure (5.29). The sulfonation group will be used as cationic exchanger alongside the hydrophobic alkyl chain to give the monolithic column mixed mode properties as a strong cationic/hydrophobic mixed mode column which may enhance the separation process.

From Figure (5.29) the peak at 910.07 cm^{-1} for epoxy groups of the GMA in the monolith that showed in Figure (5.7) was disappeared, and there are two new peaks clearly present, at 1032.23 cm^{-1} and 995.96 cm^{-1} for R-SO_3 and S-O groups respectively,[272, 273] in addition, a broad band for -OH group between

3600-3100 cm^{-1} was observed. [274] These peaks indicate that the epoxy rings were opened, and changed to R-SO_3Na group that can be used in cationic interaction mechanism besides the hydrophobic interaction mechanism. Moreover, the peaks at 1725.19 cm^{-1} for C=O, and at 1148.21 cm^{-1} for C-O ester groups are still unchanged due to non-participation of these groups in the sulfonation reaction.

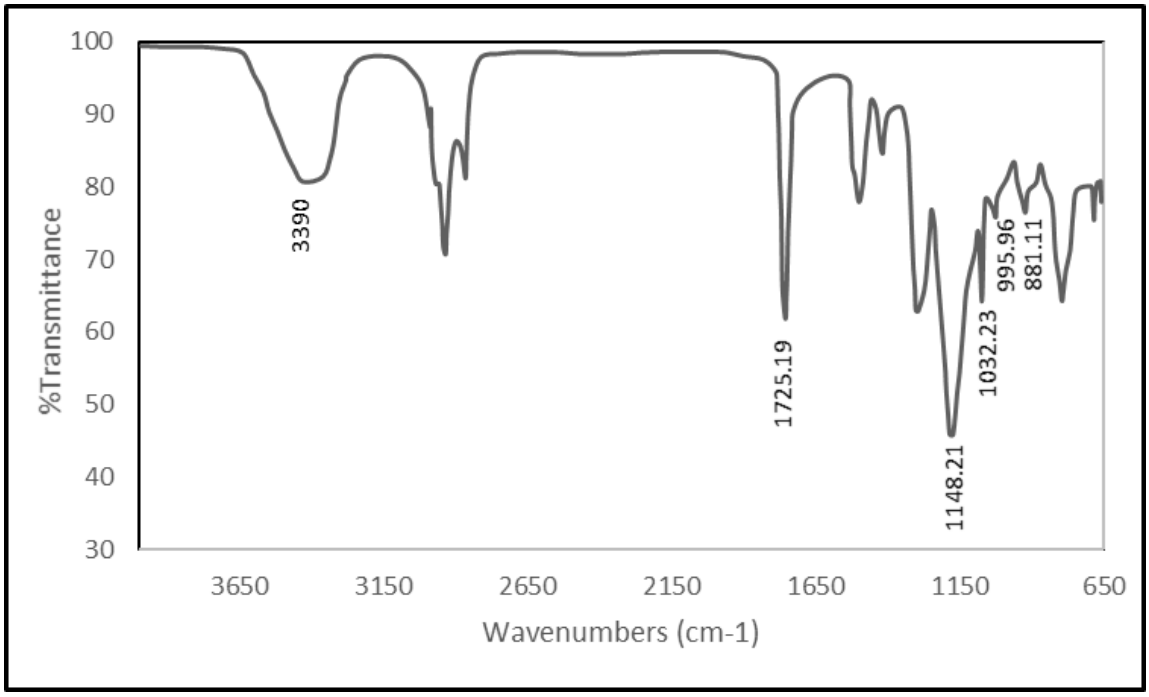

Figure 5.29 FTIR spectrum of the GMA-co-SMA-co-EDMA monolith after opening epoxy ring from 4000 cm^{-1} to 650 cm^{-1}.

5.8.3 Energy dispersive X-ray (EDX) analysis

The EDX analysis was used to investigate and determine the chemical composition of monolithic materials before and after opening the epoxy ring of the glycidyl methacrylate-co- stearyl methacrylate-co-ethylene dimethacrylate monolithic column. These results also indicate that the -SO_3Na group is present on the monolithic column after ring opening reaction using Na_2SO_3 as shown in Figures (5.30) and (5.31)

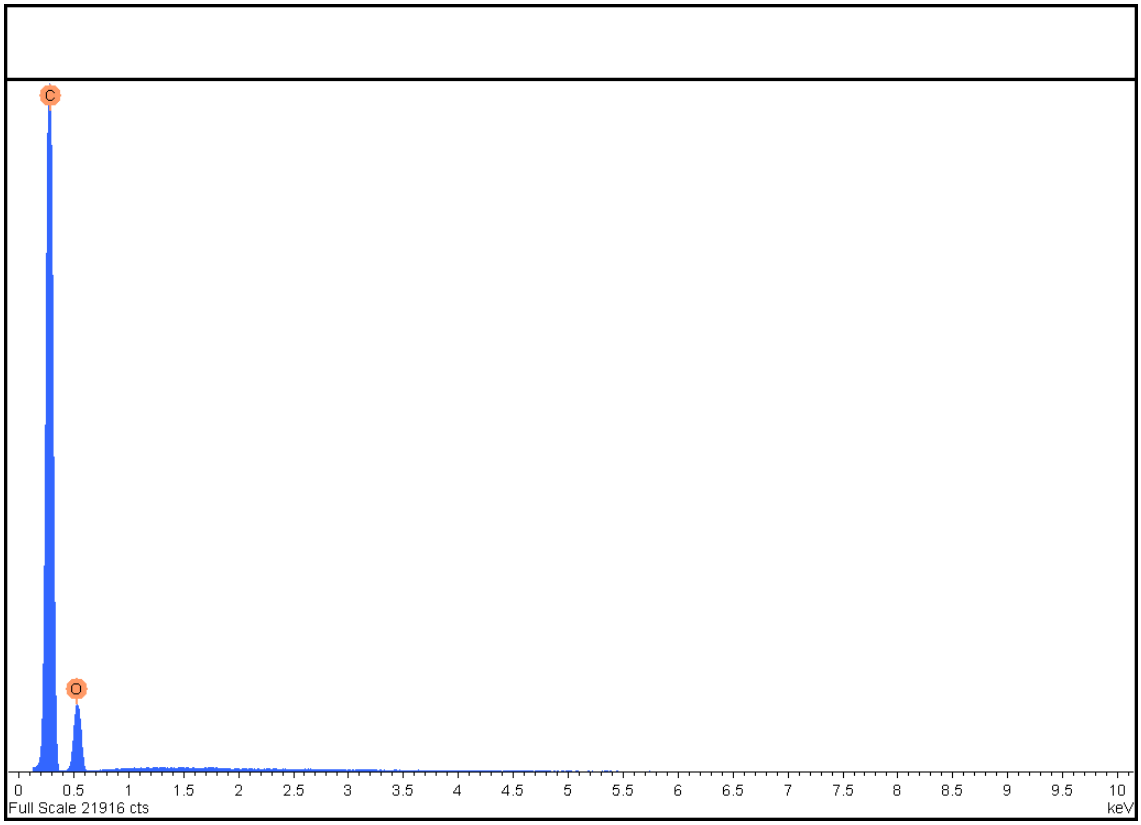

Figure 5.30 EDX analysis for GMA-co-SMA-co-EDMA monolithic column before opening the epoxy ring.

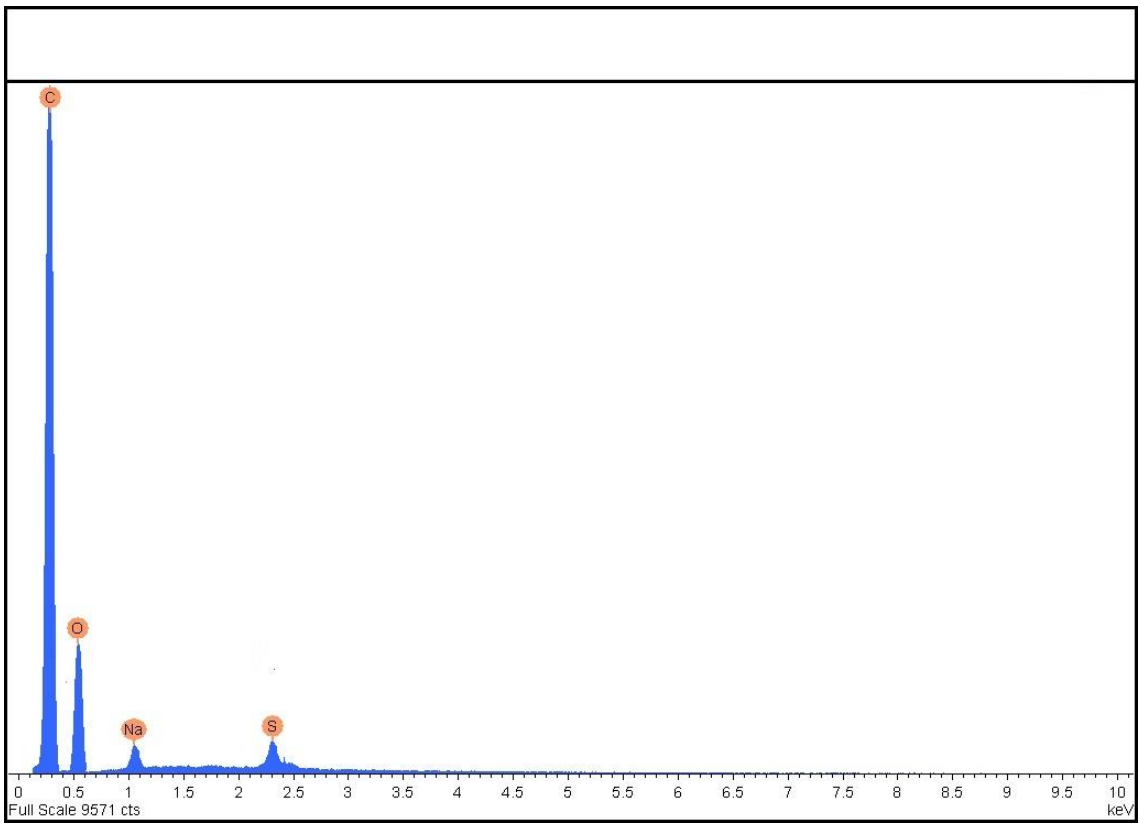

Figure 5.31 EDX analysis for GMA-co-SMA-co-EDMA monolithic column after opening the epoxy ring with Na_2SO_3.

The EDX analysis shows that the epoxy ring for glycidyl methacrylate was opened using Na_2SO_3 to form R-SO_3Na group that can be used as a strong cationic exchange group in addition to the hydrophobic chains which can be utilized to form a mixed mode monolithic column.

The CHN analysis has been carried out and proved that a significant amount of sulphur atoms were present within the monolithic column. All this data provides convincing evidence that the epoxy rings have been changed to cationic exchange groups.

5.9 Applications of glycidyl methacrylate-co-stearyl methacrylate-co- ethylene dimethacrylate as strong cation exchange/revers phase mixed mode monolithic columns.

The GMA-co-SMA-co-EDMA monolithic columns have been tested with different samples to investigate the separation behavior as mixed mode monolithic columns for LC separation. The higher surface area and large pores size compared with HILIC/Hydrophobic monoliths previously prepared should help to improve the separation for large molecules.

5.9.1 Separation of proteins

GMA-co-SMA-co-EDMA strong cationic/hydrophobic mixed mode monolithic columns were used to separate a mixture of proteins. Different proteins have been chosen depending on the difference in the isoelectric points and the difference in the molecular weight as showed in Table (5.12) were used to investigate the separation ability for these monolithic columns.

Table 5.12 Types of standard proteins that used in pre-concentration analysis.

Proteins	**Molecular weight Da**	**Isoelectric point**
Insulin	5805	5.3
Cytochrome C	12384	10.2
Lysozyme	14307	11.35
Myoglobin	17199	6.8
Trypsin	23300	4.5
Albumin chicken egg white	42700	5.3

Gradient analysis methods were used to separate these proteins, with a variety of solvents such as ammonium acetate, sodium phosphate, acetonitrile, and water used to optimize the peak shape.

It was found that sodium phosphate/acetonitrile gave better peak shapes compared to other solvents. The peaks were found to be broad and base line separation could not be achieved using water/ acetonitrile, ammonium acetate/acetonitrile, and water/ammonium acetate. Therefore, sodium phosphate/acetonitrile was used in all experiments where pH was varied. The results of the GMA-co-SMA-co-EDMA mixed mode monolithic column are shown in Figures (5.32 - 5.34)

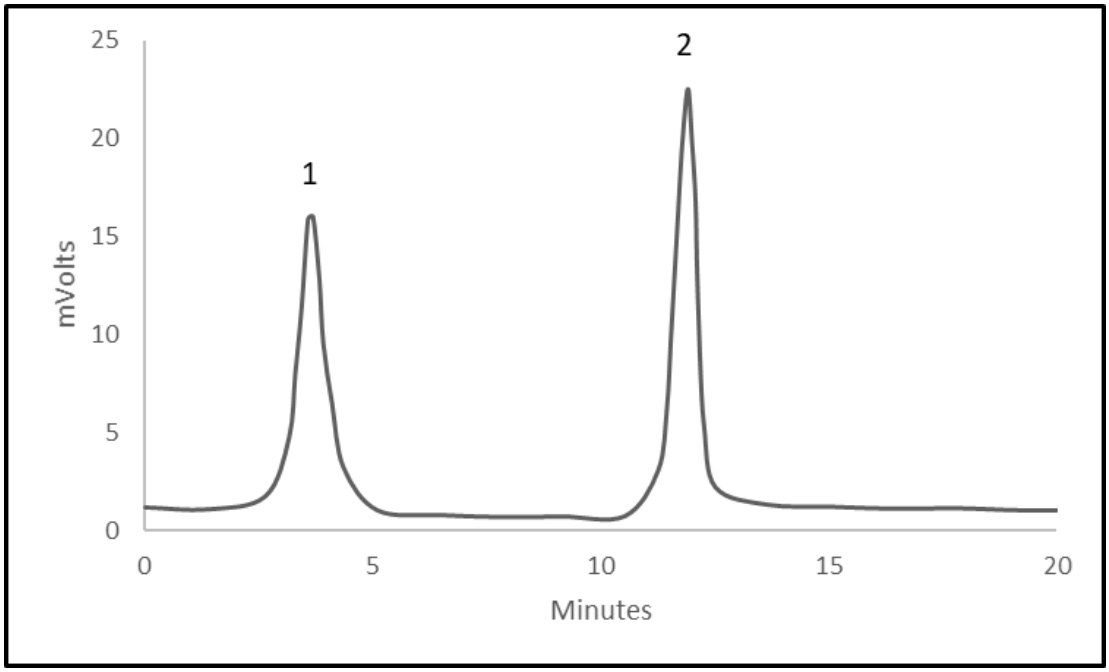

Figure 5.32 Chromatogram of proteins mixture (1) Insulin (pI=5.3), and (2) Lysozyme (pI=11.3), 10^{-5} M mixture of each with gradient no. (10) the injection volume (2.5 µL), and the detection wavelength 254 nm.

Table 5.13 Solvent composition of gradient analysis no. (10)

Time/ min.	Sodium phosphate (pH=11) %	Acetonitrile % (0.1 % TFA)	Flowrate mL/min
0:00	20	80	0.2
1:00	20	80	0.2
14:00	90	10	0.2
17:00	90	10	0.2
17.30	20	80	0.2
20:00	20	80	0.2

In polar solvents the folded structure of proteins indicates that hydrophobic amino acids will tend to be on the inside of the folded protein while the hydrophilic amino acids on the outer surface will interact with the polar solvent. The interactions between the surface of the monolith and the protein sample could also occur between the hydrophilic amino acids in the proteins and the hydrophilic part on the surface of the monolith, more than the hydrophobic interactions.

In this work because the columns are SCE/RP monolithic columns, therefore, the interactions will be between the ion exchanger ($-SO_3^-$) and the charged amino acids more than the hydrophobic interactions because the electrostatic interactions of charged molecules in ion exchange chromatography are stronger and operate longer over distances than other interactions.[271,275]

As can be seen from Figure (5.32) that, the base line separation could be obtain using SCE/RP GMA-co-SMA-co-EDMA monolithic columns with mixture of insulin and lysozyme.

The separation depended on the cationic exchange properties since all these proteins were eluted with increasing the pH of the mobile phase during the gradient analysis. In ion exchange chromatography, samples will elute depending on their charge density, however, higher charge density samples will be retained longer.[276] Increasing the pH of the mobile phase will reduce the charge density and reduce the interactions between the charged proteins with the sulfonate groups on the surface area of the monolithic column until the (pI) of each proteins is reached and all proteins are gradually released.[204] These results have proven the cationic interactions between the monolithic column and the proteins that were analyzed.

The monolithic column was also used to investigate separation of myoglobin and cytochrome C, which also have different pI values, the results are shown in Figure (5.33)

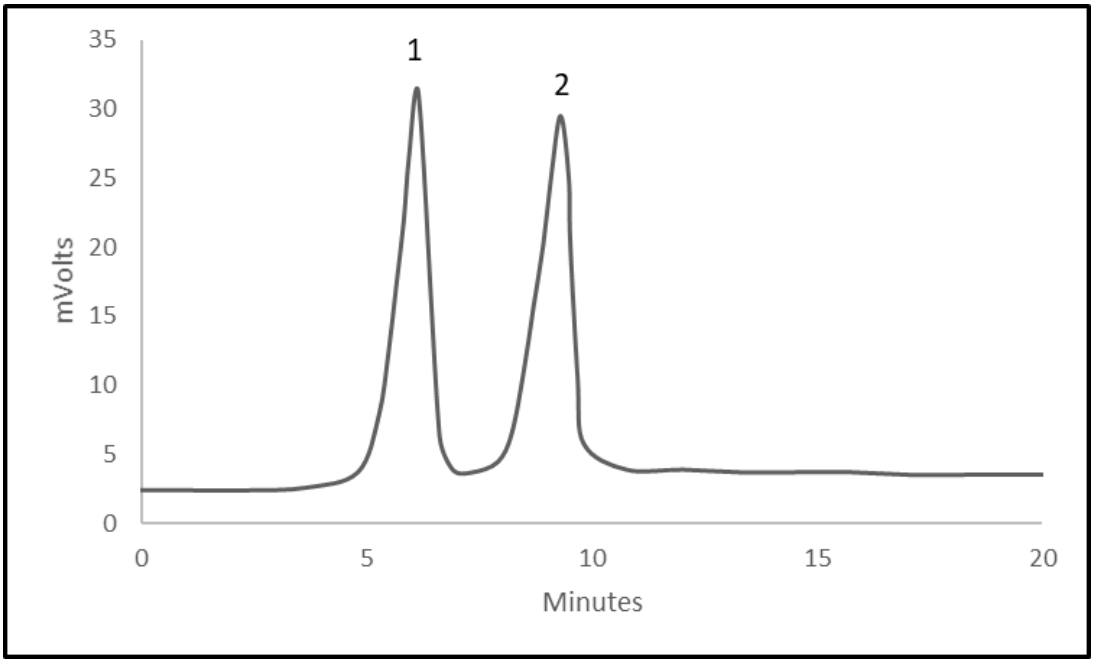

Figure 5.33 Chromatogram of proteins mixture (1) Myoglobin (pI=6.8), and (2) Cytochrome c (pI=10.2), 10^{-5} M mixture of each with gradient no. (10) the injection volume (2.5 µL), and the detection wavelength 254 nm.

Separation a mixture of trypsin (pI=4.5) and albumin egg white (pI=4.7) was carried out to investigate the separation ability of the SCE/RP monolithic columns to separate two proteins having very close pI values. The results are shown in Figure (5.34)

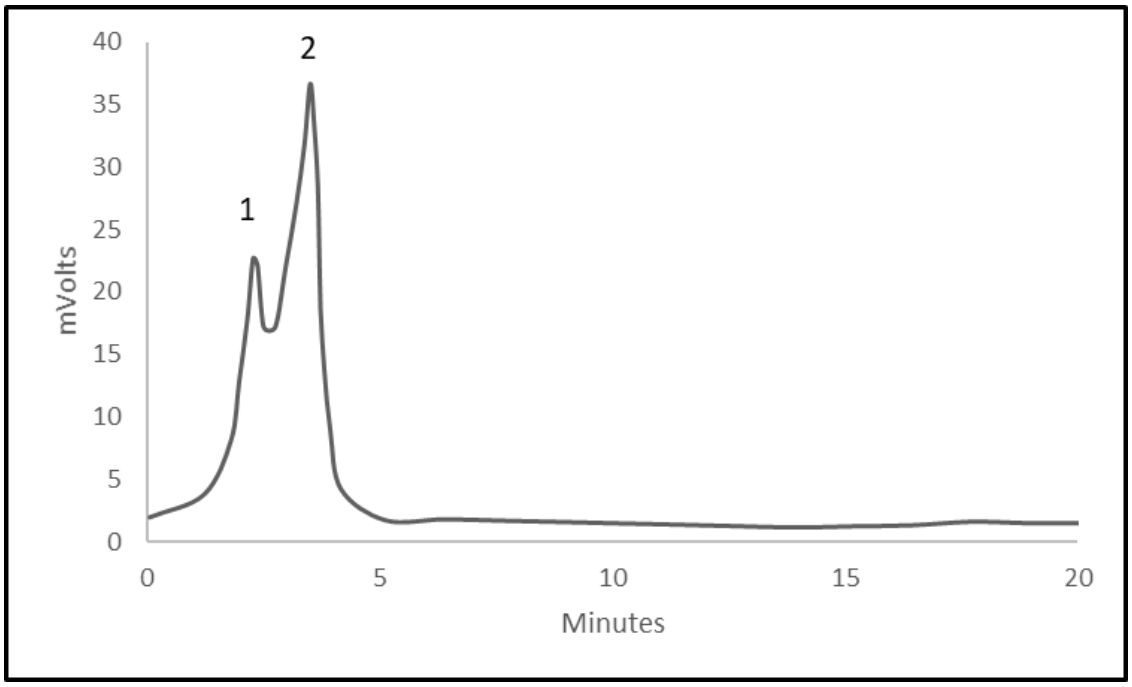

Figure 5.34 Chromatogram of a mixture of (1) trypsin (pI=4.5) and (2) albumin chicken egg white (pI=4.7), 10^{-5} M mixture of each with gradient no. (10) the injection volume (2.5 µL), and the detection wavelength 254 nm.

As can be seen from Figure (5.34) and Table (5.13), the two proteins did not have base line separation that was achieved previously in Figures (5.32), and (5.33). This could be due to the close values of pI that could lead to be the charge density of each proteins are close to each other, therefore, they could not separate, and the peaks were overlapped.

The strong cation exchange mode considered a crucial mode for peptides and proteins separation in chromatographic technique.[277] The strong cationic exchange columns with sulfonate groups have many advantages, for example, the ability to maintain the negative charge when using acidic buffer conditions such as (pH ~3) that can be used to separate peptides. While, the natural buffer pH range could be used to separate basic peptides or proteins.[278] The strong cationic exchange/revers phase monolithic columns have been used to separate three proteins in single run, the results are shown in Figure (3.35).

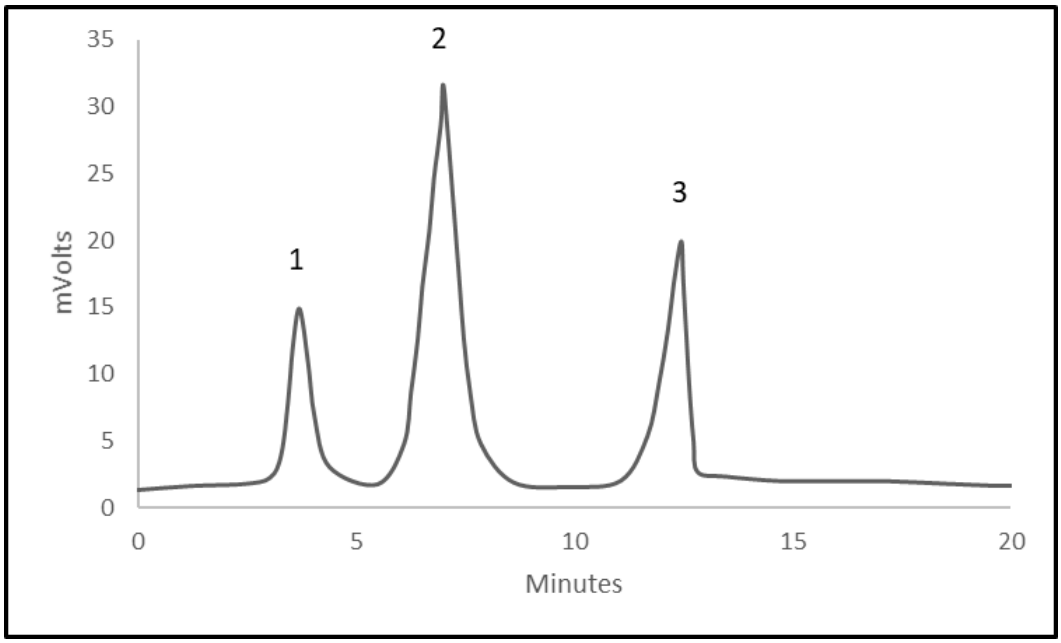

Figure 5.35 Chromatogram of proteins mixture (1) Insulin (pI=5.3), (2) Myoglobin (pI=6.8) and (3) Lysozyme (pI=11.3), 10^{-5} M mixture of each with gradient no. (10) the injection volume (2.5 µL), and the detection wavelength 254 nm.

As can be seen from Figure (5.35) that insulin (pI=5.3) was eluted firstly due to reach the pI value, after that the net charge will be negative and there are no electrostatic interactions with the cationic exchanger. The next eluent was myoglobin that have higher pI value than insulin (pI=6.8) that needs higher pH

solvent solution to elute. Ultimately, lysozyme (pI=11.3) was eluted with higher retention time compared with other proteins due to the highly interactions with ($-SO_3^-$). According to the pI, higher pH solvent solution should be used to release the proteins that have higher pI value. This can be obtained using the gradient analysis.

The N for the SCX/RP monolithic column and Rs values between each protein were calculated, and the results are shown in Table (5.14)

Table 5.14 The average number of theoretical plates (N) and the resolution value (Rs) for each protein with SCX/RP monolithic columns (n=3)

Analytes	**SCX/RP monolithic column**
N	1389
Rs for Insulin and Lysozyme	6.1
Rs for Myoglobin and Cytochrome C	1.8
Rs for Trypsin and Albumin chicken egg white	0.42
Rs Insulin and Myoglobin	2.1
Rs for Myoglobin and Lysozyme	2.7

According to the Table (5.14), The results showed that the monolithic column can provide base line separation for all the proteins that separated using SCX/RP monolithic columns with gradient analysis no (10), due to the high Rs values (more than 1.5). Yet, the base line separation was not achieved between trypsin and albumin chicken egg white Rs (0.42) due to the close pI value for each protein.

The separation process based on the difference in the pI value of each proteins which can be defined as the pH at which the proteins net charge equal to zero[279].

However, proteins will move along the monolithic column and interact with ($-SO_3^-$) groups on the surface of the monolith by electrostatic interactions and bind to the cationic exchanger. So far, each protein has a charged side chains of amino acids that gave the protein different net charge at different pH to react with ($-SO_3^-$) groups. All proteins will bind to the cationic exchanger until they reach their isoelectric points. Therefore, when proteins have several basic amino acids, the pI value will be high, on the other hand, the pI value will be low for proteins with low acidic amino acids.

5.9.2 Separation of hydrophobic compounds

Separation of hydrophobic compounds was investigated using SCX/RP monolithic columns that have higher surface area and pore size compared with HILIC/RP monolithic columns.

Four hydrophobic compounds (toluene, naphthalene, anthracene, and pyrene) were used to evaluate the performance of the monolithic columns using the same experimental conditions previously used in section (5.6.1), the results are shown in Figure (5.36)

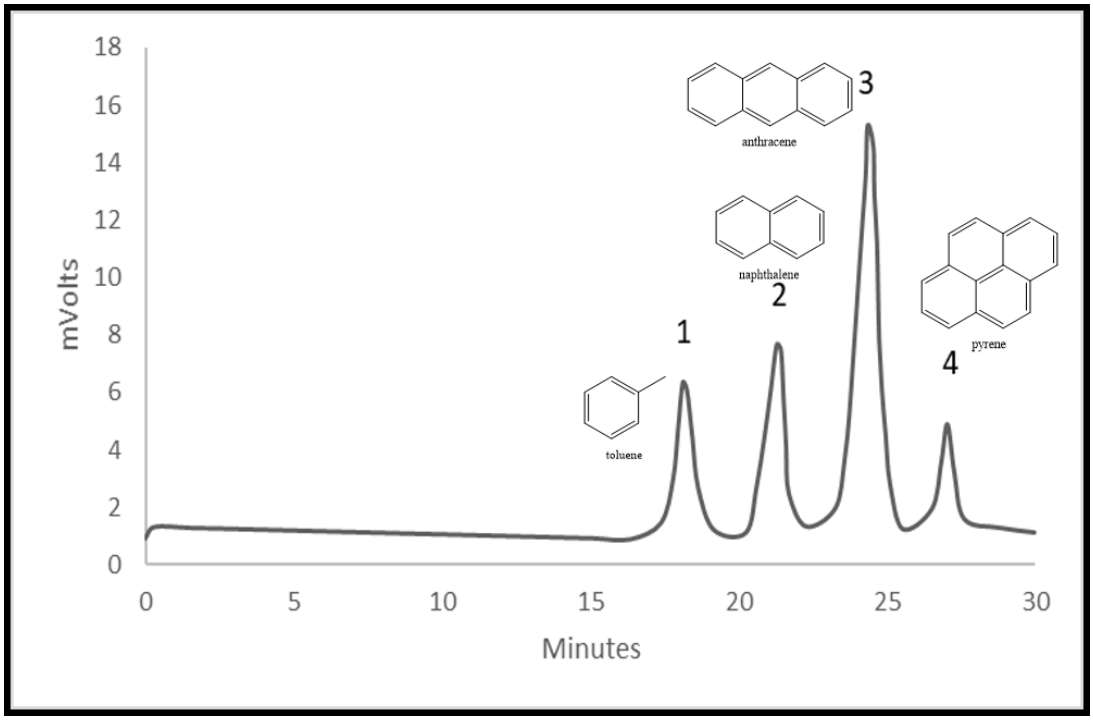

Figure 5.36 Chromatogram of a mixture of (1) toluene, (2) naphthalene, (3) anthracene, and (4) pyrene, 10^{-5} M mixture of each with gradient no. (5) the injection volume (2.5 µL), and detection wavelength 254 nm.

As can be seen from Figure (5.36), the four compounds were well separated with base line resolution. Comparing these results with these obtained from the experiment discussed in section (5.6.1), shows that the shapes of the peaks and the base line separation is better than that in Figure (5.10).

High surface area provides more binding sites on the surface of the monolithic columns; therefore, more interactions will take place between the solutes and the stationary phase which could lead to enhance the sample base line separation. Moreover, when the sample molecules are partitioning between the mobile phase and the stationary phase, the higher pore size on the surface of the SCE/RP monolithic columns compared with HILIC/RP monolithic columns might allow

more sample molecules to diffuse into the pores and increase the mass transfer rate between the mobile phase and the stationary phase.

The gradient program was used to increase the desorption rate over the adsorption rate to elute the molecules and reduce the retention factor. According to the van Deemter concept the C-term should be kept at a minimum value to increase the resolution of the peaks by reducing the H value. The N, and Rs values were calculated and compared to N, and Rs value previously obtained in section 5.6.1, the results are shown in Table (5.15)

Table 5.15 The average number of theoretical plates (N) and the resolution value (Rs) for toluene, naphthalene, anthracene, and pyrene with SCX/RP and HILIC/RP monolithic columns (n=3)

Analytes	**SCX/RP monolithic column**	**HILIC/RP monolithic column**
N for Toluene	3272	3215
Rs for Toluene and Naphthalene	1.92	1.41
Rs for Naphthalene and Anthracene	2.48	1.70
Rs for Anthracene and Pyrene	1.97	0.59

As can be seen from Table (5.15), the N and Rs values for the analytes separated using SCE/RP monolithic column were increased compared with HILIC/RP. The elution order was followed the hydrophobicity order, therefore there is no effect of the strong cationic groups on the elution order of the analytes because the

interactions were hydrophobic interactions only. More investigations were carried out to study the effect of ($-SO_3^-$) groups on the separation of small molecules.

5.9.3 Separation of hydrophilic and hydrophobic compounds

The effect of ($-SO_3^-$) on the surface of the SCX/RP monolithic columns was investigated because ($-SO_3^-$) has hydrophilic properties that could enhance the sample separation compared to the diols groups. Three compounds phenacetin, codeine, and pyrene were used with the same experimental conditions that illustrate in section (5.6.3). The results are shown in Figure (5.37)

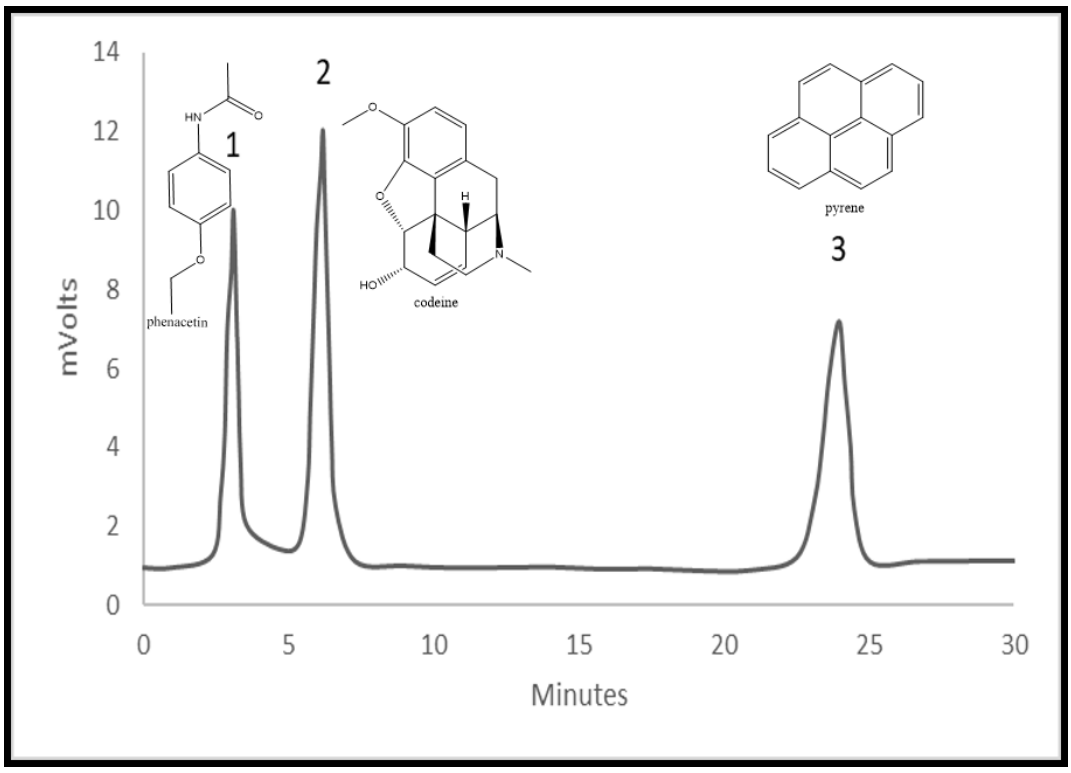

Figure 5.37 Chromatogram of a mixture of (1) phenacetin, (2) codeine, and (3) pyrene, 10^{-5} M mixture of each with gradient no. (7) the injection volume (2.5 µL), and the detection wavelength 254 nm.

As can be seen from Figure (5.37), the two hydrophilic compounds phenacetin and codeine were better separated using SCX/RP monolithic column compared with HILIC/RP monolithic column. This could be due to a contribution of ($-SO_3^-$) groups on the surface of the monolithic column that could increase the hydrophilic properties by providing alternative functional groups that could increase the interaction between the hydrophilic compound and the surface of the monolith. However, the mass transfer rate between the mobile phase and the stationary phase was increased and the retention factor was decreased. Therefore, the performance of the monolithic column was enhanced by obtaining base line separation between the hydrophilic compounds.

According to the plate theory, the separation is enhanced when the N and Rs values are increased. These parameters were calculated, and values compared with experiment results that obtained in section (5.6.3). The results are shown in Table (5.16)

Table 5.16 The average number of theoretical plates (N) and the resolution value (Rs) for phenacetin, codeine, and anthracene with SCX/RP and HILIC/RP monolithic columns (n=3)

Analytes	SCX/RP monolithic column	HILIC/RP monolithic column
N	3018	2897
Rs for Phenacetin and Codeine	2.25	0.76
Rs for Codeine and Anthracene	10.75	6.25

The N value for SCX/RP monolithic columns was increased compared with HILIC/RP monolithic column, which explains the improvement in the peak shapes. Moreover, the Rs value was changed dramatically from 0.76 to 2.25 to give clear base line separation for the hydrophilic molecules. All these results indicate that the retention mechanism could be controlled by the polar (OH) groups in addition to the ($-SO_3^-$) groups that take part in the separation process. As described in (5.6.3) The elution order did not change and did not follow the hydrophobicity order because phenacetin is more hydrophobicity than codeine[259], and still phenacetin eluted earlier, that could be due to some hydrophilic interactions with hydrophilic parts of the monolith surface.

5.9.4 Separation of peptides

The SCX/RP GMA-co-SMA-co-EDMA monolithic columns were used to separate a mixture of peptides that have different molecular weight and charge density depending on the amino acids in the side chains.

Two peptides angiotensin I (1298.48 g mol^{-1}), and angiotensin II (1046.18 g mol^{-1}) were used to investigate the separation ability of the monolithic columns using gradient analysis shown in Table (5.17), the results are shown in Figure (5.38)

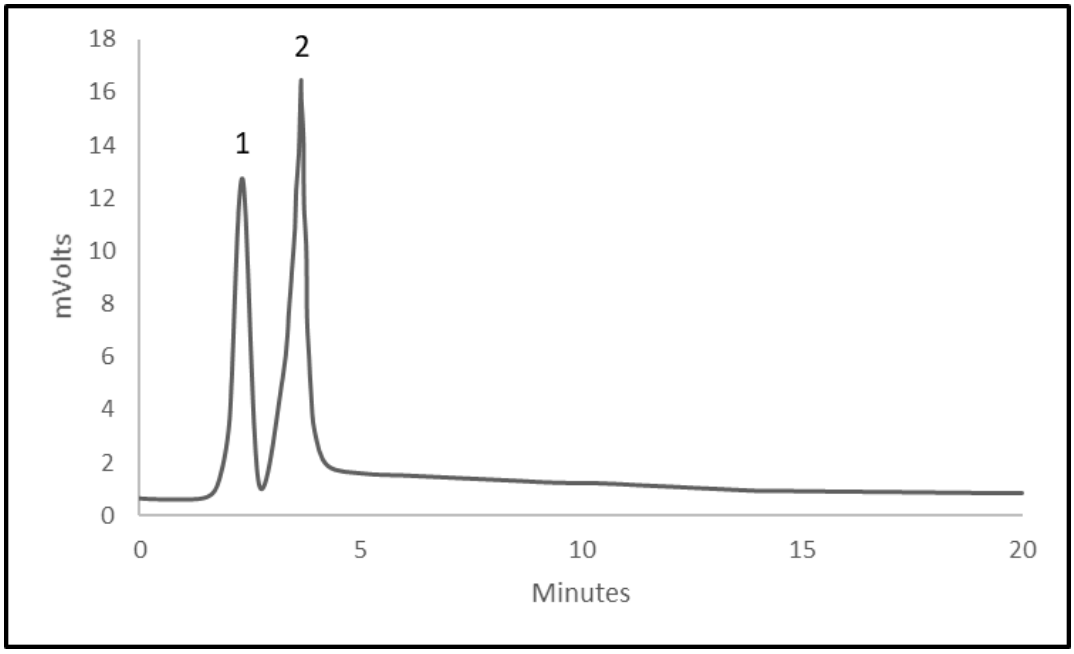

Figure 5.38 Chromatogram of proteins mixture (1) angiotensin (II), and (2) angiotensin (I), 0.5 mg mL^{-1} mixture of each with gradient no. (11) the injection volume (2.5 µL), and the detection wavelength 254 nm.

Table 5.17 Solvent composition of gradient analysis no. (11)

Time/ min.	Sodium phosphate (pH= 9) %	Acetonitrile % (0.1 % TFA)	Flowrate mL min^{-1}
0:00	0	100	0.2
1:00	0	100	0.2
16:00	70	30	0.2
18:00	70	30	0.2
18.30	0	100	0.2
20:00	0	100	0.2

The electrostatic interactions will take place between the positively charged peptides and the ($-SO_3^-$) groups on the surface of the monolithic columns. However, the retention time will differ from one peptide to another depending on their net charge densities. Therefore, when a peptide has a lower number of positively charged amino acids it will elute before the peptide that has more positively charged amino acids. Gradient analysis was used to elute the peptides by varying the pH of the solvent solution between 2.4 and 8.5.

As can be seen from Figure (5.38) that the angiotensin (II) was eluted before angiotensin (I) because the amino acids sequence of angiotensin (II) is Asp-Arg-Val-Tyr-Ile-His-Pro-Phe, while, that for angiotensin (I) is Asp-Arg-Val-Tyr-Ile-His-Pro-Phe-His-Leu. Therefore, angiotensin (II) has two positively charged amino acids (Arg, His) in addition to the positive N terminal on the (Asp) when it is fully protonated at acidic media, eventually the net charge is +3. Angiotensin (I) has three positively amino acids (Arg) and two (His) in addition to the positive N terminal on the (Asp), therefore, the net charge is +4.

According to cationic interactions the angiotensin (II) will elute first because it has less net charge compared with the angiotensin (I) that required more time to elute. In terms of the hydrophobicity, angiotensin (II) has three hydrophobic amino acids (Ile, Pro, and Phe. While angiotensin (I) has four hydrophobic amino acids (Ile, Pro, Phe, and Leu), therefore, angiotensin (I) could interact with hydrophobic alkyl chains on the surface of the monolith also leading to an increase in the retention time. The N and Rs values were calculated and shown in Table (5.18)

Table 5.18 The average number of theoretical plates (N) and the resolution value (Rs) for angiotensin (II), and angiotensin (I)with SCX/RP and HILIC/RP monolithic columns (n=3)

N	818
Rs for Angiotensin (II) and Angiotensin (I)	1.46

5.9.5 Separation of peptides from digested cytochrome C

SCX/RP GMA-co-SMA-co-EDMA monolithic column was used to separate peptides from a commercial tryptic digested cytochrome C previously examined with HILIC/RP monolithic columns (section 5.6.4) using the same experimental conditions, except that sodium phosphate (pH= 9) was used instead of water. The results are shown in Figure (5.39)

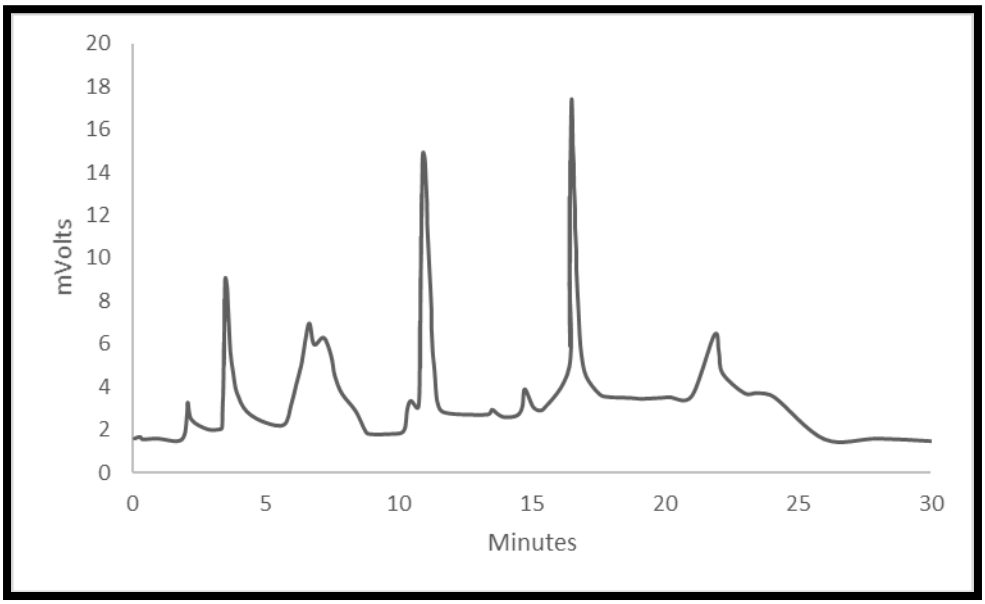

Figure 5.39 Chromatogram of commercial tryptic digested cytochrome C with gradient no. (8) using sodium phosphate instead of water, the injection volume (2.5 µL), and the detection wavelength 254 nm.

The experiments showed that, when using SCX/RP monolithic columns some peak shapes were enhanced compared with the peak shapes obtained with HILIC/RP monolithic columns as can be seen in Figures (5.39) and (5.14). These satisfactory results could be due to the presence of strong cationic interactions increasing the interactions between the charged peptides and the ionic exchanger.

On the other hand, the full separation of peptides was not achieved due to the complexity of the sample that contains substantial number of peptides having different net charge.

Possibly, a larger monolithic column may have been more successful, however, this was not possible with the equipment available.

5.10 Fabrication of strong cationic exchange/ revers phase monolithic columns inside microchip device

The SCX/RP glycidyl methacrylate-co-stearyl methacrylate-co-ethylene glycol dimethacrylate monolithic columns were fabricated inside the microchip device by in-situ polymerization to prepare monolithic columns that could be used for LC separation.

The microchip was prepared as described in section (2.9), however it contains two holes on the top layer of 1.5 mm diameter which were created using traditional glass drilling techniques for inlet and outlet of the mobile phase. The second layer consists of the milled channel that was created using a Datron M7 CNC-machine, the dimensions of the channel were 30 mm length, 1 mm width, and 500 µm depth, and the two layers were thermally bonded at 585 °C for 3 hours in a custom-made oven. The microchip design is illustrated in Figure (5.40).

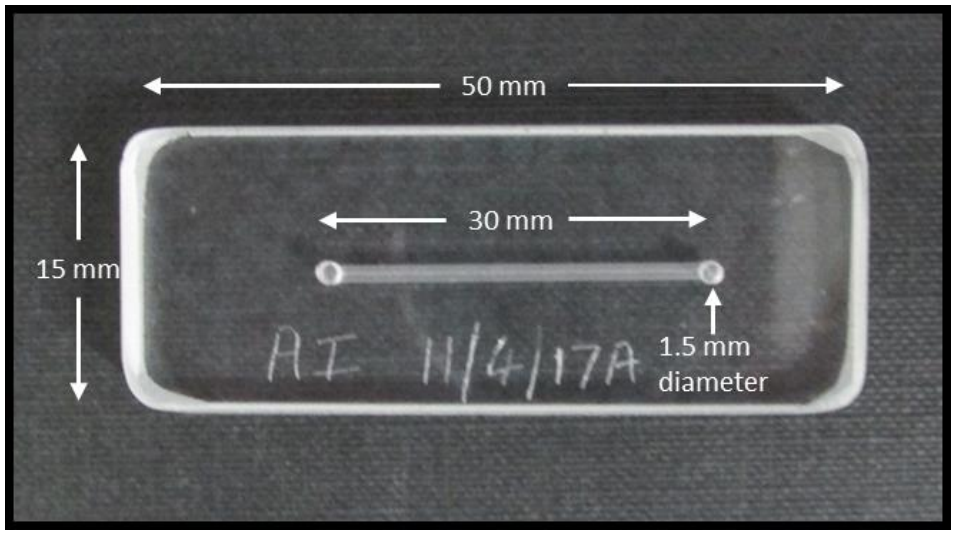

Figure 5.40 A glass microchip photograph that used for in-situ polymerization for SCX/RP monolithic columns for LC separation

PEEK tubes were glued to the microchip using epoxy glue, and it was then connected to the syringe pump for the silanization and polymerization steps described in section 2.1.1 and 2.1.2 respectively. The porogenic solvent used was a mixture of 50:50 1-propanol, and methanol with 23 min irradiation time. After that, the glycidyl methacrylate-co-stearyl methacrylate-co-ethylene glycol dimethacrylate monolith was modified to SCX/RP monolith using the epoxy ring opening reaction method illustrated in section 2.6.2. The fabricated monolith inside the microchip is shown in Figure (5.41)

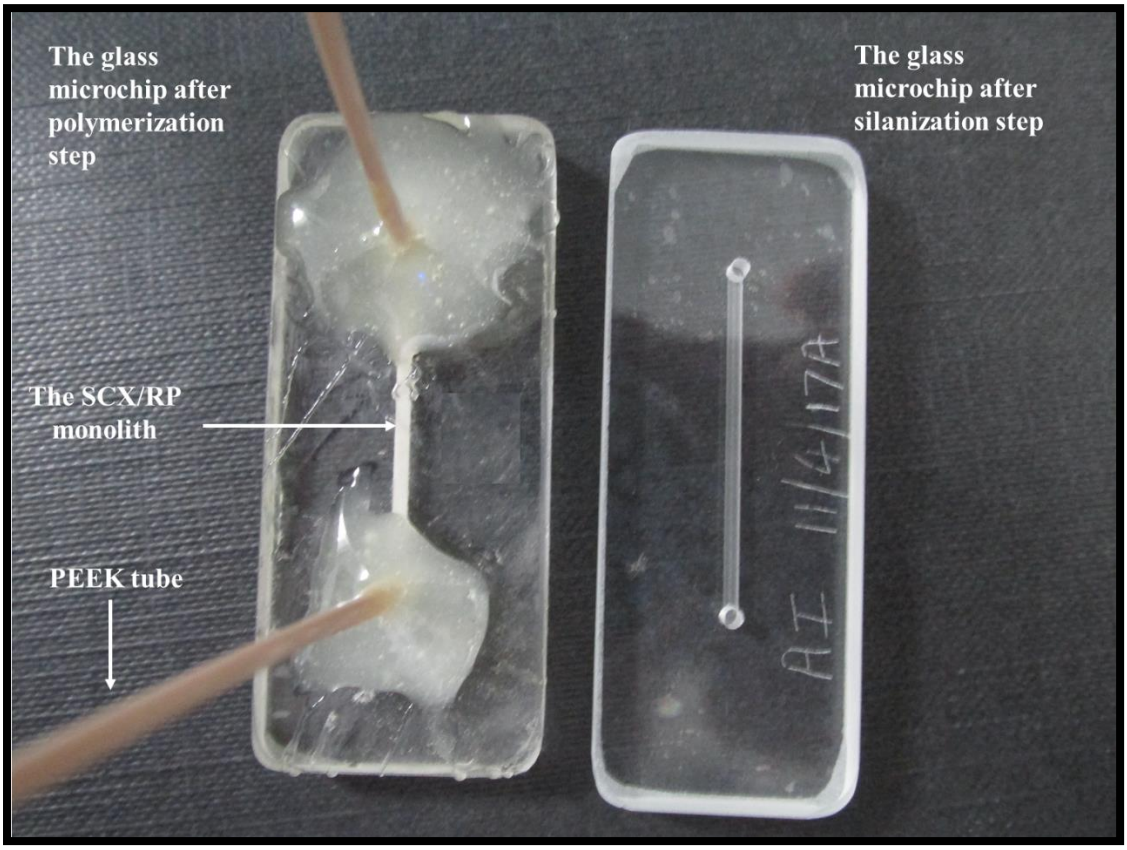

Figure 5.41 A photograph for the microchips device, on the right the microchip after silanization step, and on the left the microchip after polymerization step

5.10.1 Investigation of the flow rate inside the microchip

The flow rate was investigated to obtain the appropriate flow rate with reasonable back pressure. The microchip was connected to a hydrodynamic pump (JASCO, PU 1580, Japan) and different flow rates were investigated to evaluate the back pressure. The results are shown in Table (5.19)

Table 5.19 The effect of the flow rate on the back pressure inside the microchip (n=3)

Flow rate µL min^{-1}	**Back pressure (psi)**
4	726
6	819
8	1152
10	1370
12	1489
13	The system leaked

As can be seen from Table (5.19) that the maximum flow rate that can be used was 12 µL min^{-1} with back pressure 1489 psi. Therefore, this flow rate was used in the further experiments.

The HPLC pump used in previous experiments provides less reliable flow at rates below 10 µL min^{-1}. Therefore, the HPLC system could not be used with a microchip device especially with gradient analysis which required changing the flow rate with time. In addition, a suitable flow splitter was not available. However, another system was used to test the separation ability of the fabricated SCX/RP monolith inside the microchip.

The microchip was connected to the new system that consists of a hydrodynamic pump (JASCO, PU 1580, Japan) that can pump at a flow rate below 10 µL min^{-1}, manual injector, and UV detector (KNAUER, D-14163, Germany). The new system is shown in Figure (5.42)

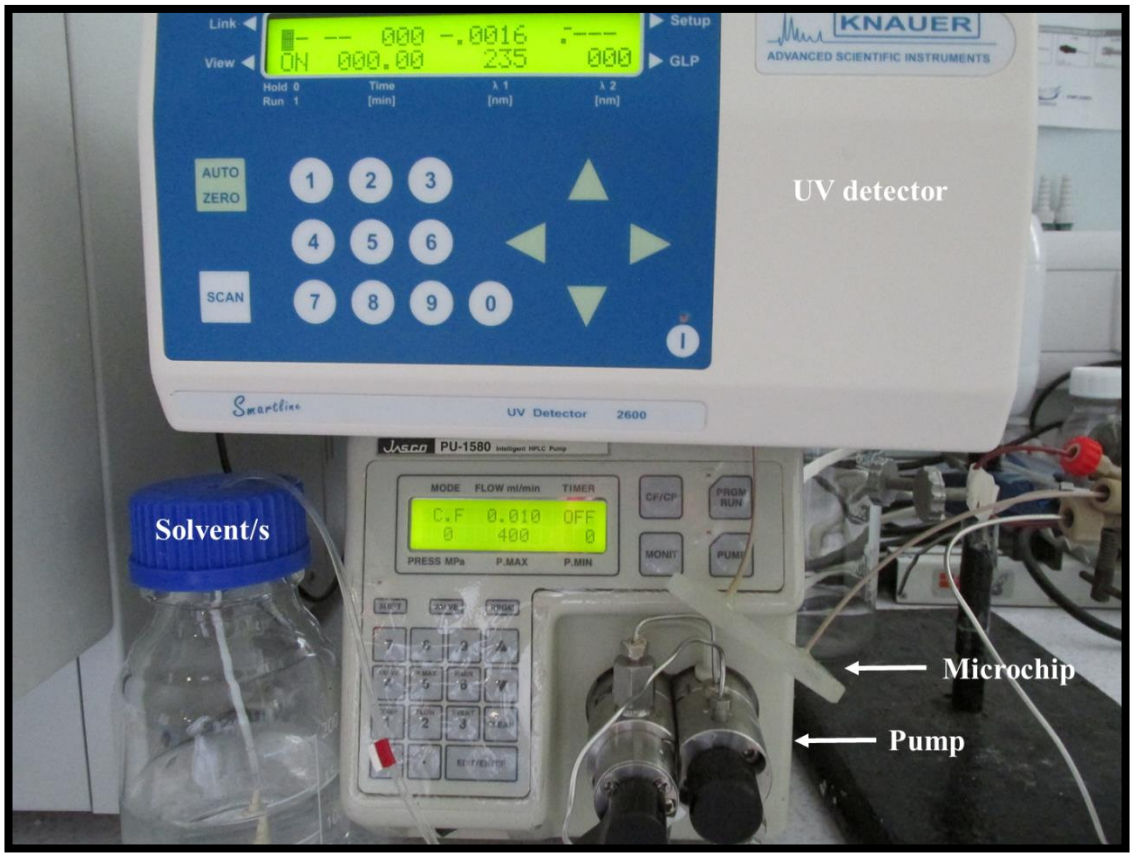

Figure 5.42 A photograph for the microchip that connected to the manual injector and UV detector.

As can be seen the new system could not use gradient analysis since there is one pump only that can pump the solvent through the system. Therefore, isocratic analysis was used to try and separate small molecules due to the high surface area that could be key factor to increase the interactions between the analyte and the stationary phase.

5.10.2 Separation of hydrophobic compounds using microchip device

The hydrophobic compounds (benzophenone, fluorene, anthracene, and pyrene) were used to investigate the separation ability of the SCX/RP monolithic columns that prepared in situ polymerization. These compounds are differed in the hydrophobicity, and the molecular weight, that could be used to separate these compounds depending on the interactions of these compounds with stationary phase. The results are shown in Figure (5.43)

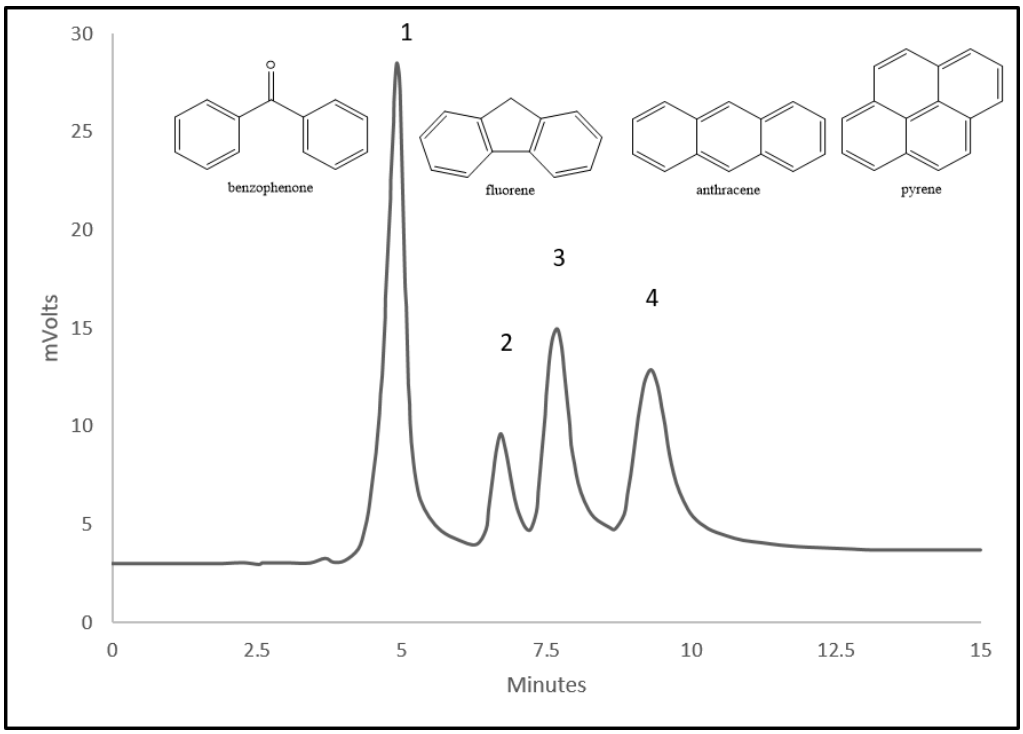

Figure 5.43 Chromatogram of a mixture of (1) benzophenone, (2) fluorene, (3) anthracene, and (4) pyrene, 10^{-5} M mixture of each with 80% ACN, 20% water, the injection volume (1.5 µL), flow rate 12 µL min^{-1}, and the detection wavelength 254 nm.

As can be seen from Figure (5.43) that the four compounds were separated successfully, and the elution order followed the hydrophobicity order therefor, benzophenone was eluted first, while pyrene has higher retention time. However,

isocratic analysis was used instead of gradient analysis for two reasons, initially, the limitation of HPLC pump to pump lower than 10 µL min^{-1}, secondly, the isocratic analysis could be used with monolith that have high surface area and enough mesopores, because it was mentioned elsewhere that the isocratic system could not provide fine separation if the monolithic column does not have enough mesopores.[191] So far, the SCX/RP monolith prepared using 1-propanol, and methanol exhibited higher surface area, and higher pore size than other monoliths prepared in this study. The high surface area and high pore size of the monolith will boost the partitioning of the analytes between the mobile phase and the hydrophobic stationary phase of the monolithic column. Consequently, the solutes will diffuse into the pores of the stationary phase and interact with the alkyl chains by hydrophobic interactions. Therefore, the amount of less polar solvent was used to enhance the mass transfer of the solutes between the stationary phase and mobile phase by reducing the retention factor of the analytes.[257] In addition, increasing the desorption rate over adsorption rate, consequently, decreasing the C-term in van Deemter equation, that can give sharp peaks with base line separation.

According to the plate theory, when the (N) value is increased the efficiency of the column is increased due to increasing the instant equilibrium of the solute between the mobile phase and the stationary phase. So far, the base line separation will be improved. The (N) and (Rs) values was calculated, and the results were shown in Table (5.20).

Table 5.20 The average number of theoretical plates (N) and the resolution value (Rs) for benzophenone, fluorene, anthracene, and pyrene using SCX/RP monolithic column inside microchip device (n=3)

N	334
Rs for Benzophenone and Fluorene	2.164
Rs for Fluorene and Anthracene	0.871
Rs for Anthracene and Pyrene	1.193

It was mentioned elsewhere that Rs can be considered acceptable when it is 0.8, while it would be significant at 1.5.[223] However, from Table (5.20) base line separation could be obtained with benzophenone and fluorene, while, it could not quite be obtained between fluorene and anthracene. Depending on the hydrophobicity index the values of log P for these chemicals are, benzophenone 3.18, fluorene 4.18, anthracene 4.4, pyrene 4.88.[268] It can be seen that there is a significant difference in the hydrophobicity between benzophenone and fluorene leading to elution of benzophenone earlier than fluorene with base line separation. While, the difference in the hydrophobicity between fluorene and anthracene is less than other compounds, therefore, the base line separation was not quite obtained.

5.10.3 Separation of pharmaceutical compounds using microchip device

The microchip device was used to investigate separation of two pharmaceutical compounds phenacetin, and codeine. These compounds were previously investigated using GMA-co-SMA-co-EDMA monolithic column as SCX/RP inside a borosilicate tube as illustrated in section (5.10.2). Similarly, the prepared monolithic column inside the microchip has ($-SO_3^-$), and (-OH) groups on the surface of the monolith that formed due to opening the epoxy ring of GMA. These groups can give hydrophilic properties beside the hydrophobic properties for the monolith which could be used as a mixed-mode monolithic column HILIC/RP. Isocratic analysis again used for the same reasons previously mentioned to separate these compounds. The results are shown in Figure (5.44)

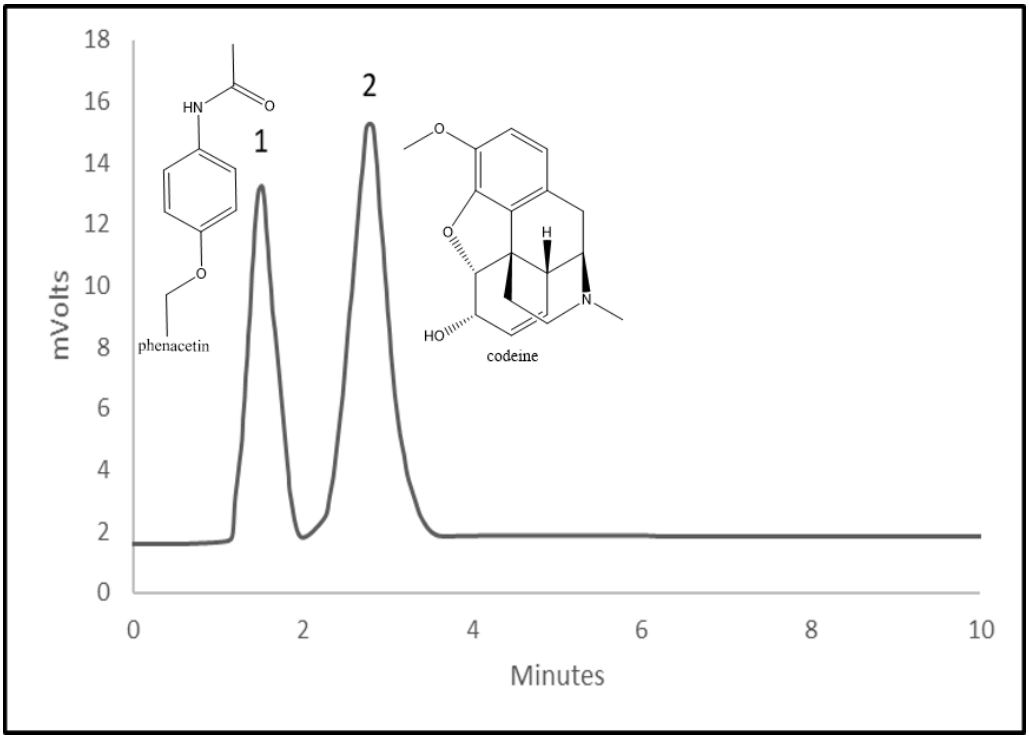

Figure 5.44 Chromatogram of a mixture of (1) phenacetin, (2) codeine, 10^{-5} M mixture of each with 20% ACN, 80% water, the injection volume (1.5 µL), flow rate 12 µL min^{-1}, and the detection wavelength 254 nm.

As can be seen from Figure (5.44) that, the two compounds were separated with base line separation. However, the retention time was changed toward lower retention time compared with the retention time in the previous experiment section (5.10.3). It could be that the desorption rate was higher than the adsorption rate when isocratic analysis was used compared with gradient analysis. Consequently, the retention factor was decreased leading to elute these compounds earlier. The efficiency of the monolithic column was investigated by calculating N and Rs value. These values were shown in Table (5.21).

Table 5.21 The average number of theoretical plates (N) and the resolution value (Rs) for phenacetin, and codeine using SCX/RP monolithic column inside microchip device (n=3)

N for Phenacetin	149
Rs for Phenacetin and Codeine	1.258

As can be seen from Table (5.21) and Figure (5.44) that the satisfying separation of pharmaceutical compounds could be achieved using SCX/RP monolithic column in microchip device with isocratic analysis.

The large molecules such as proteins and peptides were not tested because separation of these compounds required gradient analysis.

5.11 Evaluation of separation performance for SCX/RP glycidyl methacrylate-co-stearyl methacrylate-co- ethylene glycol dimethacrylate monolithic column

The separation performance for the SCX/RP GMA-co-SMA-co-EDMA monolithic columns was evaluated by investigating the long-term stability and reproducibility for the monolithic columns fabricated inside the borosilicate tube and the glass microchip. Proteins that showed based line separation in section 5.10.1 when three proteins were separated as shown in Figure (5.35). These proteins were used to investigate the run-to-run, and batch-to-batch reproducibility for the SCX/RP GMA-co-SMA-co-EDMA monolithic columns prepared inside the borosilicate tube. While, the monolithic column performance prepared inside the glass microchip was investigated using the experiment shown in section 5.11.3 based on the retention time of each sample.

The run-to-run reproducibility was carried out by separation of these compounds using the same borosilicate tube and same glass microchip for three times. Whereas, the batch-to-batch reproducibility was carried out by separation the same proteins using different borosilicate tube and glass microchip three times. The evaluation results for the SCX/RP monolithic columns prepared inside the borosilicate tube and glass microchip are shown in Tables (5.22), and (5.23).

Table 5.22 The RSD results of run-to-run and batch-to-batch for the SCX/RP monolithic column inside borosilicate tube (n=3)

	Insulin RSD%	Myoglobin RSD%	Lysozyme RSD%
Run-to-Run	3.82	3.04	3.91
Batch-to-Batch	4.48	3.66	4.27

Table 5.23 The RSD results of run-to-run and batch-to-batch for the SCX/RP monolithic column inside glass microchip (n=3)

	Phenacetin RSD%	Codeine RSD%
Run-to-Run	1.73	1.84
Batch-to-Batch	2.27	2.52

It can be seen from Tables (5.22), and (5.23) that the proteins and pharmaceutical compounds separation reproducibility using borosilicate tube and glass microchip was achieved due to the acceptable RSD% value.

The SCX/RP monolithic columns were stable and could be used several times. So far, they have been used 20 times with the borosilicate tube and 8 times with glass microchip. The life time was investigated by evaluation of the back pressure of the experiment each time. However, it was found that the life time was more than 30 days for both the borosilicate tube and glass microchip if they were stored in a solution of (50:50) acetonitrile and water. Yet, the life time was 10, and 6 days for the borosilicate tube and glass microchip respectively, if they were kept

dry due to the cracking of the monolith. Therefore, the monolith should be stored in solvent(s).

5.12 Summary

Glycidyl methacrylate-co-stearyl methacrylate-co-ethylene glycol dimethacrylate monolithic columns were prepared using different ratios of GMA:SMA such as (90:10, 50:50, 40:60, 30:70, 20:80, and 10:90)%. The most suitable irradiation time was investigated using 365 nm UV-light to form a monolith with a suitable pore matrix containing macropores and mesopores, and able to provide significant separation the results are shown in Table (5.22).

Table 5.24 The effect of irradiation time on the surface area and the pore size of the GMA-co-SMA-co-EDMA monolithic columns.

Monomers ratio (v/v) GMA:SMA mL	**Irradiation time min**	**Surface area m^2g^{-1}**	**Pore size nm**
90:10 %	100	13.2480	6.38
50:50 %	120	14.5920	5.69
40:60 %	120	16.1381	5.91
30:70 %	130	19.5938	5.12
20:80 %	140	20.3313	4.80
10:90 %	160	21.0283	4.20

It was found from Table (5.24) that the monolith was formed with all the ratios of the monomers that used. In addition, the irradiation time for each column was increased with increasing the percentage of SMA. The average surface area and

average pore size were investigated using BET analysis, however, the results showed that the higher average surface area of the monolithic columns between 19.5938-21.0283 m^2 g^{-1}, was achieved with a reduction in the average pores size was 5.12, 4.80, and 4.2 nm for (30:70, 20:80, and 10:90)% of GMA:SMA respectively. However, the monolithic column prepared using (30:70)% of GMA:SMA has been chosen for LC separation, due to the higher average pores size compared to the (20:80, and 10:90)% of GMA:SMA, which can give the monolith higher permeability and less back pressure.

FTIR analysis was used to determine the peaks of interest in the monomers, cross-linker, and the monolith. The results showed that the glycidyl methacrylate-co-stearyl methacrylate-co-ethylene glycol dimethacrylate polymer has two peaks at 1726.41 cm^{-1} and 910.07 cm^{-1} indicating the presence of (C=O) and epoxy group. While (C=C) peak a round 1637 cm^{-1} in the monomers, and cross-linker was disappeared, this is good evidence for the formation of the polymer by incorporation of both monomers and cross-linker using (C=C) bonds. Moreover, the ^{1}HNMR analysis has been investigated to demonstrate the formation of the monolith, the results show that the ($C=CH_2$) bonds around (5-6) ppm in the monomers and cross linker have disappeared in the polymer ^{1}HNMR spectrum.

The epoxy ring for glycidyl methacrylate-co-stearyl methacrylate-co-ethylene glycol dimethacrylate monolithic columns prepared using (30:70)% of GMA:SMA and irradiation time 120 minute was opened to form diol groups. These groups increase the hydrophilic properties to obtain HILIC/RP monolithic columns that could be used to separate a range of different samples. The FTIR results showed

that the peak at 910.07 cm^{-1} for the epoxy ring in the monolithic column had disappeared and a new peak at 3237.51 cm^{-1} was formed which indicate that the (-OH) was formed and the epoxy ring was opened.

The prepared monolithic columns were used to separate several types of compounds such as, hydrophobic compounds, pharmaceutical compounds, mixture of hydrophilic and hydrophobic compounds, digested cytochrome C, and proteins. The results are shown in Table (5.25).

Table 5.25 The application of HILIC/RP GMA-co-SMA-co-EDMA monolithic column with different samples.

Samples	**HILIC/RP monolithic column**
Mixture of Hydrophobic compounds	Good separation with base line separation and N (3215)
Mixture of Pharmaceutical compounds	Good separation with base line separation and N (1147)
Mixture of hydrophobic and hydrophilic compounds	Good separation with N (2897)
Peptides	Poor separation
Proteins	Poor separation

Table (5.25) showed that, a significant base line separation and (N) value could be obtained with hydrophobic, pharmaceutical, mixture of hydrophilic and hydrophobic compounds compared with GMA-co-LMA-co-EDMA monolithic columns, although proteins and digested cytochrome C could not be fully separated.

The mixed mode mechanism was investigated using two monolithic columns GMA-co-SMA-co-EDMA, and SMA-co-EDMA to separate the same sample

containing phenacetin, codeine, and anthracene. The results showed there is a significant difference in separation behavior between the two columns. There are two peaks observed with SMA-co-EDMA monolithic column the first one was a broad peak for phenacetin and codeine, and the second peak for anthracene. Whereas, with GMA-co-SMA-co-EDMA monolithic column, there are three peaks for all the compounds. In addition, the peak shape was enhanced toward sharper peaks.

The effect of porogenic solvents on the monolith formation was investigated in an attempt to obtain higher surface areas compared with that of the monolith previously prepared using 1-propanol, and 1,4-butan di-ol. Different porogenic solvents such as methanol, ethanol, hexanol, 1-dodecanol, acetonitrile, and chloroform with 1-propanol were used to prepare the monolithic columns. The monoliths were tested by BET analysis and the results are shown in Table (5.26).

Table 5.26 The effect of porogenic solvent on the surface area and the pore size of the GMA-co-SMA-co-EDMA monolithic columns.

Porogenic solvents	**Surface area m^2g^{-1}**	**Pore size nm**
1-Propanol and methanol	246.7444	3.16
1-Propanol and ethanol	8.4633	4.26
1-Propanol and hexanol	151.4761	3.56
1-Propanol and 1-dodecanol	27.0396	2.36
1-Propanol and acetonitrile	35.8386	3.75
1-Propanol and chloroform	142.9172	2.86

It can be seen from Table (5.26) that the monolithic columns prepared using 1-propanol and methanol had a higher surface area than the others. After that the ratio of the porogenic solvents 1-propanol/methanol was investigated to prepare monolithic columns that have a suitable surface area and pore size to separate large molecules. The results are shown in Table (5.27).

Table 5.27 The effect of poroginic solvent ratio 1-propanol/methanol on the surface area and the pore size of the GMA-co-SMA-co-EDMA monolithic columns.

1-Propanol : Methanol (v/v)	Surface area m^2g^{-1}	Pore size nm
1.05 : 0.60	246.7444	3.16
0.90 : 0.75	253.9917	3.04
0.85 : 0.80	262.4497	2.97
0.825 : 0.285	282.5835	2.95
0.80 : 0.85	276.4871	2.98
0.75 : 0.90	271.7542	3.03
0.60 : 1.05	246.3098	3.07

Table (5.27) showed that the 50:50 percent of 1-propanol to methanol gave better results compared with other ratios. The monolithic column was connected to the HPLC pump to evaluate the back pressure, it was found that the monolithic column was too dense and could not wash with any solvents. Therefore, the irradiation time was investigated to form the monolith with 50:50 1-propanol/methanol, the results showed that the monolith was formed after 23 minutes, which is less than the other monolithic columns. This column was used in all the further experiments.

The GMA-co-SMA-co-EDMA monolith was used to separate a mixture of three proteins, the results showed acceptable ability to separate these proteins. However, the peaks were broad and there is overlap between these peaks and complete resolution and base line separation was not possible with the monolithic column as HILIC/RP mixed mode monolithic column. However, this mechanism does not enhance the peak width and make it sharper. Therefore, another option has been investigated by changing the monolithic column to strong cationic exchange/ hydrophobic mixed mode monolithic column by opening the epoxy ring of glycidyl methacrylate using Na_2SO_3 to form a cationic exchanger.

The epoxy groups in glycidyl methacrylate-co-stearyl methacrylate-co-ethylene glycol dimethacrylate monolithic columns were opened using a sulfonation reaction. The ring opening reaction and formation of a cationic exchanger was proven using different techniques such as FTIR, EDX, and CHN. The FTIR showed the peak at 910.07 cm^{-1} for epoxy groups of the GMA in the monolith was disappeared, and there are two new peaks clearly present, at 1032.23 cm^{-1} and 995.96 cm^{-1} for R-SO_3 and S-O groups respectively, in addition, a broad band for -OH group between 3600-3100 cm^{-1} was observed. The peaks at 1725.19 cm^{-1} for C=O, and at 1148.21 cm^{-1} for C-O ester groups are still unchanged due to non-participation of these groups in the sulfonation reaction.

EDX, and CHN techniques demonstrated that the epoxy rings were opened due to presence of the S and Na in the in the EDX analysis, while S in the CHN analysis.

The SCX/RP monolithic columns were investigated to separate proteins, peptides, tryptic digested cytochrome C, hydrophobic compounds, and a mixture of hydrophilic and hydrophobic compounds. The results are shown in Table (5.28).

Table 5.28 The N and Rs values for SCX/RP and HILIC/RP GMA-co-SMA-co-EDMA monolithic columns with different samples.

Analytes	**SCX/RP monolithic column**		**HILIC/RP monolithic column**	
	Average N value	**Average Rs value**	**Average N value**	**Average Rs value**
Mixture of Hydrophobic compounds	3272	2.12	3215	1.23
Mixture of hydrophilic and hydrophobic compounds	3018	6.50	2897	3.50
Mixture of peptides	818	1.46	Poor separation	Poor separation
Mixture of proteins	1389	2.6	Poor separation	Poor separation

It was found from Tables (5.28) that the N and Rs values are higher and base line separation could be obtained using SCX/RP monolithic columns with all proteins samples, peptides, hydrophobic compounds, and mixture of hydrophilic and hydrophobic compounds compared to the HILIC/RP monolithic columns.

The SCX/RP GMA-co-SMA-co-EDMA monolithic column was prepared inside the microchip device to reduce the analytes volume that could be expensive, or the solvents volume that could be not available in substantial amounts. Moreover, reducing the reaction time due to the small size of the reactors, and enhancing the performance of the analytical device by increasing the reproducibility, and the selectivity.

Isocratic analysis was used instead of gradient analysis due to the low flow rate required for use with the microchip (maximum flow rate 12 µL min^{-1}). Therefore, another system was used based on a single pump, because the limited flow rate of the HPLC pump was 10 µL min^{-1}. Therefore, the gradient analysis could not be used. Due to this limitation the separation of the large molecules such as proteins and peptides was not investigated further. However, the high surface area and pore size compared to HILIC/RP monolith was helped to separate small molecules such as hydrophobic, and pharmaceutical compounds with base line separation.

From all the results above, it can be concluded that the GMA-co-SMA-co-EDMA monolithic columns that prepared using (50:50) 1-propanol, and methanol as a porogenic solvent showed higher surface area and pore size than other columns. These columns exhibited significant separation when they converted to SCX/RP monolithic columns compared with HILIC/RP monolithic columns.

6 Conclusions

Glycidyl methacrylate copolymer monolithic columns have been investigated using different monomers alongside to glycidyl methacrylate (GMA) such as styrene (Sty), 2-(diethylamino) ethyl methacrylate (2DEAMA), butyl methacrylate (BMA), lauryl methacrylate (LMA), and stearyl methacrylate (SMA). Ethylene glycol dimethacrylate (EDMA) was used as cross-linker, while, 2,2-dimethoxy-2-phenylacetophenone was used as initiator. All these monoliths were prepared inside the borosilicate tube by in-situ polymerization to produce mixed mode monolithic columns. The prepared columns have been tested for use in LC separation, instead of using one column for each mode (hydrophobic, hydrophilic, and ionic exchange) to save the time, effort, money and enhance the reproducibility of the analysis.

The three ratios (90:10, 50:50, and 10:90)% between the two monomers was investigated to prepare monolith with appropriate surface area and pore size that can be used to separate small and macro molecules. It was found that the (GMA-co-Sty-co-EDMA) monolithic column was formed using (90:10) % of GMA:Sty after 360 minutes of irradiation time. The BET analysis results demonstrated that the monolithic column has low average surface area 1.2104 m^2 g^{-1}, with average pore size of 17.84 nm.

The monolithic columns were connected to HPLC system to investigate the separation performance of the columns. The results showed that these columns have poor separation ability to separate different samples, due to the low surface area which lead to poor interactions between the sample and the stationary

phase. Other monomer ratios have been investigated to form the monolithic column, however, the monolith did not form using any of these other ratios.

The second monolithic column (GMA-co-2DEAMA-co-EDMA) was formed after 240 minutes with (90:10) %, and after 290 minutes with (50:50) % of GMA:2DEAMA. While, it was not formed with (10:90)%. The BET analysis results showed that the average surface area and the average pore size for (90:10)% GMA:2DEAMA were 3.0530 m^2 g^{-1}, and 15.80 nm, while, 2.2716 m^2 g^{-1}, and 14.02 nm, for (50:50)% GMA:2DEAMA. The chromatographic behavior of these columns was also poor, and no separation was achieved.

The GMA-co-BMA-co-EDMA monolithic columns showed slightly higher surface area than the monolithic columns that prepared using Sty, and 2DEAMA. The monolith was only formed using (10:90) % GMA:BMA. The average surface area was 4.9582 m^2 g^{-1}, with average pore size of 15.03 nm when irradiated for 110 minutes. The monolithic columns showed poor performance as LC columns.

The GMA-co-LMA-co-EDMA monolithic column was formed using the three ratios with different irradiation time. The (10:90) % of GMA:LMA was formed after 140 minutes irradiation time. The monolithic columns have higher average surface area compared with (50:50)% 11.4328 $m^2.g^{-1}$. Moreover, the average pore size was 4.26 nm.

The monolithic column was demonstrated to separate different samples such as hydrophilic, and hydrophobic molecules. However, large molecules (peptides and proteins) were not separated. While, The results showed that the hydrophilic compounds are eluted first flowed by hydrophobic compounds, this could be,

because the surface of the monolith has a 90% of LMA, therefore, the hydrophilic properties of the GMA that can give hydrophilic properties to the monolith, was poor compared with the hydrophobic properties.

The GMA-co-SMA-co-EDMA monolithic columns were prepared using different ratios of GMA:SMA (90:10)%, (50:50)%, (40:60)%, (30:70)%, (20:80), and (10:90)%. The irradiation time was investigated for each ratio to obtain the best ratio that can give significant surface area with reasonable pore size that can be used for LC separation.

The nitrogen adsorption analysis using BET analyzer results showed that the average surface area of the monoliths increased with increasing the ratio of SMA. The (30:70)% of the GMA:SMA was chosen in the all experiments because the average surface area of the monolith was higher than other monoliths that formed using GMA:SMA with lower ratio. While, above the (30:70) ratio the average surface area of the monoliths was increased steadily. So far, these columns have not been chosen because, they have higher hydrophobic properties and less hydrophilic properties due to low ratio of GMA, that could lead to decreasing the probability of obtaining mixed mode monolithic columns.

The GMA-co-SMA-co-EDMA as terpolymer monolithic column was demonstrated using FTIR and ^{1}HNMR analysis. The results showed that the polymer has two peaks at 1726.41 cm^{-1} and 910.07 cm^{-1} indicating the presence of (C=O) and epoxy group. While (C=C) peak a round 1637 cm^{-1} in the monomers, and cross-linker was disappeared, this is good evidence for the formation of the polymer by incorporation of both monomers and cross-linker using (C=C) bonds. The ^{1}HNMR

analysis showed that the ($C=CH_2$) bonds around (5-6) ppm in the monomers and cross linker have disappeared in the polymer ^{1}HNMR spectrum.

The monolithic columns were used as HILIC/RP monolithic columns after changing the epoxy rings of glycidyl methacrylate to diol groups to increase the hydrophilic properties of the columns. The FTIR results showed that the peak at 910.07 cm^{-1} for the epoxy ring in the monolithic column had disappeared and a new peak at 3237.51 cm^{-1} was formed which indicate that the (-OH) was formed and the epoxy ring was opened.

The prepared monolithic columns were used to separate several types of compounds such as, hydrophobic compounds, pharmaceutical compounds, mixture of hydrophilic and hydrophobic compounds, digested cytochrome C, and proteins. The results showed that, a significant base line separation could be obtained with hydrophobic, pharmaceutical, mixture of hydrophilic and hydrophobic compounds compared with GMA-co-LMA-co-EDMA monolithic columns, although proteins and digested cytochrome C could not separate properly.

The mixed mode behavior was investigated using two monolithic columns GMA-co-SMA-co-EDMA, and SMA-co-EDMA monolithic columns to separate the same sample containing phenacetin, codeine, and anthracene. It was found that there is a difference in the separation behavior between the two columns, because SMA-co-EDMA monolithic column showed two peaks for the three compounds. While, GMA-co-SMA-co-EDMA showed good separation for all the three compounds, and the elution order was not follow the hydrophobicity order.

Different porogenic solvents such as methanol, ethanol, hexanol, 1-dodecanol, acetonitrile, and chloroform with 1-propanol as porogenic solvents were used to prepare the monolithic columns instead of 1-propanol and 1,4-butan di-ol using 120 minute in an attempt to obtain higher surface areas.

The BET analysis and the results showed that the monolithic columns prepared using 1-propanol and methanol had a higher surface area than the other columns. Yet the monolithic column was blocked and could not wash. Therefore, the ratio of the porogenic solvents (1-propanol: methanol) was investigated to prepare monolithic columns that have a suitable surface area and pore size to separate large molecules. It was found that the 50:50 percent of 1-propanol to methanol gave better results compared with other ratios.

The irradiation time was investigated to form the monolith with 50:50 1-propanol:methanol, it was found that the monolith was formed after 23 minute which is less than others monolithic columns this column was used in all the further experiments.

The GMA-co-SMA-co-EDMA monolith was used to separate a mixture of three proteins, the results showed acceptable ability to separate these proteins. However, the peaks were broad and there is overlap between these peaks and complete resolution and base line separation was not possible with the monolithic column as HILIC/RP mixed mode monolithic column. However, this mechanism does not enhance the peak width and make it sharper. Therefore, another option has been investigated by changing the monolithic column to strong cationic exchange/ hydrophobic mixed mode monolithic column.

The monolithic columns were used as SCX/RP monolithic columns by changing the epoxy groups in glycidyl methacrylate-co-stearyl methacrylate-co-ethylene glycol dimethacrylate monolithic columns to (-OH) and (-SO_3Na) groups using a sulfonation reaction. The FTIR, EDX, and CHN analysis have been proven the formation of the SCX/RP monolith. However, the peak at 910.07 cm^{-1} for epoxy groups of the GMA in the monolith was disappeared, and there are two new peaks clearly present, at 1032.23 cm^{-1} and 995.96 cm^{-1} for R-SO_3 and S-O groups respectively, in addition, a broad band for -OH group between 3600-3100 cm^{-1} was observed. EDX, and CHN techniques demonstrated that the epoxy rings were opened due to presence S and Na in the EDX analysis, ans S in the CHN analysis.

The SCX/RP monolithic columns were investigated to separate proteins, peptides, tryptic digested cytochrome C, hydrophobic compounds, and a mixture of hydrophilic and hydrophobic compounds. The results showed that base line separation could be obtained using SCX/RP monolithic columns with all proteins samples tested, depending on the pI value of each protein. The hydrophobic compounds, and a mixture of hydrophilic and hydrophobic compounds showed good base line separation when tested using SCX/RP monolithic columns and compared to the HILIC/RP monolithic columns. The digested cytochrome C showed acceptable base line separation for some peptides.

The SCX/RP GMA-co-SMA-co-EDMA monolithic column was prepared inside the microchip device to reduce the analytes volume that could be expensive, or the

solvents volume that could be not available in substantial amounts. Moreover, reducing the reaction time due to the small size of the reactors, and enhancing the performance of the analytical device by increasing the reproducibility, and the selectivity.

Isocratic analysis was used instead of gradient analysis due to the low flow rate required for use with the microchip (maximum flow rate 12 µL min^{-1}). Therefore, another system was used based on a single pump, because the limited flow rate of the HPLC pump was 10 µL min^{-1}. Therefore, the gradient analysis could not be used. Due to this limitation the separation of the large molecules such as proteins and peptides was not investigated further. However, the high surface area and pore size compared to HILIC/RP monolith was helped to separate small molecules such as hydrophobic, and pharmaceutical compounds with base line separation.

7 Future work

Developing the mixed mode monolithic column by investigating other monomers that have different properties to separate different range of the samples in single run.

Investigate different porogenic solvents, that could enhance the morphological properties of the monoliths prepared in this study such as GMA-co-Sty-co-EDMA, and GMA-co-2DEAMA-co-EDMA because these monolithic columns have less hydrophobic properties compared with GMA-co-SMA-co-EDMA.

Prepared monolithic columns with wider pore size for large molecules by tuning the polymerization mixture to give monolithic columns with significantly enhanced chromatographic performance for large molecules.

Investigate the length of the GMA-co-SMA-co-EDMA monolithic columns, and the effect on the separation performance.

Application the GMA-co-SMA-co-EDMA monolithic columns in different sectors such as environmental, and forensic analysis.

Preparation of the GMA-co-SMA-co-EDMA monolith inside the microchip device to separate macro molecules

Investigating the ability of GMA-co-SMA-co-EDMA monolith to use as a solid phase sorbent for pre-concentration studies inside the borosilicate tube, capillary tube, and microchip device.

Investigation and separation of proteins and peptides from real samples

8 References

1. G. Guiochon, *Journal of Chromatography A*, 2007, **1168**, 101-168.
2. M. Kubin, P. Špaček and R. Chromeček, *Collection of Czechoslovak Chemical Communications*, 1967, **32**, 3881-3887.
3. W. D. Ross and R. T. Jefferson, *Journal of Chromatographic Science*, 1970, **8**, 386-389.
4. B. Belenkii, *Russian Journal of Bioorganic Chemistry*, 2006, **32**, 323-332.
5. T. Tennikova, F. Svec and B. Belenkii, *Journal of liquid chromatography*, 1990, **13**, 63-70.
6. D. Josić, J. Reusch, K. Löster, O. Baum and W. Reutter, *Journal of Chromatography A*, 1992, **590**, 59-76.
7. K. Nakanishi and N. Soga, *Journal of the American Ceramic Society*, 1991, **74**, 2518-2530.
8. H. Minakuchi, K. Nakanishi, N. Soga, N. Ishizuka and N. Tanaka, *Analytical Chemistry*, 1996, **68**, 3498-3501.
9. P. Jandera, *Journal of Chromatography A*, 2013, **1313**, 37-53.
10. B. Belenkii, A. Podkladenko, O. Kurenbin, V. Mal'tsev, D. Nasledov and S. Trushin, *Journal of Chromatography A*, 1993, **645**, 1-15.
11. F. Svec and J. M. Fréchet, *Analytical Chemistry*, 1992, **64**, 820-822.
12. N. Tanaka, H. Kobayashi, K. Nakanishi, H. Minakuchi and N. Ishizuka, *Journal*, 2001.
13. N. Tanaka, H. Kobayashi, N. Ishizuka, H. Minakuchi, K. Nakanishi, K. Hosoya and T. Ikegami, *Journal of Chromatography A*, 2002, **965**, 35-49.
14. A. R. Ivanov, L. Zang and B. L. Karger, *Analytical Chemistry*, 2003, **75**, 5306-5316.
15. T. Zhu and K. H. Row, *Journal of Separation Science*, 2012, **35**, 1294-1302.
16. R. D. Arrua, M. C. Strumia and C. I. Alvarez Igarzabal, *Materials*, 2009, **2**, 2429-2466.
17. T. Qi, A. Sonoda, Y. Makita, H. Kanoh, K. Ooi and T. Hirotsu, *Industrial & Engineering Chemistry Research*, 2002, **41**, 133-138.
18. C. Viklund, F. Svec, J. M. Fréchet and K. Irgum, *Chemistry of Materials*, 1996, **8**, 744-750.
19. A. I. Cooper and A. B. Holmes, *Advanced Materials*, 1999, **11**, 1270-1274.
20. A. K. Hebb, K. Senoo, R. Bhat and A. I. Cooper, *Chemistry of Materials*, 2003, **15**, 2061-2069.
21. S. Xie, F. Svec and J. M. Frechet, *Journal of Polymer Science Part A: Polymer Chemistry*, 1997, **35**, 1013-1021.
22. C. Viklund, A. Nordström, K. Irgum, F. Svec and J. M. Fréchet, *Macromolecules*, 2001, **34**, 4361-4369.
23. K. K. Unger, R. Skudas and M. M. Schulte, *Journal of Chromatography A*, 2008, **1184**, 393-415.
24. H. Oberacher and C. G. Huber, *TrAC Trends in Analytical Chemistry*, 2002, **21**, 166-174.
25. E. F. Hilder, F. Svec and J. M. Frechet, *Electrophoresis*, 2002, **23**, 3934-3953.
26. S. Miller, *Analytical Chemistry*, 2004, **76**, 99-101.

27. F. C. Leinweber, D. Lubda, K. Cabrera and U. Tallarek, *Analytical Chemistry*, 2002, **74**, 2470-2477.
28. C. W. Klampfl, *Journal of Chromatography A*, 2004, **1044**, 131-144.
29. E. S. Alzahrani, University of Hull, 2012.
30. H. Zou, X. Huang, M. Ye and Q. Luo, *Journal of Chromatography A*, 2002, **954**, 5-32.
31. W. Li, P. Xu, H. Zhou, L. Yang and H. Liu, *Science China Technological Sciences*, 2012, **55**, 387-416.
32. F. Svec, E. C. Peters, D. Sykora, C. Yu and J. Frechet, *Journal of High Resolution Chromatography*, 2000, **23**, 3-18.
33. S. Hjerten, *Industrial & Engineering Chemistry Research*, 1999, **38**, 1205-1214.
34. I. Gusev, X. Huang and C. Horvath, *Journal of Chromatography A*, 1999, **855**, 273-290.
35. S. Hjerten, J.-L. Liao and R. Zhang, *Journal of Chromatography A*, 1989, **473**, 273-275.
36. K. Hoshina, S. Horiyama, H. Matsunaga and J. Haginaka, *Journal of Chromatography A*, 2009, **1216**, 4957-4962.
37. H. Aoki, N. Tanaka, T. Kubo and K. Hosoya, *Journal of Separation Science*, 2009, **32**, 341-358.
38. Y.-f. Maa and C. Horváth, *Journal of Chromatography A*, 1988, **445**, 71-86.
39. F. Svec and J. M. Frechet, *Science-New York then Washington*, 1996, 205-210.
40. F. Svec, *Journal of Separation Science*, 2009, **32**, 3-9.
41. A. Premstaller, H. Oberacher and C. G. Huber, *Analytical Chemistry*, 2000, **72**, 4386-4393.
42. S. Xie, R. W. Allington, F. Svec and J. M. Fréchet, *Journal of Chromatography A*, 1999, **865**, 169-174.
43. E. C. Peters, M. Petro, F. Svec and J. M. Frechet, *Analytical Chemistry*, 1998, **70**, 2296-2302.
44. R. D. Arrua, M. Talebi, T. J. Causon and E. F. Hilder, *Analytica Chimica Acta*, 2012, **738**, 1-12.
45. A. Namera, A. Nakamoto, T. Saito and S. Miyazaki, *Journal of Separation Science*, 2011, **34**, 901-924.
46. F. Watanabe, T. Kubo, K. Kaya and K. Hosoya, *Journal of Chromatography A*, 2009, **1216**, 7402-7408.
47. B. W. Pack and D. S. Risley, *Journal of Chromatography A*, 2005, **1073**, 269-275.
48. N. Tanaka, H. Nagayama, H. Kobayashi, T. Ikegami, K. Hosoya, N. Ishizuka, H. Minakuchi, K. Nakanishi, K. Cabrera and D. Lubda, *Journal of Separation Science*, 2000, **23**, 111-116.
49. L. Trojer, S. H. Lubbad, C. P. Bisjak, W. Wieder and G. K. Bonn, *Journal of Chromatography A*, 2007, **1146**, 216-224.
50. M. Jančo, D. Sýkora, F. Svec, J. M. Fréchet, J. Schweer and R. Holm, *Journal of Polymer Science Part A: Polymer Chemistry*, 2000, **38**, 2767-2778.
51. I. Nischang, *Journal of Chromatography A*, 2012, **1236**, 152-163.
52. I. Nischang, I. Teasdale and O. Brüggemann, *Journal of Chromatography A*, 2010, **1217**, 7514-7522.
53. F. Svec, *Journal of Chromatography A*, 2012, **1228**, 250-262.

54. I. Nischang, I. Teasdale and O. Brüggemann, *Analytical and Bioanalytical Chemistry*, 2011, **400**, 2289-2304.
55. F. Plieva, X. Huiting, I. Y. Galaev, B. Bergenståhl and B. Mattiasson, *Journal of Materials Chemistry*, 2006, **16**, 4065-4073.
56. R. D. Arrua, T. J. Causon and E. F. Hilder, *Analyst*, 2012, **137**, 5179-5189.
57. J. Urban and P. Jandera, *Analytical and Bioanalytical Chemistry*, 2013, **405**, 2123-2131.
58. C. Bignardi, L. Elviri, A. Penna, M. Careri and A. Mangia, *Journal of Chromatography A*, 2010, **1217**, 7579-7585.
59. H. Minakuchi, K. Nakanishi, N. Soga, N. Ishizuka and N. Tanaka, *Journal of Chromatography A*, 1997, **762**, 135-146.
60. K. Cabrera, *Journal of Separation Science*, 2004, **27**, 843-852.
61. N. Manchón, M. D'Arrigo, A. García-Lafuente, E. Guillamón, A. Villares, J. Martínez, A. Ramos and M. Rostagno, *Analytical and Bioanalytical Chemistry*, 2011, **400**, 1251-1261.
62. A. Ghanem and T. Ikegami, *Journal of Separation Science*, 2011, **34**, 1945-1957.
63. H. Kobayashi, T. Ikegami, H. Kimura, T. Hara, D. Tokuda and N. Tanaka, *Analytical Sciences*, 2006, **22**, 491-501.
64. K. Nakanishi, *Journal of Porous Materials*, 1997, **4**, 67-112.
65. K. Nakanishi and N. Soga, *Journal of Non-Crystalline Solids*, 1992, **139**, 1-13.
66. M. Kato, K. Sakai-Kato and T. Toyo'oka, *Journal of Separation Science*, 2005, **28**, 1893-1908.
67. I. Gill and A. Ballesteros, *Trends in Biotechnology*, 2000, **18**, 282-296.
68. F. C. Leinweber and U. Tallarek, *Journal of Chromatography A*, 2003, **1006**, 207-228.
69. T. Gunji, M. Ozawa, Y. Abe and R. West, *Journal of Sol-Gel Science and Technology*, 2001, **22**, 219-224.
70. B. Yan, R.-F. Yao and Q.-M. Wang, *Materials Letters*, 2006, **60**, 3063-3067.
71. S. A. El-Safty, *Journal of Materials Science*, 2009, **44**, 6764.
72. N. Khimich, *Glass Physics and Chemistry*, 2004, **30**, 430-442.
73. L. Bai, H. Liu, Y. Liu, X. Zhang, G. Yang and Z. Ma, *Journal of Chromatography A*, 2011, **1218**, 100-106.
74. Q. Yao, Y. Zhou, Y. Sun and X. Ye, *Journal of Inorganic and Organometallic Polymers and Materials*, 2008, **18**, 477-484.
75. L. He and C.-S. Toh, *Analytica Chimica Acta*, 2006, **556**, 1-15.
76. L. Xu and H. K. Lee, *Journal of Chromatography A*, 2008, **1195**, 78-84.
77. C. Yao, L. Qi, H. Jia, P. Xin, G. Yang and Y. Chen, *Journal of Materials Chemistry*, 2009, **19**, 767-772.
78. P. Jandera, J. Urban and D. Moravcová, *Journal of Chromatography A*, 2006, **1109**, 60-73.
79. T. Nema, E. Chan and P. Ho, *Talanta*, 2010, **82**, 488-494.
80. C. Hou, J. Ma, D. Tao, Y. Shan, Z. Liang, L. Zhang and Y. Zhang, *Journal of Proteome Research*, 2010, **9**, 4093-4101.
81. L. Zhang, B. Chen, H. Peng, M. He and B. Hu, *Journal of Separation Science*, 2011, **34**, 2247-2254.
82. H. Zhong, G. Zhu, J. Yang, P. Wang and Q. Yang, *Microporous and Mesoporous Materials*, 2007, **100**, 259-267.

83. E. J. Nassar, R. R. Gonçalves, M. Ferrari, Y. Messaddeq and S. J. Ribeiro, *Journal of Alloys and Compounds*, 2002, **344**, 221-225.
84. K. Nishio and T. Tsuchiya, *Solar Energy Materials and Solar Cells*, 2001, **68**, 295-306.
85. Y. Wei, D. Jin, J. Xu, G. Baran and K. Y. Qiu, *Polymers for Advanced Technologies*, 2001, **12**, 361-368.
86. M. L. Ferrer, F. Del Monte, C. R. Mateo, J. Gomez and D. Levy, *Journal of Sol-Gel Science and Technology*, 2003, **26**, 1169-1172.
87. K. Noble, A. Seddon, M. Turner, P. Chevalier and D. Ou, *Journal of Sol-Gel Science and Technology*, 2003, **26**, 419-423.
88. J. Sun, E. K. Akdogan, L. C. Klein and A. Safari, *Journal of Non-Crystalline Solids*, 2007, **353**, 2807-2812.
89. K. Nakanishi, H. Shikata, N. Ishizuka, N. Koheiya and N. Soga, *Journal of Separation Science*, 2000, **23**, 106-110.
90. C. Barner-Kowollik, T. P. Davis and M. H. Stenzel, *Polymer*, 2004, **45**, 7791-7805.
91. L. Snyder, *Analyst*, 1991, **116**, 1237-1244.
92. K. Robards, P. R. Haddad and P. E. Jackson, *Principles and practice of modern chromatographic methods*, Academic Press, 1994, p.59.
93. J. Nikelly, *HPLC and CE: Principles and Practice By Andrea Weston and Phyllis R. Brown. Academic Press: San Diego. 1997.*
94. L.-R. Snyder, *Journal of Chromatographic Science*, 1972, **10**, 200-212.
95. J. J. Van Deemter, F. Zuiderweg and A. v. Klinkenberg, *Chemical Engineering Science*, 1956, **5**, 271-289.
96. F. J. S. A.Braithwaite, *Chromatographic Methods*, . Chapman & Hall, New York, 4th edn., 1990, p. 138.
97. J. H. Knox, *Journal of Chromatographic Science*, 1980, **18**, 453-461.
98. www.chromacademy.com.
99. Y. Xiang, Y. Liu and M. L. Lee, *Journal of Chromatography A*, 2006, **1104**, 198-202.
100. V. Bansal, *Journal of Global Pharma Technology*, 2010, **2**.
101. S. Abidi, *Journal of Chromatography A*, 1991, **587**, 193-203.
102. Y. Ma, N. Tanaka, A. Vaniya, T. Kind and O. Fiehn, *Journal of Agricultural and Food Chemistry*, 2016, **64**, 505-512.
103. R. P. Scott, *Chrom-Ed Book Series*, 2003, **1**.
104. L. R. Snyder, J. J. Kirkland and J. W. Dolan, *Introduction to modern liquid chromatography*, John Wiley & Sons, 2011, p.187.
105. R. Scott, *Advance Chromatgraphy*, 1982, **20**, 167-172.
106. B.-Y. Zhu, C. T. Mant and R. S. Hodges, *Journal of Chromatography A*, 1992, **594**, 75-86.
107. H. Willard, L. Meritt, J. Dean and F. Settle, *Instrumental Methods of Analysis, New Delhi*, 1986, p.172.
108. A.K.Connors, *A Text Book of Pharmaceutical Analysis. , 3rd edition,* A Wiley Interscience publication, 2005, p.*373*.
109. C. F. Poole and S. K. Poole, *Chromatography Today*, Elsevier, 2012, p.553 .
110. M. J. Wells and C. R. Clark, *Analytical Chemistry*, 1992, **64**, 1660-1668.
111. W. Melander and C. Horvath, *Academic Press, New York*, 1980, **2**, 176.
112. J. M. Miller and D. T. Burns, *Chromatography Concepts and Contrasts*, Wiley, New York, 1989. p. 297.

113. D. E. Martire and R. E. Boehm, *The Journal of Physical Chemistry*, 1983, **87**, 1045-1062.
114. K. A. Dill, *Journal of Physical Chemistry*, 1987, **91**, 1980-1988.
115. K. A. Dill, J. Naghizadeh and J. Marqusee, *Annual review of physical chemistry*, 1988, **39**, 425-461.
116. J. G. Dorsey and K. A. Dill, *Chemical Reviews*, 1989, **89**, 331-346.
117. J. G. Dorsey and W. T. Cooper, *Analytical Chemistry*, 1994, **66**, 857A-867A.
118. P. R. Haddad and P. E. Jackson, *Ion Chromatography*, Elsevier, 1990. p 92.
119. J. S. Fritz, *Journal of Chromatography A*, 2004, **1039**, 3-12.
120. C. A. Lucy, *Journal of Chromatography A*, 2003, **1000**, 711-724.
121. U. M. Kent, *Methods in Molecular Biology*, 1999, **115**, 19-22.
122. C. T. Mant and R. S. Hodges, *Journal of Separation Science*, 2008, **31**, 2754-2773.
123. P. R. Levison, *Journal of Chromatography B*, 2003, **790**, 17-33.
124. Y. Yang, H. R. Hebron and J. Hang, *Journal of Biomolecular Techniques*, 2008, **19**, 205.
125. H. L. Knudsen, R. L. Fahrner, Y. Xu, L. A. Norling and G. S. Blank, *Journal of Chromatography A*, 2001, **907**, 145-154.
126. P. Hajós and L. v. Nagy, *Journal of Chromatography B: Biomedical Sciences and Applications*, 1998, **717**, 27-38.
127. G. Bonn, *Journal of Chromatography A*, 1987, **387**, 393-398.
128. A. A. Zagorodni, *Ion exchange materials: properties and applications*, Elsevier, 2006. p 19.
129. A. P. E. J. P.R.Haddad, *Journal of Chromatography*, 1990, **46**, 230-232.
130. P. M. Cummins, O. Dowling and B. F. O'Connor, *Protein Chromatography: Methods and Protocols*, 2011, 215-228.
131. P. Hong, S. Koza and E. S. Bouvier, *Journal of Liquid Chromatography & Related Technologies*, 2012, **35**, 2923-2950.
132. N. Nelson and N. Kitagawa, *Journal of Liquid Chromatography*, 1990, **13**, 4037-4050.
133. M. Potschka, *Journal of Chromatography A*, 1993, **648**, 41-69.
134. S. Fekete, I. Molnár and D. Guillarme, *Journal of Pharmaceutical and Biomedical Analysis*, 2017, **137**, 60-69.
135. L. A. Kennedy, W. Kopaciewicz and F. E. Regnier, *Journal of Chromatography A*, 1986, **359**, 73-84.
136. Y. Yang and X. Geng, *Journal of Chromatography A*, 2011, **1218**, 8813-8825.
137. G. Zhao, X.-Y. Dong and Y. Sun, *Journal of Biotechnology*, 2009, **144**, 3-11.
138. Y. Li, J. Yang, J. Jin, X. Sun, L. Wang and J. Chen, *Journal of Chromatography A*, 2014, **1337**, 133-139.
139. Q. Wang, M. Ye, L. Xu and Z.-g. Shi, *Analytical Chimical Acta*, 2015, **888**, 182-190.
140. Y. Liu, Q. Du, B. Yang, F. Zhang, C. Chu and X. Liang, *Analyst*, 2012, **137**, 1624-1628.
141. H. Qiu, M. Zhang, T. Gu, M. Takafuji and H. Ihara, *Chemistry-A European Journal*, 2013, **19**, 18004-18010.
142. X. Liu and C. A. Pohl, *Journal of Separation Science*, 2010, **33**, 779-786.
143. N. H. Davies, M. R. Euerby and D. V. McCalley, *Journal of Chromatography A*, 2007, **1138**, 65-72.

144. R. Nogueira, M. Lämmerhofer and W. Lindner, *Journal of Chromatography A*, 2005, **1089**, 158-169.
145. C. Cabanne, J. Pezzini, G. Joucla, A. Hocquellet, C. Barbot, B. Garbay and X. Santarelli, *Journal of Chromatography A*, 2009, **1216**, 4451-4456.
146. S. C. Burton and D. R. Harding, *Journal of Biochemical and Biophysical Methods*, 2001, **49**, 275-287.
147. X. Geng, C. Ke, G. Chen, P. Liu, F. Wang, H. Zhang and X. Sun, *Journal of Chromatography A*, 2009, **1216**, 3553-3562.
148. J. Dong, C. Xie, R. Tian, R. Wu, J. Hu and H. Zou, *Electrophoresis*, 2005, **26**, 3452-3459.
149. M. Bedair and Z. E. Rassi, *Electrophoresis*, 2002, **23**, 2938-2948.
150. D. Allen and Z. El Rassi, *Electrophoresis*, 2003, **24**, 408-420.
151. D. Allen and Z. El Rassi, *Journal of Chromatography A*, 2004, **1029**, 239-247.
152. W. Wieder, C. P. Bisjak, C. W. Huck, R. Bakry and G. K. Bonn, *Journal of Separation Science*, 2006, **29**, 2478-2484.
153. R. a. Wu, H. Fu, W. Jin and M. Ye, *Electrophoresis*, 2002, **23**, 1239-1245.
154. Q. Tang and M. L. Lee, *Journal of Chromatography A*, 2000, **887**, 265-275.
155. K. Ohyama, Y. Shirasawa, M. Wada, N. Kishikawa, Y. Ohba, K. Nakashima and N. Kuroda, *Journal of Chromatography A*, 2004, **1042**, 189-195.
156. M. Zhang, C. Yang and Z. El Rassi, *Analytical Chemistry*, 1999, **71**, 3277-3282.
157. L. Xu, Y.-Q. Feng, Z.-G. Shi, S.-L. Da and F. Wei, *Journal of Chromatography A*, 2004, **1033**, 161-166.
158. D. Hoegger and R. Freitag, *Journal of Chromatography A*, 2003, **1004**, 195-208.
159. G. Ding, Z. Da, R. Yuan and J. J. Bao, *Electrophoresis*, 2006, **27**, 3363-3372.
160. D. Allen and Z. El Rassi, *Analyst*, 2003, **128**, 1249-1256.
161. H. Fu, C. Xie, H. Xiao, J. Dong, J. Hu and H. Zou, *Journal of Chromatography A*, 2004, **1044**, 237-244.
162. H. Fu, C. Xie, J. Dong, X. Huang and H. Zou, *Analytical Chemistry*, 2004, **76**, 4866-4874.
163. X. Dong, J. Dong, J. Ou, Y. Zhu and H. Zou, *Electrophoresis*, 2006, **27**, 2518-2525.
164. B.-Y. Zhu, C. T. Mant and R. S. Hodges, *Journal of Chromatography A*, 1991, **548**, 13-24.
165. E. F. Hilder, F. Svec and J. M. Fréchet, *Journal of Chromatography A*, 2004, **1053**, 101-106.
166. J. P. Hutchinson, P. Zakaria, A. R. Bowie, M. Macka, N. Avdalovic and P. R. Haddad, *Analytical Chemistry*, 2005, **77**, 407-416.
167. R. Wu, H. Zou, M. Ye, Z. Lei and J. Ni, *Electrophoresis*, 2001, **22**, 544-551.
168. P. Zakaria, J. P. Hutchinson, N. Avdalovic, Y. Liu and P. R. Haddad, *Analytical Chemistry*, 2005, **77**, 417-423.
169. V. Pucci, M. A. Raggi, F. Svec and J. M. Fréchet, *Journal of Separation Science*, 2004, **27**, 779-788.
170. Z. Jiang, N. W. Smith, P. D. Ferguson and M. R. Taylor, *Journal of Separation Science*, 2008, **31**, 2774-2783.
171. M. Lämmerhofer, F. Svec, J. M. Fréchet and W. Lindner, *Journal of Chromatography A*, 2001, **925**, 265-277.
172. Z. Jiang, N. W. Smith, P. D. Ferguson and M. R. Taylor, *Analytical Chemistry*, 2007, **79**, 1243-1250.

173. F. Ye, Z. Xie and K. Y. Wong, *Electrophoresis*, 2006, **27**, 3373-3380.
174. T. Ikegami, K. Horie, J. Jaafar, K. Hosoya and N. Tanaka, *Journal of Biochemical and Biophysical Methods*, 2007, **70**, 31-37.
175. M. A. Strege, S. Stevenson and S. M. Lawrence, *Analytical Chemistry*, 2000, **72**, 4629-4633.
176. C. Mant, L. Kondejewski and R. Hodges, *Journal of Chromatography A*, 1998, **816**, 79-88.
177. E. Hartmann, Y. Chen, C. T. Mant, A. Jungbauer and R. S. Hodges, *Journal of Chromatography A*, 2003, **1009**, 61-71.
178. K. D. Safa and M. H. Nasirtabrizi, *Polymer Bulletin*, 2006, **57**, 293-304.
179. E.-R. Kenawy, F. I. Abdel-Hay, A. E.-R. R. El-Shanshoury and M. H. El-Newehy, *Journal of Controlled Release*, 1998, **50**, 145-152.
180. B. Reddy and S. Balasubramanian, *European polymer journal*, 2002, **38**, 803-813.
181. R. Balaji, D. Grande and S. Nanjundan, *Polymer*, 2004, **45**, 1089-1099.
182. M. Espinosa, P. Del Toro and D. Silva, *Polymer*, 2001, **42**, 3393-3397.
183. E. G. Vlakh and T. B. Tennikova, *Journal of Separation Science*, 2007, **30**, 2801-2813.
184. R. J. Groarke and D. Brabazon, *Materials*, 2016, **9**, 446.
185. S. Eeltink, L. Geiser, F. Svec and J. M. Fréchet, *Journal of Separation Science*, 2007, **30**, 2814-2820.
186. P. Holdšvendová, J. Suchánková, M. Bunček, V. Bačkovská and P. Coufal, *Journal of Biochemical and Biophysical Methods*, 2007, **70**, 23-29.
187. Y. Li, B. Gu, H. D. Tolley and M. L. Lee, *Journal of Chromatography A*, 2009, **1216**, 5525-5532.
188. E. Nesterenko, O. Yavorska, M. Macka, A. Yavorskyy and B. Paull, *Analytical Methods*, 2011, **3**, 537-543.
189. E. Maksimova, E. Vlakh and T. Tennikova, *Journal of Chromatography A*, 2011, **1218**, 2425-2431.
190. E. Maksimova, E. Vlakh, E. Sinitsyna and T. Tennikova, *Journal of Separation Science*, 2013, **36**, 3741-3749.
191. H. Zhang, J. Ou, Y. Wei, H. Wang, Z. Liu, L. Chen and H. Zou, *Analytica Chimica Acta*, 2015, **883**, 90-98.
192. E. J. Carrasco-Correa, G. Ramis-Ramos and J. M. Herrero-Martínez, *Journal of Chromatography A*, 2013, **1298**, 61-67.
193. S.-L. Lin, Y.-R. Wu, T.-Y. Lin and M.-R. Fuh, *Analytica Chimica Acta*, 2015, **871**, 57-65.
194. A. Darvishi, M. J. Zohuriaan Mehr, G. B. Marandi, K. Kabiri, H. Bouhendi and H. Bakhshi, *Designed Monomers and Polymers*, 2013, **16**, 79-88.
195. G. G. Godwin, C. J. Selvamalar, A. Penlidis and S. Nanjundan, *Reactive and Functional Polymers*, 2004, **59**, 197-209.
196. P. a. Song, Y. Zhang and J. Kuang, *Journal of Materials Science*, 2007, **42**, 2775-2781.
197. C. Monnereau, E. Blart, V. Montembault, L. Fontaine and F. Odobel, *Tetrahedron*, 2005, **61**, 10113-10121.
198. C. Selvamalar, P. Vijayanand, A. Penlidis and S. Nanjundan, *Journal Application Polymer Science*, 2004, **91**, 3604-3612.

199. D. Horák, M. J. Beneš, K. Gumargalieva and G. Zaikov, *Journal Application Polymer Science.*, 2001, **80**, 913-916.
200. S. He, W. Wu, R. Wang, W. Pu and Y. Chen, *Polymer-Plastics Technology and Engineering*, 2011, **50**, 719-726.
201. E. J. Carrasco-Correa, G. Ramis-Ramos and J. M. Herrero-Martínez, *Journal of Chromatography A*, 2015, **1379**, 100-105.
202. F. Svec and J. M. Frechet, *Journal of Chromatography A*, 1995, **702**, 89-95.
203. C. Viklund, F. Svec, J. M. Frechet and K. Irgum, *Biotechnology Progress*, 1997, **13**, 597-600.
204. J. C. Masini, *Analytical and Bioanalytical Chemistry*, 2016, **408**, 1445-1452.
205. Y. Ueki, T. Umemura, J. Li, T. Odake and K.-i. Tsunoda, *Analytical Chemistry*, 2004, **76**, 7007-7012.
206. J. Wang, H. Lü, X. Lin and Z. Xie, *Electrophoresis*, 2008, **29**, 928-935.
207. D. N. Gunasena and Z. El Rassi, *Electrophoresis*, 2012, **33**, 251-261.
208. J. Lin, X. Wu, X. Lin and Z. Xie, *Journal of Chromatography A*, 2007, **1169**, 220-227.
209. C. Yu, F. Svec and J. M. Frechet, *Electrophoresis*, 2000, **21**, 120-127.
210. I. M. Lazar, L. Li, Y. Yang and B. L. Karger, *Electrophoresis*, 2003, **24**, 3655-3662.
211. S. Le Gac, J. Carlier, J.-C. Camart, C. Cren-Olivé and C. Rolando, *Journal of Chromatography B*, 2004, **808**, 3-14.
212. X. Jiao, S. Shen and T. Shi, *Journal of Chromatography B*, 2015, **1007**, 100-109.
213. H. Ren, X. Zhang, Z. Li, Z. Liu and J. Li, *Journal of Separation Science*, 2017, **40**, 826-833.
214. C. Viklund, E. Pontén, B. Glad, K. Irgum, P. Hörstedt and F. Svec, *Chemistry of Materials*, 1997, **9**, 463-471.
215. Z. Lin, H. Huang, X. Sun, Y. Lin, L. Zhang and G. Chen, *Journal of Chromatography A*, 2012, **1246**, 90-97.
216. X. Lin, J. Wang, L. Li, X. Wang, H. Lü and Z. Xie, *Journal of Separation Science*, 2007, **30**, 3011-3017.
217. A. Sabarudin, J. Huang, S. Shu, S. Sakagawa and T. Umemura, *Analytica Chimica Acta*, 2012, **736**, 108-114.
218. L. Terborg, J. C. Masini, M. Lin, K. Lipponen, M.-L. Riekolla and F. Svec, *Journal Advance Research*, 2015, **6**, 441-448.
219. A. Bruchet, V. Dugas, C. Mariet, F. Goutelard and J. Randon, *Journal of Separation Science*, 2011, **34**, 2079-2087.
220. M. Wang, J. Xu, X. Zhou and T. Tan, *Journal of Chromatography A*, 2007, **1147**, 24-29.
221. Y. Wei, X. Huang, R. Liu, Y. Shen and X. Geng, *Journal of Separation Science*, 2006, **29**, 5-13.
222. P. Watts and S. J. Haswell, *Current Opinion in Chemical Biology*, 2003, **7**, 380-387.
223. H. A. Al Lawati, *PhD Thesis,* University of Hull, 2007.
224. T. Rohr, D. F. Ogletree, F. Svec and J. M. Fréchet, *Advanced Functional Materials*, 2003, **13**, 264-270.
225. C. Zhang, J. Xu, W. Ma and W. Zheng, *Biotechnology Advances*, 2006, **24**, 243-284.
226. S.-E. Ong, S. Zhang, H. Du and Y. Fu, *Frontiers in Bioscience*, 2008, **13**, 2757-2773.
227. Y. Yang, C. Li, K. H. Lee and H. G. Craighead, *Electrophoresis*, 2005, **26**, 3622-3630.

228. N. Lion, T. C. Rohner, L. Dayon, I. L. Arnaud, E. Damoc, N. Youhnovski, Z. Y. Wu, C. Roussel, J. Josserand and H. Jensen, *Electrophoresis*, 2003, **24**, 3533-3562.
229. P. Kallio and J. Kuncova, *Microfluidics*, TEKES, 2004, **158,** 33-48.
230. A. G. Crevillén, M. Hervás, M. A. López, M. C. González and A. Escarpa, *Talanta*, 2007, **74**, 342-357.
231. K. W. Ro, R. Nayak and D. R. Knapp, *Electrophoresis*, 2006, **27**, 3547-3558.
232. G. M. Janini and H. J. Issaq, *Chromatographic Science*, 1993, **64**, 119-119.
233. N. Anastos, S. W. Lewis, N. W. Barnett, J. R. Pearson and K. P. Kirkbride, *Journal of Forensic Science*, 2005, **50**, JFS2004183-2004186.
234. E. Heftmann, *Chromatography: A Laboratory Handbook of Chromatographic and Electrophoretic Methods. 3d Ed*, Van Nostrand Reinhold Company, New York, NY, **1975**, p. 23.
235. V. Pretorius, B. J. Hopkins and J. Schieke, *Journal of Chromatography A*, 1974, **99**, 23-30.
236. J. W. Jorgenson and K. D. Lukacs, *Analytical Chemistry*, 1981, **53**, 1298-1302.
237. K. Lukacs and J. Jorgenson, *Journal of Separation Science*, 1985, **8**, 407-411.
238. K. Altria, N. Smith and C. Turnbull, *Chromatographia*, 1997, **46**, 664-674.
239. F. J. Holler, D. A. Skoog and S. R. Crouch, *Principles of Instrumental Analysis (6th ed.). Cengage Learning*, 2007, p. 9.
240. I. Mikšík and P. Sedláková, *Journal of Separation Science*, 2007, **30**, 1686-1703.
241. J. Simal-Gándara, *Critical Reviews in Analytical Chemistry*, 2004, **34**, 85-94.
242. Q. Tang and M. L. Lee, *TrAC Trends in Analytical Chemistry*, 2000, **19**, 648-663.
243. C. Schwer and E. Kenndler, *Analytical Chemistry*, 1991, **63**, 1801-1807.
244. S. Van den Bosch, S. Heemstra, J. Kraak and H. Poppe, *Journal of Chromatography A*, 1996, **755**, 165-177.
245. M. M. Dittmann and G. P. Rozing, *Journal of Chromatography A*, 1996, **744**, 63-74.
246. D. S. Peterson, T. Rohr, F. Svec and J. M. Fréchet, *Analytical Chemistry*, 2003, **75**, 5328-5335.
247. S. Paul and B. Rånby, *Macromolecules*, 1976, **9**, 337-340.
248. P. D. Fletcher, S. J. Haswell, P. He, S. M. Kelly and A. Mansfield, *Journal of Porous Materials*, 2011, **18**, 501-508.
249. J. Courtois, M. Szumski, E. Byström, A. Iwasiewicz, A. Shchukarev and K. Irgum, *Journal of Separation Science*, 2006, **29**, 14-24.
250. I. Nischang, O. Brueggemann and F. Svec, *Analytical and Bioanalytical Chemistry*, 2010, **397**, 953-960.
251. D. Bandilla and C. D. Skinner, *Journal of Chromatography A*, 2003, **1004**, 167-179.
252. C. Yu, M. Xu, F. Svec and J. M. Fréchet, *Journal of Polymer Science Part A: Polymer Chemistry*, 2002, **40**, 755-769.
253. S. Yu, F. L. Ng, K. C. C. Ma, A. A. Mon, F. L. Ng and Y. Y. Ng, *Journal Application Polymer. Science*, 2013, **127**, 2641-2647.
254. Y. Huo, P. J. Schoenmakers and W. T. Kok, *Journal of Chromatography A*, 2007, **1175**, 81-88.
255. J. M. Armenta, B. Gu, C. D. Thulin and M. L. Lee, *Journal of Chromatography A*, 2007, **1148**, 115-122.
256. T. Rohr, E. F. Hilder, J. J. Donovan, F. Svec and J. M. Frechet, *Macromolecules*, 2003, **36**, 1677-1684.

257. A. M. K. Weed, J. Dvornik, J. J. Stefancin, A. A. Gyapong, F. Svec and Z. Zajickova, *Journal of Separation Science*, 2013, **36**, 270-278.
258. A.-M. Siouffi, *Journal of Chromatography A*, 2006, **1126**, 86-94.
259. www.pubchem.ncbi.nlm.nih.gov.
260. P. Li, Y. Shen, X. Li and X. Yang, *Polymer-Plastics Technology and Engineering*, 2011, **50**, 29-35.
261. J. Zhou, L. Wang, X. Dong, Q. Yang, J. Wang, H. Yu and X. Chen, *European Polymer Journal*, 2007, **43**, 1736-1743.
262. H. V. Harris and S. J. Holder, *Polymer*, 2006, **47**, 5701-5706.
263. A. Polic, T. Duever and A. Penlidis, *Journal of Polymer Science Part A: Polymer Chemistry*, 1998, **36**, 813-822.
264. P. M. Johnson, J. W. Stansbury and C. N. Bowman, *Journal of Combinatorial Chemistry*, 2007, **9**, 1149-1156.
265. K. A. Berchtold, B. Hacioğlu, L. Lovell, J. Nie and C. N. Bowman, *Macromolecules*, 2001, **34**, 5103-5111.
266. G. Litvinenko and V. Kaminsky, *Progress in Reaction Kinetics*, 1994, **19**, 139-193.
267. A. J. Alpert, *Journal of Chromatography A*, 1990, **499**, 177-196.
268. A. R. Oyler, B. L. Armstrong, J. Y. Cha, M. X. Zhou, Q. Yang, R. I. Robinson, R. Dunphy and D. J. Burinsky, *Journal of Chromatography A*, 1996, **724**, 378-383.
269. L. Riddle and G. Guiochon, *Chromatographia*, 2006, **64**, 1-7.
270. O. G. Potter and E. F. Hilder, *Journal of Separation Science*, 2008, **31**, 1881-1906.
271. C. E. Harland, *Ion exchange: Theory and Practice*, Royal Society of Chemistry, 2007, p. 49.
272. L. Wang, Y.-l. Su, L. Zheng, W. Chen and Z. Jiang, *Journal of Membrane Science*, 2009, **340**, 164-170.
273. Y. Liu and A. Laskin, *The Journal of Physical Chemistry A*, 2009, **113**, 1531-1538.
274. M. S. Refat, L. A. Ismail and A. M. A. Adam, *International Journal of Chemical Sciences*, 2013, **11,** 24-38.
275. O. V. Krokhin, R. Craig, V. Spicer, W. Ens, K. Standing, R. Beavis and J. Wilkins, *Molecular & Cellular Proteomics*, 2004, **3**, 908-919.
276. J. Dai, C. H. Shieh, Q.-H. Sheng, H. Zhou and R. Zeng, *Analytical Chemistry*, 2005, **77**, 5793-5799.
277. K. M. Gooding, F. E. Regnier and A. Townshend, *Analytica Chimica Acta*, 1990, **236**, 511-512.
278. B. Gu, Z. Chen, C. D. Thulin and M. L. Lee, *Analytical Chemistry*, 2006, **78**, 3509-3518.
279. A. Norden, F. Flynn, L. Fulcher and J. Richards, *Journal of Clinical Pathology*, 1989, **42**, 59-62.

9 Publications

1- The 6th PhD experience conference (poster), university of Hull 2015.

2- RSC the 13th material chemistry division poster symposium (poster), London 2016.

3- The 7th PhD experience conference (poster), university of Hull 2016.

4- RSC organic division north east regional meeting (poster), university of Durham 2017.

5- RSC analytical research forum (poster), London 2017

10 Appendix

Applications of glycidyl methacrylate-co- lauryl methacrylate-co-ethylene dimethacrylate monolithic column

Chromatograms of hydrophobic compounds

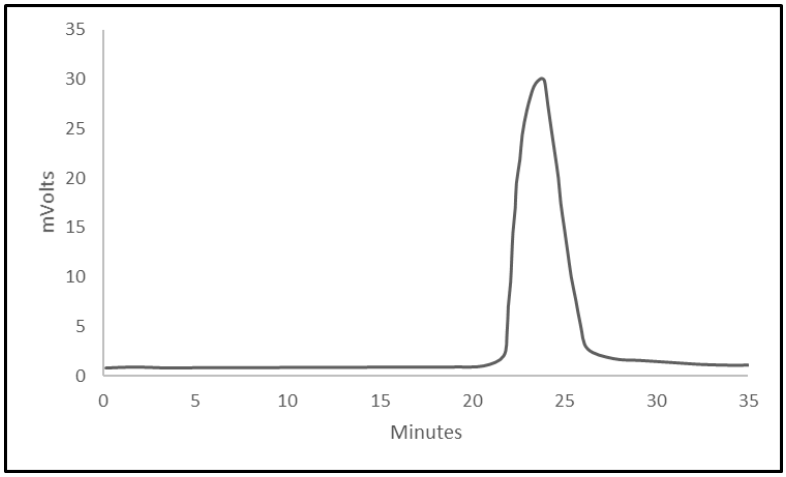

Figure (1) Chromatogram of naphthalene, 10^{-4} M with gradient analysis no (1), the injection volume (2.5 µL), and the detection wavelength 254 nm.

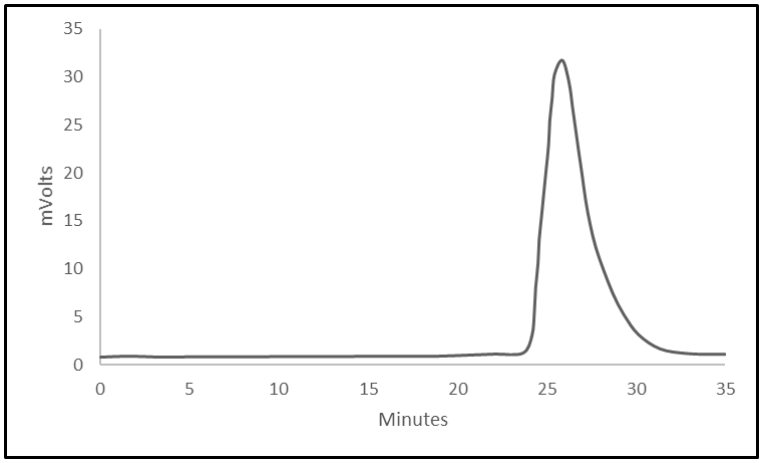

Figure (2) Chromatogram of benzophenone, 10^{-4} M with gradient analysis no (1), the injection volume (2.5 µL), and the detection wavelength 254 nm.

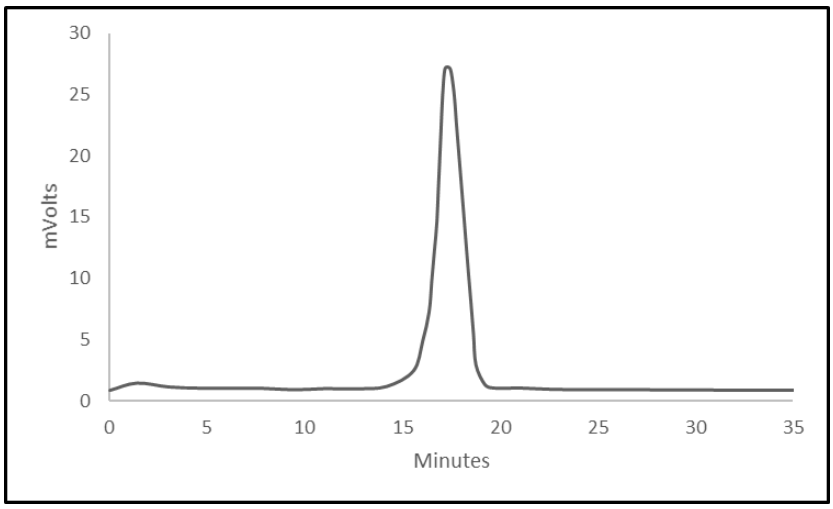

Figure (3) Chromatogram of naphthalene, 10^{-4} M with gradient no. (2), the injection volume (2.5 µL), and the detection wavelength 254 nm.

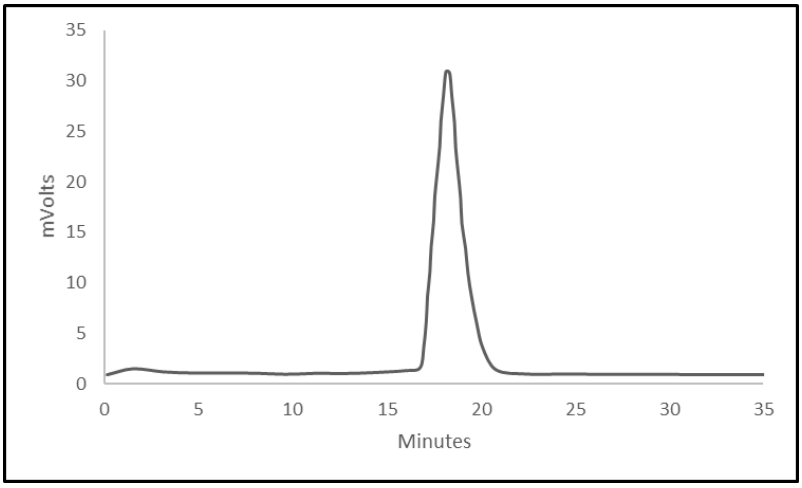

Figure (4) Chromatogram of benzophenone, 10^{-4} M with gradient no. (2), the injection volume (2.5 µL), and the detection wavelength 254 nm.

Chromatograms of hydrophobic compounds

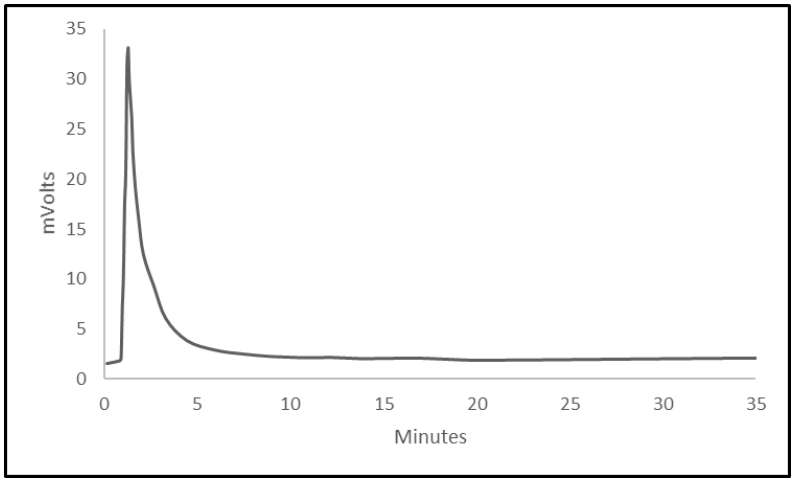

Figure (5) Chromatogram of codeine, 10^{-4} M with gradient no. (2) the injection volume (2.5 µL), and the detection wave length 254 nm.

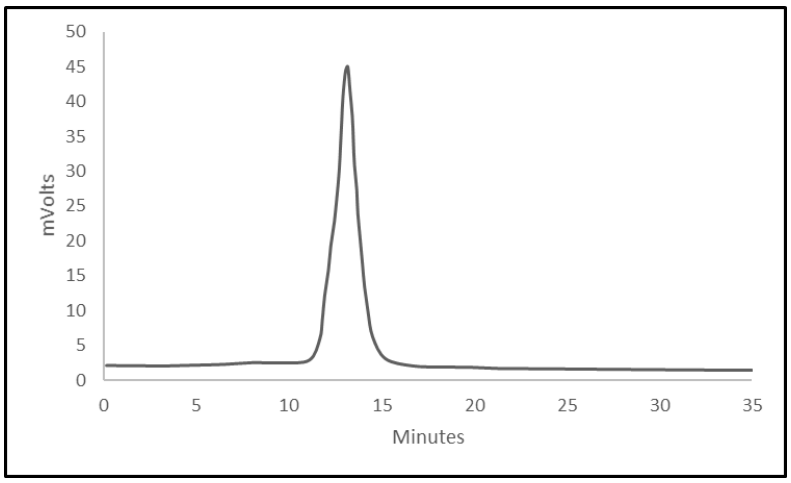

Figure (6) Chromatogram of phenacetin, 10^{-4} M with gradient no. (2) the injection volume (2.5 µL), and the detection wave length 254 nm.

Chromatograms for the compounds that used to prove the mixed mode mechanism with Lauryl methacrylate-co-ethylene glycol dimethacrylate monolithic columns

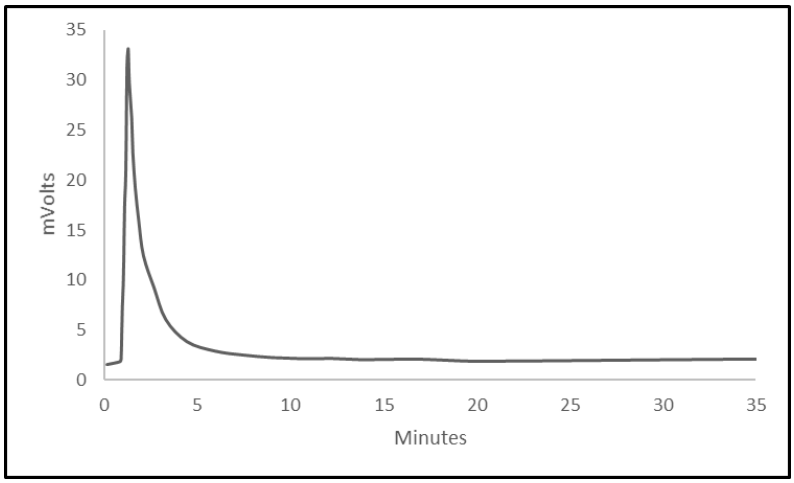

Figure (7) Chromatogram of Codeine with C12 column, 10^{-4} M with gradient no. (4) the injection volume (2.5 µL), and the detection wave length 254 nm.

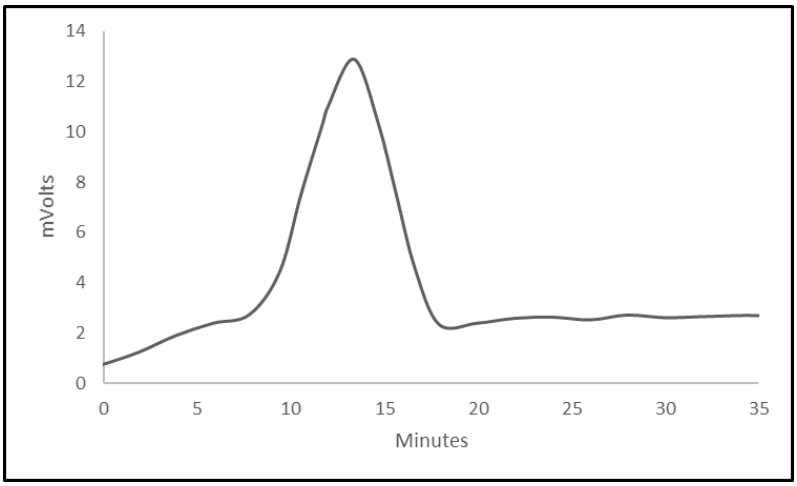

Figure (8) Chromatogram of Phenacetin with C12 column, 10^{-4} M with gradient no. (4) the injection volume (2.5 µL), and the detection wave length 254 nm.

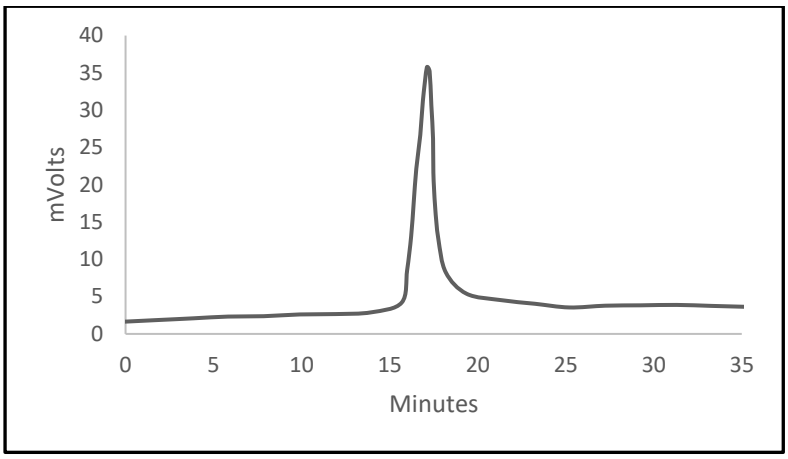

Figure (9) Chromatogram of benzophenone with C12 column, 10^{-4} M with gradient no. (4) the injection volume (2.5 µL), and the detection wave length 254 nm.

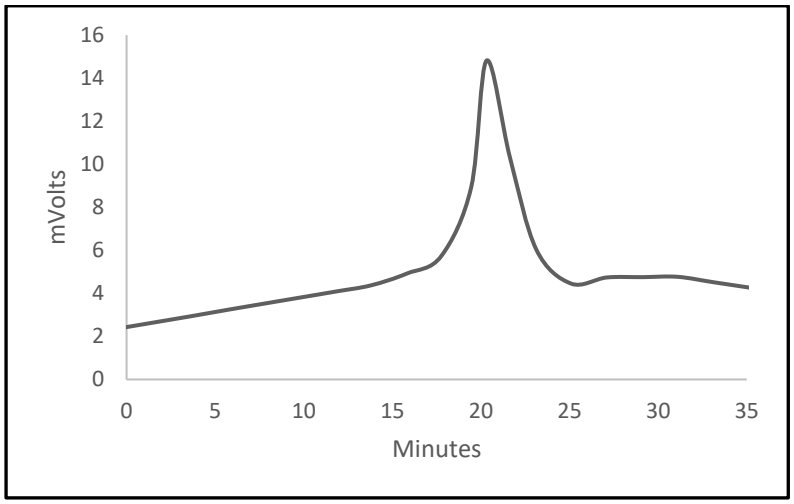

Figure (10) Chromatogram of fluorene with C12 column, 10^{-4} M with gradient no. (4) the injection volume (2.5 µL), and the detection wave length 254 nm.

Chromatograms for the compounds that used to prove the mixed mode mechanism with glycidyl methacrylate-co-lauryl methacrylate-co-ethylene glycol dimethacrylate monolithic columns

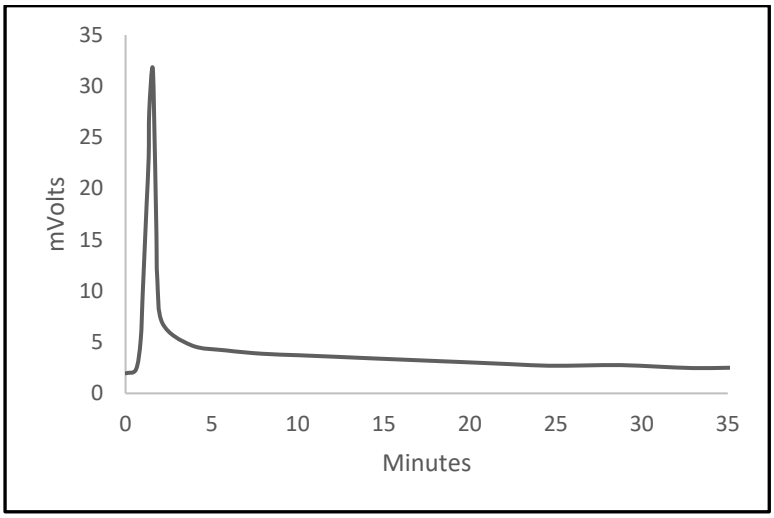

Figure (11) Chromatogram of Codeine with GMA-co-LMA-EDMA column, 10^{-4} M with gradient no. (4) the injection volume (2.5 µL), and the detection wave length 254 nm.

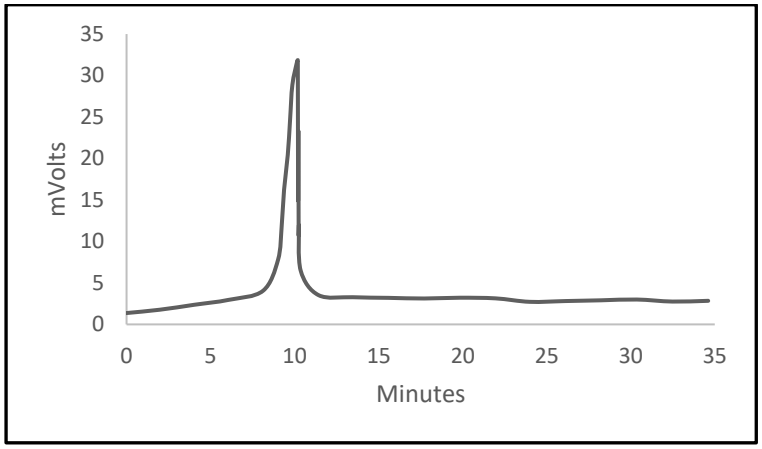

Figure (12) Chromatogram of Phenacetin with GMA-co-LMA-EDMA column, 10^{-4} M with gradient no. (4) the injection volume (2.5 µL), and the detection wave length 254 nm.

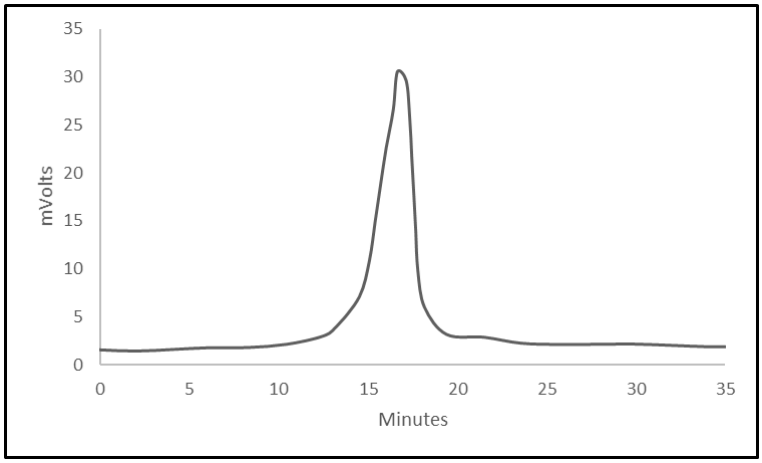

Figure (13) Chromatogram of benzophenone with GMA-co-LMA-EDMA column, 10^{-4} M with gradient no. (4) the injection volume (2.5 µL), and the detection wave length 254 nm.

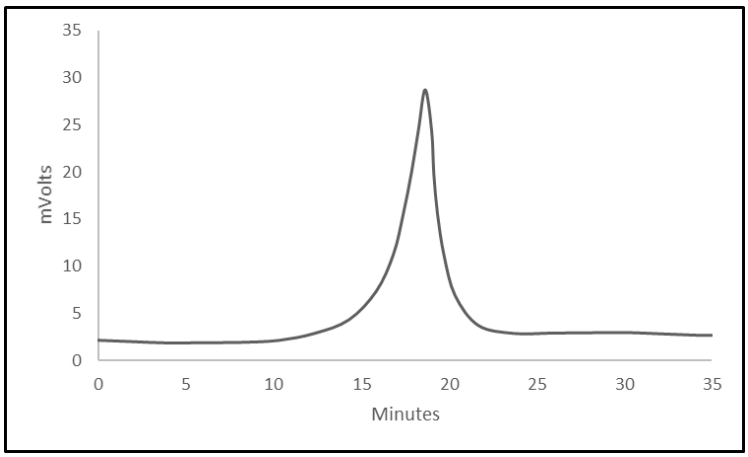

Figure (14) Chromatogram of fluorene with GMA-co-LMA-EDMA column, 10^{-4} M with gradient no. (4) the injection volume (2.5 µL), and the detection wave length 254 nm.

Applications of HILIC/RP glycidyl methacrylate-co-stearyl methacrylate-co-ethylene glycol dimethacrylate monolithic column.

Chromatograms of hydrophobic compounds

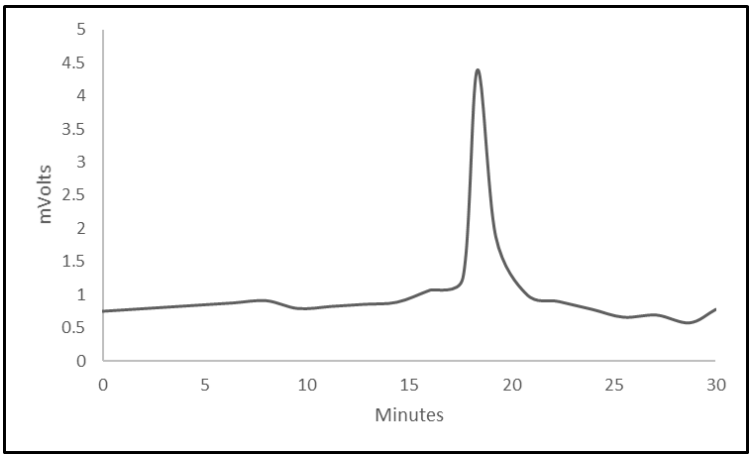

Figure (15) Chromatogram of toluene, 10^{-5} M with gradient no. (5) the injection volume (2.5 µL), and the detection wavelength 254 nm.

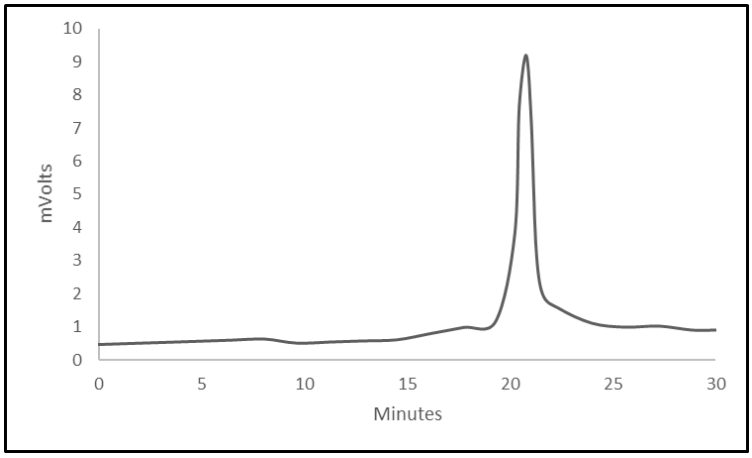

Figure (16) Chromatogram of naphthalene, 10^{-5} M with gradient no. (5) the injection volume (2.5 µL), and the detection wavelength 254 nm.

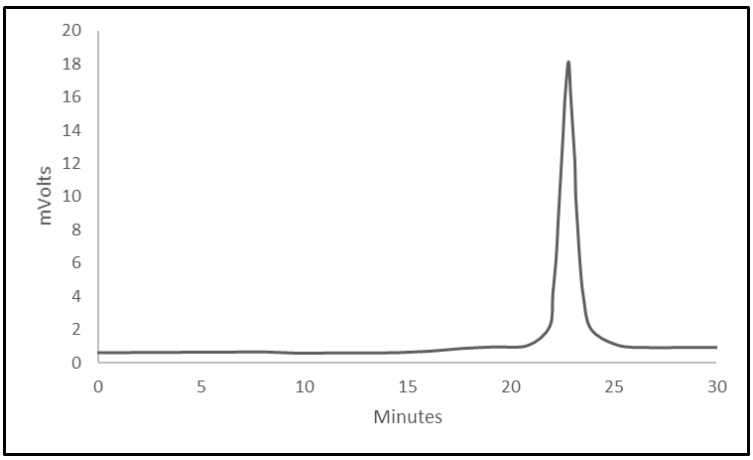

Figure (17) Chromatogram of anthracene, 10^{-5} M with gradient no. (5) the injection volume (2.5 µL), and the detection wavelength 254 nm.

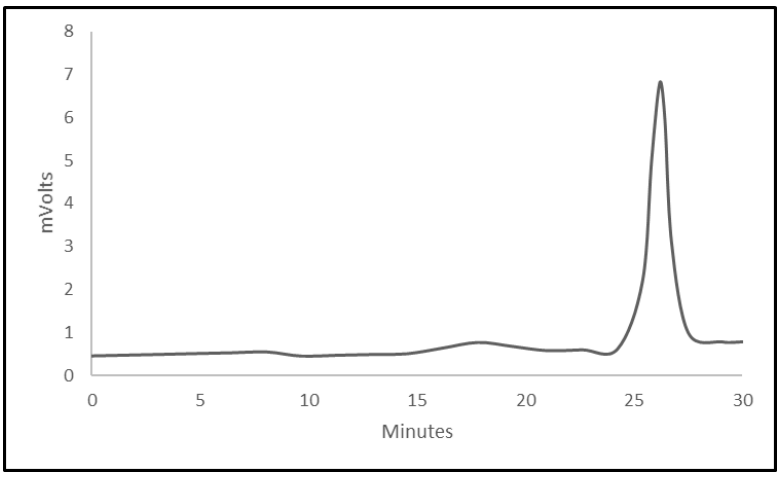

Figure (18) Chromatogram of pyrene, 10^{-5} M mixture with gradient no. (5) the injection volume (2.5 µL), and the detection wavelength 254 nm.

Chromatograms of pharmaceutical compounds

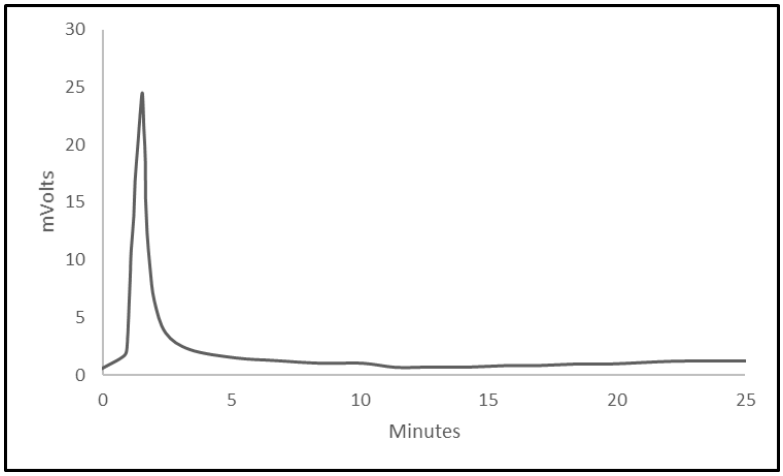

Figure (19) Chromatogram of caffeine, 10^{-5} M with gradient no. (6) the injection volume (2.5 µL), and the detection wavelength 254 nm.

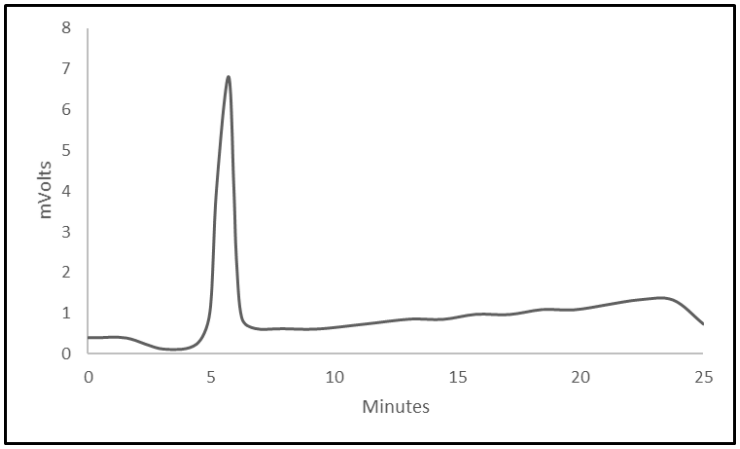

Figure (20) Chromatogram of Paracetamol, 10^{-5} M with gradient no. (6) the injection volume (2.5 µL), and the detection wavelength 254 nm.

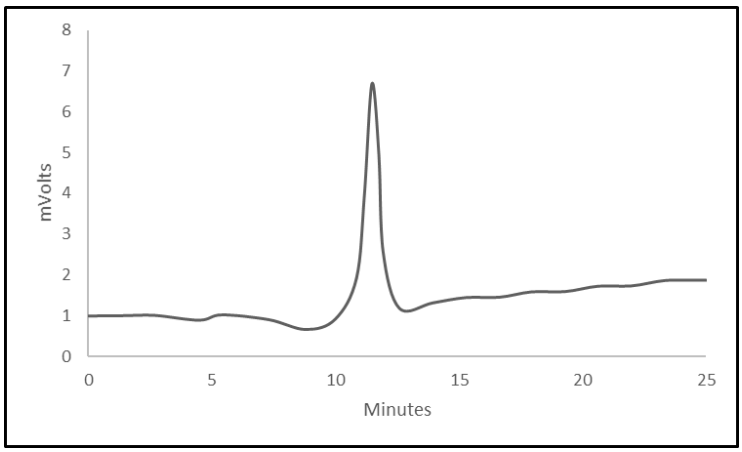

Figure (21) Chromatogram of ibuprofen, 10^{-5} M with gradient no. (6) the injection volume (2.5 µL), and the detection wavelength 254 nm.

Chromatograms of hydrophobic and hydrophilic compounds

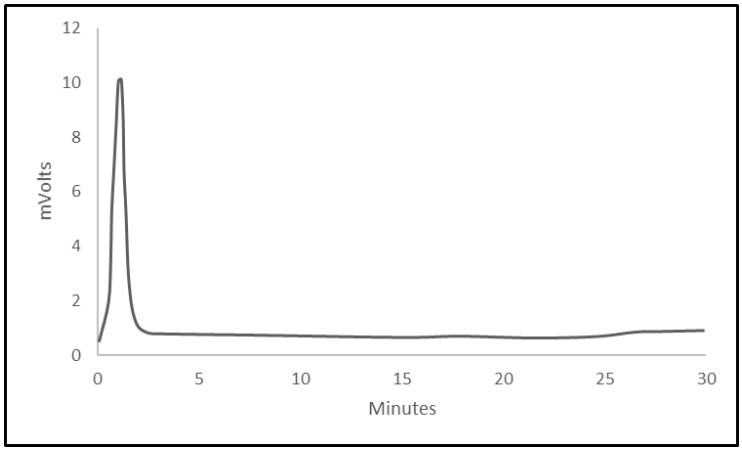

Figure (22) Chromatogram of phenacetin, 10^{-5} M with gradient no. (7) the injection volume (2.5 µL), and the detection wavelength 254 nm.

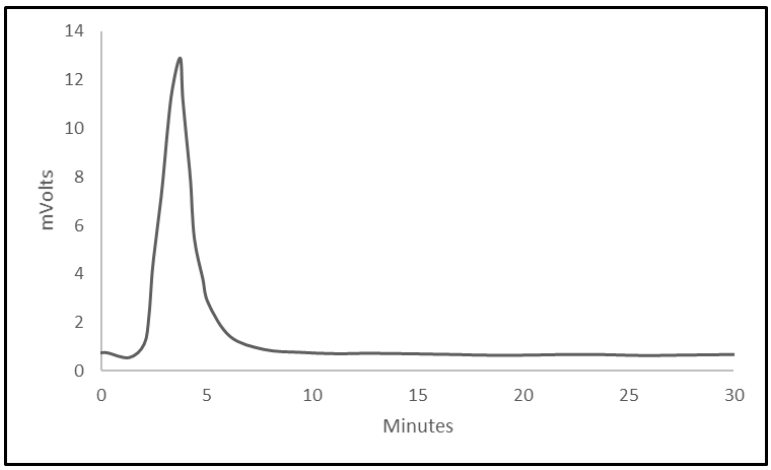

Figure (23) Chromatogram of codeine, 10^{-5} M with gradient no. (7) the injection volume (2.5 µL), and the detection wavelength 254 nm.

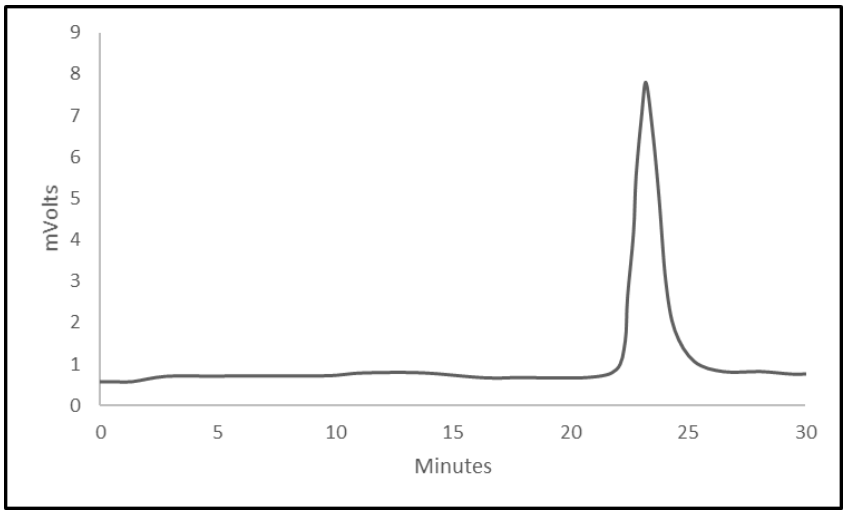

Figure (24) Chromatogram of pyrene, 10^{-5} M with gradient no. (7) the injection volume (2.5 µL), and the detection wavelength 254 nm.

Chromatograms for cyclohexanol and cumene

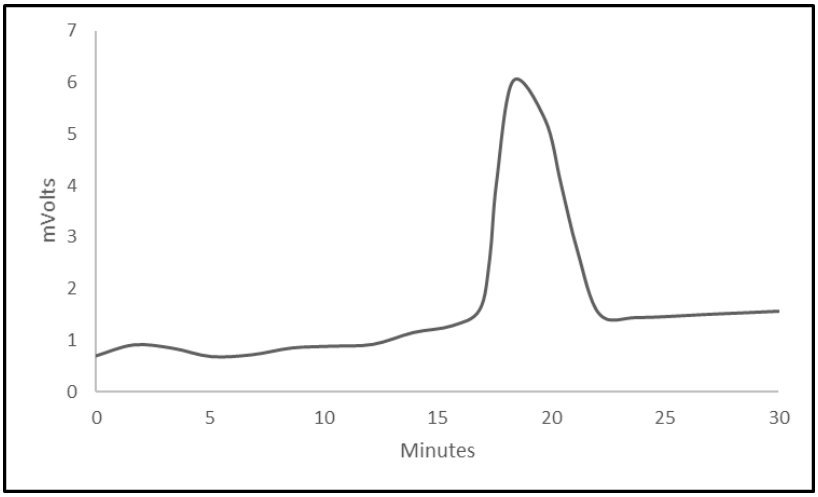

Figure (25) Chromatogram of cyclohexanol, 10^{-5} M with gradient no. (7) the injection volume (2.5 µL), and the detection wavelength 254 nm.

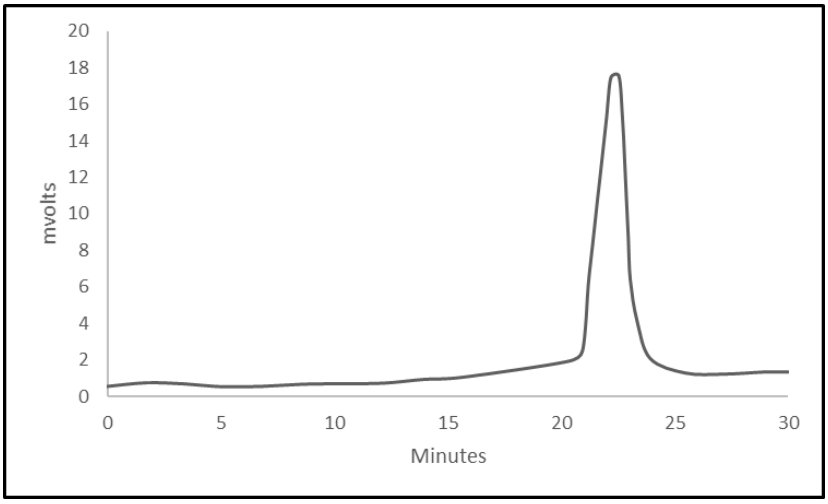

Figure (26) Chromatogram of cumene, 10^{-5} M with gradient no. (7) the injection volume (2.5 µL), and the detection wavelength 254 nm.

Chromatograms for the compounds that used to prove the mixed mode mechanism with stearyl methacrylate-co-ethylene glycol dimethacrylate

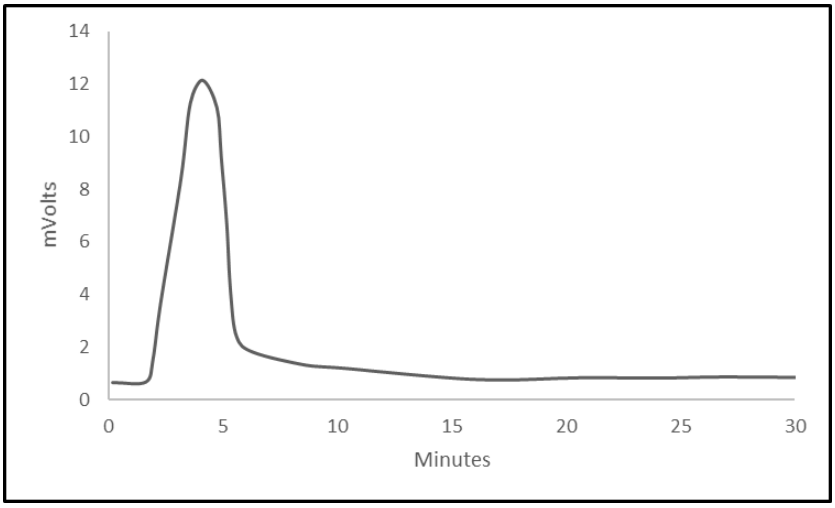

Figure (27) Chromatogram of phenacetin, 10^{-5} M using SMA-co-EDMA monolithic column, with gradient no. (7) the injection volume (2.5 µL), and the detection wavelength 254 nm.

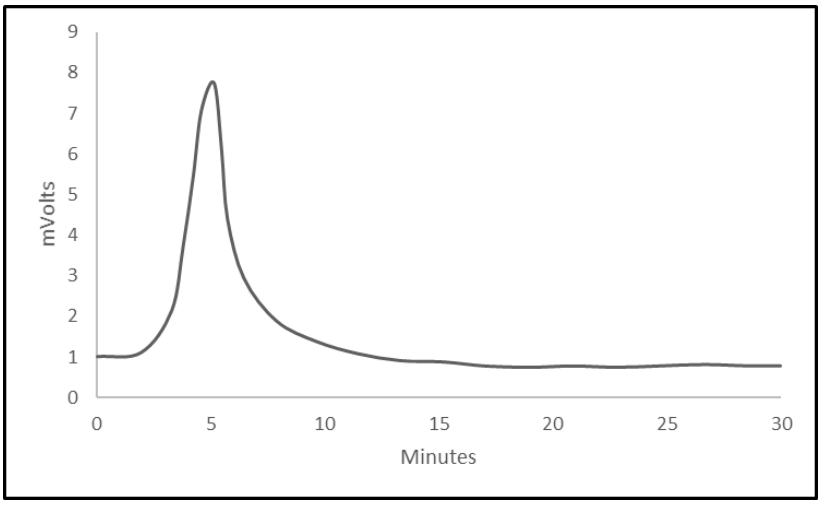

Figure (28) Chromatogram of Codeine, 10^{-5} M using SMA-co-EDMA monolithic column, with gradient no. (7) the injection volume (2.5 µL), and the detection wavelength 254 nm.

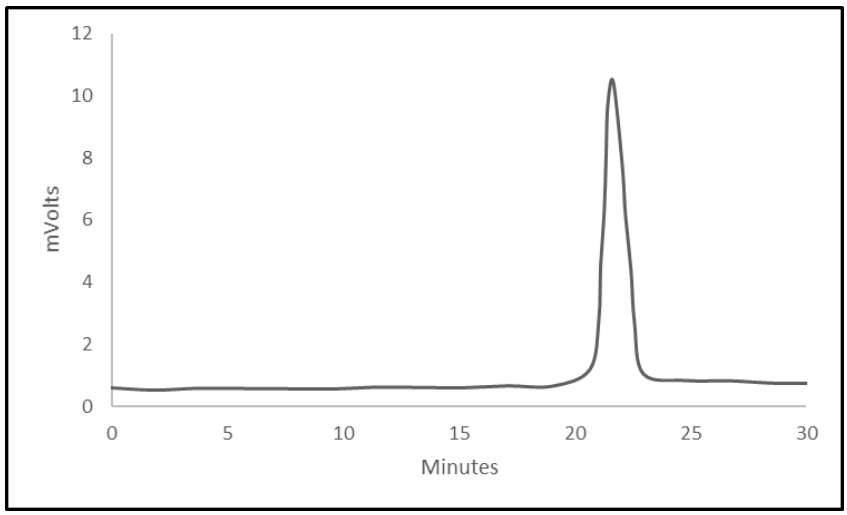

Figure (29) Chromatogram of anthracene, 10^{-5} M using SMA-co-EDMA monolithic column, with gradient no. (7) the injection volume (2.5 µL), and the detection wavelength 254 nm.

Chromatograms for proteins that separated using glycidyl methacrylate-co-stearyl methacrylate-co-ethylene glycol dimethacrylate with (1-propanol and methanol) porogenic solvent

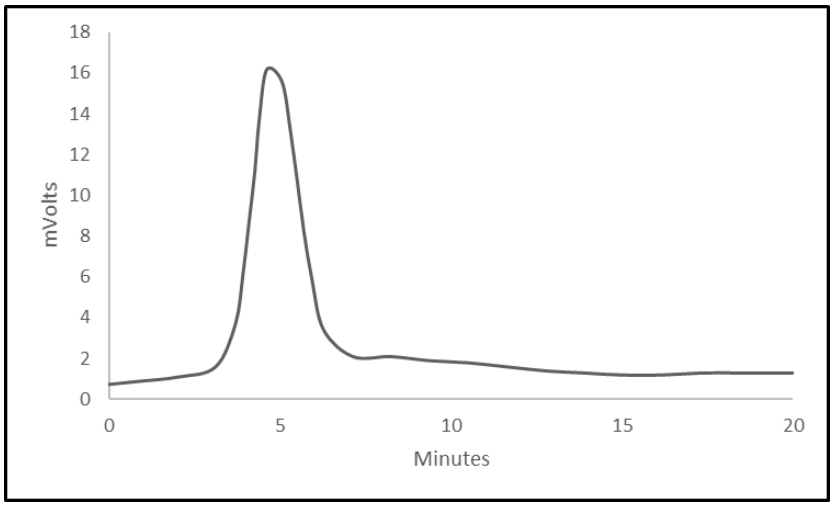

Figure (30) Chromatogram of apo-transferrin, 10^{-5} M with gradient no. (9) the injection volume (2.5 µL), and the detection wavelength 254 nm.

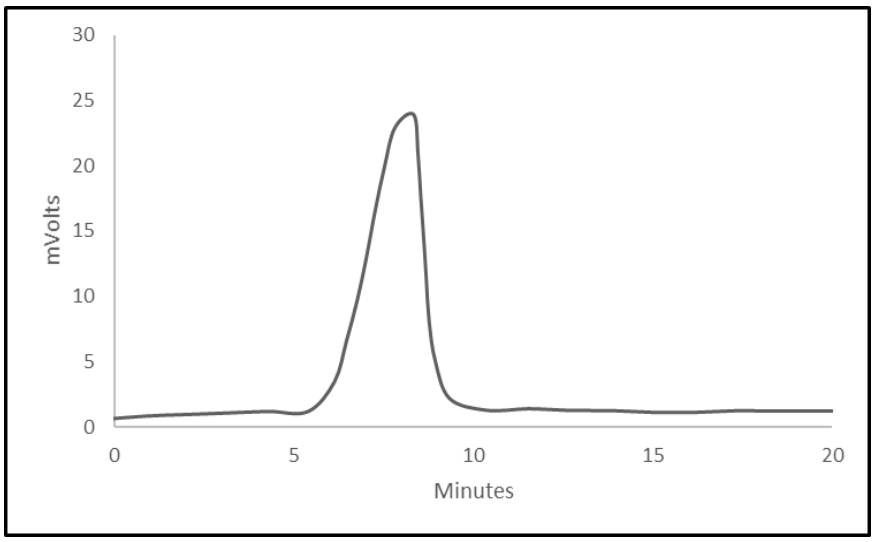

Figure (31) Chromatogram of bovine serum albumin, 10^{-5} M with gradient no. (9) the injection volume (2.5 µL), and the detection wavelength 254 nm.

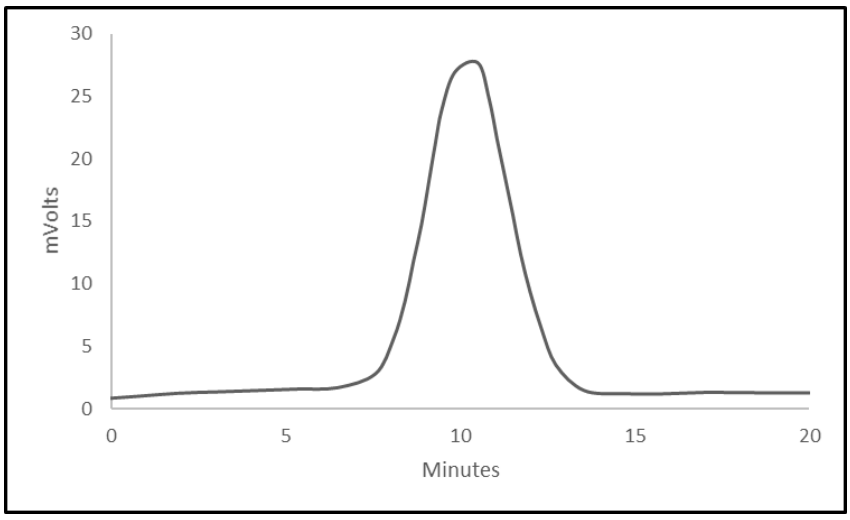

Figure (32) Chromatogram of Cytochrome C, 10^{-5} M mixture with gradient no. (9) the injection volume (2.5 µL), and the detection wavelength 254 nm.

Applications of SCX/RP glycidyl methacrylate-co-stearyl methacrylate-co-ethylene glycol dimethacrylate monolithic column.

Chromatograms of proteins

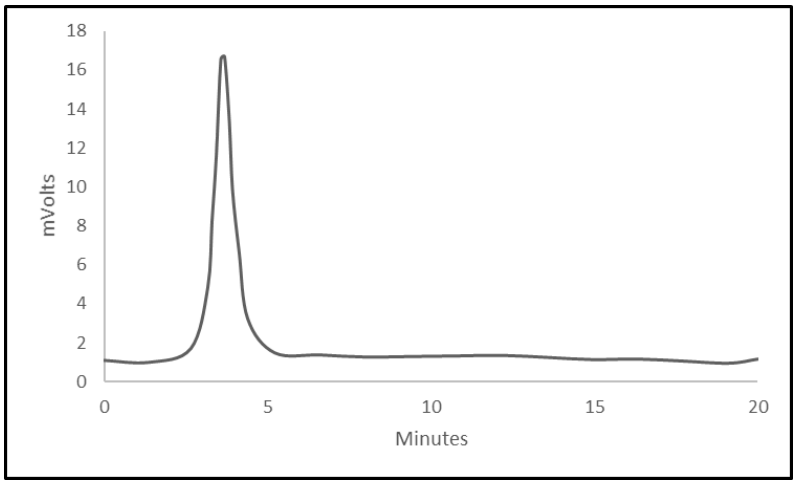

Figure (33) Chromatogram of Insulin, 10^{-5} M with gradient no. (9) the injection volume (2.5 µL), and the detection wavelength 254 nm.

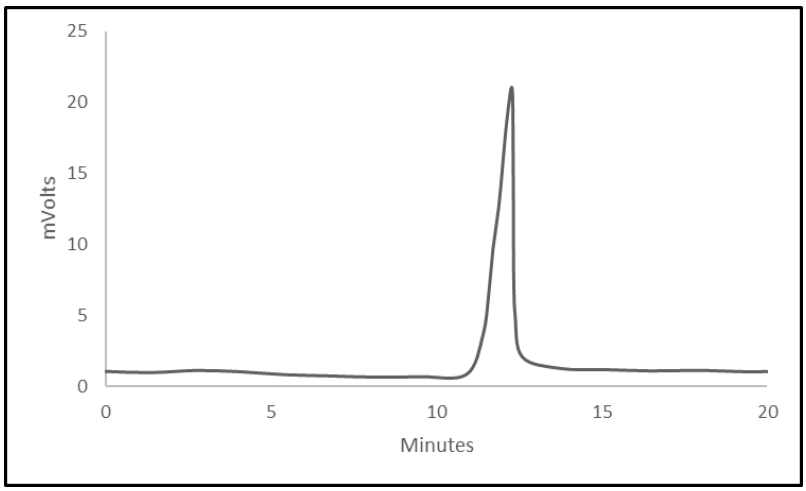

Figure (34) Chromatogram of lysozyme, 10^{-5} M with gradient no. (9) the injection volume (2.5 µL), and the detection wavelength 254 nm.

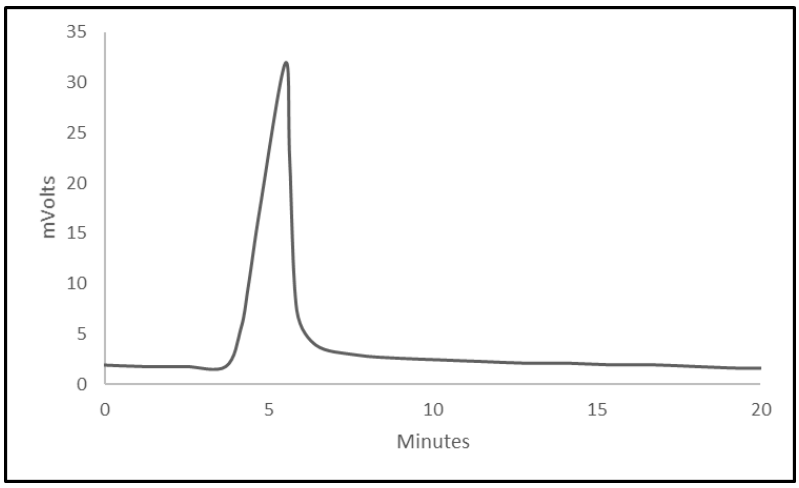

Figure (35) Chromatogram of Myoglobin, 10^{-5} M with gradient no. (7) the injection volume (2.5 µL), and the detection wavelength 254 nm.

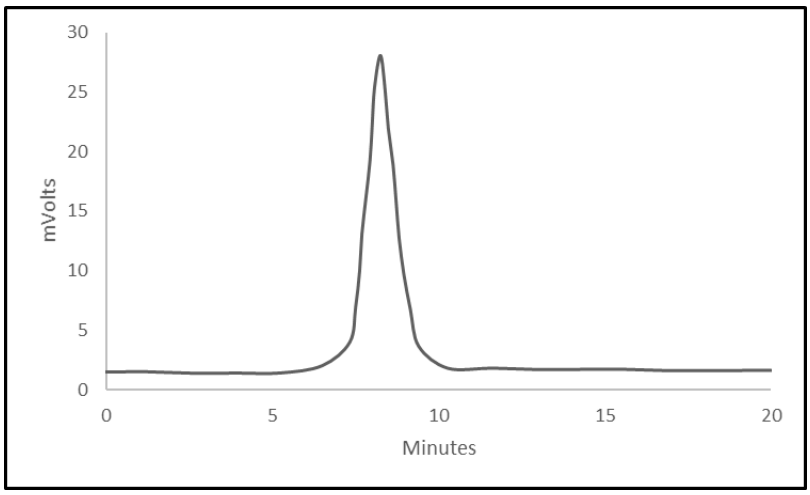

Figure (36) Chromatogram of Cytochrome C, 10^{-5} M with gradient no. (9) the injection volume (2.5 µL), and the detection wavelength 254 nm.

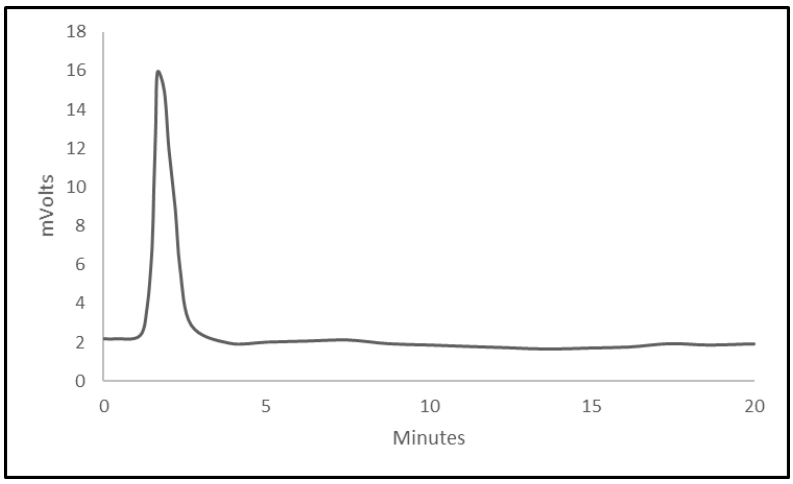

Figure (37) Chromatogram of trypsin, 10^{-5} M with gradient no. (9) the injection volume (2.5 µL), and the detection wavelength 254 nm.

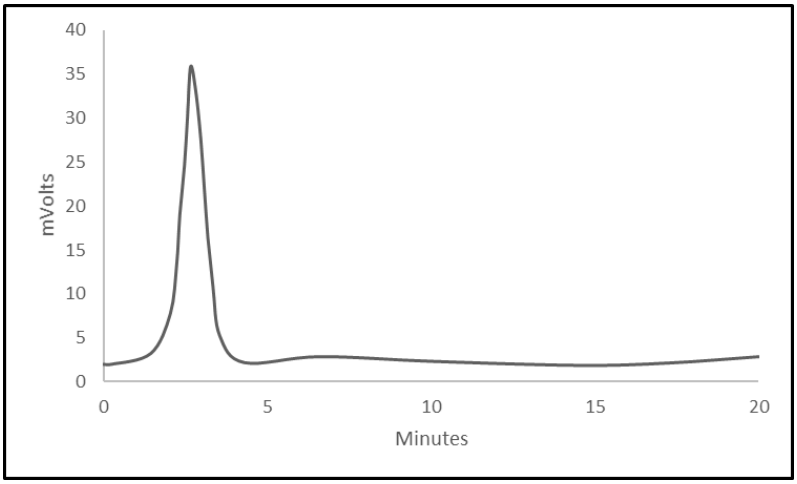

Figure (38) Chromatogram of albumin chicken egg white, 10^{-5} M mixture of each with gradient no. (9) the injection volume (2.5 µL), and the detection wavelength 254 nm.

Chromatograms of hydrophobic compounds

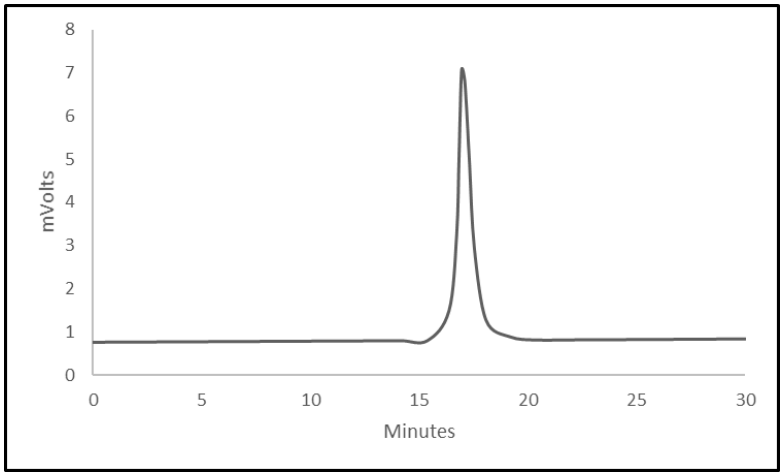

Figure (39) Chromatogram of, 10^{-5} M with gradient no. (5) the injection volume (2.5 µL), and detection wavelength 254 nm.

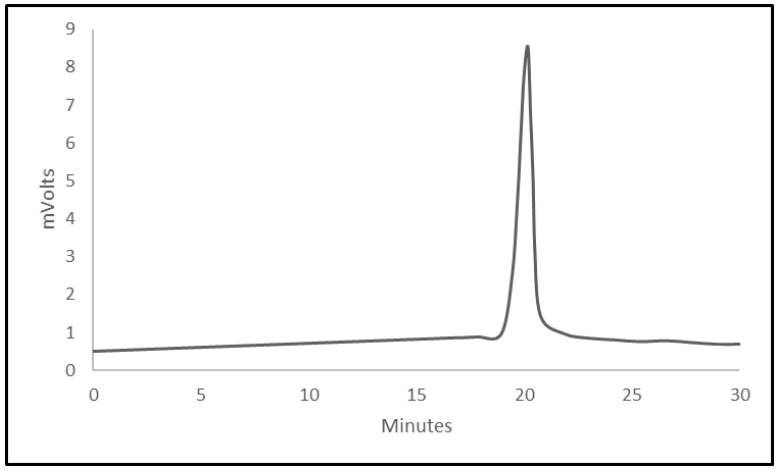

Figure (40) Chromatogram of naphthalene, 10^{-5} M with gradient no. (5) the injection volume (2.5 µL), and detection wavelength 254 nm.

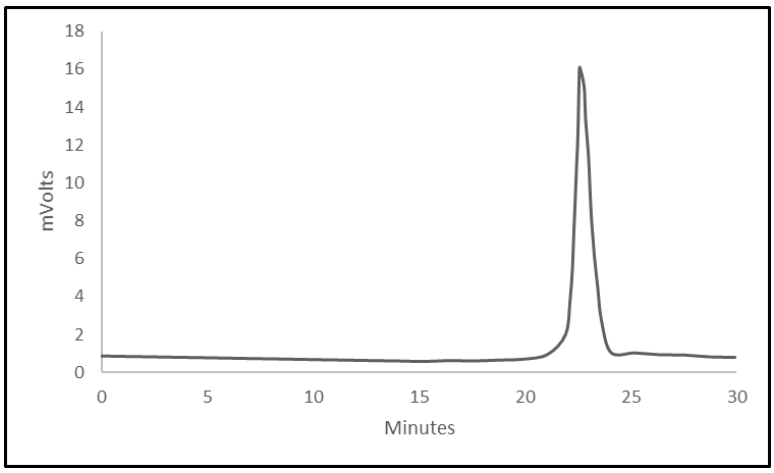

Figure (41) Chromatogram of anthracene, 10^{-5} M with gradient no. (5) the injection volume (2.5 µL), and detection wavelength 254 nm.

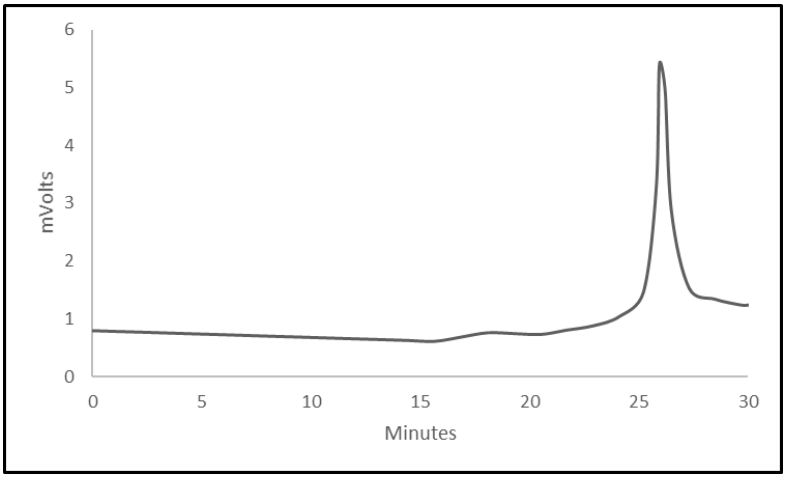

Figure (42) Chromatogram of pyrene, 10^{-5} M with gradient no. (5) the injection volume (2.5 µL), and detection wavelength 254 nm.

Chromatograms of hydrophilic and hydrophobic compounds

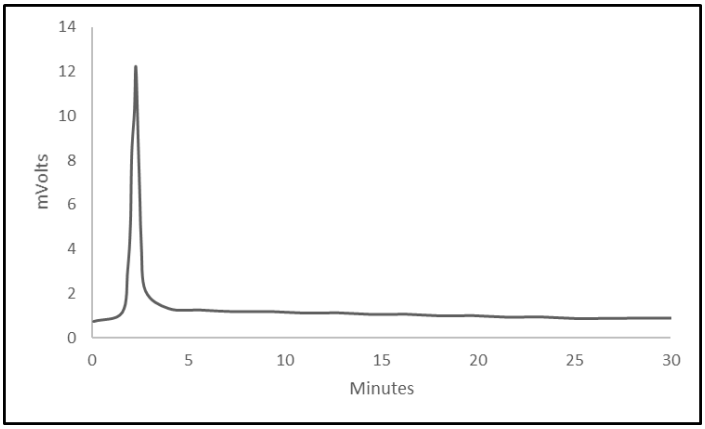

Figure (43) Chromatogram of phenacetin, 10^{-5} M with gradient no. (7) the injection volume (2.5 µL), and the detection wavelength 254 nm.

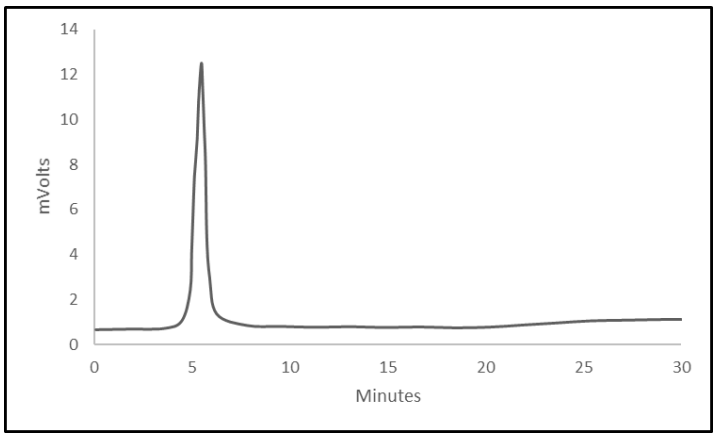

Figure (44) Chromatogram of codeine, 10^{-5} M with gradient no. (7) the injection volume (2.5 µL), and the detection wavelength 254 nm.

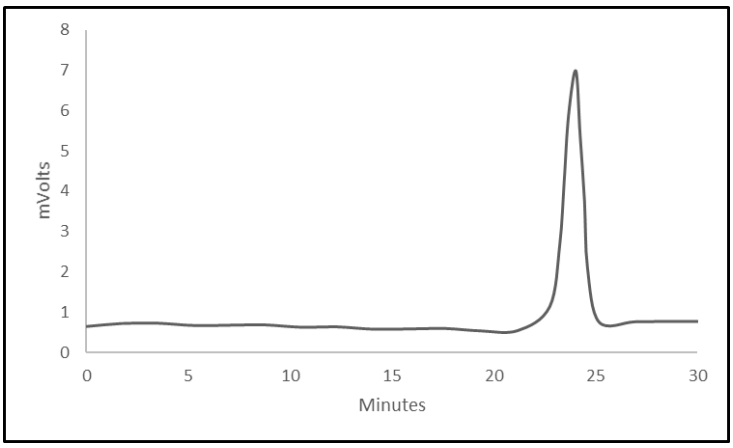

Figure (45) Chromatogram of pyrene, 10^{-5} M with gradient no. (7) the injection volume (2.5 µL), and the detection wavelength 254 nm.

Chromatograms of peptides

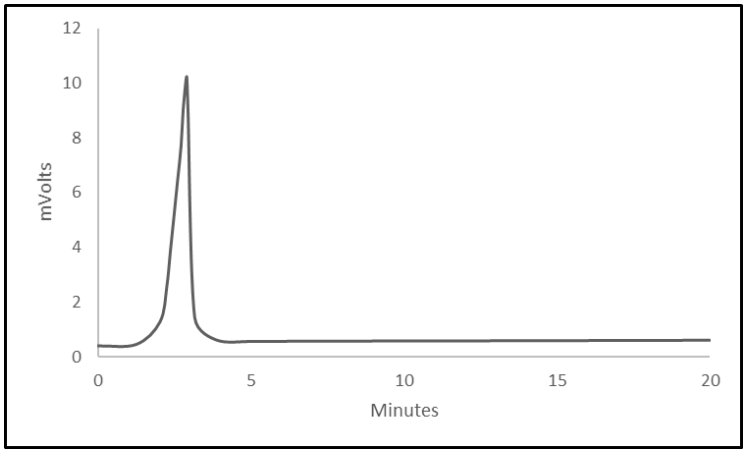

Figure (46) Chromatogram of angiotensin (II), 0.5 mg mL^{-1} with gradient no. (10) the injection volume (2.5 µL), and the detection wavelength 254 nm.

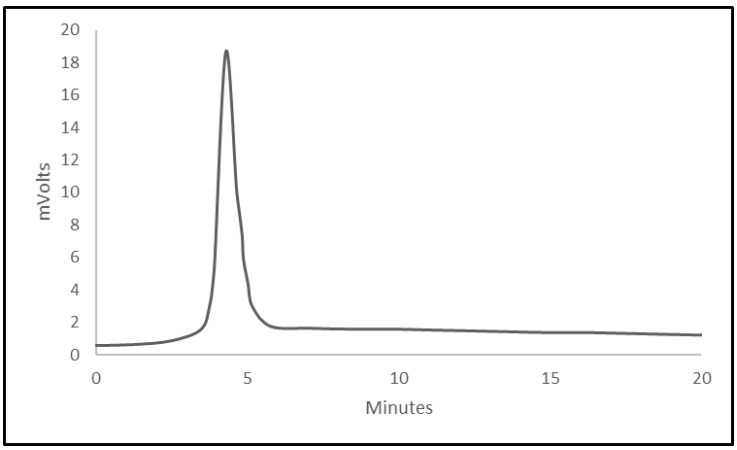

Figure (47) Chromatogram of angiotensin (I), 0.5 mg mL^{-1} with gradient no. (10) the injection volume (2.5 µL), and the detection wavelength 254 nm.

Microchip device

Chromatograms of hydrophobic compounds using microchip device

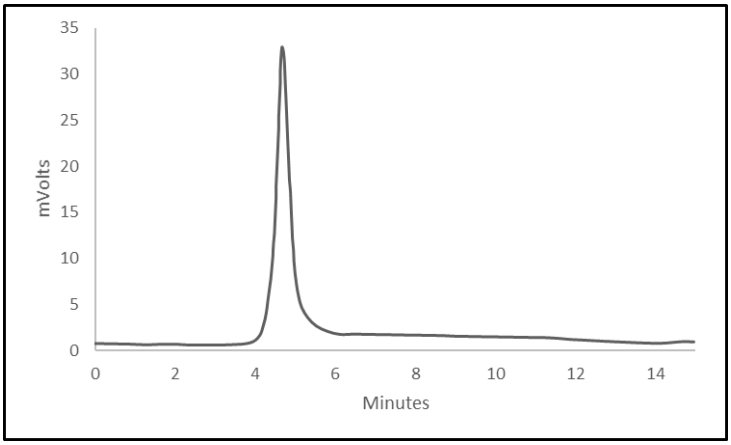

Figure (48) Chromatogram of benzophenone, 10^{-5} M with 80% ACN, 20% water, the injection volume (1.5 µL), flow rate 12 µL min^{-1}, and the detection wavelength 254 nm.

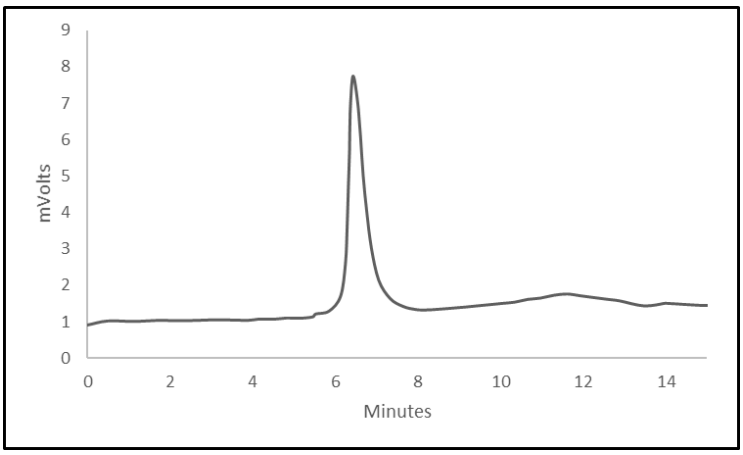

Figure (49) Chromatogram of fluorene, 10^{-5} M with 80% ACN, 20% water, the injection volume (1.5 µL), flow rate 12 µL min^{-1}, and the detection wavelength 254 nm.

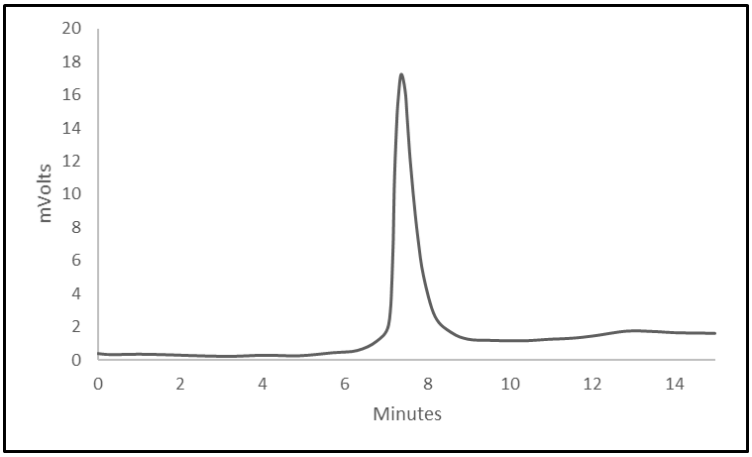

Figure (50) Chromatogram of anthracene, 10^{-5} M with 80% ACN, 20% water, the injection volume (1.5 µL), flow rate 12 µL min^{-1}, and the detection wavelength 254 nm.

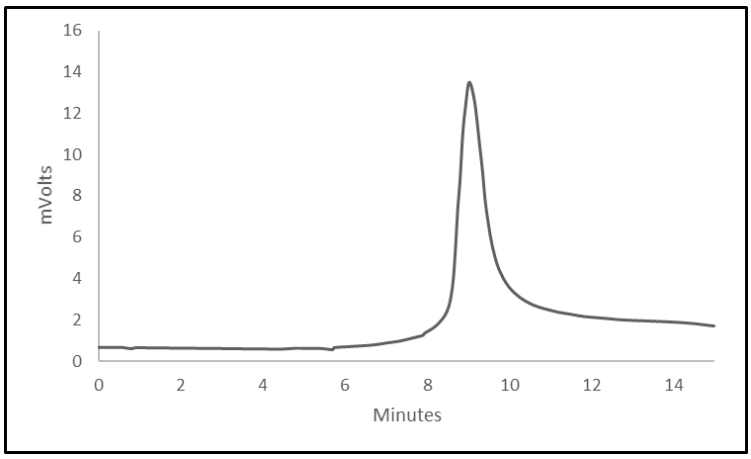

Figure (51) Chromatogram of pyrene, 10^{-5} M with 80% ACN, 20% water, the injection volume (1.5 µL), flow rate 12 µL min^{-1}, and the detection wavelength 254 nm.

Chromatograms of hydrophilic compounds

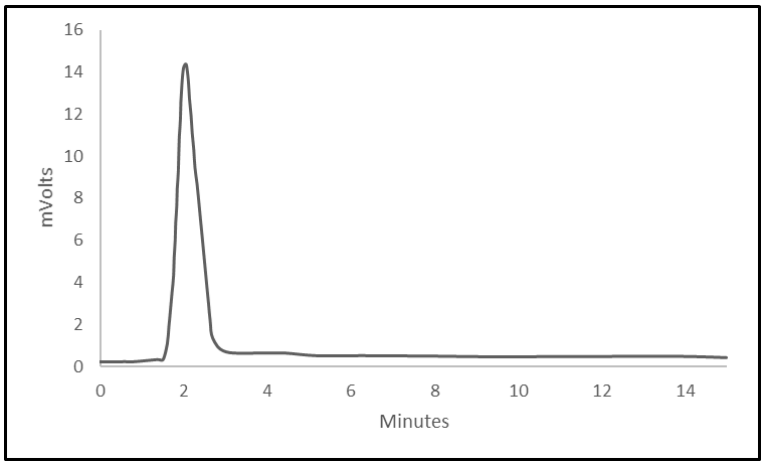

Figure (52) Chromatogram of phenacetin, 10^{-5} M with 20% ACN, 80% water, the injection volume (1.5 µL), flow rate 12 µL min^{-1}, and the detection wavelength 254 nm.

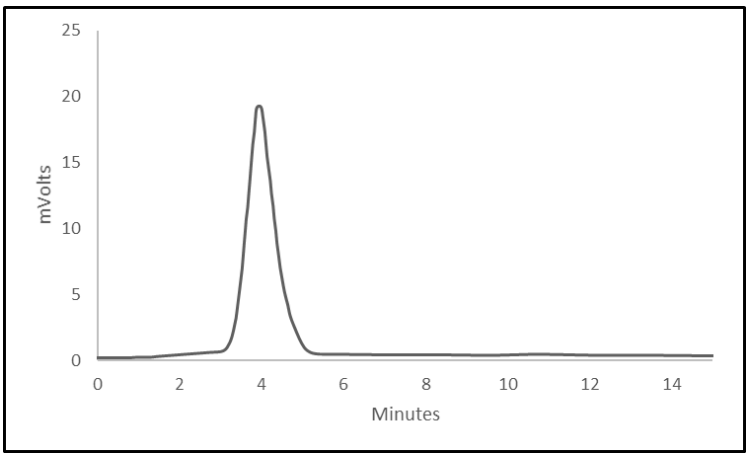

Figure (53) Chromatogram of codeine, 10^{-5} M with 20% ACN, 80% water, the injection volume (1.5 µL), flow rate 12 µL min^{-1}, and the detection wavelength 254 nm.